

Proliposome Technology for Protein Delivery

by

Basel Tawfiq Arafat

A thesis submitted in partial fulfilment for the requirements of the degree of Doctor of
Philosophy at the University of Central Lancashire

April 2013

DECLARATION

I declare that while registered as a candidate for this research degree, I have not been an enrolled student or registered candidate for any other award from an academic or professional institution. No portion of the work referred to in the thesis has been used in any other submission for an academic award and is solely my own work.

ABSTRACT

Growing attention has been given to the potential of the respiratory tract for systemic delivery of macromolecules, particularly proteins and peptides. However, limitations such as short transit time and loss of activity of some proteins and peptides in the respiratory tract need to be overcome. Consequently, the utility of controlled drug delivery systems such as liposomes as protein carriers appear promising. Unfortunately, liposomes are unstable in aqueous dispersions. Additionally, conventional liposome preparation methods such as the thin film hydration are difficult to scale-up, and also demonstrate low entrapment efficiencies for hydrophilic materials.

The aim of this work was to develop novel submicron mucoadhesive liposomes entrapping the protein immunoglobulin g (IgG) using the proliposome method. Additionally, this work explored the potential of the generated liposomes for respiratory tract delivery via medical nebulisers and nasal sprays with different operating principles.

Liposomes generated from the proliposome technology were multilamellar as cryo-TEM studies revealed. The generated liposomes were capable of entrapping considerable concentrations of salbutamol sulfate (59.1%), ovalbumin (43.3 %) and IgG (29.9 %). Also, the generated liposomes demonstrated superior entrapment efficiency of IgG to other liposome preparation methods (thin film and particulate-based proliposome technology). Reduction of liposome size to 400 nm and the incorporation of the mucoadhesive agent sodium alginate markedly enhanced the entrapment of IgG in liposomes (up to 50 %). The secondary structure and immunological reactivity of IgG were also maintained following its incorporation in liposomes as demonstrated by circular dichroism and microagglutination assay, respectively.

Nebulisation was found to fragment liposomes as well as reduce the activity of the entrapped IgG. The degree of liposome fragmentation and loss of activity of IgG varied markedly among different medical nebulisers. Liposome size distribution and IgG immune reactivity studies elucidated that vibrating-mesh nebuliser was least disruptive to liposome structure and the immunoreactivity of the incorporated IgG was least affected following its use (retained activity of 83% versus 24% and 39% for the ultrasonic and air-jet nebulisers, respectively). Contrary to medical nebulizers, this work illustrated that all studied nasal devices preserved both the integrity of liposomes and the incorporated IgG.

In conclusion, the findings of this study demonstrate potential benefits in drug delivery employing both intranasal administration and proliposome technology offer with great promise in using proliposome formulations for intranasal protein delivery.

TABLE OF CONTENTS

DECLARATION	ii
ABSTRACT	iii
TABLE OF CONTENTS	iv
LIST OF FIGURES	viii
LIST OF TABLES	xiv
ACKNOWLEDGEMENTS	xv
LIST OF ABBREVIATIONS AND ACRONYMS	xvi
CHAPTER 1: INTRODUCTION	1
1.1 Drug delivery to the respiratory tract.....	2
1.2 Pulmonary route	2
1.2.1 Historical background	2
1.2.2 Anatomy and physiology of the respiratory system	4
1.2.3 Advantages and limitations of pulmonary delivery	5
1.2.4 Devices for pulmonary delivery	6
1.3 Nasal delivery.....	15
1.3.1 Historical background	15
1.3.2 Anatomy and physiology of the nose	16
1.3.3 Advantages of nasal drug delivery	16
1.3.4 Limitations of nasal delivery	18
1.3.5 Applications of nasal delivery	18
1.3.6 Nasal delivery devices.....	19
1.4 Liposomes	21
1.4.1 Historical background	21
1.4.2 Molecular composition of liposomes.....	21
1.4.3 Classification of liposomes	24
1.4.4 Advantages and drawbacks of liposomal delivery	25
1.4.5 Preparation of liposomes.....	27
1.5 Liposomes in respiratory tract delivery	30
1.5.1 Liposomes in nasal delivery:	31
1.5.2 Liposomes in pulmonary delivery	33
1.5.3 Safety and fate of liposomes in the respiratory tract	37
1.6 Hypothesis and objectives	38

CHAPTER 2: GENERAL METHODOLOGY	40
2.1 Materials	41
2.2 Methods.....	41
2.2.1 Preparation of liposomes.....	41
2.2.2 Hydration of phospholipid thin films or particulate-based proliposomes.....	43
2.2.3 Size reduction of liposomes	44
2.2.4 Phospholipid assay	45
2.2.5 Size analysis of the liposomes.....	46
2.2.6 Liposome morphology, Cryo Transmission Electronic Microscopy (Cryo-TEM)	48
2.2.7 Zeta potential analysis	48
2.2.8 Drug entrapment studies	49
2.2.9 Determination of the secondary structure of IgG	51
2.2.10 Immunoreactivity of IgG	52
2.2.11 Determination of nebuliser performance.....	53
2.2.12 Determination of aerosol size distribution	54
2.2.13 Determination of the shot weight and dose accuracy of nasal devices	56
2.2.14 Determination of nasal spray characteristics	57
2.2.15 Statistical Analysis.....	59
CHAPTER 3: CHARACTERISATION OF LIPOSOMES GENERATED FROM ETHANOL BASED PROLIPOSOMES	62
3.1 Introduction	63
3.2 Methodology.....	64
3.2.1 Preparation of liposomes.....	64
3.2.2 Characterisation of liposomes	65
3.2.3 Phospholipid assay	66
3.2.4 Size reduction of ethanol based liposomes	66
3.2.5 Formulation of mucoadhesive ethanol-based liposomes.....	67
3.3 Results and discussion	67
3.3.1 Formulation of empty ethanol-based proliposomes	67
3.3.2 Preparation of SS liposomes	72
3.3.3 Preparation of OVA liposomes.....	76
3.3.4 Size reduction of empty liposomes.....	78
3.3.5 Effect of extrusion on the properties of liposomes entrapping SS or OVA	83
3.3.6 Inclusion of chitosan in liposome formulations.....	85
3.4 Conclusions	88

CHAPTER 4: FORMULATION OF IgG LIPOSOMES USING THE ETHANOL-BASED PROLIPOSOMES	
METHOD	90
4.1 Introduction	91
4.2 Methodology.....	92
4.2.1 Manufacture of IgG liposomes.....	92
4.2.2 Characterisation of liposomes	93
4.2.3 Formulation of mucoadhesive ethanol-based liposomes.....	94
4.2.4 Size reduction of ethanol-based liposomes	94
4.2.5 Secondary structure and activity of IgG.....	95
4.3 Results and discussion	95
4.3.1 Entrapment of IgG.....	95
4.3.2 Size distribution of IgG liposomes.....	97
4.3.3 Addition of mucoadhesive agents to IgG liposomes generated from ethanol-based proliposomes	101
4.3.4 Size reduction of IgG liposomes.....	106
4.3.5 Structural determination and activity of IgG.	112
4.3.6 Effect of temperature on the structure of IgG.....	115
4.3.7 Effect of size reduction on the structure and activity of IgG	115
4.4 Conclusions	120
CHAPTER 5: DELIVERY OF LIPOSOMES GENERATED FROM ETHANOL-BASED PROLIPOSOMES	
VIA MEDICAL NEBULISERS	122
5.1 Introduction	123
5.2 Methodology.....	125
5.2.1 Preparation of IgG liposomes.....	125
5.2.2 Determination of nebuliser performance.....	125
5.2.3 Determination of aerosol size distribution	125
5.2.4 Characterisation of liposomes	126
5.2.5 Determination of structure and activity of IgG.....	126
5.3 Results and discussion	127
5.3.1 Determination of nebuliser performance.....	127
5.3.2 Aerosol droplet size and Respirable output.....	133
5.3.3 Influence of nebulisation on the size distribution and morphology of liposomes ..	138
5.3.4 Structure and activity of IgG following nebulisation	145
5.4 Conclusions	154

CHAPTER 6: DELIVERY OF LIPOSOMES VIA NASAL SPRAYS	155
6.1 Introduction	156
6.2 Methodology.....	158
6.2.1 Preparation of IgG liposomes.....	158
6.2.2 Determination of the shot weight and dose accuracy of nasal devices	158
6.2.3 Determination of nasal spray characteristics	158
6.2.4 Characterisation of liposomes following spraying.....	159
6.2.5 Determination of structure and activity of IgG.....	159
6.3 Results and discussion:	159
6.3.1 Priming and tail off characteristics	159
6.3.2 Droplet size distribution (DSD)	164
6.3.3 Spray pattern and plume geometry.....	170
6.3.4 Liposomes before and after spraying	176
6.3.5 Effect of spraying on the structure and activity of IgG	177
6.4 Conclusions	184
CHAPTER 7: GENERAL CONCLUSIONS AND FUTURE WORK	185
CHAPTER 8: REFERENCES	191

LIST OF FIGURES

CHAPTER 1: INTRODUCTION

Figure 1.1: Papers published in the field of respiratory tract delivery since 1953.	3
Figure 1.2: Images of (a) the Mudge inhaler (b) the Sales Giro pressurized inhaler and (c) Medihaler® advert sheet.	4
Figure 1.3: Schematic representations of the human respiratory tract.	7
Figure 1.4: Schematic representation of a pMDI device.....	8
Figure 1.5: The design of a conventional air-jet nebuliser and the movement of the droplets inside the nebuliser following inspiration and expiration.	11
Figure 1.6: Proposed mechanisms for aerosol generation in ultrasonic nebulisers: (A) droplet formation via cavitation theory; (B) droplet formation via capillary wave theory.....	13
Figure 1.7: Schematic representation of a passively vibrating-mesh nebuliser showing the generation of the aerosol from the mesh plate.	14
Figure 1.8: Schematic representation of an actively vibrating-mesh nebuliser showing the generation of the aerosol from the mesh plate.	15
Figure 1.9: Cross-Section of nasal cavity.....	17
Figure 1.10: The structure of a PC molecule.....	22
Figure 1.11: Schematic representation of the assembly of phospholipids in liposomes.	23
Figure 1.12: Chemical structure of cholesterol.....	23
Figure 1.13: Schematic representations of types of liposomes.....	24
Figure 1.14: Papers published in the field of liposomal delivery systems since 1976.....	26

CHAPTER 2: GENERAL METHODOLOGY

Figure 2.1: A schematic presentation of laser diffraction.....	47
Figure 2.2: A schematic representation of DLS in the Zetasizer instrument.	47
Figure 2.3: A schematic representation of the mechanism of action of LDV in the Zetasizer instrument.	49
Figure 2.4: Schematic diagram illustrating analysis of aerosol droplets generated from a nebuliser via the laser diffraction principle.	55
Figure 2.5: FPF output equations: (1) FPF output in relation to mass output; (2) FPF output in relation to active protein output	56

Figure 2.6: A schematic representation of: (A) the impaction technique used to determine the spray pattern of the nasal devices (B) spray pattern example, showing the maximum (Dmax) and minimum (Dmin) diameters. 60

Figure 2.7: A schematic representation of the high speed photography technique used to determine the spray pattern of the nasal devices. 61

CHAPTER 3: CHARACTERISATION OF LIPOSOMES GENERATED FROM ETHANOL BASED PROLIPOSOMES

Figure 3.1: Relationship between (A) vortexing duration and liposome size and (B) size distribution of the generated liposomes during hydration steps. 68

Figure 3.2: Size of liposomes during one week storage at 5 ± 1 °C. 70

Figure 3.3: SPAN of liposomes during a week interval of storage at a temperature of 5 ± 1 °C. . 71

Figure 3.4: Zeta potential of liposomes during a week interval of storage at a temperature of 5 ± 1 °C. 71

Figure 3.5: Chemical structure of salbutamol sulphate. 73

Figure 3.6: The assembly of cholesterol between phospholipid molecules. 74

Figure 3.7: Relationship between cholesterol concentration in the lipid phase and particle size distribution of liposomes. 76

Figure 3.8: The entrapment efficiency of OVA prepared in a range of concentrations. 78

Figure 3.9: Phospholipid content in the supernatant for liposomes processed at various conditions: (I) liposomes without processing; (II) liposomes after probe sonication to 100 nm vesicles; (III) liposomes after ultracentrifugation; (IV) liposomes after probe sonication to 100 nm vesicles followed by centrifugation; (V) liposomes after probe sonication into 400 nm vesicles; (VI) liposomes after probe sonication into 400 nm vesicles followed by centrifugation. 80

Figure 3.10: Size and polydispersity of liposomes reduced in size using bath sonication, probe sonication or extrusion. 81

Figure 3.11: Relationship between number of extrusion cycles through the different membrane filters (5, 1, 0.8 and 0.4 μm pore size) on the (A) size of liposomes and (B,C,D) size distribution following 0, 3 and 5-7 extrusion cycles, respectively. (B-D) represents typical size distribution monographs generated by the Zetasizer Nanoseries analysis software. 82

Figure 3.12: Entrapment efficiency of OVA and SS before and after extrusion of liposomes. 85

Figure 3.13: Zeta potential of liposomes upon inclusion of chitosan in a range of concentrations. 87

Figure 3.14: Effect of chitosan concentration on the entrapment efficiency of OVA in liposomes.....	88
---	----

CHAPTER 4: FORMULATION OF IgG LIPOSOMES USING THE ETHANOL-BASED PROLIPOSOMES METHOD

Figure 4.1: Entrapment efficiency of IgG used at various concentrations in liposomes manufactured using the thin film hydration or proliposome methods.....	98
Figure 4.2: Size of liposomes prepared using ethanol-based proliposomes, particulate-based proliposomes or thin film hydration.....	99
Figure 4.3: Size distribution of liposomes prepared using ethanol-based proliposomes, particulate-based proliposomes or thin film hydration.....	100
Figure 4.4: Zeta potential of liposomes prepared using ethanol-based proliposomes, particulate-based proliposomes or thin film hydration.....	101
Figure 4.5: Effect of mucoadhesive agents' (chitosan and alginate) concentration on size of generated liposomes.....	102
Figure 4.6: Effect of Mucoadhesive agents' (chitosan and alginate) concentration on SPAN of generated liposomes.....	103
Figure 4.7: Effect of mucoadhesive agents' (chitosan and alginate) concentration on size of generated liposomes.....	104
Figure 4.8: Mucoadhesive agents' (chitosan and alginate) concentration and its effect on entrapment efficiency of IgG in the generated liposomes.	106
Figure 4.9: Probe sonication time and its effect on size and Pdi of the generated liposomes.	108
Figure 4.10: Cryo-TEM images of liposomal multilamellar structure (A) before and (B) after sonication.....	109
Figure 4.11: Effect of probe sonication on the zeta potential of liposomes.	110
Figure 4.12: Effect of probe sonication on the entrapment efficiency of IgG in the generated liposomes.....	111
Figure 4.13: Secondary structure of IgG, both free in solution or incorporated into liposomes, as determined via CD.	113
Figure 4.14: Activity of IgG free in solution or incorporated into liposomes, determined using the IgG easytitre kit.....	114
Figure 4.15: CD spectra of IgG in solution at temperatures between 20 oC and 70 oC. A 3D representation of (A) all the spectra combined and (B) the individual spectra at each temperature.....	116

Figure 4.16: CD spectra of IgG incorporated in liposomes at temperatures between 20 oC and 70 oC. A 3D representation of (A) all the spectra combined and (B) the individual spectra at each temperature.....	117
Figure 4.17: Secondary structure of IgG free and incorporated into liposomes before and after sonication.....	118
Figure 4.18: Activity of IgG free and incorporated into liposomes before and after sonication.....	119

CHAPTER 5: DELIVERY OF LIPOSOMES GENERATED FROM ETHANOL-BASED PROLIPOSOMES VIA MEDICAL NEBULISERS

Figure 5.1: Nebulisation time of IgG solution and IgG liposomes before and after probe-sonication using Pari Turboboy (air-jet), Omron MicroAir (vibrating-mesh) and Polygreen (ultrasonic) nebulisers.....	127
Figure 5.2: Sputtering duration of IgG solution and IgG liposomes before and after probe-sonication using Pari (air-jet), Omron (vibrating-mesh) and the Polygreen (ultrasonic) nebulisers.....	128
Figure 5.3: Mass output for IgG solution and IgG liposomes before and after probe-sonication using; (a) Pari (air-jet), (b) Omron (vibrating-mesh) and (c) the Polygreen (ultrasonic) nebulisers.....	131
Figure 5.4: Output rate of IgG solution and IgG liposomes before or after sonication using; (a) Pari (air-jet), (b) Omron (vibrating-mesh) and (c) Polygreen (ultrasonic) nebulisers.....	132
Figure 5.5: Droplet size measured using the TOF and laser diffraction Spraytec for (a) IgG solution, (b) non-sonicated liposomes and (c) sonicated liposomes.....	135
Figure 5.6: SPAN of the droplets measured using the TOF and laser diffraction technology for (a) IgG solution, (b) non-sonicated liposomes and (c) sonicated liposomes.....	136
Figure 5.7: FPF from the different nebulisers using the TOF and laser diffraction technology for (a) IgG solution, (b) non-sonicated liposomes and (c) sonicated liposomes.....	139
Figure 5.8: FPF output from the different nebulisers using the TOF and laser diffraction technology for (a) IgG solution, (b) non-sonicated liposomes and (c) sonicated liposomes.....	140
Figure 5.9: Cryo-TEM images of liposomes (non-sonicated) following nebulisation via (a) Pari air-jet nebuliser, (b) Omron vibrating-mesh nebuliser and (c) Polygreen ultrasonic nebuliser.....	147
Figure 5.10: Cryo-TEM images of liposomes (sonicated) following nebulisation via (a) Pari air-jet nebuliser, (b) Omron vibrating-mesh nebuliser and (c) Polygreen ultrasonic nebuliser.....	148

Figure 5.11: Nebulisation of (A) IgG and IgG bound to liposomes ((B) non-sonicated and (C) sonicated), via Pari, Omron and Polygreen nebulisers, and its effect on the secondary structure of IgG.....	149
Figure 5.12: Nebulisation of IgG bound to liposomes ((A) non-sonicated and (B) sonicated) and (C) IgG solution, via Pari, Omron and Polygreen nebulisers, and its effect on the activity of IgG.....	150
Figure 5.13: Nebulisation of IgG and IgG bound to liposomes (non-sonicated and sonicated), via (A) Pari, (B) Omron and (C) Polygreen nebulisers, and its effect on the activity of IgG relative to before nebulisation.	151
Figure 5.14: FPF output% relative to the active IgG delivered, using the (A) TOF and (B) laser diffraction technologies for the, IgG solution, non-sonicated liposomes and sonicated liposomes.....	153

CHAPTER 6: DELIVERY OF LIPOSOMES VIA NASAL SPRAYS

Figure 6.1: Number of actuations required priming the nasal devices, number of full actuations generated and number of actuations in the tail-off phase for the different formulations in nasal devices: (A) MAD (B) nasal spray A (C) nasal spray B.	161
Figure 6.2: The emitted dose from the nasal devices for the different formulations.....	162
Figure 6.3: The time required per actuation for the different formulations through the nasal devices..	163
Figure 6.4: Time course frames (40 ms) of an evolving plume from nasal spray A showing the different phases of cloud spray development..	165
Figure 6.5: Time course frames (40 ms) of an evolving plume from nasal spray B showing the different phases of cloud spray development.	166
Figure 6.6: Time course frames (40 ms) of an evolving plume from the MAD showing the different phases of cloud spray development..	167
Figure 6.7: Images of the plumes and the spray patterns using the MAD for (A) the IgG solution (B) non-sonicated IgG liposomes and (C) sonicated IgG liposomes.....	172
Figure 6.8: Images of the plumes and the spray patterns using nasal spray A for (A) the IgG solution (B) non-sonicated IgG liposomes and (C) sonicated IgG liposomes.....	173
Figure 6.9: Images of the plumes and the spray patterns using nasal spray B for (A) the IgG solution (B) non-sonicated IgG liposomes and (C) sonicated IgG liposomes.....	174
Figure 6.10: Size and size distribution of (A) non-sonicated liposomes and (B) sonicated vesicles using different nasal devices.....	178
Figure 6.11: Cryo-TEM images of multilamellar liposomes (non-sonicated) following spraying via the (A) MAD, (B) nasal spray A and (C) nasal spray B.....	179

Figure 6.12: Cryo-TEM images of multilamellar liposomes (sonicated) following spraying via the (a) MAD, (b) nasal spray A and (c) nasal spray B.	180
Figure 6.13: Spraying of (A) IgG and IgG bound to liposomes ((B) non-sonicated and (C) sonicated), using a MAD and two nasal pump sprays A and B, and its effect on the secondary structure of IgG.....	181
Figure 6.14: Spraying of IgG and IgG bound to liposomes (non-sonicated or sonicated), using a MAD and two nasal pump sprays A and B, and its effect on the activity of IgG.	182
Figure 6.15: Spraying of IgG and IgG bound to liposomes (non-sonicated and sonicated), using a MAD and two nasal pump sprays A and B, and its effect on the activity of IgG relative to before nebulisation.....	183

LIST OF TABLES

CHAPTER 1: INTRODUCTION

Table 1.1: Entrapment efficiency of different drugs in alcohol-based proliposomes.	30
---	----

CHAPTER 3: CHARACTERISATION OF LIPOSOMES GENERATED FROM ETHANOL BASED PROLIPOSOMES

Table 3.1: Size, SPAN and zeta potential of liposomes before and after dilution..	69
Table 3.2: Effect of sample volume on size, SPAN and zeta potential of the generated liposomes.	72
Table 3.3: Comparison between liposomes with and without SS.	73
Table 3.4: Size, zeta potential and SS entrapment efficiency using liposome formulations having different cholesterol concentrations..	73
Table 3.5: Size, SPAN and zeta potential of liposomes having a range of OVA.	77
Table 3.6: Size, SPAN and zeta potential of liposomes incorporating SS or OVA..	84
Table 3.7: Size and size distribution of freshly prepared liposomes prepared with a range of chitosan concentrations.....	86

CHAPTER 5: DELIVERY OF LIPOSOMES GENERATED FROM ETHANOL-BASED PROLIPOSOMES VIA MEDICAL NEBULISERS

Table 5.1: Size and size distribution of non-sonicated liposomes before nebulisation, after nebulisation and what is remaining in the nebuliser reservoir. Measurements were carried out using laser diffraction or dynamic light scattering (DLS).....	142
Table 5.2: Size Size and size distribution of sonicated liposomes before nebulisation, after nebulisation and what is remaining in the nebuliser reservoir. Measurements were carried out using dynamic light scattering (DLS)..	143

CHAPTER 6: DELIVERY OF LIPOSOMES VIA NASAL SPRAYS

Table 6.1: The droplet size, SPAN and particle fraction < 10 µm for the different formulations using different nasal devices.....	169
Table 6.2: The (A) plume geometry and (B) spray pattern of the generated spray cloud.....	175

ACKNOWLEDGEMENTS

All praises and thanks be to Allah the Almighty for giving me the strength, patience and grace to reach the end of this remarkable period. It is also a great pleasure to convey my sincere thanks to the many people who have made this PhD journey possible.

My first debt of gratitude must go to my advisor Dr Abdelbary Elhissi. He patiently provided the vision, advice and encouragement necessary for me to pursue my doctoral program and complete my dissertation. I want to also convey my many thanks to my second supervisor Prof Antony D'Emanuelle for his continuous support. I cannot overstate my gratitude to UCLAN for funding my project. I am also immensely grateful to the technical and support staff at UCLAN for their continuous help.

Many thanks are due to several academics with whom I have had the good fortune of working with during my study. I am especially thankful to Prof. Waqar Ahmed, Dr. Sarah Dennison, Mr Ian Portman, Mr David McCarthy and Dr Michael Flynn.

I am also indebted to friends and colleagues. Especially to Mohamed Alhnan, Hisham Al-Obaidi, Sulaf Assi, Basel Barghouti, Bilal Qadoura, Adli abu-Fazaa, Khaled Bazzari, Naser Damis, Abdallah Yaghi, Alicia D'souza, Sufian Khawaldeh, Rakesh Tekade, Maha Nasr, Rami Basyouni, Ahmad Utaibi, Amanda Clark, Banu Abdalla, Kanar Hidayat, Iftikhar Khan, Nozad Hussein and Huner Omar.

Most of all, I wish to express my utmost gratitude to my beloved family. I would not have reached this far without my family's support and encouragement. They have always been there for me particularly: my love and wife-to-be Monika, my brother Tareq, my sister Beesan and brother in law Mohamed. Most of all, I wish to express my deep and sincere thanks to my parents Tawfiq and Nadia for their unflagging love, patience and support. To them all I dedicate this thesis.

LIST OF ABBREVIATIONS AND ACRONYMS

- APS** – Aerodynamic particle sizer
- BCA** – Bicinchoninic acid
- BDP** – Beclomethasone dipropionate
- BSA** – Bovine serum albumin
- CD** – Circular dichroism
- CDC** – Colloidal drug carrier
- CDER** – Center for drug evaluation and research
- CF** – Carboxyfluorescein
- CFC** – Chlorofluorocarbon
- CNS** – Central nervous system
- COPD** – Chronic obstructive pulmonary disease
- CsA** – Cyclosporine A
- CSF** – Cerebrospinal fluid
- DLPC** – Dilauroylphosphatidylcholine
- DLS** – Dynamic light scattering
- DMPC** – Dimyristoylphosphatidylcholine
- DPI** – Dry powder inhaler
- DPPC** – Dipalmitoylphosphatidylcholine
- DSD** – Droplet size distribution
- DSPC** – Distearoylphosphatidylcholine
- FDA** – Food and drug Administration
- FP** – Fluticasone propionate
- FPF** – Fine particle fraction
- G0-G25** – Generation 0-25
- HPLC** – High performance liquid chromatography
- Ig** – Immunoglobulin
- IVIG** – Intravenous immunoglobulin
- LDV** – Laser Doppler Velocimetry
- LEU** – Leuprorelin acetate
- LUV** – Large unilamellar vesicle
- MAD** – Mucosal atomisation device

MLV – Multilamellar vesicle

MMAD – Mass median aerodynamic diameter

NB – Nicotine base

NS – Nicotine salt

OLV – Oligolamellar vesicle

OVA – Ovalbumin

PC – Phosphatidylcholine

Pdi – Polydispersity index

PH – Propranolol hydrochloride

pMDI – Pressurized metered dose inhaler

PVP – Polyvinylpyrrolidone

SG – Soybeansterylglucoside

SPC – Soya phosphatidylcholine

SPAN – A unit-less term introduced by Malvern Instruments Ltd. to express the width of the distribution.

SS – Salbutamol sulfate

SUV – Small unilamellar vesicle

TBT– Tracheobronchial tree

TLC – Thin layer chromatography

TOF – Time-of-flight

TT – Tetanus toxoid

VMD – Volume median diameter

CHAPTER 1

INTRODUCTION

1.1 Drug delivery to the respiratory tract

The respiratory tract has been used as a route of drug administration for many decades. In addition to being the standard route for local therapeutic delivery, especially for treating chronic obstructive pulmonary disease (COPD) and asthma (which affects more than 300 million people in the world), it has also been proven to have immense potential in systemic drug delivery (Kleinstreuer *et al.*, 2008). Figure 1.1 illustrates the number of papers published since 1953 incorporating the keywords “respiratory tract delivery” (using the Web of Science citation manager). Moreover, the number of papers published on nasal delivery and pulmonary delivery alone were found to follow the same increasing trend, thus reflecting the great interest and potential of the respiratory route. Furthermore, both pulmonary and nasal delivery are amongst the top four positions in the drug delivery market, together with oral controlled release and parenteral delivery (Koch, 2003). The potential growth of those sectors is also extensive, as both nasal and pulmonary deliveries are showing promise in the delivery of proteins and peptides.

1.2 Pulmonary route

1.2.1 Historical background

The earliest recordings of inhalation therapy were in the Ebers papyrus from ancient Egypt, dating to 1554 BC (Smyth *et al.*, 2011), and for a long time now the smoke generated from burning compounds has been inhaled for therapy and enjoyment. The modern era of aerosol therapy and the first use of the word “inhaler” began in 1778 with the Mudge inhaler, devised by Dr. John Mudge. Later in the 18th century the first pressurized inhaler was invented by the French physician Sales Giro in 1858. Many other inhalers were also introduced in the late 19th and early 20th centuries.

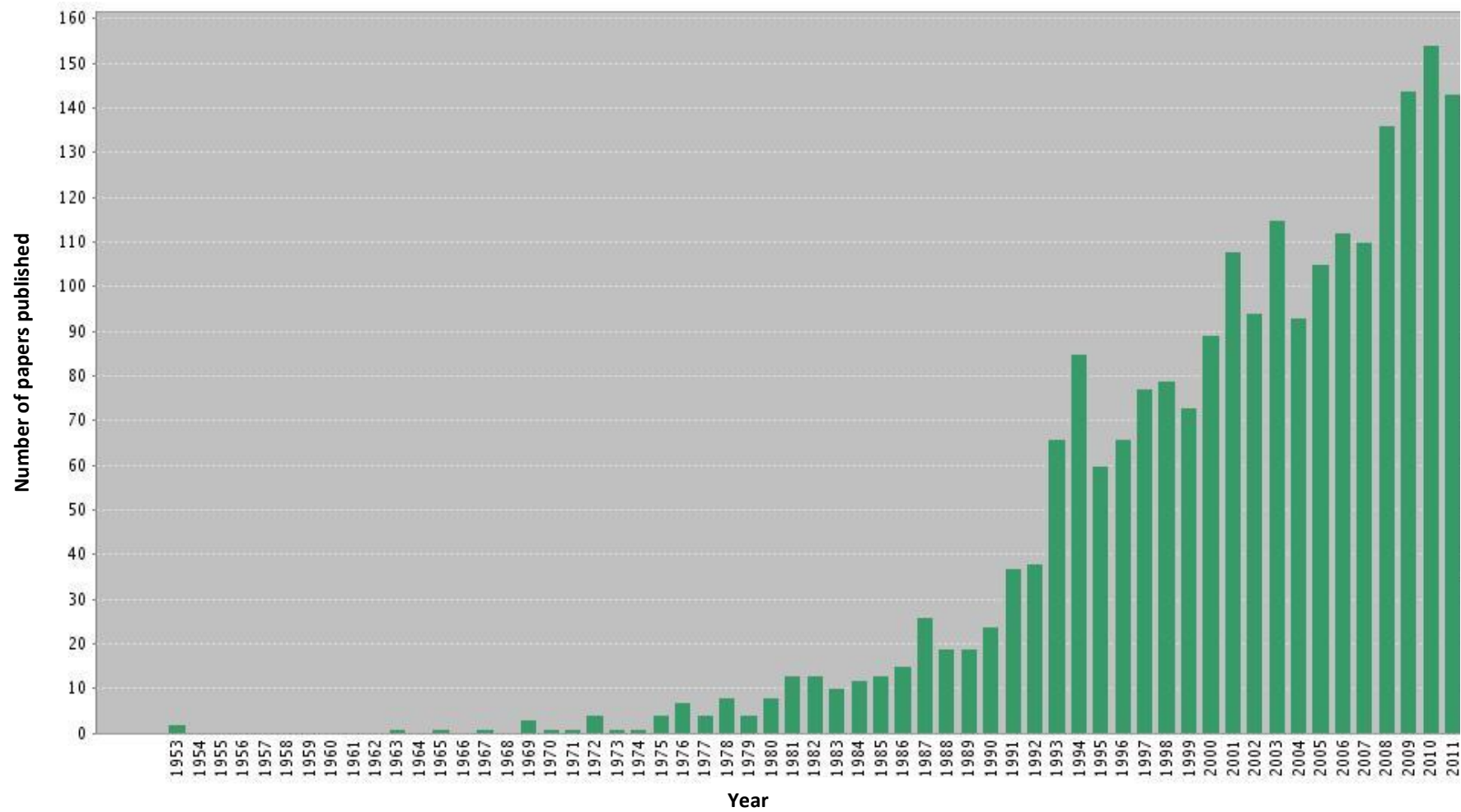


Figure 1.1: Papers published in the field of respiratory tract delivery since 1953. (informed via Web of Science citation manager)

A huge advancement in aerosol technology was in the 1950s with the development of the pressurized metered dose inhalers Medihaler® by Charlie Thiel and colleagues, which with minor modifications continues to be the most popular form of aerosol delivery nowadays (Rubin, 2010; Smyth *et al.*, 2011).

Throughout the last century, the world has witnessed increased interest in the development and use of inhalation therapy for both local and systemic diseases. Figure 1.2 illustrates images of the Mudge inhaler, the Sales Giro pressurized inhaler and the Medihaler® advert sheet.



Figure 1.2: Images of (a) the Mudge inhaler (b) the Sales Giro pressurized inhaler and (c) Medihaler® advert sheet. (Taken from Smyth *et al.*, 2011)

1.2.2 Anatomy and physiology of the respiratory system

The respiratory system can be divided anatomically into the upper respiratory tract and the lower respiratory tract. The upper respiratory tract includes structures found in the head and neck and comprises the nose, pharynx and larynx. The lower respiratory tract comprises structures found in the thorax or chest regions, including the trachea, bronchi and lungs. The lungs comprise bronchioles, alveolar ducts and alveoli (Jindal *et al.*, 2011).

Functionally, the respiratory system can be divided into two zones: the conducting zone and the respiratory zone. The conducting zone, whereby air is conducted in a continuous passageway to the respiratory zone, includes the nose, pharynx, larynx, trachea, bronchi and bronchioles. The respiratory zone (the gas exchange region) comprises structures found in the deep lung, and includes respiratory bronchioles, alveolar ducts and alveoli (Jindal *et al.*, 2011). Figure 1.3 shows schematic representation of the respiratory system in humans.

The function of the nose is to filter, warm and humidify the air entering the body. Following nasal or oral inhalation, the air and inhaled particles pass through the pharynx. The lowest region of the pharynx divides into the oesophagus and larynx through which air passes to the trachea. The trachea comprises what is recognised as generation 0 (G0) of the tracheobronchial tree (TBT), and every subsequent branching leads to a new generation. The trachea further divides into the left and right bronchi, comprising the (G1) of the TBT. Like the trachea, the bronchi are also supported by the C shaped cartilage rings, however further down the respiratory tract those cartilages become smaller and smooth muscles become more abundant. The right bronchus further branches into three lobar bronchi, whilst the left branches into two lobar bronchi. These lobar bronchi further branch into segmental bronchi. These lobar bronchi and segmental bronchi comprise (G2) and (G3), respectively. The segmental bronchi lead to bronchioles and ultimately to terminal bronchioles (G16), where the conducting region of the TBT ends and the respiratory region starts, comprising the respiratory bronchioles (G17) which lead to the alveolar sacs (G23), see Figure 1.3 c (Bisgaard *et al.*, 2001; Abdelrahim, 2009).

1.2.3 Advantages and limitations of pulmonary delivery

The lung is the most relevant site for treating respiratory tract disorders and the delivery of mucolytic and antiasthma drugs. Pulmonary delivery of drugs for local disorders provides many advantages over other routes of delivery, such as improved bioavailability of drugs, reduction of drug dose, lower enzymatic drug

degradation in the lung, avoidance of first pass hepatic effect and enhanced patient compliance (because pulmonary delivery is a needle-free). Moreover, the high vascularity of the lungs and its large surface area permit rapid drug absorption into the systemic circulation when systemic therapeutic effect is needed, as in case of the delivery of proteins, vaccines and anticancer drugs (Farr *et al.*, 1987; Adjei and Gupta, 1994; Torchilin, 2006).

Despite the many advantages of pulmonary delivery, the complicated morphology of the lung makes the delivery of the whole dose into the deep lung a difficult task. Furthermore, the mucociliary clearance in the mucosal surfaces of the respiratory tract and the presence of some enzymatic activity causes significant reduction in the lower airway deposition (Adjei and Gupta, 1994).

1.2.4 Devices for pulmonary delivery

A variety of devices can be used for the generation of aerosols for medical inhalation, namely pressurized metered dose inhalers, dry powder inhalers, nebulisers and soft mist inhalers.

1.2.4.1 Pressurized metered dose inhalers (pMDIs)

Since the 1950s, pMDIs have been recognised as the most popular delivery devices for treatment of lung diseases (Rathbone *et al.*, 2003; Smyth *et al.*, 2011). A pMDI consists of a pressurized canister containing the therapeutic material, a propellant and other excipients such as preservatives, surfactants and dispersing agents (Hess *et al.*, 2012) (Figure 1.4).

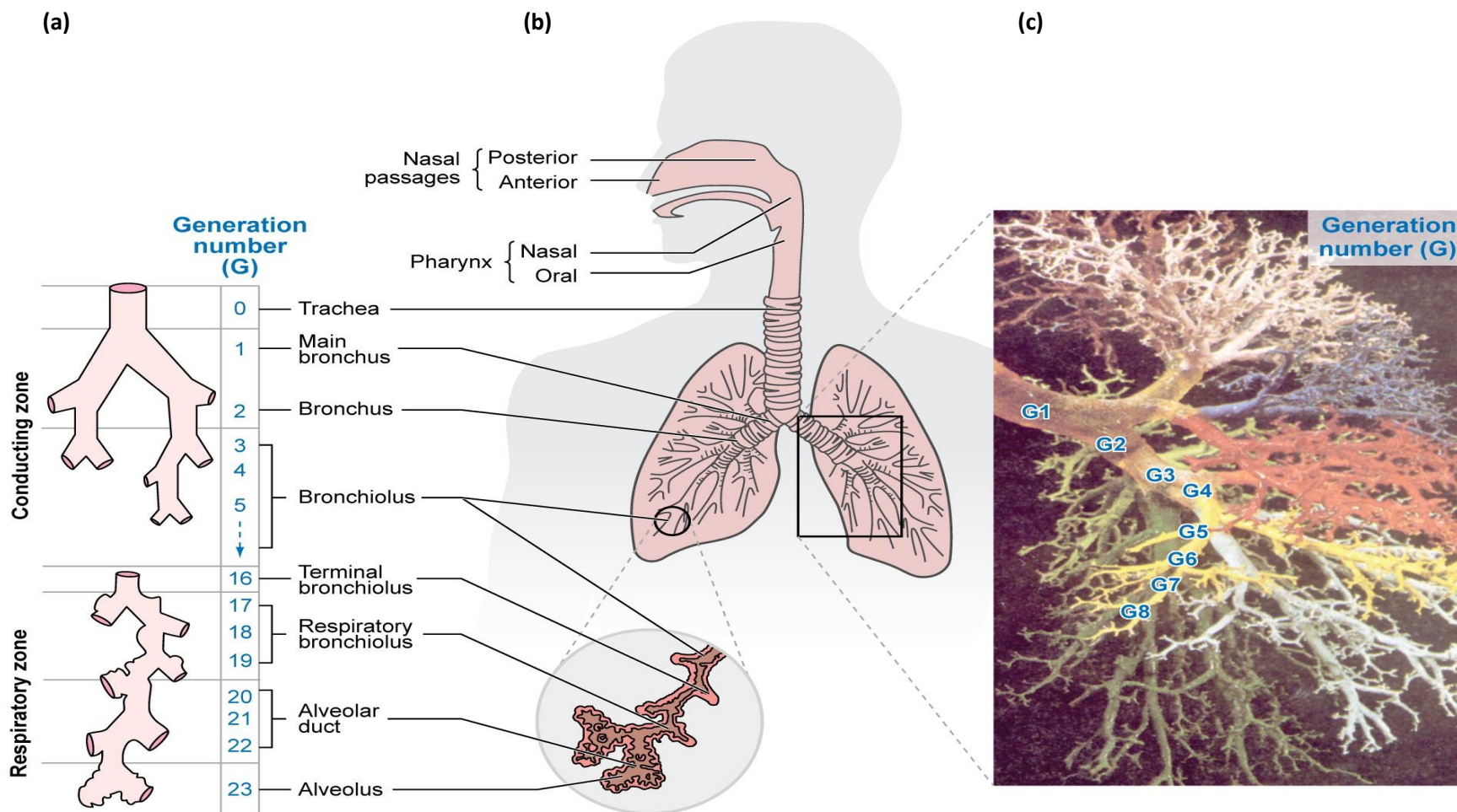


Figure 1.3: Schematic representations of the human respiratory tract. (Adapted from Kleinstreuer *et al.*, 2008)

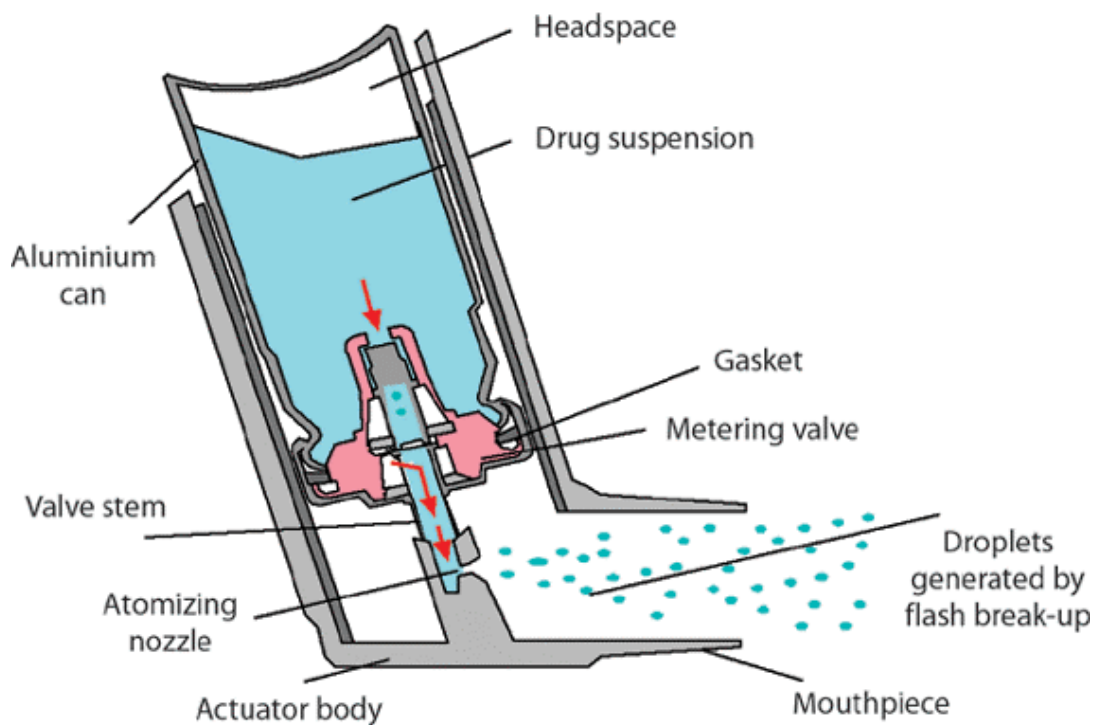


Figure 1.4: Schematic representation of a pMDI device. (Adapted from Pritchard, 2005)

Typically, 200 high pressure actuations (e.g. >10 atm) can be generated and inhaled via pMDIs, and by each puff a drug dose of 0.02-5 mg in metered volumes of 25–100 μL can be delivered (Kleinstreuer *et al.*, 2008).

Propellants in pMDIs are liquefied compressed gases that are nontoxic, non-flammable, stable and compatible with the drug, having a boiling point between -15 to -30°C . The first propellant systems introduced were chlorofluorocarbons (CFCs) (Noakes, 2002). Recently, however, because of the damaging effect CFCs have on the ozone layer, their use has been banned (Molina and Rowland, 1974), and the greenhouse gases tetrafluoroethane (HFA-134a) and heptafluoropropane (HFA-227) were found to be suitable replacements, and are now used in the market (Newman, 2005).

pMDIs have the advantage of protecting their contents from bacteria and atmospheric conditions, being highly portable and relatively cheap compared to other inhalation devices (Abdelrahim, 2009). However, a major limitation of a pMDI is the patient's inability to use it correctly. In a study by Saunders (1965),

25 out of 46 patients were found to use the pMDI incorrectly. This was also found by Shim and Williams (1980), who reported that only 14 patients from a total of 30 used their pMDIs correctly.

Another problem with the use of pMDIs is the difficulty of determining the remaining dose inside a pMDI. In a study by Rubin and Durotoye (2004), 74% of the 50 patients questioned did not know how many actuations remained in their pMDI device, hence the method of using the device adopted by all patients was to use it until they no longer heard the actuation of the medication.

1.2.4.2 Dry powder inhalers (DPIs)

DPIs first appeared in the market in the late 1960s with the introduction of the Spinhaler® by Fisons. GlaxoSmithKline (GSK) also introduced the Rotahaler® and the Diskhaler® in the late 1970s and early 1980s. In 1988 Astra Zeneca developed the first multidose gravity feed DPI, the Turbuhaler® (Crompton, 2004).

DPIs consist of the powder container, the metering system, the disintegration aid and the mouthpiece (Abdelrahim, 2009). The powders for inhalation in DPIs are usually micronized drug particles loaded onto inert carrier particles to enhance the flow properties of the powders (Maggi *et al.*, 1999).

DPI devices are either single-dose or multi-dose inhalers. The multi-dose inhalers can be further divided into multi-unit dose inhalers, in which several single dose units are available as individual capsules or multi-strip packages; and multi-dose reservoir inhalers, in which a bulk supply of dose is preloaded into the device (Chrystyn, 2007).

Minimal coordination is necessary on the part of patients as DPI devices are intrinsically breath activated. Moreover, they are propellant-free, and may achieve higher pulmonary deposition than pMDIs (Crompton, 2004; Rubin, 2010).

However, DPI devices have limitations, since moderate to high inspiratory flow by the patient is required to inhale the powder, thus it is unsuitable for young children and patients with compromised lung functions (Kleinstreuer *et al.*, 2008). Moreover, DPIs are sensitive to humidity, and the exhaled breath of patients might cause humidification of the powders in the inhaler, leading to reduced fractions of drug delivered upon inhalation (Maggi *et al.*, 1999).

1.2.4.3 Nebulisers

Nebulisers are devices that transform solutions or suspensions into an aerosol that is suitable for inhalation. Unlike pMDIs and DPIs, they are capable of delivering relatively large volumes of propellant-free liquid formulations. Nebulisers can also be employed to deliver aerosols to patients who have difficulties in using DPIs and pMDIs, such as children and old people, where the aerosolised drug can be inhaled during normal tidal breathing using a facemask or mouthpiece (McCallion *et al.*, 1996a). Based on the mechanism of atomisation, medical nebulisers can be divided into three types; air-jet, ultrasonic, and vibrating-mesh nebulisers.

(1) Air-jet nebulisers

Air-Jet nebulisers, also simply called jet nebulisers, have been used for many years to deliver aerosols to the respiratory tract. The use of jet nebulisers can be traced back to the early twentieth century. The 1930s witnessed the introduction of a compressor nebuliser in Germany (the Pneumostat), and the introduction of glass-bulb nebulisers such as the Parke-Davis Glaseptic, followed by the introduction of plastic-bulb nebulisers (i.e. AsthmaNefrin) in the 1940s (Anderson, 2005; Smyth *et al.*, 2011). These old-fashioned nebulisers generated aerosols of wide particle size distribution and much of their output

was non-respirable (Muers, 1997), necessitating the development of new generations of air-jet nebulisers.

Jet nebulisers use compressed gas to generate aerosols (Mercer *et al.*, 1968). A jet of high velocity gas is passed through a Venturi nozzle (with a diameter of about 0.3-0.7 mm), creating an area of negative pressure, resulting in pulling the liquid from the nebuliser reservoir via the “Bernoulli effect” (McCallion *et al.*, 1996a). The liquid is drawn into the airstream as fine ligaments, which then collapse into primary aerosol droplets under the effect of surface tension (O’Callaghan and Barry, 1997). These primary droplets usually have a very large size (15-500 μm) (Nerbrink *et al.*, 1994). Due to the baffling system inside the nebuliser, only a proportion of the droplets leave the nebuliser and enter the airstream as secondary inhalable aerosols (Dennis *et al.*, 1990), while the non-respirable portion of the droplets (primary aerosol) are recycled into the reservoir for further atomisation (Figure 1.5) (O’Callaghan and Barry, 1997). This can lead to solvent evaporation, resulting in concentration of the solutes in the reservoir (Ferron *et al.*, 1976), and a drop in the temperature of the nebuliser solution by 10-15°C (Clay *et al.*, 1983; Cockcroft *et al.*, 1989).

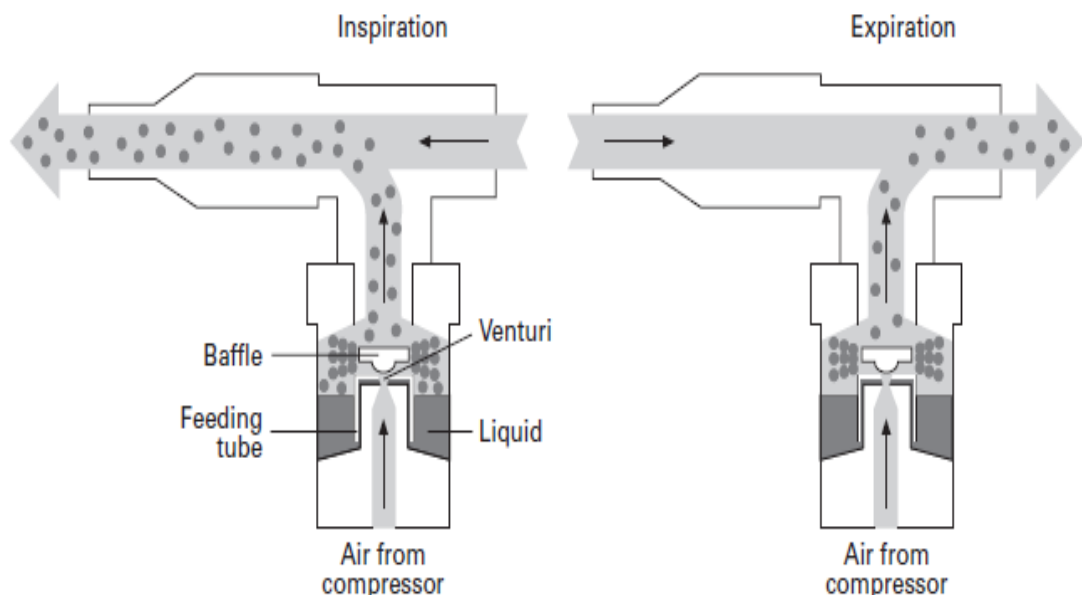


Figure 1.5: The design of a conventional air-jet nebuliser and the movement of the droplets inside the nebuliser following inspiration and expiration. (Taken from O’Callaghan and Barry, 1997)

The design and operating parameters of jet-nebulisers are the main factors that affect the aerosol performance, including the output and droplet size (Loffert *et al.*, 1994).

One major limitation for the use of the conventional air-jet nebuliser is the very large amount of aerosols wasted during expiration (Figure 1.5). Several nebuliser designs have been introduced to resolve this problem (Hess, 2000), including the use of reservoir bags (e.g. Circulaire, Westmed, USA), open vent nebulisers (e.g. Sidestream, Medic-Aid, UK), breath-enhanced (e.g. Pari LC Plus, Pari GmbH, Germany) or breath-actuated nebulisers (e.g. AeroEclipse nebuliser, Monaghan Medical Corporation, USA) (Rau *et al.*, 2004).

(2) Ultrasonic nebulisers

The development of ultrasonic nebulisers began in the late 1950s (Smyth *et al.*, 2011). These nebulisers utilise a high frequency vibrating piezoelectric crystal transducer (e.g. quartz), which produces high frequency sound waves (1-2.5 MHz) to atomize the liquid into aerosols (Flament *et al.*, 1999).

Two theories have been proposed for aerosol generation in ultrasonic nebulisers. At low frequencies, cavitation is speculated to be the main mechanism leading to droplet formation. On the other hand, at high frequencies the formation of capillary waves is thought to occur (Figure 1.6) (Taylor and McCallion, 1997; Barreras *et al.*, 2002). Moreover, it has also been suggested that both mechanisms contribute to droplet formation, whereby cavitation bubbles are postulated to initiate and drive capillary waves (Boguslaskii and Eknadiosyants, 1969; Taylor and McCallion, 1997).

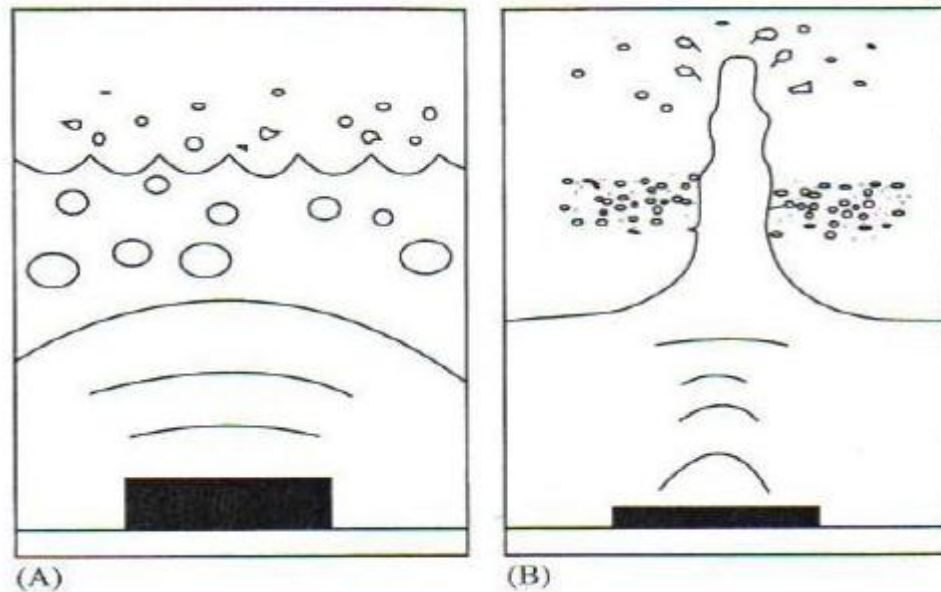


Figure 1.6: Proposed mechanisms for aerosol generation in ultrasonic nebulisers: (A) droplet formation via cavitation theory; (B) droplet formation via capillary wave theory. (Taken from Taylor and McCallion, 2002)

Like air-jet nebulisers, ultrasonic nebulisers include baffles in their design, therefore large droplets may be recycled to the reservoir whilst smaller droplets (secondary aerosols) are released for inhalation (Elhissi *et al.*, 2011b). Moreover, contrary to air-jet nebulisers, ultrasonic nebulisers heat the medical fluid, hence increasing its temperature (Taylor and Hoare, 1993). This can be a major drawback when thermo-labile drugs or proteins are used.

(2) Vibrating-mesh nebulisers

Vibrating-mesh nebulisers, also called perforated membrane nebulisers, employ vibrating-mesh plates with multiple micro-sized apertures to generate the aerosol. Several manufacturers have developed different devices that utilise this technology. Based on the mechanism of operation, vibrating-mesh devices can be divided into passively and actively vibrating-mesh nebulisers (Newman and Gee-Turner, 2005; Elhissi *et al.*, 2011b).

Passively vibrating-mesh devices (e.g. Omron MicroAir NE-U22 nebuliser) employ a vibrating piezoelectric crystal (e.g. quartz) attached to a transducer horn. In front of this there is a perforated plate consisting of around 6000 tapered holes, each of $3\mu\text{m}$ in diameter. When an electrical current is applied, the piezoelectric crystal vibrates at high frequency which is then transmitted to the transducer horn. The transmitted vibrations induce passive upward and downward vibrations in the perforated plate, which causes the extrusion of the fluid through the holes and generation of the aerosol (Figure 1.7) (Dhand, 2003).

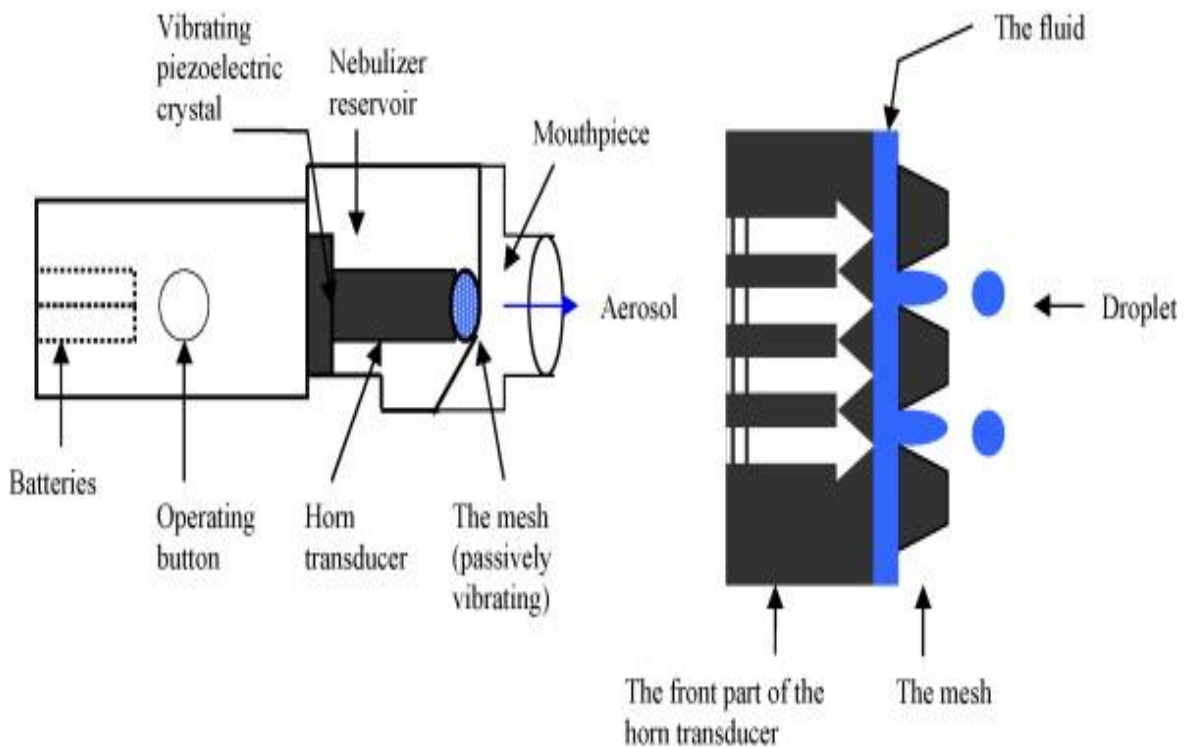


Figure 1.7: Schematic representation of a passively vibrating-mesh nebuliser showing the generation of the aerosol from the mesh plate. (Adapted from Ghazanfari et al., 2007)

Actively vibrating nebulisers (e.g. Aeroneb Pro nebuliser) consist of a vibrational element and around 1000 electroformed dome-shaped apertures. When an electrical current is supplied, the vibrational element expands and contracts, resulting in an upward and downward movement of the plate, causing a “micropump” effect that extrudes the fluid through the holes to generate slow moving aerosols (Figure 1.8) (Dhand, 2003).

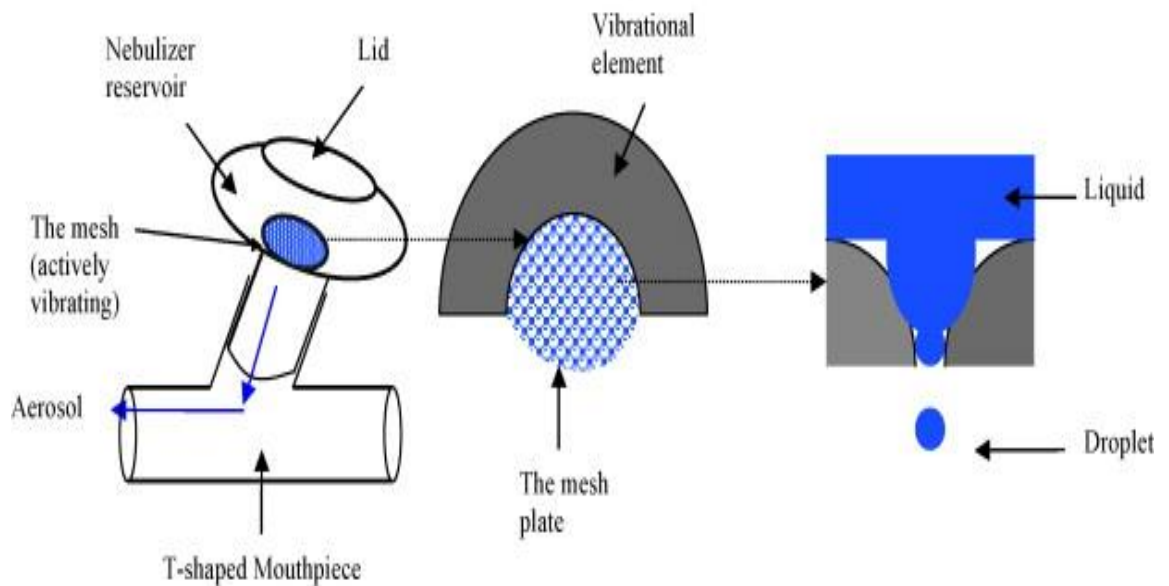


Figure 1.8: Schematic representation of an actively vibrating-mesh nebuliser showing the generation of the aerosol from the mesh plate. (Adapted from Ghazanfari et al., 2007)

1.3 Nasal delivery

1.3.1 Historical background

Since the past decade, the application of the nose as a route for drug delivery has been an area of great curiosity and the world market has noticed a boost in the number of drugs marketed as nasal formulations (Pires *et al.*, 2009; Devillier *et al.*, 2010; Wen, 2011). The nasal route became a popular route for the administration of tobacco from the 17th century in the form of snuff, and it remains a common route for the administration of drugs of abuse, notably cocaine (Davis, 1999a).

With the advancement in drug delivery and discovery, nasal delivery is now recognised as a very promising route for the delivery of therapeutic compounds, for both systemic and local effects (Ugwoke *et al.*, 2005).

1.3.2 Anatomy and physiology of the nose

The nose is the primary entrance to the respiratory tract and also contains the region that is essential for the sense of smell (olfactory region). The nostrils are external openings of the nose and they open at the back into the nasopharynx and lead to the trachea and oesophagus (Washington *et al.*, 2001).

The nasal cavity is an irregularly-shaped chamber approximately 7.5 cm long and 5 cm high in the front of the head (Ghosh and Jasti, 2005). The nasal region in man has a length of 60 mm, a volume of 20 ml (Aulton, 2007) and a surface area of 180 cm² (Ghosh and Jasti, 2005). The nose is subdivided into the right and left halves by a cartilaginous wall called the midline septum. Each half consists of three regions. Firstly, the vestibule, which comprises the outermost part of the nose and runs for about 15 mm from the nostril to the nasal valve, has an area of 0.6 cm². Secondly, the olfactory region, which occupies 10% of the total nasal area, is situated in the roof of the nasal cavity. The third region of the nasal cavity is the respiratory region (Mygind and Dahl, 1998). The respiratory region consists of three folds or indentations known as the inferior, the middle and the superior turbinates which divide the air spaces into thin slits and are the reason for the relatively large surface area of the nasal cavity (Figure 1.9) (Costantino *et al.*, 2007).

Although the nose is the organ of smell, only a small region is involved in this sense and the rest of the nasal cavity is involved in respiration (Aulton, 2007). Inside the nose, the inspired air of temperatures between -20 and +55 °C can be brought to within 10°C above or below the body temperature (Washington *et al.*, 2001).

1.3.3 Advantages of nasal drug delivery

The abundantly supplied vascular nature of nasal mucosa and its high permeability owing to its thin porous epithelium makes the nasal route an

attractive option for macromolecular drug delivery (Ghosh and Jasti, 2005). In addition, the availability of large surface area for drug absorption helps in offering a rapid onset of therapeutic effect (Costantino *et al.*, 2007).

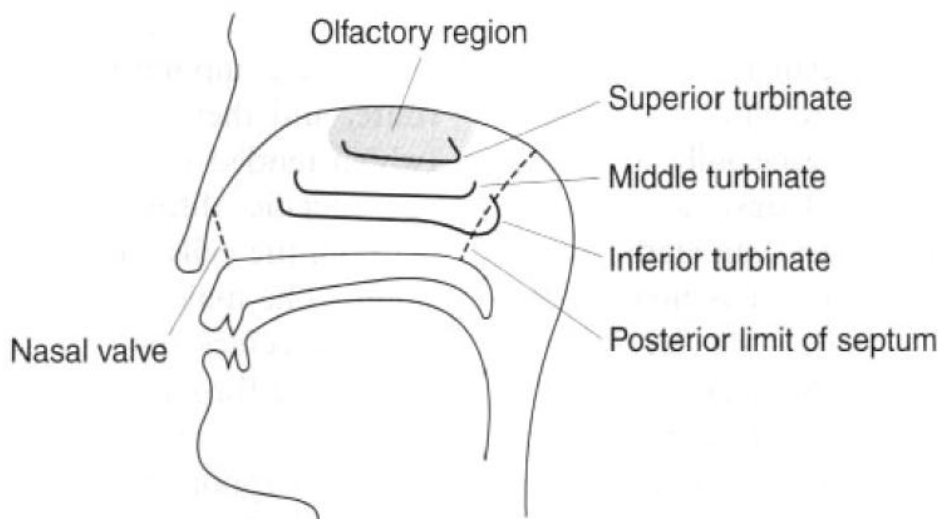


Figure 1.9: Cross-Section of nasal cavity. (Adapted from Costantino *et al.*, 2007)

Another advantage of the nasal route is that substances via this route are transported directly to the systemic circulation, avoiding the effect of hepatic first pass or gut wall metabolism (Chien *et al.*, 1989).

Moreover, the lower enzymatic activity in the nasal cavity and the fact that enzyme inhibitors are more effective in this region compared to the gastrointestinal tract could increase the bioavailability of therapeutic materials (Ugwoke *et al.*, 2005). In addition, unlike the lung, which is a very difficult organ for medication to access, regardless whether one is using solution or a powder formulation, it is easy to deliver the whole dose to the nasal cavity (Davis, 1999a). Another unique feature of nasal delivery is that drugs can be absorbed directly into the central nervous system (CNS) via its olfactory epithelium and/or the trigeminal nerves (Hussain, 1998; Mistry *et al.*, 2009). In terms of self-medication, nasal delivery has not only proven to be cost-effective but also

attractive in relation to its capability of enhancing patient compliance and reducing the risk of overdose (Quraishi *et al.*, 1997; Ugwoke *et al.*, 2005).

1.3.4 Limitations of nasal delivery

In spite of its advantages, there are some limitations associated with nasal delivery, such as possible local tissue irritation (Dondeti *et al.*, 1996), rapid drug clearance (Soane *et al.*, 1999; Illum, 2003), low permeability of larger macromolecules (McMartin *et al.*, 1987), and possible degradation of proteins and peptides by the endopeptidases present in the nasal cavity (Morimoto *et al.*, 1991; Arora *et al.*, 2002).

1.3.5 Applications of nasal delivery

For many years, drugs have been administered intranasally for both local and systemic effects, and the world market has shown an increasing number of drugs being marketed as nasal formulations (Kublik and Vidgren, 1998).

Its promising areas of application include:

- Local delivery
- Systemic delivery
- Drug delivery to CNS
- Vaccine delivery

The intranasal route could be used for local delivery of drugs directly to the nose, thereby enabling the use of lower drug doses and minimizing systemic adverse effects (Schata *et al.*, 1991; Salib and Howarth, 2003; Stanaland, 2004; Norris and Rowe-Jones, 2006; Wallace *et al.*, 2008). Prominent examples of intranasal formulations for local delivery include nasal decongestants, antimicrobial drugs, antihistamines and corticosteroids.

Due to the rapid onset of action offered by intranasal delivery, products used in emergency or those needed to produce immediate effects may be given

intranasally. For instance, in acute pain, panic attacks, sleep induction, erectile dysfunction, nausea, heart attacks and Parkinson's disease, drugs would be highly advantageous if delivered via this route. In addition, the ease of application of nasal sprays makes long-term treatments relatively convenient (Gardner et al., 1993; Kaiser *et al.*, 1995; Aulton, 2007; Costantino *et al.*, 2007; Rozgony *et al.*, 2010).

Another application of great interest is CNS targeting via the nasal route. Drugs delivered intranasally might be transported along the olfactory epithelium and/or the trigeminal nerves to yield significant concentrations in the cerebrospinal fluid (CSF) (Misra *et al.*, 2003). Born *et al.*, (2002) found evidence of direct nose-to-brain transport, and access to the CSF of three neuropeptides, bypassing the bloodstream, has been reported in human trials.

1.3.6 Nasal delivery devices

The selection of suitable delivery system depends upon the physicochemical properties of the drug used, the proposed indication, the basic compliance of the patients and marketing preferences (Kublik and Vidgren, 1998).

Nasal formulations can be applied via a variety of dosage forms (e.g. solutions, emulsions, suspensions, powders and gels). Liquid preparations mainly water-based formulations are the most widely used for intranasal delivery. One major advantage of aqueous-based formulations is the humidification effect they offer, enabling the drying of the mucous membrane that is associated with many allergic and chronic diseases to be ameliorated (Kublik and Vidgren, 1998). On the other hand, water-soluble formulations suffer from a major drawback, which is the microbiological instability and the resultant need for preservatives in their formulation. Many preservatives may induce a damaging effect to the mucociliary function (Joki *et al.*, 1996) and their long-term use might lead to rhinitis medicamentosa (Graf *et al.*, 1995).

A variety of liquid formulations for intranasal delivery are available nowadays, including mechanical pump sprays, drops, propellant-driven metered dose

inhalers, squeeze bottles and compressed air nebulisers (Kublik and Vidgren, 1998). Amongst those formulations, metered dose sprays and nasal drops are the most common. Most of the pharmaceutical nasal preparations on the market are delivered by metered dose pump sprays. Solutions, emulsions and suspensions can all be formulated into nasal sprays. Moreover, due to the availability of actuators and metered dose pumps, they can deliver a defined dose (25 μ l and 200 μ l) with high accuracy (Kushwaha *et al.*, 2011).

Nasal drops, as alternatives to nasal sprays, are simple and convenient, easy to manufacture and cost-effective. However, these systems lack dose precision (Kushwaha *et al.*, 2011), and the bioavailability of drugs following delivery via nasal drop devices has been reported to be lower than that of drugs administered via nasal sprays (Harris *et al.*, 1986; Daley-Yates and Baker, 2001). Daley-Yates and Baker (2001) compared the systemic bioavailability of fluticasone propionate (FP) aqueous nasal spray and a new nasal drop formulation. Eight-time lower bioavailability of FP following nasal drops compared with the nasal spray system was reported. Similar findings were reported by Harris *et al.*, (1986), who found a two- to three-fold increase in the bioavailability of desmopressin after administration via nasal sprays compared to nasal drops.

Nasal powder dosage forms, which offers more stability to formulations and abnegates the need for preservatives, can be delivered via multi-dose inhalers or insufflators in nasal delivery systems. However, the general nasal irritation sometimes caused by powders comprises a drawback to the nasal administration of powdered formulations (Aurora, 2002).

Amongst the other systems that gained attention lately with the recent development of precise dosing devices are nasal gels. Viscous thickened solutions or suspensions are administered as nasal gel systems, producing less post-administration nasal drip, less aroma impact and less irritability due to soothing excipients (Aurora, 2002). However, nasal gel systems tend to coagulate in specific areas, not spreading in the nasal cavity without special (e.g. clinical) application hence, occupying a narrow distribution area that impairs effective medication administration (Kublik and Vidgren, 1998).

Particles can be deposited into various regions of the respiratory tract by a variety of mechanisms. There are three main mechanisms by which significant particle deposition can occur within the respiratory tract: inertial impaction, sedimentation and brownian diffusion. Other less important mechanisms contributing to deposition within the respiratory tract also exist, including electrostatic precipitation and interception (Smola *et al.*, 2008; Phalen and Phalen, 2011). A key factor affecting the deposition in the respiratory tract is the size of the inhaled particles (Heyder *et al.*, 1975; 1982; 1986).

1.4 Liposomes

1.4.1 Historical background

During the past few decades, colloidal carrier systems (e.g. liposomes) have gained considerable attention in drug delivery and targeting (Crommelin and Sindelar, 1997). Recent studies have shown that more than 95% of new therapeutic molecules have poor pharmacokinetics (Brayden, 2003). Appropriate formulation technologies are believed to solve this problem. Among these technologies, colloidal drug carriers (CDCs) have gained most attention, as they may modify the *in vivo* distribution of the associated materials and improve their therapeutic index by increasing their efficacy or reducing toxicity (Nastruzzi, 2005). Liposomes have attracted the most interest among CDCs (Crommelin and Sindelar, 1997).

Liposomes were first described by A.D Bangham in 1961, who, in his investigation of the role of phospholipids on blood and blood clots, reported that phospholipids can form spherical vesicles in aqueous dispersions (Bangham *et al.*, 1965).

1.4.2 Molecular composition of liposomes

Liposomes mainly are mainly consisted of phospholipids, which are amphipathic molecules consisting of hydrophilic headgroups attached to long non-polar

hydrophobic tails. The hydrophilic head typically consists of a phosphate group, whereas the hydrophobic tail is made of two long hydrocarbon chains (Marjan and Allen, 1996). Phospholipids with different hydrophilic headgroups can be functionalised for conjugation, whilst hydrophobic tail regions of different chain lengths and saturation can be used to modify the properties of liposomes (Edwards and Baeumner, 2006). The most common phospholipids are phosphatidylcholines (PCs), which are amphipathic molecules comprising a glycerol bridge that links a phosphocholine hydrophilic polar head group with a pair of hydrophobic acyl (hydrocarbon) chains (Figure 1.10) (New, 1990; Hernández and Scholz, 2008).

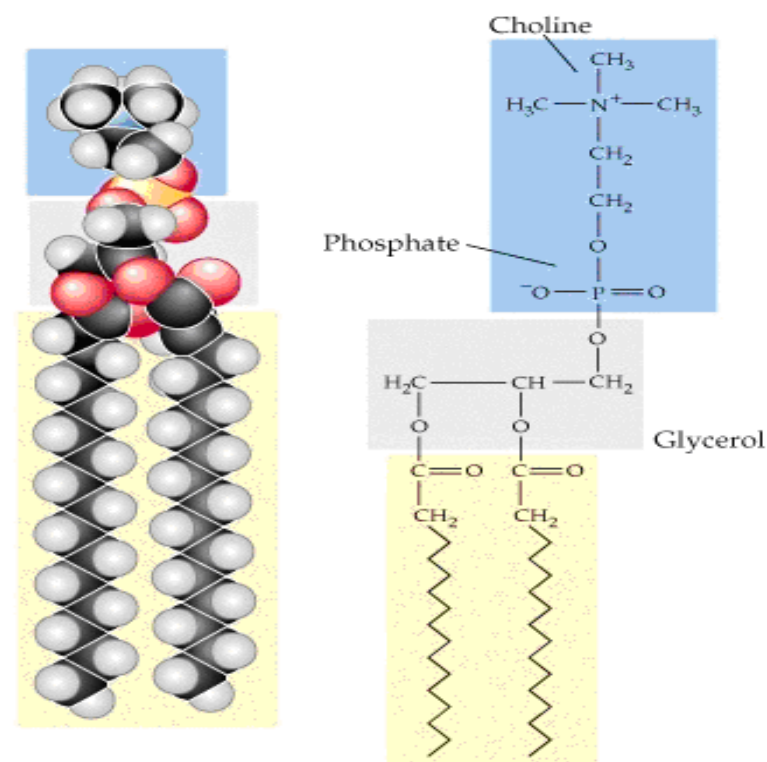


Figure 1.10: The structure of a PC molecule. (Adapted from Chasin, 2010)

PC molecules are insoluble in water; hence they align themselves closely in planar bilayer sheets in aqueous media to minimise the unfavourable interactions between the bulk aqueous phase and the long fatty acid chains. Those interactions are eliminated when the sheets fold themselves to form sealed vesicles (Figure 1.11) (New, 1990).

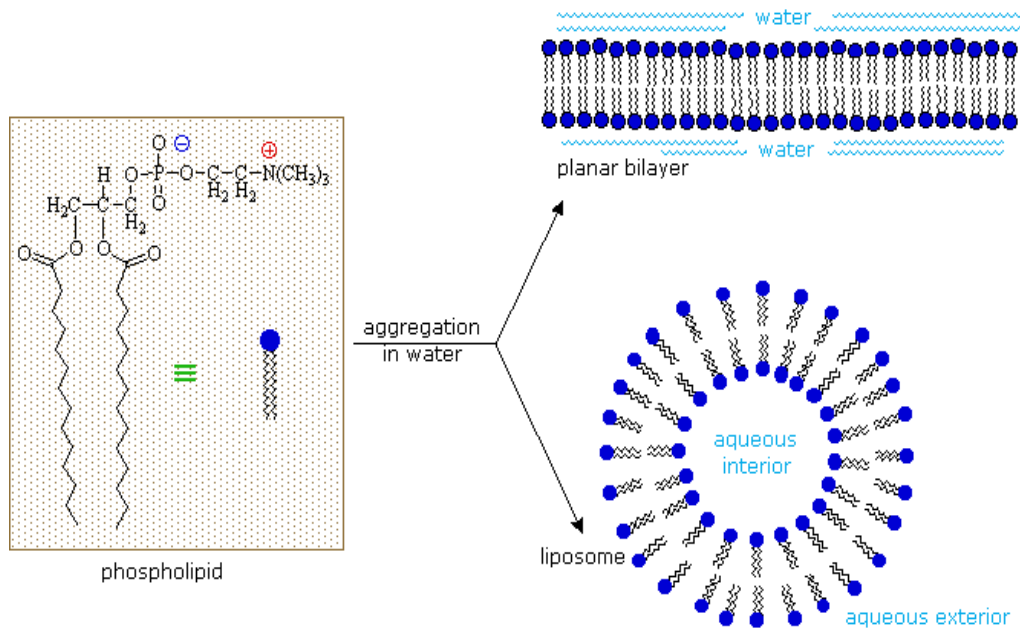


Figure 1.11: Schematic representation of the assembly of phospholipids in liposomes. (Adapted from Reusch, 1999)

Sterols are also important components of most biological membranes, and their incorporation into liposome bilayers can bring about major changes in the properties of the membranes. Manipulating the fluidity and improving the stability of the membranes may reduce the permeability of water-soluble molecules across the membranes (Vemuri and Rhodes, 1995). Cholesterol (Figure 1.12) is the predominant sterol in mammals (Law, 2000).

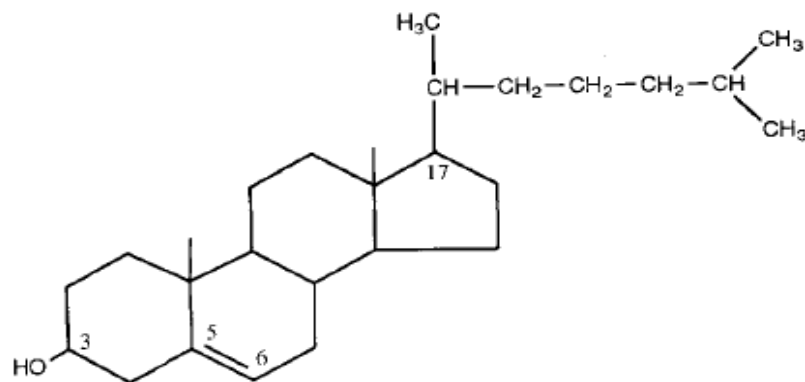


Figure 1.12: Chemical structure of cholesterol. (Adapted From Vemuri and Rhodes, 1995)

1.4.3 Classification of liposomes

There are various classes of liposomes. Liposomes are classified either by the number of bilayers present, their size or the method of their preparation (Vemuri and Rhodes, 1995).

When liposomes are described based on the number of bilayers, they are either unilamellar vesicles (ULVs), multilamellar vesicles (MLVs) or oligolamellar vesicles (OLVs). While MLVs have five to twenty lipid bilayers, OLVs have two to five bilayers. Another type of vesicles that could form is the multivesicular vesicles (MVs). A MVV is made up of a large vesicle incorporating smaller vesicles (Figure 1.13) (Rongen *et al.*, 1997; Segata *et al.*, 2006).

Based on their size, liposomes range from small unilamellar vesicles (SUV), with diameters generally below 100 nm, to OLVs, MLVs and large unilamellar vesicles (LUV), having sizes ranging from 100 nm to several micrometres (Rongen *et al.*, 1997; Kirby and Gregoriadis, 1999). Figure 1.13 illustrates the types of vesicles according to their lamellarity.

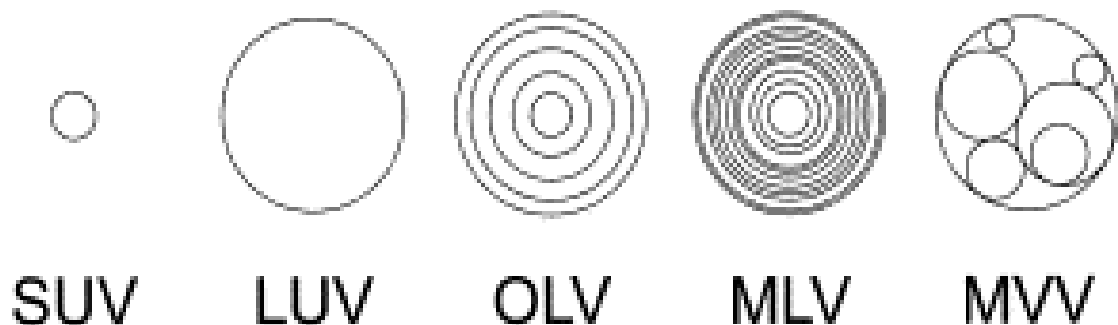


Figure 1.13: Schematic representations of types of liposomes. (Adapted from Rongen *et al.*, 1997)

1.4.4 Advantages and drawbacks of liposomal delivery

Extensive investigations on liposomal carriers have been observed recently and are found to be increasing by time due to promises of advances in that field. Figure 1.14 illustrates the number of papers published on liposomes since 1976 incorporating the keywords “liposomal delivery systems” (using the Web of Science citation manager).

Amongst all the delivery systems that have been devised to beneficially modulate the pharmacokinetics and/or tissue distribution of the drug, liposomes attracted the most interest (Storm and Crommelin, 1998). This is mainly due to their low toxicity, high biocompatibility and biodegradability and ability to entrap a wide variety of materials (Crommelin and Sindelar, 1997; Allen, 1998; Gomez-Hens and Fernandez-Romero, 2006).

Despite the extensive amount of work and significant improvements in manufacturing technologies over the past few decades, the commercial success of liposomes is limited, mainly due to stability issues, both physical (as manifested by drug leakage and vesicle aggregation or fusion) and chemical (due to hydrolysis of the ester bonds or oxidation of unsaturated acyl groups of the phospholipid molecules) (Gregoriadis, 1988; Storm and Crommelin, 1998; Felnerova *et al.*, 2004; Sabin *et al.*, 2006). Also, with liposomes, batch-to-batch variation and inconsistencies in producing large batches have been reported (Kirby and Gregoriadis, 1999; Gomez-Hens and Fernandez-Romero, 2006). Additionally, the rapid clearance of liposomes from the blood circulation after intravenous administration is a serious problem that should be considered in the formulation of liposomes that have potential suitability for commercial use (Allen and Chonn, 1987). A study by Allen and Everest (1983) has shown that about 85% of large egg phosphatidylcholine liposomes were found in the spleen and liver 0.5 hours post-injection in rats. This is attributed to the clearance of liposomes by the reticuloendothelial system.

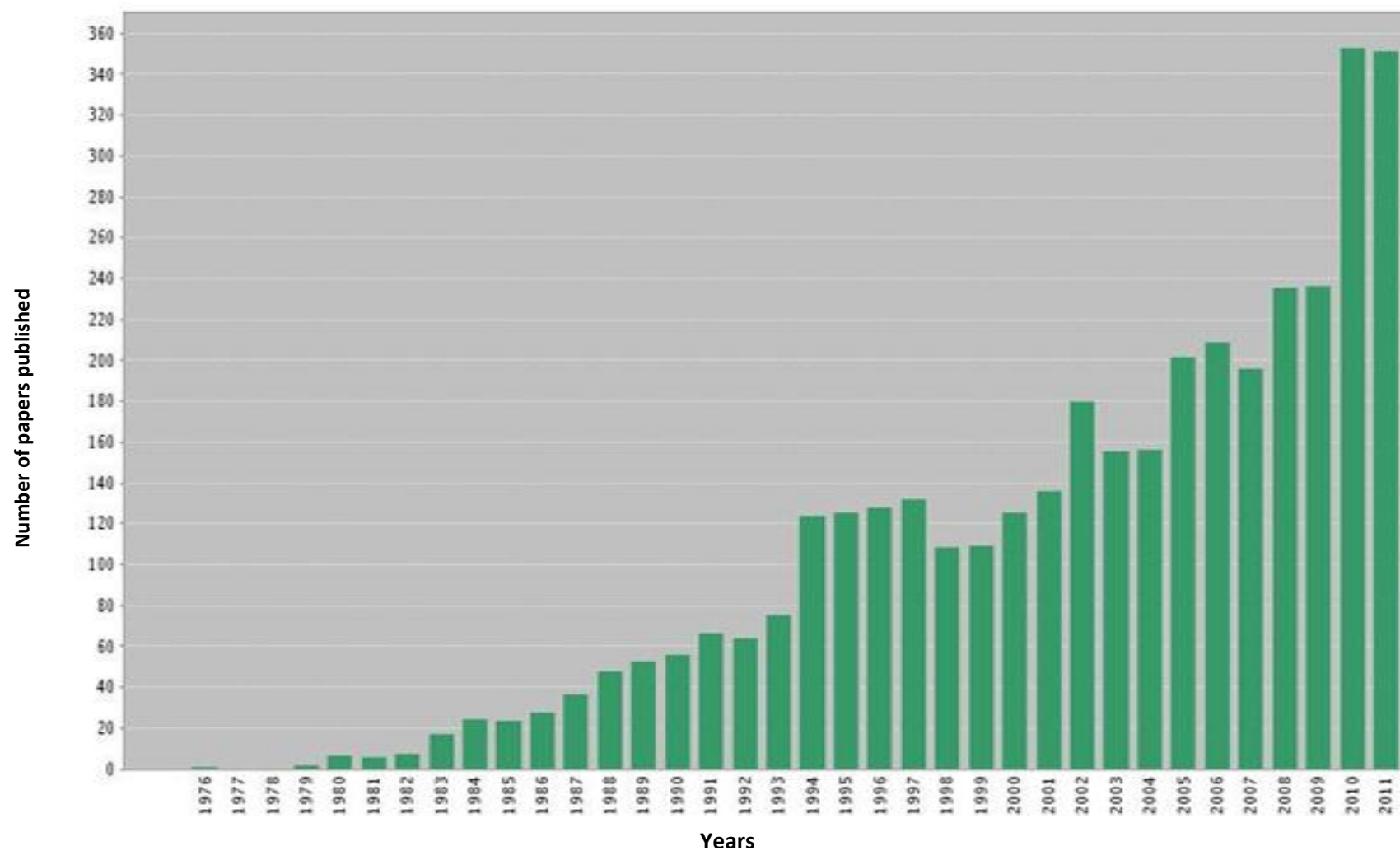


Figure 1.14: Papers published in the field of liposomal delivery systems since 1976. (Generated via Web of Science citation manager)

1.4.5 Preparation of liposomes

Various methods have been proposed for the preparation of liposomes. However, the underlying principle of the formation of liposomes is the interactions between the lipid-lipid and lipid-water molecules. The input of energy (e.g. by shaking, sonication, homogenization etc.) results in the arrangement of the phospholipid molecules into bilayered vesicles in order to achieve thermodynamic stability in the aqueous environment (Lasic *et al.*, 2001; Mozafari, 2005).

1.4.5.1 Proliposomes

Despite the fact that liposomes are promising, broadly applicable and highly researched novel delivery systems, they suffer from instability problems, such as sedimentation, aggregation, fusion and phospholipid hydrolysis and/or oxidation (Betageri and Yatvin, 2002; Yan-yu *et al.*, 2006).

In order to improve the stability of liposomes, Payne *et al.*, (1986a; 1986b) introduced a novel method for the manufacture of liposomes using the concept of proliposomes, which are defined as dry, free flowing granules which, on addition of aqueous phase, form MLVs.

These proliposomes can overcome the stability problems associated with liposomes (Ahn *et al.*, 1995a; Yan-yu *et al.*, 2006). In addition, due to their free flowing properties, proliposomes might be considered for the manufacture of various dosage forms including tablets and capsules (Song *et al.*, 2002; Ning *et al.*, 2005). Nowadays, proliposomes may be classified into two main types: particulate-based proliposomes and alcohol-based proliposomes (Elhissi *et al.*, 2006b).

(1) Particulate-based proliposomes

This type comprises a granular free flowing material of a lipid and drug coated onto soluble carrier particles by which, on hydration, liposomal suspensions are generated (Payne *et al.*, 1986a; Payne *et al.*, 1986b). Various carrier materials have been investigated for their suitability in the manufacture of proliposomes, such as lactose (Shah *et al.*, 2006), sodium chloride (Payne *et al.*, 1986b), mannitol (Yan-yu *et al.*, 2006; Gupta *et al.*, 2008), fructose and sorbitol (Payne *et al.*, 1986a; Ahn *et al.*, 1995a; Song *et al.*, 2002; Ning *et al.*, 2005).

The particle size of the carrier may influence the size and polydispersity of the liposomes produced (New, 1990; Ahn *et al.*, 1995a). Amongst the studied carrier materials, sorbitol appeared to offer the best compromise because of its acceptability for clinical use and due to its low osmotic activity when compared to the other lower molecular weight compounds (Payne *et al.*, 1986b; New, 1990; Song *et al.*, 2002).

The entrapment efficiency of hydrophobic materials is generally high in liposomes generated from particulate-based proliposomes. Payne *et al.*, (1986a) reported an entrapment efficiency of 100% for Amphotericin B. In another study by Yan-yu *et al.*, (2006), the entrapment efficiency of silymarin was reported to be more than 90%. Conversely, unlike hydrophobic drugs, hydrophilic drugs such as propranolol hydrochloride (PH) were reported to have low entrapment efficiency values, for instance 10%, as reported by Ahn *et al.*, (1995a).

Many studies have been performed on particulate-based proliposomes. including research on the intravenous administration of methotrexate (Park *et al.*, 1994), cyclosporin A (Lee *et al.*, 1999), doxorubicin (Lee *et al.*, 1996) and amphotericin B (Payne *et al.*, 1986a). In nasal delivery, proliposomes containing propranolol hydrochloride (Ahn *et al.*, 1995a; b) and nicotine (Jung *et al.*, 2000) have been investigated. Hwang *et al.*, (1997) also explored the transdermal delivery of nicotine proliposomes. Furthermore, the topical delivery of proliposomes of aceclofenac was studied by Gupta *et al.*, (2008) and entrapment efficiencies of more than 90% were reported for this drug. Also, the

production of effervescent particulate-based proliposomes was examined and described by Katare *et al.*, (1990), who employed effervescent granules as carriers and used a fluidised bed method for the phospholipid coating on the carrier particles. High entrapment efficiency values (nearly 100%) were reported by this method for the non-steroidal anti-inflammatory drugs ibuprofen (Katare *et al.*, 1990) and indometacin (Katare *et al.*, 1995).

(2) Solvent-based proliposomes

Solvent-based proliposomes, also referred to as alcohol-based proliposomes or ethanol-based proliposomes (depending on the solvent used to dissolve the lipid) are formulation technologies first introduced by Perrett *et al.*, (1991) to offer a relatively simple means of generating liposomes from alcoholic phospholipid solutions. Solvent-based proliposomes comprise concentrated alcoholic solutions of lipids which upon addition of aqueous phase and shaking generate liposomes (Perrett *et al.*, 1991; Dufour *et al.*, 1996). Ethanolic-based proliposomes were found to coexist in a stacked precipitated bilayers in the ratio of (5:4:10) lipid: ethanol: buffer w/w/w (Perrett *et al.*, 1991). Hydration of alcohol-based proliposomes was found to generate a mixture of OLVs and MLVs (Gregoriadis, 1993; Elhissi *et al.*, 2006a).

High entrapment efficiencies were reported for hydrophilic drugs encapsulated in liposomes prepared via the alcohol-based proliposome method; depending on the lipid composition of the proliposomes, the entrapment efficiency can range between 65 and 80% (Perrett *et al.*, 1991). Formulation parameters such as hydration rates and hydration temperatures were also found to significantly affect the properties of the liposomes and thus the entrapment efficiencies. Table 1.1 shows the entrapment efficiency values reported by Turanek *et al.*, (1997) for drugs encapsulated in liposomes using the alcohol-based proliposome method. Moreover, entrapment efficiency values of (81%) for amphotericin b (Amb) and (61%) for salbutamol sulfate (SS) using the ethanol-based proliposome method has been previously demonstrated (Albasarah *et al.*, 2010; Elhissi *et al.*, 2011a).

Table 1.1: Entrapment efficiency of different drugs in alcohol-based proliposomes. (Adapted from Turanek *et al.*, 1997)

Entrapped moiety	Entrapment efficiency (%)
Neomycin	65
Gentamycin	69
Carboxyfluorescein	81
Adamantylamide dipeptide	87
Muramyl dipeptide	62
B-D-GlcNAc-norMurNAc-L-Abu-D-isoGln	85
Mesotetra-(parasulfophenyl)-porphin	65

1.5 Liposomes in respiratory tract delivery

The delivery of drugs to the respiratory tract offers considerable advantages over other routes of administration both for local and systemic delivery of drugs.

The rapid onset of action following respiratory tract delivery (owing to its relatively large surface area and high vascularity, the evasion of first pass metabolism and harsh gastrointestinal environment and its non-invasive nature) makes the respiratory tract a very interesting route for the administration of drugs, particularly macromolecules such as peptides and proteins. Despite the advantages the respiratory tract offers, the duration of activity following administration is short, and some metabolic activity still exists in the respiratory tract. Consequently, controlled drug delivery systems such as liposomes have been investigated and are postulated to overcome those limitations of respiratory tract delivery by offering sustained release and enhancing the local retention time of medicaments (Gregoriadis, 1993). In addition, liposomes contain lipids similar to those found in the pulmonary walls (Finley *et al.*, 1968).

1.5.1 Liposomes in nasal delivery:

The potential and usefulness of liposomes for intranasal delivery was previously explored. Alpar *et al.*, (1992) studied the effect of equimolar distearoylphosphatidylcholine (DSPC) and cholesterol liposomes incorporating tetanus toxoid (TT) in guinea pigs. The results from their study indicated that liposomes formulations significantly improved the immune response when delivered via the nasal cavity compared to free antigen. This was also confirmed by Tafaghodi *et al.*, (2006), who evaluated the efficacy of equimolar PC and cholesterol liposomes for entrapping TT after intranasal administration in rabbits. The results from their study demonstrated that intranasal administration of liposomes preserved the immunoreactivity of TT (100.5 ± 1.3 % that of original TT) and induced no or little system IgG immune response and a high mucosal immune IgA response. Moreover, lack of toxicity or local irritation was observed after the intranasal delivery of liposomes.

Law *et al.*, (2001) investigated liposomes containing calcitonin after intranasal delivery in rabbits. The data from their study indicated that liposomes not only exhibited a higher bioavailability than calcitonin solution alone but also resulted in an increase in the residence time in the nasal cavity.

Furthermore, Muramatsu *et al.*, (1999) investigated the benefit of using cholesterol, soybean-derived sterol or soybean sterylglucoside (SG) modified dipalmitoylphosphatidylcholine (DPPC) liposomes for the intranasal delivery of insulin. The results from their study indicated that, contrary to the insulin solution alone, all DPPC modified liposomes resulted in a hypoglycaemic effect. SG modified DPPC liposomes, however, caused the highest hypoglycaemic effect, which was attributed to the higher fluidity in the liposomal membranes using SG-modified DPPC liposomes in comparison to cholesterol and SS modified DPPC liposomes.

The usefulness of liposomes for the nasal delivery of nefidipine (Vyas *et al.*, 1995), levonorgestrel (Ding *et al.*, 2007) and the synthetic peptide vaccine 366–374 peptide (Ninomiya *et al.*, 2002) have also been previously reported. Moreover, the DNA-hsp65 vaccine complexed with cationic liposomes was also

found to illicit a cellular immune response comparable to that induced by four intramuscular doses of the naked DNA (Rosada *et al.*, 2008).

The potential of intranasal delivery of liposomes for brain delivery has also been previously examined. Arumugan *et al.*, (2008) investigated the usefulness of soya lecithin and cholesterol (4:1) based liposomes for the delivery of rivastigmine to rat brains following intranasal delivery. The results from their study indicated a higher bioavailability of rivastigmine in the brain of the rats after intranasal administration of the rivastigmine liposomes in comparison to the intranasal drug alone and the oral rivastigmine solution. AUC values of rivastigmine were 6.58, 12.99 and 36 ($\text{mg}/\text{min}/\text{ml}^{-1}$) for free drug oral, free drug intranasal and liposomes, respectively. Additionally, the rivastigmine were also found to have longer half-life in the brain after the delivery via liposomes intranasally in comparison to orally and intranasally administered free drug.

The possibility of achieving sustained delivery of drugs via proliposomes formulations was also previously studied. Ahn *et al.*, (1995b) investigated the bioavailability and plasma profiles of PH entrapped inside sorbitol particulate-based proliposomes and loaded into sorbitols delivered intranasally into rats and compared to the oral and intravenous solution of PH. The results from the study demonstrated the high bioavailability of PH proliposomes compared to that of IV solutions (100%), PH loaded sorbitols (96.2%) and intranasal PH (103%), and much higher than that of the oral solution (14.2%). The plasma profile for the PH proliposomes, on the other hand, was significantly different from those of the solution formulation, and plasma concentrations were lowest at the initial phase and higher than the other formulations after 180 minutes, illustrating that proliposomes can be a good candidate for sustained delivery of drugs.

Jung *et al.*, (2000) investigated particulate-based proliposomes for nasal delivery of nicotine base (NB) and nicotine hydrogen tartarate salt (NS) in rats. The bioavailabilities of NB and NS proliposomes following intranasal delivery were comparable to those of the NB and NS intranasal saline solutions. The AUC values for the NB were 65.8 ± 27.9 and 56.1 ± 34.7 ($\mu\text{g}/\text{ml}/\text{min}$) for the solution and proliposomes, respectively, whilst for the NS the AUCs were

27.8±7.12 and 39.0±12.8 (µg/ml/min), respectively. The mean residence time and plasma half-life ($T_{1/2}$) of NB and NS on the other hand were much longer than those using the saline solutions, thus giving an indication of the advantages provided when proliposomes are employed.

The addition of mucoadhesive materials to liposomal formulations delivered via the intranasal route was also found to significantly enhance the bioavailability and sustained delivery of the drug. Shahiwala and Misra (2006) have investigated the effect of incorporating chitosan into liposome formulations containing leuprorelin acetate (LEU) for intranasal delivery. The data from their study indicated that nasal delivery of liposomes entrapping LEU resulted in a higher bioavailability (27.83%) than that of the drug alone (10.89%). Furthermore, the addition of chitosan to both the LEU alone and liposomal formulation lead to an increase in the bioavailability to 49.13% and 88.90%, respectively. The release of LEU was found to be delayed for the liposomal formulation in comparison to the free drug and even further delayed after the addition of chitosan to the formulation.

The delivery of liposomes as mucoadhesive nasal gels using acyclovir as a model drug was studied by Alsarra *et al.*, (2008), who found that the liposomal gel incorporating acyclovir not only prolonged the contact between the acyclovir and the absorptive sites in the nasal cavity, but also facilitated the direct absorption through the nasal mucosa. The bioavailability of acyclovir given intranasally was as low as 5.3% using the liposome-free gel and as high as 60.72% using the liposomal gel formulation.

1.5.2 Liposomes in pulmonary delivery

The ability of liposomes to entrap drugs and deliver them in a sustained manner and the fact that they are nontoxic has drawn a lot of interest due to their potential use in pMDIs, DPIs and nebulisers.

The feasibility of using pressurized packs for the delivery of liposomes was first investigated by Farr *et al.*, (1987). In their study, egg phosphatidylcholine was dissolved into a chlorofluorohydrocarbon blend, and the possibility of *in situ* formation of liposomes following deposition in the respiratory tract was demonstrated. This was further confirmed by Vyas and Sakthivel (1994).

For the use in DPIs, liposomal formulations encapsulating the drugs are homogenized, dispersed into carriers and converted into DPI by freeze or spray drying. On inhalation, the liposome powders get hydrated by the deposition on the surface of the respiratory tract, forming the liposome vesicles (Chougule *et al.*, 2007). The use of freeze drying for the generation of liposome powders for DPI was also investigated by Joshi and Misra (2001) and Huang *et al.*, (2010). The results from their studies suggested the suitability of the liposomal formulation to be delivered into the deep lung.

Alves and Santana (2004) and Chougule *et al.*, (2008) also investigated the use of spray drying for the generation of the liposomal powders suitable for inhalation. The results from their investigation demonstrated the usefulness of spray drying as a technique to generate homogeneous lipid spherical particles suitable for pulmonary delivery. Furthermore, the feasibility of preparing isoniazid (INH) proliposome powders for inhalation has also been investigated (Rojanarat *et al.*, 2011). Cell culture results from their study have demonstrated that the INH-proliposomes were nontoxic to respiratory-associated cells and offered a significantly higher efficacy than the free INH against alveolar macrophages infected.

Unlike DPIs and pMDIs, nebulisers can deliver liposomes directly to the respiratory systems without need to form dried liposomal formulations or the incorporation of a propellant (Taylor *et al.*, 1990a).

The potential of jet nebulisation for delivery of liposomes have been intensively examined (Taylor *et al.*, 1990a; Waldrep *et al.*, 1994; Bridges and Taylor, 2000; Bridges and Taylor, 2001; Elhissi *et al.*, 2011b). Various reports have demonstrated that jet nebulisation leads to the fragmentation of the liposomes after nebulisation (Taylor *et al.*, 1990a; Saari *et al.*, 1999; Elhissi *et al.*, 2006a). In addition to the fragmentation of liposomes, air-jet nebulisation of liposomes

has been found to cause leakage of hydrophilic materials from the liposomal formulations (Niven and Schreier, 1990; Niven *et al.*, 1991; Niven *et al.*, 1992; Desai *et al.*, 2002). Like jet nebulisation, nebulisation of liposomes via ultrasonic nebulisers has been previously reported to fragment the liposomes and cause leakage of the entrapped material (Leung *et al.*, 1996; Finlay and Wong, 1998).

Amongst the different kinds of nebulisers studied for liposome delivery, vibrating-mesh nebulisers seem to be the least disruptive to liposomes (Elhissi *et al.*, 2007; Kleemann *et al.*, 2007), and leakage of the entrapped materials following nebulisation was reported to be less using these devices compared to air-jet nebulizers (Elhissi *et al.*, 2006a).

Elhissi *et al.*, (2006a) compared the entrapment efficiency of SS entrapped inside liposomes generated from ethanol-based proliposomes following nebulisation through an air-jet nebuliser (Pari plus) and three different vibrating-mesh nebulisers (Omron NE U22), (Aeroneb Pro small mesh) and (Aeroneb Pro large mesh). The results from their study revealed that liposomes following nebulisation through the different vibrating-mesh nebulisers retained a higher amount of entrapped drug in comparison to the air-jet nebuliser, 0.239 mg SS after nebulisation through the Pari and 0.380, 0.344 and 0.263 following nebulisation through the Omron NE U22, Aeroneb Pro small mesh and Aeroneb Pro large mesh, respectively. Kleemann *et al.*, (2007) also reported a significant reduction in the leakage of materials following nebulisation through an Aeroneb vibrating-mesh nebuliser when compared to an Optineb ultrasonic nebuliser and a Pari LC air-jet nebuliser.

Various methods have been proposed to enhance the stability of liposomes to nebulisation, including the incorporation of cholesterol into the liposomal formulation (Leung *et al.*, 1996), and freeze drying of liposomes with the addition of a suitable cryoprotectant (Bridges and Taylor, 2001). Furthermore, size reduction of the liposomes has been previously reported as one of the methods to enhance delivery through nebulisers and reduce the leakage of the drugs from the liposomes following nebulisation (Finlay and Wong, 1998). Niven *et al.*, (1991) prepared MLV liposomes entrapping carboxyfluorescein (CF) of sizes between 0.2 to 5 μm using extrusion via polycarbonate membrane filters.

Results from their study indicated that the leakage of CF from the vesicles was dependent on the liposome size and ranged from $7.9\pm 0.4\%$ for $0.2\ \mu\text{m}$ vesicles to $76.8\pm 5.9\%$ for non-extruded liposomes.

Growing attention has been given to the potential of a pulmonary route for systemic delivery of macromolecules, particularly peptides and proteins. Since most proteins are stored as an aqueous concentrate rather than in a bulk powder, the use of nebulisers is a logical first choice for pulmonary delivery of proteins (Niven *et al.*, 1996). However, for the use of aerosols for inhalation, special precautions must be taken, especially when aerosolizing biologically active substances (i.e. proteins), since alteration in their biological activity might occur due to their aerosolisation (Fangmark and Carpin, 1996). Different reports exist demonstrating the loss of activity of proteins following aerosolisation (Niven and Brain, 1994; Niven *et al.*, 1994; Ip *et al.*, 1995; Niven *et al.*, 1995; Fangmark and Carpin, 1996; 1998; Khatri *et al.*, 2001).

Liposomal carriers have been proposed for stabilising proteins to nebulisation (Kanaoka *et al.*, 1999; Khatri *et al.*, 2004; Anabousi *et al.*, 2006; Huang and Wang, 2006). Furthermore, the incorporation of drugs in liposomes has also been found to reduce their toxicity. Gilbert *et al.*, (1997) investigated the tolerance of human volunteers to an aerosol of dilauroylphosphatidylcholine (DLPC) liposome entrapping cyclosporine A (CsA). The results from their investigation demonstrated that whilst the delivery of cyclosporine alone leads to intermittent coughing and tracheal irritation, DLPC entrapping CsA has been found to be safe and induced no irritation or coughing to patients. Moreover, the biological activity and safety of an aerosol of Interleukin-2 liposomes were demonstrated following their delivery to dogs (Khanna *et al.*, 1997) and humans, whilst eliminating the fever, malaise and local swelling side effects following the administration of the free drug (Ten *et al.*, 2002).

1.5.3 Safety and fate of liposomes in the respiratory tract

Amongst the main advantages of liposome delivery to the respiratory tract is their non-toxic nature. The fact that liposomes are made of lipids similar to those found in the pulmonary walls of mammals explain their safety *in vivo* and give an indication of their possible fate in the respiratory tract. Finley *et al.*, (1968) performed a morphological and lipid analysis of the lining of the alveoli in dogs. They found that the major pulmonary surfactants present in the mammalian alveoli surface are PC (51.2%) and cholesterol (11.9%).

Various reports have previously assessed the safety of liposomes in the respiratory tract (Thomas *et al.*, 1991; Schreier *et al.*, 1992; Schreier *et al.*, 1993). Thomas *et al.*, (1991) investigated the effect of inhaled SPC on the pulmonary function and on oximetry in ten healthy human volunteers. Results from their investigation demonstrated that SPC liposomes caused no acute deleterious effects on oxygenation or spirometric values.

Waldrep *et al.*, (1994; 1997) also studied the effect of DLPC liposomes, and DLPC liposomes entrapping beclomethasone dipropionate (BDP) aerosols on the spirometry and clinical chemistry evaluations. That was accompanied by a complete blood count in 10 healthy volunteers. The results from their study demonstrated the safety of liposomal aerosols on the respiratory system and the absence of side effects upon their delivery.

Lung surfactants such phosphatidylcholine (PC) and phosphatidylglycerol (PG) are synthesized by alveolar epithelial Type-II cells. An existing balance between release and clearance maintains a stable surfactant film in the lung. The main mechanism of clearance of those surfactants via the lung is following phagocytosis by alveolar macrophages (Kellaway and Farr, 1990).

The mechanism of liposomal clearance in the respiratory tract depends mainly on the location in which it is deposited, and liposomes reaching the alveoli in the same way as other lung surfactants are cleared via microphages (Kellaway and Farr, 1990). Liposomal formulations can also take advantage of opsonisation by delivering the drug to sites inside the phagolysosomes, where

intracellular microorganisms such as *Francisella tularensis*, *Mycobacterium avium-intracellulare*, *Mycobacterium tuberculosis* and *Pseudomonas pseudomallei* are known to reside. Conley *et al.*, (1997) investigated the potential of liposomes encapsulating ciprofloxacin versus the free ciprofloxacin drug for the treatment of mice infected with *Francisella tularensis*. Results from their study showed that whilst mice treated with ciprofloxacin alone suffered 100% mortality, all mice treated with liposomes encapsulating ciprofloxacin were found to survive the infection.

In addition to the deposition site of liposomes, other factors, including the constituents and dosage of the lipid in the liposomes and the charge of the vesicles, affect the clearance of the liposomes through the respiratory tract (Oguchi *et al.*, 1985; Woolfrey *et al.*, 1988; Kellaway and Farr, 1990).

The area of liposomal formulations for respiratory tract delivery is still in its infancy, thus no FDA approved products incorporating liposomes for intranasal or pulmonary delivery have been marketed.

1.6 Hypothesis and objectives

Despite the advantages of drug delivery via the respiratory tract, the duration of activity following drug administration is short. Also, activity of some proteins and peptides might be compromised upon delivery to the respiratory tract. Liposome carriers are a promising approach for overcoming the limitations of drug delivery via the respiratory route. The use of liposomes is postulated to offer sustained release and enhance the local retention time of liposome-entrapped drugs. However, issues like liposome instability to nebulisation and scaling-up difficulty need more research. Also, debatable information regarding role of nebulisation in efficient delivery and stability of proteins requires further examination. Furthermore, as yet, no study has been conducted to examine the effect of nasal spray devices on the physical stability of liposomes and activity of proteins, and the validity of proliposome technology for the entrapment of immunoglobulins (Ig) has never been addressed.

Working Hypothesis: Can proliposome technology be exploited successfully to deliver drugs via the respiratory tract.

Main Aims: (1) To explore the validity of the ethanol-based proliposome technology for generating mucoadhesive liposome formulations entrapping IgG; and (2) to investigate the potential of IgG liposomes for respiratory tract delivery via medical nebulisers and nasal sprays of different operating principles.

Specific objectives:

- To establish optimal formulation parameters required to manufacture submicron mucoadhesive liposomes via the ethanol-based proliposome technology.
- To compare conventional liposome preparation methods to the ethanol-based proliposome approach for the entrapment of IgG.
- To investigate the effect of IgG entrapment in liposomes on the immunoreactivity and secondary structure of the protein.
- To examine the influence of mucoadhesive agents' incorporation in liposomal structure on the characteristics of liposomes.
- To study the relation between formulation (i.e. IgG solution or IgG liposomes) and device (whether a medical nebuliser or nasal spray), and its effect on the performance of the device and characteristics of generated cloud.
- To determine the effect of nebulisation or spraying on physical stability of liposomes and integrity of IgG.
- To examine the viability of size reduction of liposomes as a technique to enhance the stability of liposomes during nebulisation or spraying.
- To analyse the data and write up the PhD thesis.

CHAPTER 2

GENERAL METHODOLOGY

2.1 Materials

Soya phosphatidylcholine (SPC; Lipoid S 100) was obtained from Lipoid (Steinhausen, Switzerland). Ammonium thiocyanate and ferric chloride of analytical grade were purchased from VWR, UK. Salbutamol sulfate (SS) (99%) was purchased from Alfa-Aesar, UK. Sucrose $\geq 99.5\%$ GC, sodium alginate derived from brown algae (low viscosity), absolute ethanol, cholesterol 99%, albumin from chicken egg white (ovalbumin (OVA)) $\geq 98\%$ and phosphate buffered saline tablets were purchased from Sigma Aldrich, UK. Protasan G213, an ultrapure chitosan glutamate salt, was obtained from Novamatrix, Belgium. High performance liquid chromatography (HPLC) grade water, methanol, bicinchoninic acid (BCA) protein assay kit, immunoglobulin G (IgG) easy-titre kit and chloroform were all supplied by Fisher Scientific Ltd., UK. The drug FlebogammaDif® 5% 50 mg/ml intravenous immunoglobulin (IVIG) was supplied by Instituto GRIFOLS (Barcelona, Spain).

2.2 Methods

2.2.1 Preparation of liposomes

A variety of methods for preparing liposomes exist, as outlined earlier (Section 1.4.5). In this study three methods for preparing liposomes were used:

- Liposomes made by using thin film hydration method
- Liposomes generated from ethanol-based proliposomes
- Liposomes generated from particulate-based proliposomes

a) Liposomes made by thin film hydration

Lipid phase comprising SPC (40 mg) and cholesterol (10 mg) in a mole ratio of 2:1 were dissolved in 5 mls of chloroform within a 100 ml pear-shaped flask. The flask was then attached to a rotary evaporator (Rotavap, Büchi,

Switzerland) under negative pressure (<50mbar) using a vacuum pump (V-700, Büchi, Switzerland). The temperature of the rotary evaporator's water bath was adjusted to 30°C, and rotation speed was set at maximum (280 rpm). After 1 hour the vacuum pump was turned off to release the negative pressure. The thin film formed on the inner walls of the flask was then hydrated, as outlined in Section 2.2.2, to generate liposomes.

b) Particulate-based proliposomes

In this study sucrose was used as carrier particles in the preparation of proliposomes. Sucrose was first ground using a pestle and mortar and sieved in order to collect particles having the size cut of 300–500 µm. Particulate-based proliposomes (1:5 w/w SPC to sucrose ratio) were manufactured by placing sucrose (2.5 g) in a 100 ml pear-shaped flask. The flask was attached to a rotary evaporator (Rotavap, Büchi, Switzerland) under a negative pressure (<50mbar) using a vacuum pump (V-700, Büchi, Switzerland), the water bath was set at 30°C and the rotation speed was set at 280 rpm. This was followed by dissolving SPC (400 mg) and cholesterol (100 mg) in HPLC grade chloroform (15 ml). The chloroformic solution was sprayed in portions (0.5-1 ml each) via a feed-line tube attached within the rotary evaporator. After each injection, the chloroformic solution was allowed to evaporate before injecting the next portion. After injecting the chloroformic solution, the flask was left on the rotary evaporator for 1 hour to ensure complete solvent evaporation. The vacuum was then released and the sucrose-based proliposomes were collected and placed in a vial and stored in the freezer (-18°C). Proliposomes were hydrated and annealed according to the procedure performed for the thin film method (Section 2.2.2).

c) Ethanol-based proliposomes

Liposomes were prepared using an ethanol-based proliposome approach by modifying the method originally introduced by Perrett *et al.*, (1991). Lipid phase (50 mg) consisting of SPC and cholesterol (2:1) was dissolved in 60 mg ethanol (76 μ l) at 70°C (to aid the dissolution of cholesterol) for two minutes in an 8 ml glass vial to yield a clear lipid solution (i.e. the proliposomes). SS (1 mg/ml), OVA (1.7, 2.5, 3.2 or 4 mg/ml) or IVIG (0.5, 1, 1.25, 2.5 or 5 mg/ml) in HPLC water were previously prepared and 0.5 ml was quickly added to the proliposomes and vortexed for two minutes using the WhirlMixer™ (Fisherbrand, Fisher, UK) to generate concentrated liposomal suspensions (primary hydration step). The suspensions were further diluted to 5 ml with HPLC water and vortexed again for two minutes (secondary hydration step) to yield the final liposomal suspension. Liposomal suspensions were then left on the bench at room temperature for 1 hour to anneal.

2.2.2 Hydration of phospholipid thin films or particulate-based proliposomes

The desired amount of HPLC water was added at room temperature to the flask containing the phospholipid film or the particulate-based proliposomes. The resultant suspension was shaken for 10-15 minutes using a vortex WhirlMixer™ (Fisherbrand, Fisher, UK). The dispersion was then left for 1-2 hours to anneal at room temperature prior to use or conducting further experiments.

For the preparation of the IgG based liposomes, different concentrations of IgG in HPLC water (0.5, 1, 1.25, 2.5 or 5 mg/ml) were prepared and added to the phospholipid film or the particulate-based proliposomes to make a final volume of 5 ml.

2.2.3 Size reduction of liposomes

Liposome dispersions were reduced in size via ultrasonic vibrations or extrusion. The principle of sonication involves the use of high frequency pulsed sound waves to fragment the liposomes into smaller vesicles (Uhumwangho and Okor, 2005).

Two types of sonicators were used in this study:

1) Bath sonicator:

A volume of 30 mls of liposomal suspension were placed in a 100 ml beaker. The beaker was then covered with three layers of parafilm and placed in a bath sonicator (Fisherbrand FB11004, UK) at a temperature of 40°C. Samples of the liposomal suspension were then taken at one minute intervals to have its size measured (as described in Section 2.2.5). Sonication proceeded until the desired size was achieved.

2) Probe sonicator:

For size reduction via probe sonication, 30 ml liposomal suspension was placed in a 100 ml beaker and placed under a probe sonicator (Vibra cell sonicator, Sonics and Materials Inc., Newtown, USA). Samples were then taken from the beaker at one-minute intervals to have its size measured (as described in Section 2.2.5). Probe sonication proceeded until desired size was achieved. To avoid overheating of the phospholipids via the probe sonicator, intervals of one minute sonication were followed by intervals of two minutes immersion of the liposome flask in ice bath.

As an alternative to sonication, extrusion was employed for size reduction using a Lipofast mini-extruder (Avestin, Canada). Liposomal dispersions were sequentially passed through a series of polycarbonate membrane filters having a pore size of 2, 1, 0.8 and 0.4 μm , to yield liposomes of the desired size.

2.2.4 Phospholipid assay

The phospholipid assay was performed to investigate the efficiency of ultracentrifugation in pelleting the liposomes. These experiments were performed to investigate the efficiency of separating the liposomes from the continuous phase. Phospholipid assay was performed according to the protocol of Elhissi *et al.*, (2006b). Samples (1 ml) of the liposomal dispersions were placed in glass vials, to each of which 1 ml absolute ethanol was added to disrupt the liposomes and convert the dispersion into a clear ethanolic solution. Vials were kept overnight in a 90 °C oven to evaporate the solvent and leave the phospholipid as a film on the inner walls of the vial. Chloroform (2 ml) was added to the glass vial to dissolve the phospholipid, followed by addition of an equal volume of ammonium ferrothiocyanate solution (prepared by dissolving 6 g of ammonium thiocyanate (NH₄SCN) and 5.4 g of ferric chloride (FeCl₃·6H₂O) in 200 ml of deionised water). The phospholipid film develops a colour when the phospholipid molecules react with ammonium ferrothiocyanate in chloroformic solution (Stewart, 1980). The samples were then vortexed for one minute using the WhirlMixer™ (Fisherbrand, Fisher, UK) and left to stand for two hours. The lower chloroformic layer was aspirated and the amount of phospholipid complexed with ammonium ferrothiocyanate was estimated at 488 nm using a BioChrom WPA Biowave II UV/Visible Spectrophotometer (Biochrom WPA Ltd., UK).

For the preparation of the calibration curve, 100 mg of SPC was dissolved in 2 ml chloroform in a 100 ml pear-shaped flask and a thin film was prepared and hydrated (as described in Sections 2.2.1 and 2.2.2, respectively). A series of dilutions were then performed on the lipid suspensions to generate concentrations between 0.2 mg/ml and 2 mg /ml. Stewart assay was then performed for the calibration curve samples, as described earlier in this section.

2.2.5 Size analysis of the liposomes

Liposomes generated from proliposomes were diluted with water and their size and size distribution were measured using: (1) laser diffraction employing the Malvern Mastersizer 2000 instrument (Malvern Instruments Ltd., UK) or (2) dynamic light scattering (DLS) employing the Malvern Zetasizer Nanoseries (Malvern Instruments Ltd., UK). When using the Malvern's laser diffraction instrument, volume median diameter (VMD) and SPAN were used to express the size and size distribution, respectively. The SPAN is a unit-less term introduced by Malvern Instruments Ltd. to express the width of the distribution based on the 10%, VMD (50%) and 90% quantile, and it is calculated as $SPAN = (90\% \text{ undersize} - 10\% \text{ undersize})/VMD$. When DLS was employed the size and size distribution were expressed as Z_{average} and polydispersity index (Pdi), respectively.

Laser diffraction is amongst the most commonly used techniques for size measurements due to its convenience and rapid measurement. During laser diffraction measurements a laser beam was focused on particles which, depending on their size, scattered the laser beam. The intensity and angle of the scattered light was then measured by a series of photosensitive detectors. Those detectors were attached to a computer which then calculated the size and size distribution or span of particles (Figure 2.1).

Unlike the Mastersizer, which used the principle of laser diffraction to measure the size of particles, the Zetasizer Nanoseries measured the size of particles via the process of DLS. DLS measured the brownian motion of the particles, which was then related to its size. This was done by focusing a beam of laser at the particles and measuring the scattering intensity fluctuations caused by the motion of the particles. Figure 2.2 shows a schematic presentation of the process of DLS (Malvern-Instruments, 2004).

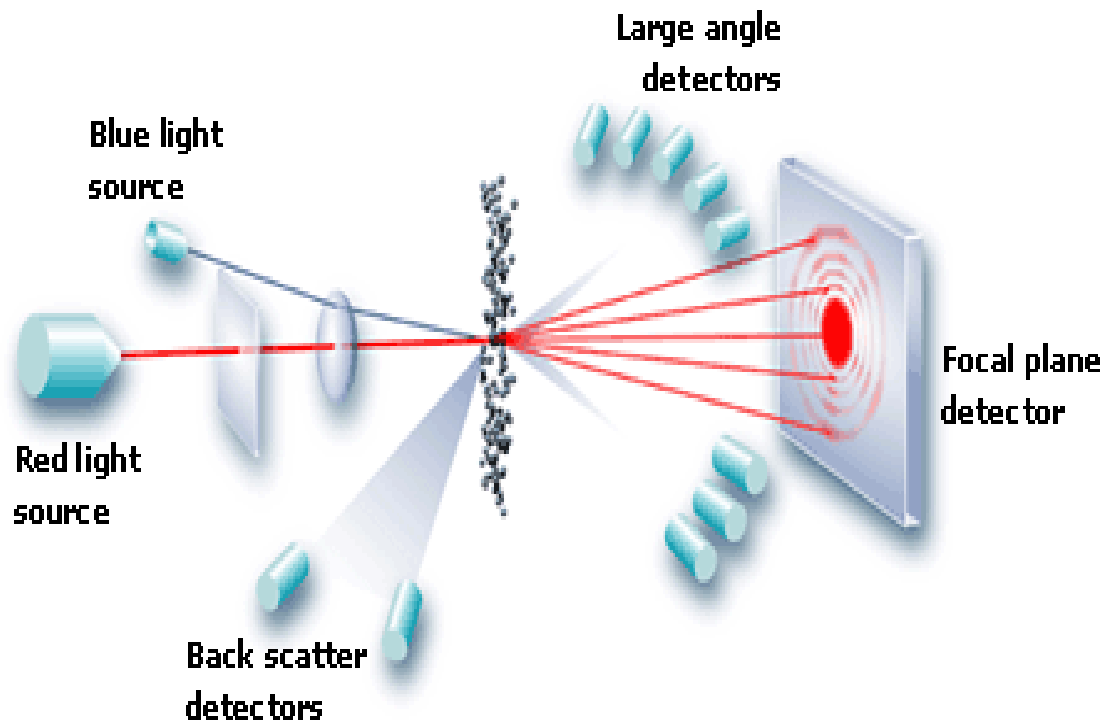
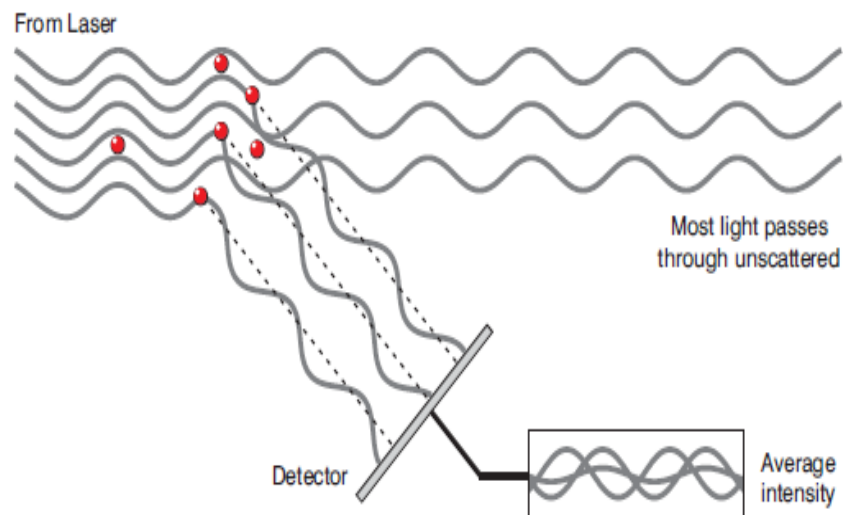


Figure 2.1: A schematic presentation of laser diffraction. (Adapted from Malvern-Instruments, 2011)



The scattered light falling on the detector.

Figure 2.2: A schematic representation of DLS in the Zetasizer instrument. (Adapted from Malvern-Instruments, 2004)

2.2.6 Liposome morphology, Cryo Transmission Electronic Microscopy (Cryo-TEM)

A volume of 10 microlitres of liposome suspension was blotted onto a glow discharged 300 mesh lacey carbon grid (Agar Scientific, UK) for three to six seconds and plunged into nitrogen chilled liquid ethane. Samples were then imaged on a Jeol 2010F (Jeol Ltd., Tokyo, Japan) using a Gatan Ultrascan 4000 (Gatan Ltd., USA).

2.2.7 Zeta potential analysis

The zeta potential of liposomes was analysed using a Zetasizer Nanoseries (Malvern Instruments Ltd., UK). Liposomal suspension was shaken and 70 μl was transferred using a Gilson pipette into a polystyrene latex cell (Malvern Instruments Ltd., UK). The temperature was set at 25°C and an equilibration time of two minutes was allowed.

The zeta potential is a term used to describe the potential difference between a conducting liquid and the surface of a solid particle immersed in the liquid (Maherani *et al.*, 2012). It is calculated by determining the velocity of particles in an electric field, also known as the electrophoretic mobility of the particles (Equation 1):

$$U_E = \frac{2\varepsilon z f(ka)}{3\eta} \quad (1)$$

where,

U_E : Electrophoretic mobility

ε : Dielectric constant

z : Zeta potential

η : Viscosity

$f(ka)$: Henry's function.

Laser Doppler Velocimetry (LDV) is the technique used to measure the electrophoretic mobility of particles in the Zetasizer instrument. LDV measures the light scattering fluctuation intensity of particles proportional to their speed in an electric field (Figure 2.3) (Malvern-Instruments, 2004).

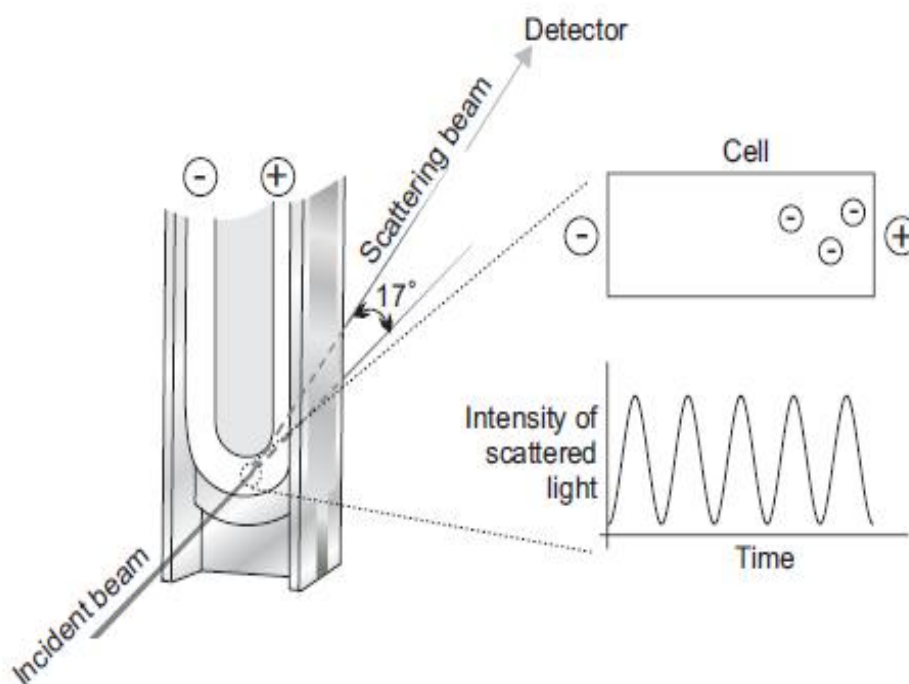


Figure 2.3: A schematic representation of the mechanism of action of LDV in the Zetasizer instrument. (Adapted from Malvern-Instruments, 2004)

2.2.8 Drug entrapment studies

The liposomal suspensions were centrifuged using a Beckman LM-80 ultracentrifuge with a 70.1 Ti fixed angle rotor (Beckman Coulter Instruments, UK) at a speed of 55,000 rpm (277,000 x g) for 45 minutes at 6 °C. The supernatant was then collected and analysed for SS, OVA or IgG.

The concentration of SS was assessed using UV spectrophotometry Biowave II UV/Visible Spectrophotometer (Biochrom WPA Ltd., UK) at 288 nm. A calibration curve of SS was constructed using SS drug concentrations between 1 to 100 µg/ml, and drug in the supernatant of the liposome samples

was quantified accordingly. The entrapment efficiency was calculated using Equation 2:

$$\text{Entrapment efficiency} = \frac{W_{\text{total drug}} - W_{\text{free drug}}}{W_{\text{total drug}}} \quad (2)$$

where “ $W_{\text{total drug}}$ ” represents the total mass of the drug initially used and “ $W_{\text{free drug}}$ ” represents the mass of the free drug detected in the supernatant after centrifuging the liposomal dispersion.

Bicinchoninic acid (BCA) colorimetric method was used for the analysis of OVA (Smith *et al.*, 1985). This method based on the reduction of Cu^{+2} ions by the protein, reduced Cu^{+2} into Cu^{+1} employing OVA. This caused the reduced copper ions to chelate with 2 molecules of bicinchoninic acid, forming a water-soluble, purple-coloured complex which could be detected at 595 nm.

Samples (25 μl each) were pipetted into a 96-well Nunc-Immuno Maxisorp polystyrene plates (Fisher Scientific, UK), followed by the addition of 200 μl of the working reagent. The well plate was then placed on a plate shaker for 30 seconds and incubated at 37°C for 30 min. The plate was then transferred to an Anthos HTII Absorbance Microplate Reader (Anthos, Krefeld, Germany) and their absorbance was measured at 595 nm. There was no specific end point when this method was used, since the colour continued to develop over time. Therefore, the plate was quickly transferred from the incubator and immediately assayed. The working reagent in this method was prepared by mixing 25 ml of working reagent A, containing sodium carbonate, sodium bicarbonate, bicinchoninic acid and sodium tartrate in 0.1 M sodium hydroxide; and 0.5 ml working reagent B, containing 4% cupric sulphate, as described in the BCA protein assay kit instruction manual (Pierce scientific, 2011). A calibration curve of OVA was constructed using OVA protein at standard concentrations of 25-2000 $\mu\text{g}/\text{ml}$, and the protein in the samples was quantified accordingly.

HPLC analysis was performed to determine the entrapment efficiency of IgG using an Agilent SEC5 5 μM - 300A column. The detection wavelength was 280 nm using an Agilent 1200 series HPLC system (Agilent Technologies,

Palo Alto, CA). The mobile phase used was PBS (pH 7.2) at a flow rate of 1 ml/min. A calibration curve was constructed by measuring the peak area of protein standards with concentrations between 10-500 ng/ml using an injection volume of 20 μ l.

The peak areas of the samples were recorded and compared against the standard curve peak areas to determine the amount of protein present in the supernatant, thereby estimating the entrapment efficiency of the protein in the liposomal dispersions.

2.2.9 Determination of the secondary structure of IgG

The secondary structure of IgG was determined in this study using the technology of Circular Dichroism (CD). CD measured the difference in absorbance between the left- and right-handed circularly polarised light by optically active substances as a function of wavelength (Fasman, 1996; Whitmore and Wallace, 2008). Based on the sensitivity of far-UV CD to the conformation of IgG, the % α -helix, β -sheet, β -turns and unordered contents of IgG molecules were determined (Kelly *et al.*, 2005; Martin and Schilstra, 2008).

CD experiments were performed using a J-815 spectropolarimeter (Jasco, UK) coupled to a Peltier Jasco CFF-426S system for temperature control, as previously described by Greenfield (2006). Far-UV CD spectra were collated at 20°C for IgG in water (2.59 μ M) and incorporated into the liposomal structure. Four scans per sample were performed over a wavelength range of 260 to 180 nm, 0.5 nm intervals with a band width of 1 nm, a scan speed of 100 nm/min and a path length of 1 mm. The overall secondary structure for each CD spectra was estimated using a secondary structure algorithm CDSSTR (protein ref. set 3 comprising 37 proteins) using DICHROWEB (Greenfield, 2006). Furthermore, using a thermostated optical cell, the measurements were performed at temperature intervals of 10°C within the

range between 20 and 80°C, and the secondary structure was determined at each temperature.

2.2.10 Immunoreactivity of IgG

An IgG Easy titre kit was used to measure the immunoreactivity of the protein. Polystyrene beads coated with anti-IgG antibodies were used in this assay. Those beads absorb light at 405 and 340 nm and aggregate when mixed with samples containing IgG. As a result of aggregation a decrease in absorption of light occurs.

For the assay of the active IgG present in the samples, the microsensitized IgG beads were first mixed vigorously to avoid sedimentation, and 20 µl were pipetted into a 96 well microtiter plates (Nunc-Immuno Maxisorp, Fisher UK). Samples were then diluted to 1:40,000 using the dilution buffer provided by the kit, and 20 µl of the diluted samples were then added into the wells containing the beads. The microplate was then mixed for 5 minutes in a plate shaker. 100 µl of the blocking buffer was then added to the wells and vigorous shaking for 10 minutes then took place. The absorbance of the microplate was then read at 405 and 340 nm using a Tecan Genios Pro™ microplate reader (Durham, NC, USA). A standard curve of IgG was constructed via dilution of IgG (concentration of 100 µg/mL) using the dilution buffer provided with the kit to obtain concentrations between 25-2000 ng/ml. The standard curve samples were run simultaneously to the IgG samples in each well of the plate. The standard curve data were then plotted on a semi-log scale and the IgG concentration in the samples was determined by interpolating between the points on the curve (Pierce scientific, 2010).

2.2.11 Determination of nebuliser performance

As elucidated in Section 1.2.4.3, various kinds of nebulizers exist. In this study, three types of nebulizers were used:

- 1) Pari Turbo boy air-jet/Pari Master compressor (Pari GmbH, Germany),
- 2) Polygreen ultrasonic nebuliser (Clement Clarke International, UK),
- 3) Omron Micro Air NE-U22 vibrating-mesh nebuliser (Omron Healthcare, UK Ltd., UK).

For the determination of the nebulisation time several end points exist, and determination is dependent on whether the nebulisation time is determined until all the mist production is ceased, or until nebulisation becomes erratic (Kradjan and Lakshminarayan, 1985). In this study, the time required for aerosol generation to become erratic was determined as the “nebulisation time”. Further tapping of the nebuliser leads to continuation of the erratic aerosolisation that is referred to as “sputtering” and the duration of this behaviour until complete cessation of aerosol generation (“dryness”) was also determined in the study and referred to as the “sputtering duration”.

IgG solution, non-sonicated liposomes or probe-sonicated liposomes (5 ml) were placed in the nebulizer; positioned against a vacuum line. The nebulisation time and sputtering duration of the different formulations in the different nebulisers was then determined.

Furthermore, aerosol mass output (%) was determined gravimetrically by measuring the difference in the weight of the nebulizer before nebulization and after achieving “dryness” (Equation 3):

$$\text{Mass output (\%)} = \frac{\text{weight of nebulised formulation}}{\text{weight of formulation present in the nebuliser prior to nebulisation}} \quad (3)$$

Also, the aerosol output rate was determined for the different formulations using the different nebulisers (Equation 4):

$$\text{Aerosol output rate (mg/min)} = \frac{\text{weight of nebulised formulation}}{\text{time required to reach dryness}} \quad (4)$$

2.2.12 Determination of aerosol size distribution

The fluid (5 ml) was placed in the nebulizer, which was then clamped 2.5 cm away from the beam centre of the Malvern Spraytec laser diffraction instrument (Malvern Instruments Ltd., UK) or the Model 3321 Aerodynamic Particle Sizer[®] (APS) Spectrometer (TSI, UK).

The Malvern Spraytec uses the technique of laser diffraction to measure the droplet size distribution (Figure 2.5). The aerosol clouds generated from the nebulisers were drawn through the laser beam of the Spraytec and the angular intensity of the scattered light was measured. These measured intensities are used to determine the VMD and size distribution (SPAN) of droplets. The lens systems used in the Malvern Spraytec are 300 and 750 mm, covering a 0.1 – 2000 micron dynamic range (Malvern spraytec manual).

On the other hand, the APS spectrometer uses the TOF technology to measure the mass median aerodynamic diameter (MMAD) of the aerosol particles. The APS accelerates the aerosol through an accelerating orifice into two partially overlapping laser beams in the detection area. As the particles cross these overlapping beams they get scattered and by means of an elliptical mirror the scattered light is collected and focused onto a photodetector. The use of two partially overlapping laser beams results in the generation of a single two-crested signal by each particle. The time difference between the two signal peaks are then used to determine the aerodynamic particle size of the aerosol (Mitchell *et al.*, 2003).

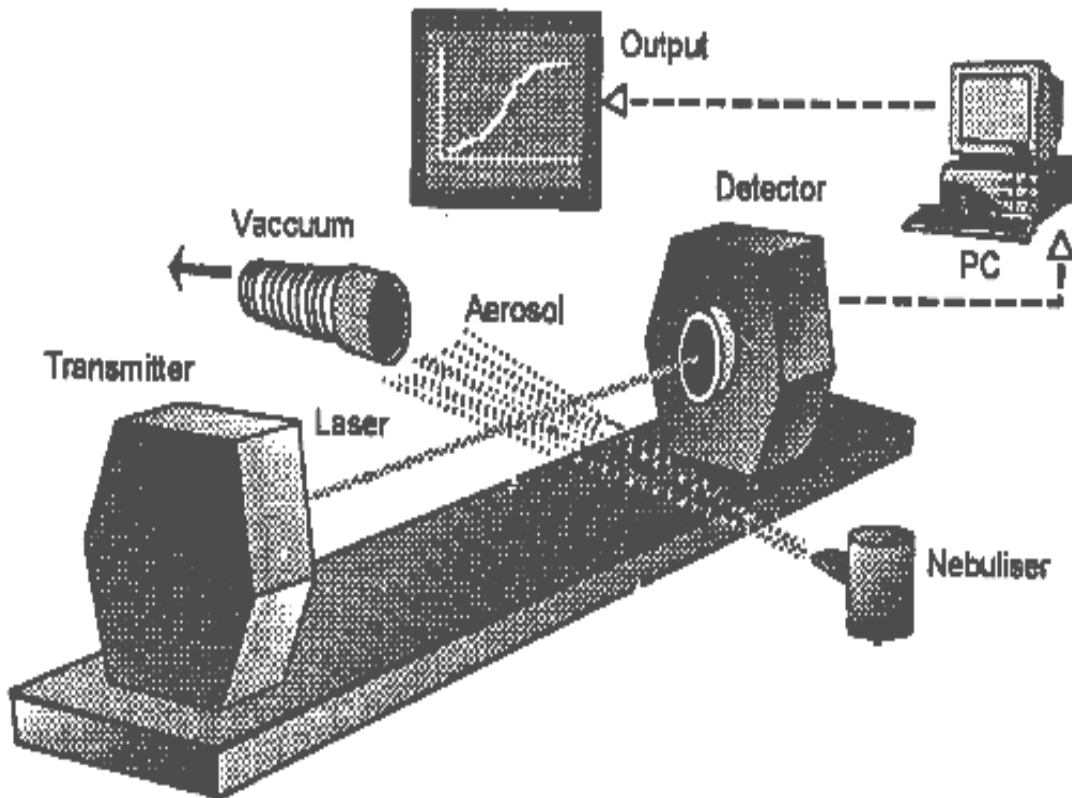


Figure 2.4: Schematic diagram illustrating analysis of aerosol droplets generated from a nebuliser via the laser diffraction principle. (Adapted from Elhissi, 2005)

In addition to the average aerosol size and SPAN, the percentage of aerosol droplets below $5\mu\text{m}$, also referred to as “fine particles fraction (FPF)” (O’Callaghan and Barry, 1997), was also examined in this study. Furthermore, the FPF output was also determined. The FPF output was determined in relation to (1) mass output or (2) active protein output (Figure 2.6).

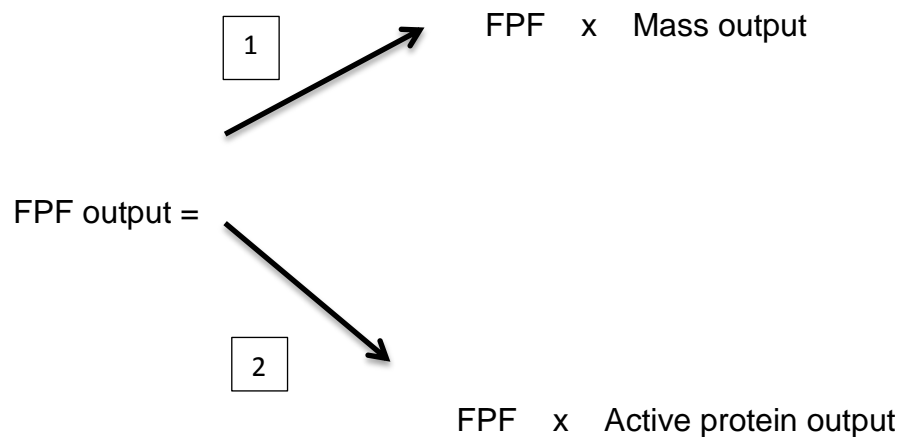


Figure 2.5: FPF output equations: (1) FPF output in relation to mass output; (2) FPF output in relation to active protein output

2.2.13 Determination of the shot weight and dose accuracy of nasal devices

In this study, three commercially available nasal devices were used: A mucosal atomisation device (MAD) (Wolfe Tory Medical, Inc., Salt Lake City, UT) and two different metered dose nasal pump sprays, which were referred to as device A (Model VP3/93, Valois) from a Beconase[®] aq. nasal spray, and device B (Model VP7/100, Valois) from a Nasacort[®] aq. nasal spray. The metered dose pump spray containers were emptied from the original formulations and washed thoroughly with water and water and ethanol mixture and left to dry overnight at 37 °C before conducting further experiments.

Prior to the use of nasal sprays, a number of priming actuations are required to purge the air off the system and dip tube to achieve the full dose (Marx and Birkhoff, 2011). The number of actuations required to prime the nasal devices, and the number of full actuations delivered by the nasal devices were determined. Moreover, as the volume of formulation in the nasal device becomes low, degradation in the accuracy of the device can be noticed (i.e. non-uniform dose emitted). This observation, known as “tailing-off” (Schultz, 1995), continued until complete cessation of spray generation. The number of actuations required in the tail-off phase was also determined in this study for the different nasal devices and formulations.

In addition to the number of actuations required by each nasal device, the shot weight, which was a measure of the emitted dose from a single actuation through the nasal devices (Guo and Doub, 2006), was also determined. This was achieved by recording the weight of the nasal device before and after each actuation. The shot weight could be used to confirm the dose consistency of the nasal devices. Also, shot weight could give indication on the number of actuations required to prime the device, number of full actuations delivered and number of actuations in the tail-off phase.

IgG solution, non-sonicated liposomes or probe-sonicated liposomes (5 ml) were placed in the nasal devices and the number of actuations required to prime the different devices were determined. Moreover, the number of full actuations delivered via the devices and the number of actuations in the tail-off phases were determined. Furthermore, the shot weight was measured for the different formulations using the different nasal devices.

2.2.14 Determination of nasal spray characteristics

The characteristics of the spray cloud generated from the nasal devices could be assessed by a variety of means, including droplet size distribution (DSD), spray pattern and plume geometry.

DSD studies were performed as outlined earlier in Section 2.2.12, using the principle of laser diffraction via the Spraytec instrument. Spray pattern and plume geometry provided information about the shape of the expanding cloud as it evolved upon actuation. Spray pattern involved measuring the cross sectional uniformity of the spray at specified distances away from the nozzle tip of the nasal spray devices.

Two different measurement techniques were previously described in Centre for Drug Evaluation and Research (CDER) guidelines (2003) for the determination of spray patterns (Mestecky *et al.*, 1997): These techniques were described as impaction and non-impaction techniques. In this study the

impaction technique was employed, which involved the upward firing of the spray into a thin layer chromatography (TLC) sheet (Figure 2.7). Spray pattern was measured at 5 cm from the nozzle tip to the TLC sheet. A phenol red dye was incorporated into the formulations to allow the splatter pattern to be visualized on the TLC plate, making the technique easier and more reliable.

Spray pattern was characterised by the metrics D_{max} , D_{min} and ovality ratio, according to CDER guidelines (2002; 2003). D_{max} was defined as the longest diameter measured on the resulting spray pattern image, whilst D_{min} was the shortest diameter measured on the spray pattern image. The ovality ratio, on the other hand, was the ratio of D_{max} to D_{min} . The ovality provided a quantitative value for the overall shape of the spray (e.g. round or ellipsoid shape).

Plume geometry data involved visualizing and measuring the shape of the emitted plume generated from the nasal devices from a sideward looking view (i.e. parallel to the plume axis). Regulatory guidelines of CDER (2002; 2003) have described two plume geometry visualization techniques: (1) high-speed photography; and (2) laser light sheet and high-speed digital camera.

In this study the high-speed photography technique was employed, which involves the upward firing of the spray against a clear white background and placing a high-speed camera to record the process of nasal spray generation (Figure 2.8).

The time history provided by the high-speed digital imaging for plume geometry analysis could also be used to determine the different phases of spray cloud development (Mestecky *et al.*, 1997): These included (1) the formation phase, wherein the pressure and flow rate through the pump were both low; (2) a fully developed phase, which occurred once the correct atomisation was reached; and (3) a dissipation phase, wherein the flow rate through the pump tailed off towards the end of the actuation cycle (Farina, 2010). The CDER recommended image analysis to be carried out at a time delay corresponding to the fully developed phase of the plume, while the plume was still in contact with the nozzle tip (CDER, 2002; 2003).

Emitted plumes were captured as movie clips at a rate of 25 frames/second using a professional digital camera - LSH Canon 550 D 55 mm – 08 (Cannon Ltd., Tokyo). The clips were then transferred to an Aperture® 3.3.1 software (Apple Inc., US) on a MacBook Pro (OS x Version 10.7.4) for image processing. The frame containing the most fully developed plume was then printed and the resultant image was characterised using the following metrics: the plume angle (measured from the vertex of the spray cone that occurs at or near the nozzle tip), plume width (i.e. the width of the plume at a specified height from the nozzle tip) and plume height per CDER guidance (CDER, 2002; 2003). Spray angles and plume width were determined using a protractor from photographic images printouts whilst the plume height was determined according to corresponding ruler marks displayed on the background.

2.2.15 Statistical Analysis

All experiments were performed in triplicates and values were expressed as mean \pm standard deviations of the mean. Statistical significance was assessed using (ANOVA) and student's t-test, as appropriate. Values with $P < 0.05$ indicate that the difference is statistically significant.

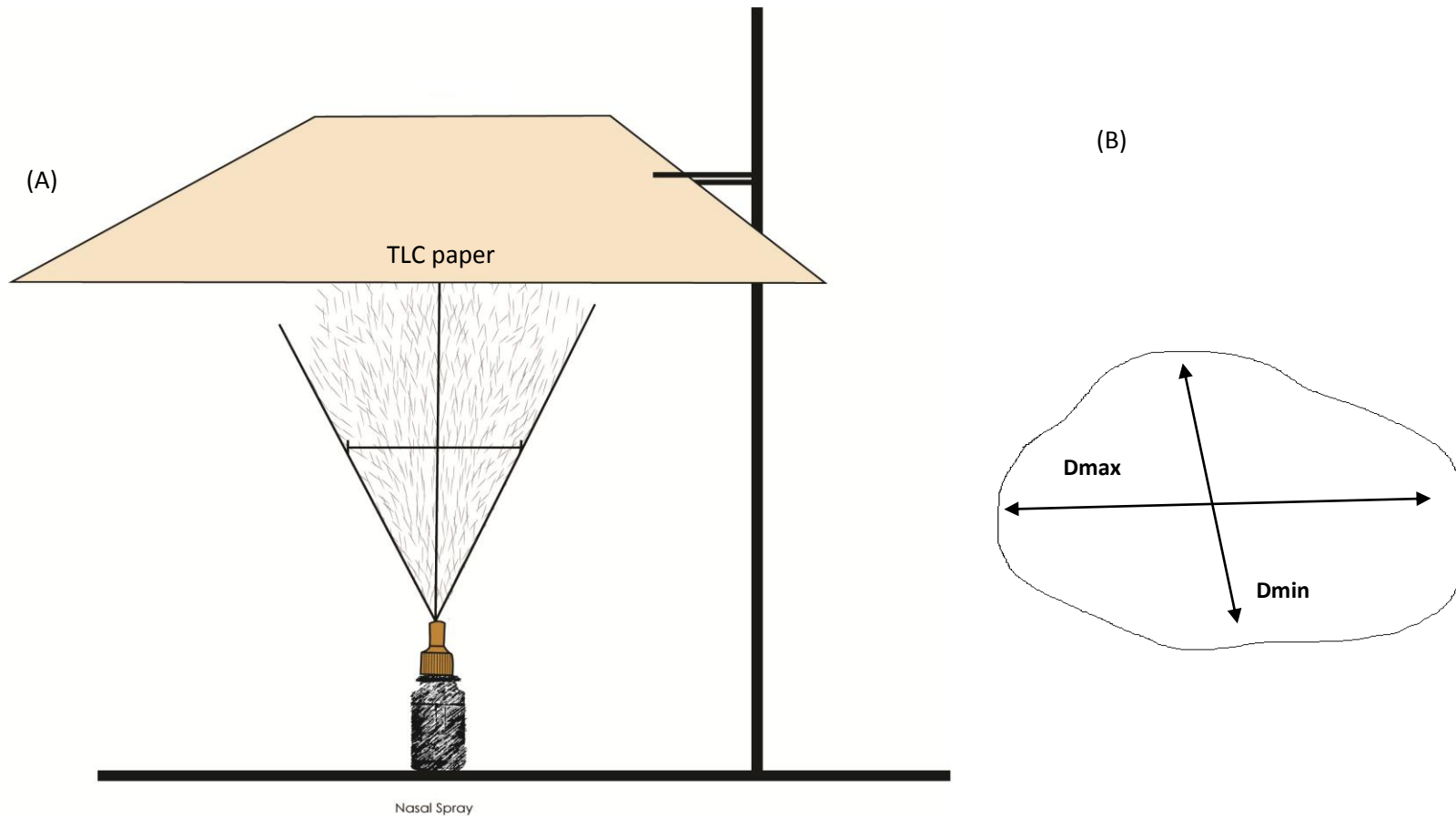


Figure 2.6: A schematic representation of: (A) the impactation technique used to determine the spray pattern of the nasal devices (B) spray pattern example, showing the maximum (D_{max}) and minimum (D_{min}) diameters.

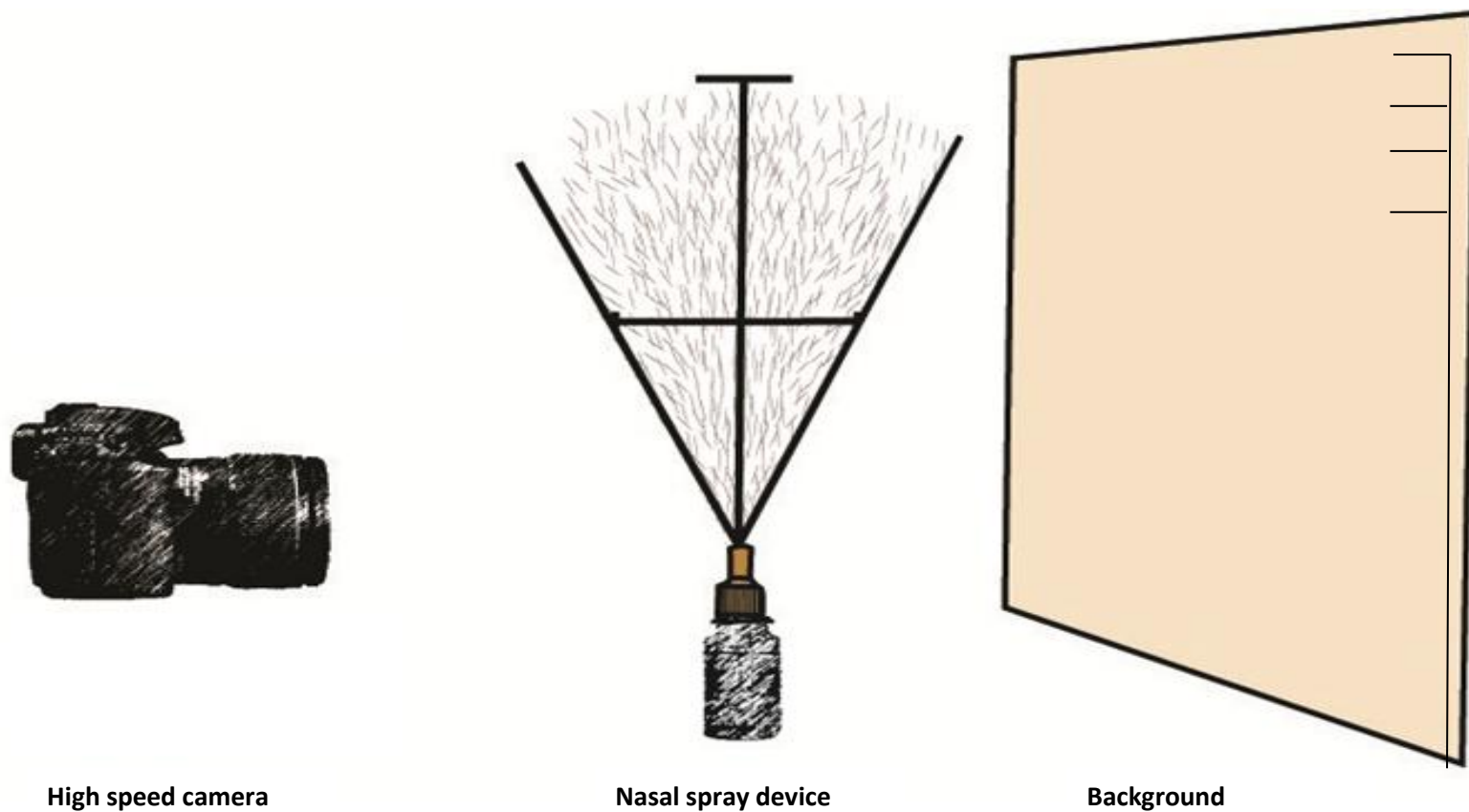


Figure 2.7: A schematic representation of the high speed photography technique used to determine the spray pattern of the nasal devices.

CHAPTER 3

CHARACTERISATION OF LIPOSOMES GENERATED FROM ETHANOL BASED PROLIPOSOMES

3.1 Introduction

Since their discovery, liposomes have become a very common topic in literature, and the field has progressed enormously. Their unique versatility with respect to size, composition and capacity for encapsulating materials has elicited great interest in their application in several areas, ranging from targeted drug and gene delivery to cosmetics (Jesorka and Orwar, 2008). The use of liposomes in drug delivery offers many advantages, mainly due to their being composed of naturally occurring lipids, which makes them biocompatible, biodegradable and non-immunogenic. Moreover, their amphiphilicity allows them to conjugate with both hydrophobic and hydrophilic therapeutic agents. Furthermore, particle size and surface properties of liposomes can easily be manipulated (Webster, 2010). Various methods of liposome preparation have been introduced, giving rise to vesicles of different lamellarities and sizes (Gregoriadis, 1993; Basu and Basu, 2002; Weissig, 2010).

Despite the many advantages liposomes offer, liposome stability is a major problem. Furthermore, other factors that limit the use of conventional liposomes are their low entrapment efficiencies, their large-scale manufacturing difficulties, and short circulation half-lives (Jesorka and Orwar, 2008).

Various strategies have been employed to overcome these limitations; one strategy is by employing proliposome technologies. Proliposomes are stable phospholipid formulations which readily generate liposomes upon the addition of an aqueous phase, thereby overcoming the instability of liposomes (Payne *et al.*, 1986a; Payne *et al.*, 1986b; Perrett *et al.*, 1991).

The physical and chemical characteristics of liposomes determine their *in vitro* and *in vivo* behaviour and various analytical techniques are now understood to establish these characteristics (Torchilin and Weissig, 2003). Amongst the most important parameters to consider when describing a liposome are their size and size distribution. Predictable and reproducible particle size distribution is necessary, since the size of liposomes gives an indication of their circulation time and biodistribution (Litzinger *et al.*, 1994). Furthermore, the surface charge of liposomes can also help to predict their fate *in vivo* (Maherani *et al.*, 2012). In

addition, entrapment efficiency is also a very important factor to be studied when characterising liposomes.

Many approaches have been proposed to enhance the entrapment efficiencies of drugs in liposomes. Amongst those are the incorporation of cholesterol in the liposomal formulation, which enhances the rigidity of the liposomal membrane, thus possibly increasing the entrapment efficiency of drugs and reducing the leakage of the drug encapsulated (Düzgüneş, 2005). Moreover, the addition of mucoadhesive agents to liposomal formulations has also been proposed to enhance the bioavailability of entrapped drugs by prolonging their residence time on mucosal surfaces (Karn *et al.*, 2011). Furthermore, many reports have demonstrated an enhancement in entrapment efficiencies following the addition of mucoadhesive agents to liposomal formulations (Phetdee *et al.*, 2008; Albasarah *et al.*, 2010).

Studies in this chapter involved preparing liposomes using the ethanol-based proliposome method for the entrapment of the model hydrophilic drug SS and the model protein OVA. Parameters involved in the preparation of the liposomes were evaluated in these studies and optimum conditions were established.

In addition, the effect of size reduction of liposomes and the incorporation of the mucoadhesive agent chitosan were evaluated. Liposomes prepared in this chapter were characterised in terms of particle size and size distribution, zeta potential and entrapment efficiency.

3.2 Methodology

3.2.1 Preparation of liposomes

Liposomes were manufactured as previously described in Section 2.2.1 by adapting the ethanol-based proliposome method described by Perrett *et al.*, (1991). Lipid phase (50 mg) comprising SPC or SPC:cholesterol was dissolved in 76 μ l ethanol to form to yield a clear lipid solution (i.e. the proliposomes). For the encapsulating of SS or OVA, SS (1 mg/ml) or OVA (1.7, 2.5, 3.2 or 4 mg/ml)

solutions in HPLC water were prepared and 0.5 ml was quickly added to the proliposomes and vortexed for two minutes to generate concentrated liposomal suspensions (primary hydration step). The suspensions were then further diluted to 5 ml with HPLC water and vortexed again for 2 minutes to yield the final liposomal suspension (secondary hydration step).

3.2.2 Characterisation of liposomes

Liposomes prepared in this study were characterised for (a) size distribution, (b) zeta potential and (c) entrapment efficiency of SS or OVA.

(a) Size of liposomes

The size distribution of generated liposomes was analysed as previously described in Section 2.2.5 using the technologies of: (1) laser diffraction employing the Malvern Mastersizer 2000 instrument (Malvern Instruments Ltd, UK) for measuring the size distribution of liposomes before size reduction; or (2) dynamic light scattering (DLS) employing the Malvern Zetasizer Nanoseries (Malvern Instruments Ltd, UK) for measuring the size of liposomes after size reduction.

(b) Zeta potential

The zeta potential of the generated liposomes was analysed via the (LDV) technique using the Zetasizer Nanoseries instrument (Malvern Instruments Ltd, UK), as elucidated in Section 2.2.7.

(c) Entrapment studies

Entrapment studies were performed as previously described in Section 2.2.8. The liposomal suspensions were centrifuged using a Beckman LM-80 ultracentrifuge device with a 70.1 Ti fixed angle rotor (Beckman Coulter Instruments) at a speed of 55,000 rpm (277,000 x g) for 45 minutes. The supernatant was then collected and analysed for SS or OVA. The concentration of SS was assessed using UV spectrophotometry (Cary 3E UV-Visible spectrophotometer) at 288 nm. BCA colorimetric method was used for the analysis of OVA (Smith *et al.*, 1985).

3.2.3 Phospholipid assay

The phospholipid assay was performed as outlined in Section 2.2.4 to investigate the efficiency of ultracentrifugation in pelleting the liposomes. The protocol of Elhissi *et al.*, (2006b) was performed to form phospholipid films from liposome dispersions. These phospholipid films were then quantified colorimetrically using the Stewart assay (Stewart, 1980).

3.2.4 Size reduction of ethanol based liposomes

Three methods were employed for the size reduction of the generated liposomes, as previously outlined in Section 2.2.3. The first two techniques of size reduction used ultrasonic vibrations via either a bath sonicator (Fisherbrand FB11004, UK) or a probe sonicator (Vibra cell sonicator, Sonics and Materials Inc., Newtown, USA). The third method for size reduction was extrusion using a Liposofast-mini extruder (Avestin, Canada), whereby the liposomal dispersion was sequentially passed through a series of polycarbonate membrane filters having a pore size of 2, 1, 0.8 and 0.4 μm , to yield liposomes of the desired size.

3.2.5 Formulation of mucoadhesive ethanol-based liposomes.

Different concentrations (0.1, 0.2 and 0.3% w/v) of the mucoadhesive agent Protasan G213, an ultrapure chitosan glutamate salt (Novamatrix, Belgium) were dissolved in 4.5 ml HPLC water. The resultant solutions were then employed in the secondary hydration step of the ethanol-based liposomes to generate the mucoadhesive liposome dispersions.

3.3 Results and discussion

3.3.1 Formulation of empty ethanol-based proliposomes

In this section, several factors and their effect on the characteristics of empty liposomal suspensions are explored. These factors were vortex mixing duration, dilution, storage stability and sample volume.

(a) Vortex mixing duration

As indicated in Section 3.2.1, the ratio of lipid to ethanol (50:60 w/v) was used in the preparation of liposomes, which was adapted from the method introduced by Elhissi *et al.*, (2006a). However, unlike the aforementioned method, to optimize the shaking of the liposomal dispersions, vortex mixing was employed instead of manual shaking during both the primary and secondary hydration. The effect of vortexing duration on the size and SPAN of liposomes was investigated (Figure 3.1). As illustrated in Figure 3.1a, when the vortexing duration was prolonged from 30 seconds to 120 seconds, the size of the liposomes generated significantly decreased ($p < 0.05$) from $4.73 \pm 0.51 \mu\text{m}$ to $3.68 \pm 0.32 \mu\text{m}$. However, further increase in the vortexing duration to 180 seconds did not have any significant effect on the size of liposomes ($p > 0.05$), as the liposome size was $3.57 \pm 0.29 \mu\text{m}$. The same effect was also found for the SPAN (Figure 3.1b) so that when vortexing

duration was increased from 30 seconds to 120 seconds the SPAN value decreased ($p < 0.05$) from 2.60 ± 0.36 to 1.73 ± 0.21 , respectively. Further increase in vortexing time to 180 seconds did not cause any significant change ($p > 0.05$) in the SPAN of liposomes (SPAN = 1.55 ± 0.17). The initial decrease in size and size distribution of liposomes might be attributed to the deaggregation of liposomes and possibly some size reduction of large vesicles.

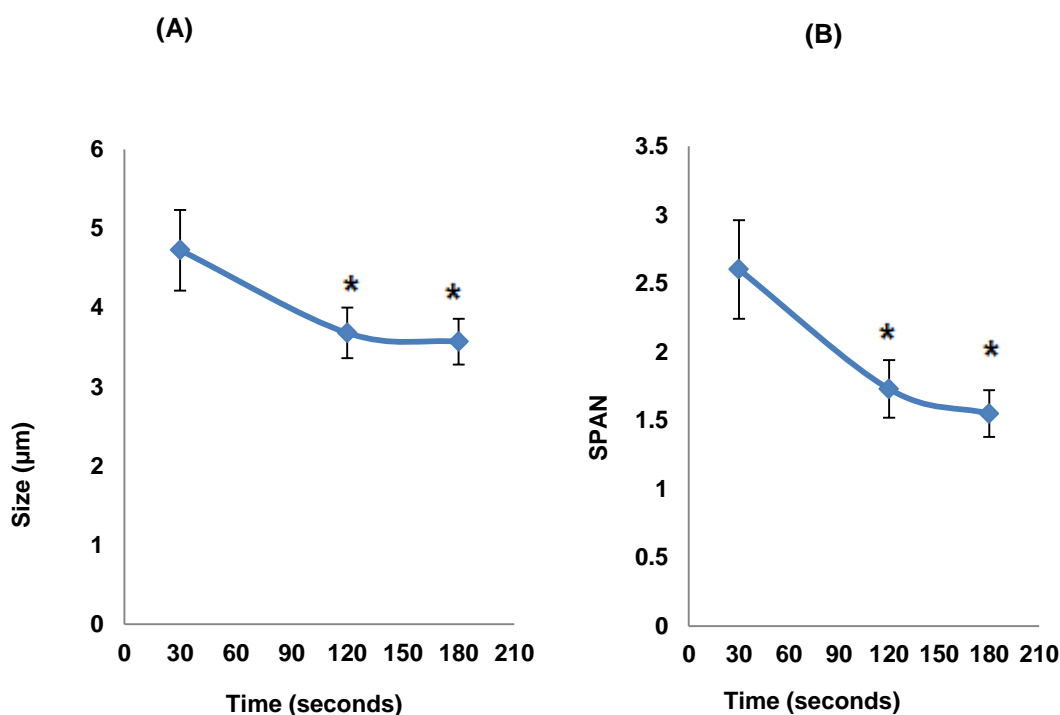


Figure 3.1: Relationship between (A) vortexing duration and liposome size and (B) size distribution of the generated liposomes during hydration steps. Data are mean \pm SD, $n=3$; * $p < 0.05$ for 120 seconds and 150 seconds compared to 30 seconds.

Early experiments by Payne *et al.*, (1986a) indicated that if liposomes were hydrated under extremely mild conditions in the absence of high shear forces (i.e. no shaking), a significant upward shift in the size of liposome could happen. When the duration of vortexing increased above 120 seconds no significant changes ($p > 0.05$) in the SPAN and VMD of the generated liposomes were found, thus indicating that 120 seconds is the optimal vortexing duration in the study. The outcome of the vortexing time optimization was found to be analogous to that of the method followed by Dufour *et al.*, (1996).

(b) Dilution of liposomes

The effect of dilution on the size, size distribution and zeta potential of liposomes was also investigated (Table 3.1). As demonstrated in Table 3.1, dilution of the liposomal dispersions did not have any influence on the size, SPAN or zeta potential of the liposomes ($p > 0.05$).

Table 3.1: Size, SPAN and zeta potential of liposomes before and after dilution. Data are mean \pm SD, n=3; $p > 0.05$ for all measured parameters.

	Size (μm)	SPAN	Zeta potential (mV)
Original sample (10 mg/ml)	3.28 \pm 0.35	1.43 \pm 0.37	-4.67 \pm 0.62
Diluted sample (5 mg/ml)	3.40 \pm 0.51	1.39 \pm 0.23	-4.31 \pm 0.54

(c) Stability of liposomes

The physical stability of liposomes upon storage in the fridge at (5 ± 1 °C) for one week was investigated. Liposomes properties such as size, polydispersity and zeta potential have been previously used to monitor the stability of liposomes and can give an indication of the possible degradation, aggregation or fusion of liposomes (Du Plessis *et al.*, 1996; Sabin *et al.*, 2005; 2006).

In a study conducted by Sabin *et al.*, (2005), the stability of liposomes to the addition of Ca^{2+} and La^{3+} ions was monitored by means of measuring the size, polydispersity and surface charge. Results from their study have demonstrated that aggregation of liposomes was demonstrated by an increase in the size and polydispersity of the liposomes, whilst fusion of liposomes was demonstrated only by an increase in the liposome size not polydispersity. A decrease in the zeta potential values was also observed as a result of fusion or aggregation.

In this study, liposomes were stored in the fridge (5 ± 1 °C) for one week, and every day a sample of the liposome dispersion was taken and analysed for size, SPAN and zeta potential (Figure 3.2). Figure 3.2 illustrates that the size of liposomes did

not markedly change ($p>0.05$) upon storage over the duration of one week, with no apparent trend of particle size increase or decrease.

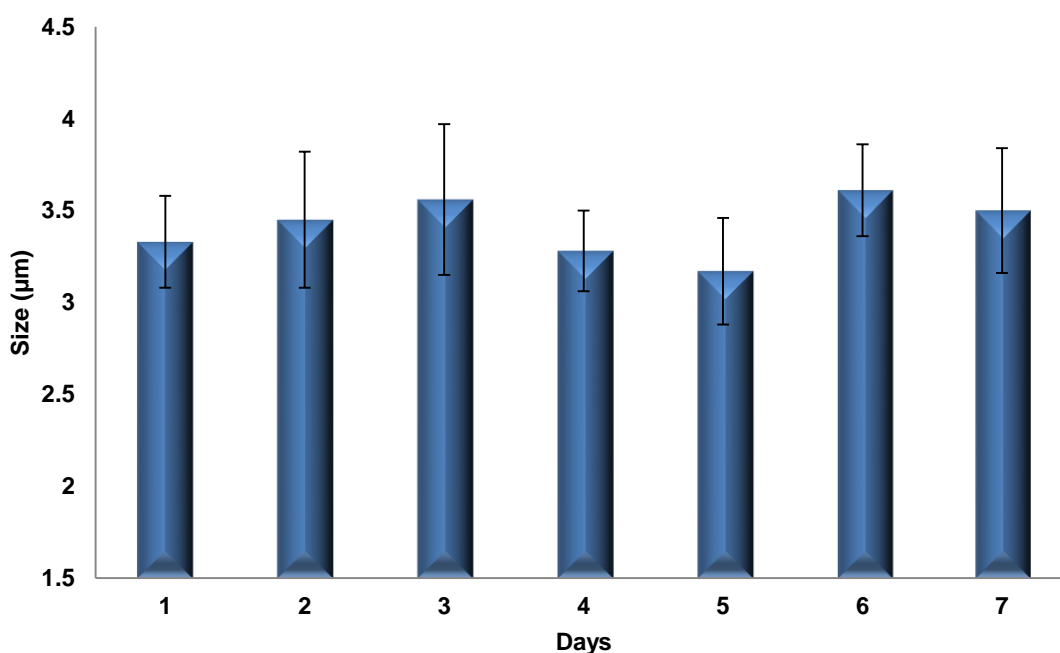


Figure 3.2: Size of liposomes during one week storage at 5 ± 1 °C. Data are mean \pm SD, $n=3$; $p>0.05$ for all.

The SPAN of liposomes was also measured for the same duration and no significant change ($p>0.05$) was observed. Moreover, no trend of increase or decrease in the SPAN values was apparent (Figure 3.3). Size and SPAN measurements therefore indicated that no fragmentation or aggregation occurred to the liposomes over the one week of storage at 5 ± 1 °C. The zeta potential values were also not affected ($p>0.05$) by the storage for one week (Figure 3.4), giving further indication that liposomes generated from ethanol-based proliposomes does not aggregate or fuse when stored at 5 ± 1 °C for a duration of at least one week.

Early findings by Hernandez-Caselles *et al.*, (1990) demonstrated that storage at 4 °C may stabilise liposomes by reducing the rate of lecithins hydrolysis into lysolecithins. Furthermore, the slightly negative charge on the liposomal surfaces could also decrease the fusion and aggregation between liposomes, since repulsion between liposomes could decrease the rate of fusion and enhance the physical stability of liposomes (Riaz, 1995).

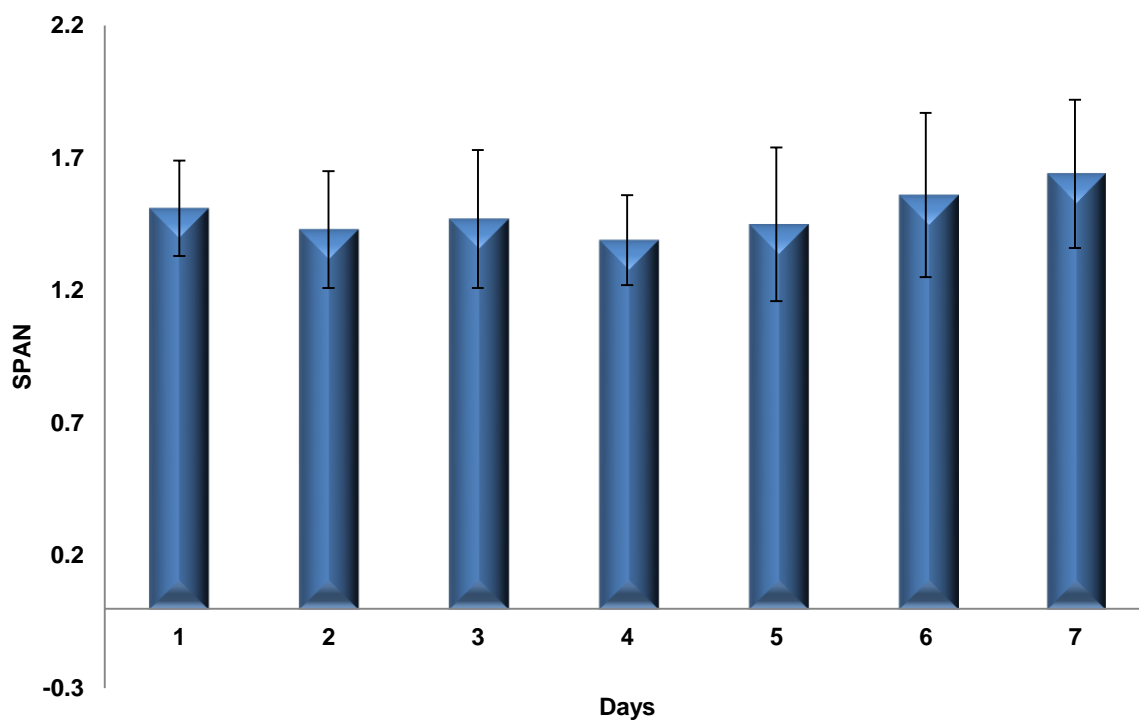


Figure 3.3: SPAN of liposomes during a week interval of storage at a temperature of 5 ± 1 °C. Data are mean \pm SD, $n=3$; $p>0.05$ for all.

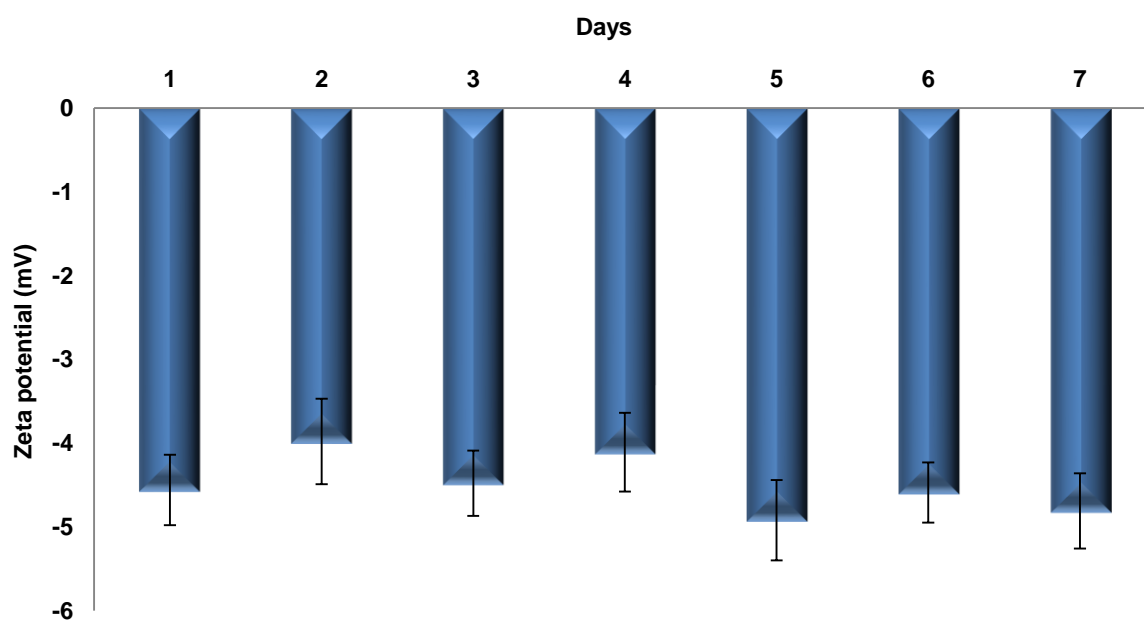


Figure 3.4: Zeta potential of liposomes during a week interval of storage at a temperature of 5 ± 1 °C. Data are mean \pm SD, $n=3$; $p>0.05$ for all zeta potential measurements.

(d) Sample volume

Another study that was performed is investigating whether manufacturing large volumes of the liposomes would affect their properties. This study might indicate whether further work to explore the scaling-up potential of liposomes is worth consideration. The ratios of lipid, ethanol and aqueous phase were kept constant and the effect of preparing samples of final volumes of 5, 10, 20 and 30 ml was studied (Table 3.2).

As can be seen in Table 3.2, the size, zeta potential and SPAN of the liposomes were not affected ($p>0.05$) by sample volume. This finding could thus be advantageous and give an indication of the possible scaling-up potential of liposomes prepared via the ethanol-based proliposome method.

Table 3.2: Effect of sample volume on size, SPAN and zeta potential of the generated liposomes. Data are mean \pm SD, n=3; $p>0.05$ for all.

Formulation	Size (μm)	SPAN	Zeta potential (mV)
5 ml sample (10 mg/ml)	3.39 \pm 0.41	1.61 \pm 0.34	-4.53 \pm 0.28
10 ml sample (10 mg/ml)	3.45 \pm 0.33	1.48 \pm 0.26	-4.31 \pm 0.46
20 ml sample (10 mg/ml)	3.10 \pm 0.52	1.55 \pm 0.23	-4.43 \pm 0.39
30 ml sample (10 mg/ml)	3.28 \pm 0.27	1.39 \pm 0.41	-4.70 \pm 0.23

3.3.2 Preparation of SS liposomes

A small hydrophilic bronchodilator molecule of pKa 9.2, SS (Figure 3.5), was considered for entrapment in liposomes. The effect of incorporation of SS in the liposomal formulation on the size, SPAN and zeta potential was investigated in this study (Table 3.3).

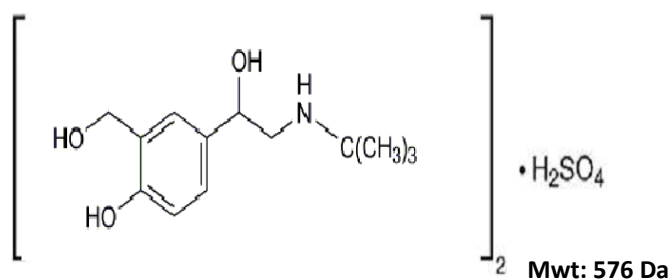


Figure 3.5: Chemical structure of salbutamol sulphate.

As demonstrated in Table 3.3, when compared to drug-free vesicles, inclusion of SS in the liposome formulation caused no significant effects ($p>0.05$) on size, SPAN or zeta potential.

Table 3.3: Comparison between liposomes with and without SS. Data are mean \pm SD, n=3; $p>0.05$ for all.

Formulation	Size (μm)	SPAN	Zeta potential (mV)
Empty liposomes	3.39 \pm 0.41	1.61 \pm 0.34	-4.53 \pm 0.28
SS liposomes	3.25 \pm 0.32	1.53 \pm 0.26	-4.66 \pm 0.37

The effect of cholesterol incorporation in SS-containing formulations on size, size distribution, zeta potential and entrapment efficiency of SS was also investigated (Table 3.4).

Table 3.4: Size, zeta potential and SS entrapment efficiency using liposome formulations having different cholesterol concentrations. Data are mean \pm SD, n=3; * $p<0.05$ for SPC:Cholesterol (1:1) or SPC:Cholesterol (2:1) compared to SPC (no cholesterol).

Formulation	Size (μm)	SPAN	Zeta potential (mV)	Entrapment efficiency (%)
SPC (no cholesterol)	3.25 \pm 0.32	1.53 \pm 0.26	-4.66 \pm 0.37	46.31 \pm 3.97
SPC: cholesterol (2:1)	3.37 \pm 0.28	1.61 \pm 0.31	-4.44 \pm 0.45	59.12 \pm 5.18 *
SPC: cholesterol (1:1)	3.41 \pm 0.55	2.42 \pm 0.43 *	-4.51 \pm 0.52	59.53 \pm 5.09 *

It was proposed by Presti *et al.*, (1982) that cholesterol may associate itself with the phospholipid chains by forming hydrogen bonds between its β -OH groups and the carbonyl groups of the phospholipid molecules, resulting in changes in the properties of the liposomal membranes. As shown in Figure 3.6, cholesterol is incorporated into the phospholipid bilayers by orienting its hydroxyl group towards the aqueous phase and inserting its hydrophobic chain alongside the hydrocarbon chains of the phospholipid. This assembly of cholesterol in the lipid bilayer tends to reduce the motion of the alkyl chain of the lipid whilst giving more space to the terminal carbons to move (New, 1990).

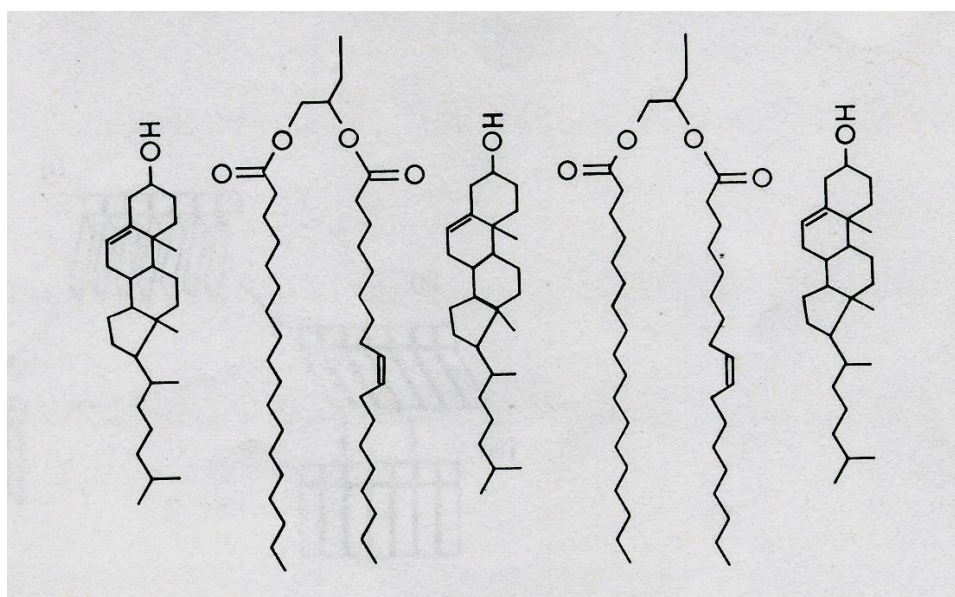


Figure 3.6: The assembly of cholesterol between phospholipid molecules. (Adapted from New, 1990).

As demonstrated in Table 3.4, cholesterol concentration did not affect the size or zeta potential of liposomes ($p > 0.05$). This finding was in agreement with that of Rengel *et al.*, (2002), who reported that cholesterol inclusion does not affect the surface charge of liposomes. Also, using the ethanol-based proliposome method, Elhissi *et al.*, (2006a) reported no change in the size of liposomes entrapping SS when different ratios of cholesterol were included.

Whilst inclusion of cholesterol had no effects on the size and zeta potential of the liposomes, it was found to markedly increase the SPAN value ($p < 0.05$) at high

cholesterol concentrations (SPC: cholesterol, 1:1) (Table 3.4). This increase in the SPAN could be an indication of liposome aggregation. Figure 3.7 compares the size distribution for both the 1:1 and 2:1 SPC: cholesterol liposomes. As demonstrated in Figure 3.7, the size distribution of liposomes having 1:1 (SPC: cholesterol) is broader than that of liposomes having the ratio 2:1, indicating the presence of liposome aggregates upon inclusion of high cholesterol concentrations. This possibly indicates that cholesterol was not fully accommodated by the liposome bilayers, suggesting that using lower cholesterol concentrations (e.g. 2:1 phospholipid to cholesterol ratio) may be most appropriate when the ethanol-based proliposome method is employed.

It has been demonstrated that when the proportion of cholesterol is higher than that of phospholipid, the lipid bilayers become too rigid and the fluidity of the membrane decreases, causing lower entrapment efficiency (Wang and Huang, 2003), necessitating the optimisation of bilayer rigidity.

Moreover, as shown in Table 3.4, the entrapment efficiency of SS was found to significantly increase ($p < 0.05$) when cholesterol was included. However, no difference in drug entrapment efficiency was found upon using phospholipid to cholesterol ratios of 2:1 or 1:1. The entrapment efficiency values of the cholesterol-based liposomes (approximately 60%) were highly similar to those found by Elhissi *et al.*, (2006a), that the entrapment of SS in liposomes generated from ethanol-based proliposomes was 62.2%.

The enhanced entrapment as a result of inclusion of cholesterol might be attributed to the fact that the presence of cholesterol in liposomal preparations decreased the liposome membrane fluidity, which thus reduced the leakage of the encapsulated material, as also previously reported by other investigators (Betageri, 1993). Inclusion of cholesterol leads to a decrease in the rotational freedom of the hydrophobic phospholipid chains and may eliminate the phase transition of the phospholipid, leading to reduction of drug leakage (Sharma and Sharma, 1997; Zhang *et al.*, 2009).

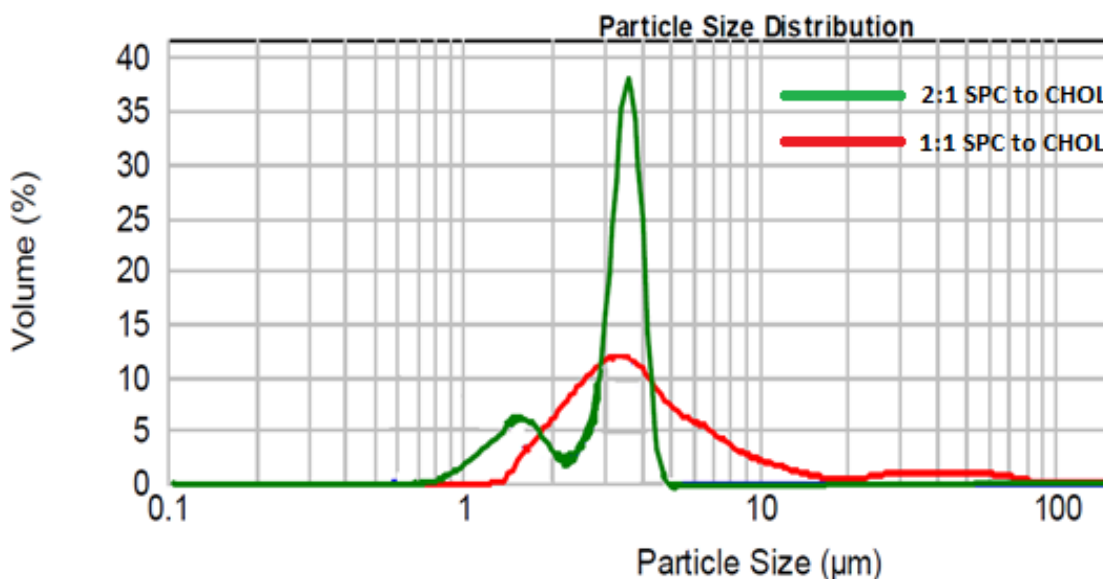


Figure 3.7: Relationship between cholesterol concentration in the lipid phase and particle size distribution of liposomes. Data are mean \pm SD, n=3; Typical of 3 different experiments.

3.3.3 Preparation of OVA liposomes

OVA is a 45 kDa protein purified from chicken eggs and widely used in immunology (McCullough and Summerfield, 2009). Due to the high expense of vaccines, and the promise shown by OVA as a model protein in liposome characterisation, OVA has been used as an alternative to protein vaccines in characterisation studies (McCullough and Summerfield, 2009).

The effect of incorporating different concentrations of OVA into the liposome formulations and the effect of that on size, SPAN, zeta potential and entrapment efficiency was investigated in this study.

The inclusion of different concentrations of OVA has been found not to markedly affect ($p > 0.05$) the size or SPAN of the generated liposomes (Table 3.5). The size and SPAN values of the liposomes remained unaffected even when OVA concentrations were as high as 4.0 mg/ml. These results agree with the findings of Dini *et al.*, (1991), who also found no change in the size of liposomes as a result of using different concentrations of bovine serum albumin (BSA), which is of similar structure to OVA.

Table 3.5: Size, SPAN and zeta potential of liposomes having a range of OVA. Data are mean \pm SD, n=3; $p>0.05$ for size and SPAN; * $p<0.05$ for zeta potential.

Concentration of OVA (mg/ml)	Size (μm)	SPAN	Zeta potential (mV)
0.0	3.39 \pm 0.41	1.61 \pm 0.34	-4.66 \pm 0.37
1.7	3.46 \pm 0.38	1.56 \pm 0.29	-6.37 \pm 0.47*
2.5	3.37 \pm 0.54	1.64 \pm 0.31	-6.71 \pm 0.39*
3.2	3.29 \pm 0.46	1.51 \pm 0.37	-6.68 \pm 0.51*
4.0	3.25 \pm 0.33	1.39 \pm 0.44	-6.80 \pm 0.45*

Unlike size and size distribution, the zeta potential was markedly affected by OVA inclusion. The zeta potential has significantly increased ($p<0.05$) by becoming more negative as a result of inclusion of 1.7 mg/ml OVA. This could be attributed to the fact that OVA exhibits a negative charge in aqueous media (Brgles *et al.*, 2008). However, when the concentration of OVA was increased above 1.7 mg/ml there was no significant change ($p>0.05$) in the zeta potential of the liposomes, possibly indicating that higher OVA concentrations do not associate with the liposome bilayers and hence no further effect on the liposome surface charge was observed.

The effect of increasing OVA concentration in the liposomal formulation on the entrapment efficiency of the protein was also investigated (Figure 3.8). Figure 3.8 shows that the entrapment of OVA protein in liposomes was significantly dependent ($p<0.05$) on the protein concentration, with higher OVA concentrations resulting in lower entrapment efficiencies. The highest entrapment value was 43.30 \pm 3.91% (OVA concentration = 1.7 mg/ml), whilst the lowest was 25.82 \pm 4.18 (OVA concentration = 4 mg/ml). These results suggest that OVA is associated with the liposome bilayers, which may have certain capacity to accommodate the protein.

Korsholm *et al.*, (2007) reported similar findings, whereby the binding of OVA to liposomes decreased by more than 60% when the concentration of OVA increased from 1 mg/ml to 10 mg/ml. Similarly, Wang and Huang (2003) have demonstrated that for BSA liposome formulations, an increase in BSA content from 1 to 3 mg was associated with a drop in the entrapment efficiency by 30%.

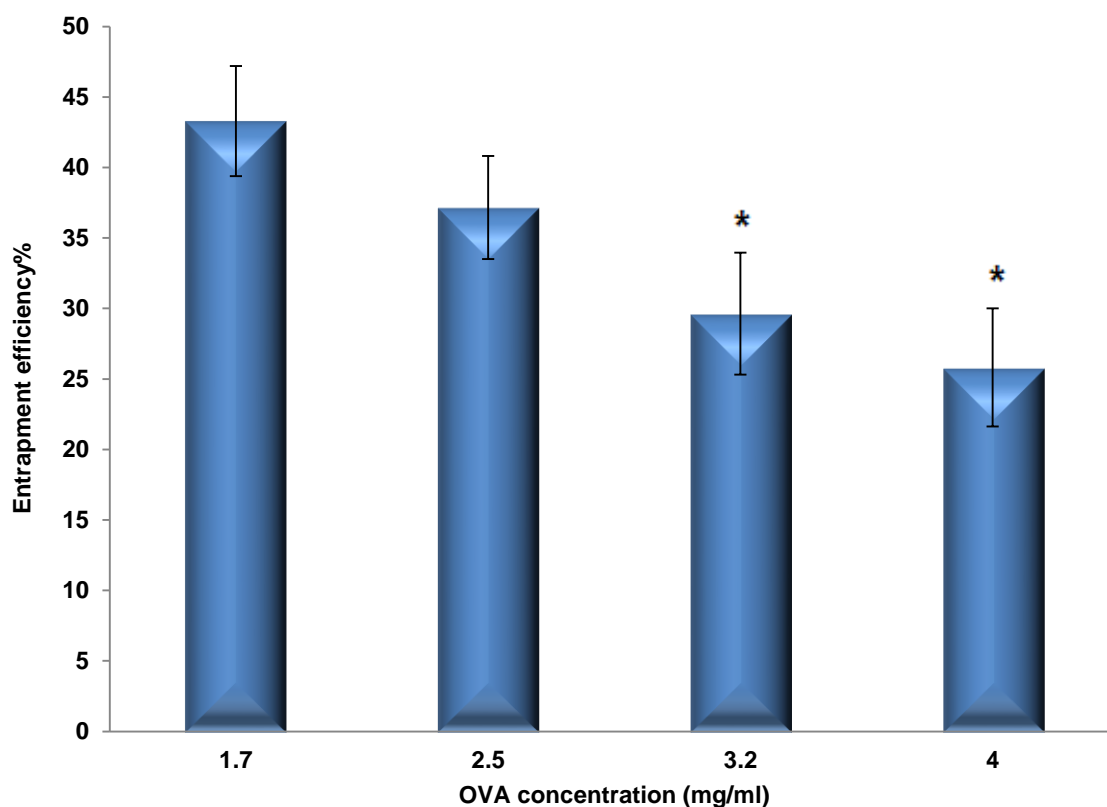


Figure 3.8: The entrapment efficiency of OVA prepared in a range of concentrations. Data are mean \pm SD, n=3; * $p < 0.05$ for 3.2 and 4 mg compared to lower concentrations.

Similar entrapment efficiency values of OVA were previously reported for albumin, 38% using reverse phase evaporation method (Szoka *et al.*, 1980) and 44.6% in liposomes generated using the ethanol injection method (Wang and Huang, 2003). Moreover, Ishikawa *et al.*, (2004) reported an entrapment efficiency of 41.9% for BSA in liposomes generated from proliposomes.

3.3.4 Size reduction of empty liposomes

Size reduction of liposomes may offer a lot of benefits, such as better uptake by cells (Zou *et al.*, 1995). However, liposome size is an important determinant of the entrapment efficiency of hydrophilic drugs inside the central aqueous core of the liposomes, since size reduction leads to decreased entrapped volume (Winslow, 2006). Therefore, engineering of liposomes having the right size is necessary for achieving the best formulations.

In this study, the characteristics of liposomes were evaluated using three methods of size reduction:

- 1- Bath sonication
- 2- Probe sonication
- 3- Extrusion

Initially, empty liposomes incorporating cholesterol at a ratio of 2:1 SPC to cholesterol were successfully reduced in size to 100 nm vesicles using any of the three above methods of size reduction listed above. However, difficulties were encountered when trying to sediment the 100 nm vesicles by ultracentrifugation, in agreement with the findings of Tortorella *et al.*, (1993) and Zhan (1999). The difficulty of sedimenting SUVs might be attributed to the low density of the liposomes. Figure 3.9 illustrates the effect of ultracentrifugation and probe sonication of the liposomal formulations on the amount of lipid present in the sample as determined by the Stewart essay. Lower amounts of the lipid in the supernatant indicate that the separation of liposomes from the supernatant is efficient.

As demonstrated in Figure 3.9, liposomes that were not ultracentrifuged or sonicated (i.e. before size reduction and separation) exhibited a lipid concentration of $94.50 \pm 3.12\%$. However, when liposomes were probe-sonicated to have a size of approximately 100 nm, lipid content was found to be $81.14 \pm 4.58\%$. This marked decrease ($p < 0.05$) in lipid content is due to losses of some lipids during the sonication procedure. Moreover, when liposomes were ultracentrifuged without sonication, a pellet of liposomes was formed at the bottom of the centrifuge tube and the amount of lipid in the supernatant was as low as $2.43 \pm 1.79\%$, indicating the high effectiveness of ultracentrifugation of liposomes. However, when liposomes were probe-sonicated prior to ultracentrifugation, the amount of lipid in the supernatant after pellet formation was as high as $22.61 \pm 5.23\%$, giving an indication that ultracentrifugation at a speed of 65,000 rpm for 4 hours did not sediment all of the liposomes, and a significant percentage of vesicles have remained dispersed in the supernatant.

In comparison to the liposomes having a size approximately 100 nm, liposomes (400 nm) were easier to prepare and sediment. After probe sonication into 400 nm

vesicles and ultracentrifugation the amount of lipid found in the supernatant was considerably low, being $5.35\% \pm 1.84$. Therefore, size reduction to obtain liposomes having a size of 400 nm was applied throughout the study.

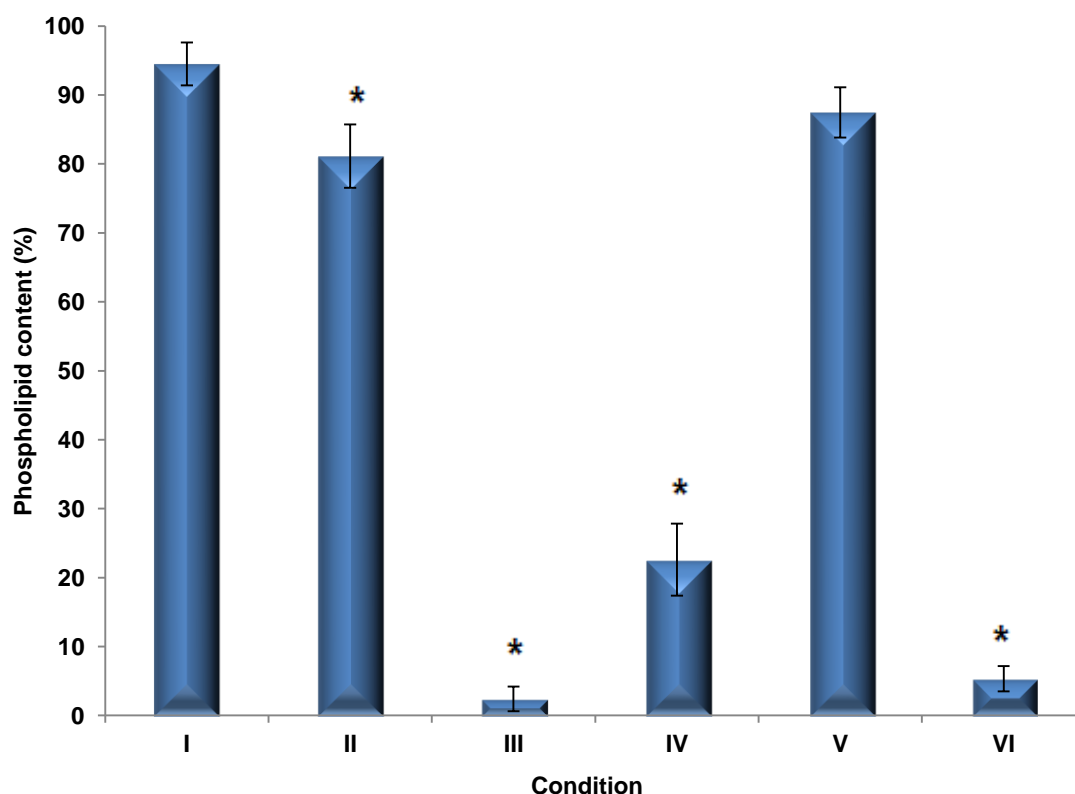


Figure 3.9: Phospholipid content in the supernatant for liposomes processed at various conditions: (I) liposomes without processing; (II) liposomes after probe sonication to 100 nm vesicles; (III) liposomes after ultracentrifugation; (IV) liposomes after probe sonication to 100 nm vesicles followed by centrifugation; (V) liposomes after probe sonication into 400 nm vesicles; (VI) liposomes after probe sonication into 400 nm vesicles followed by centrifugation. Data are mean \pm SD, $n=3$; * $p<0.05$ for II, III, IV, VI compared to I; $p>0.05$ for V compared to I.

All different methods of size reductions generated 400 nm liposomes. The properties of the generated liposomes after size reduction were investigated in this section in terms of size and polydispersity (Figure 3.10). The time required to reduce the size of liposomes to 400 nm was 22 minutes using bath sonication, and as short as 5 minutes using probe sonication. The Pdi was also significantly higher ($p<0.05$) for bath sonication when compared to probe sonication, being 0.679 ± 0.051 and 0.494 ± 0.041 , respectively. These findings demonstrate that

probe sonication not only saves time but also may offer a better control for the size distribution of liposomes, which is attributed to the direct contact between the probe and the liposomes, resulting in more efficient size reduction.

On the other hand, when extrusion was employed to reduce the size of liposomes, the Pdi was significantly lower (i.e. 0.291 ± 0.033) compared to the other methods of size reduction. Additionally, unlike probe sonication, extrusion through polycarbonate membrane filters does not contaminate the liposomes with any residues such as titanium, and hence no purification procedure is required.

Thus, due to the narrower size distribution of the liposomes generated by extrusion and the absence of titanium residues, extrusion was chosen for size reduction of liposomes in this study. The advantages of extrusion over other methods of size reduction have been previously demonstrated with other liposome formulations (Lapinski *et al.*, 2007).

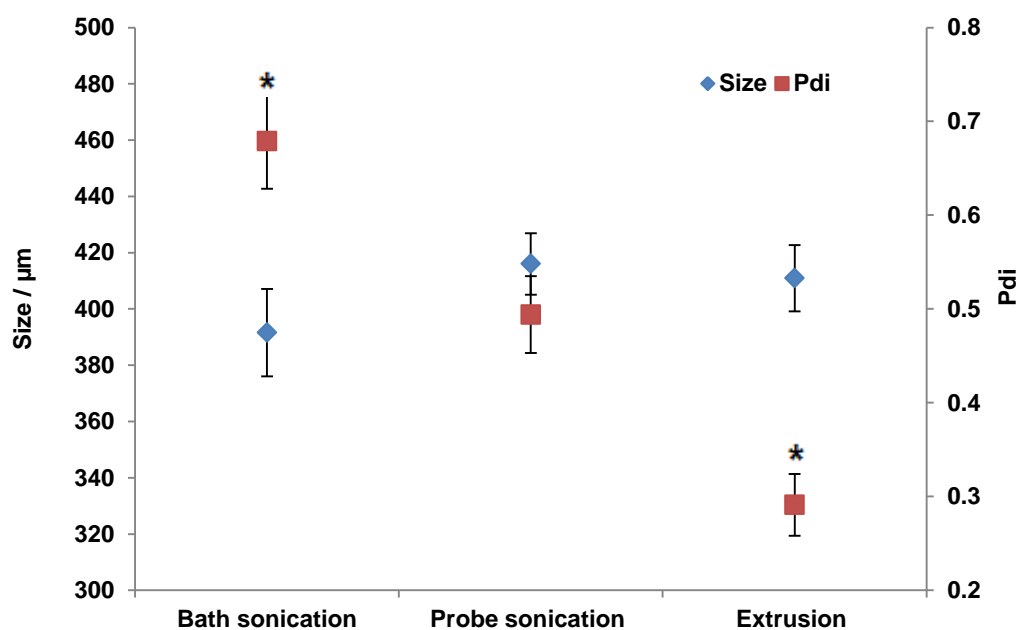


Figure 3.10: Size and polydispersity of liposomes reduced in size using bath sonication, probe sonication or extrusion. Data are mean \pm SD, $n=3$; $p>0.05$ for size measurements; * $P<0.05$ for the Pdi of Bath sonication and Extrusion compared to Probe Sonication.

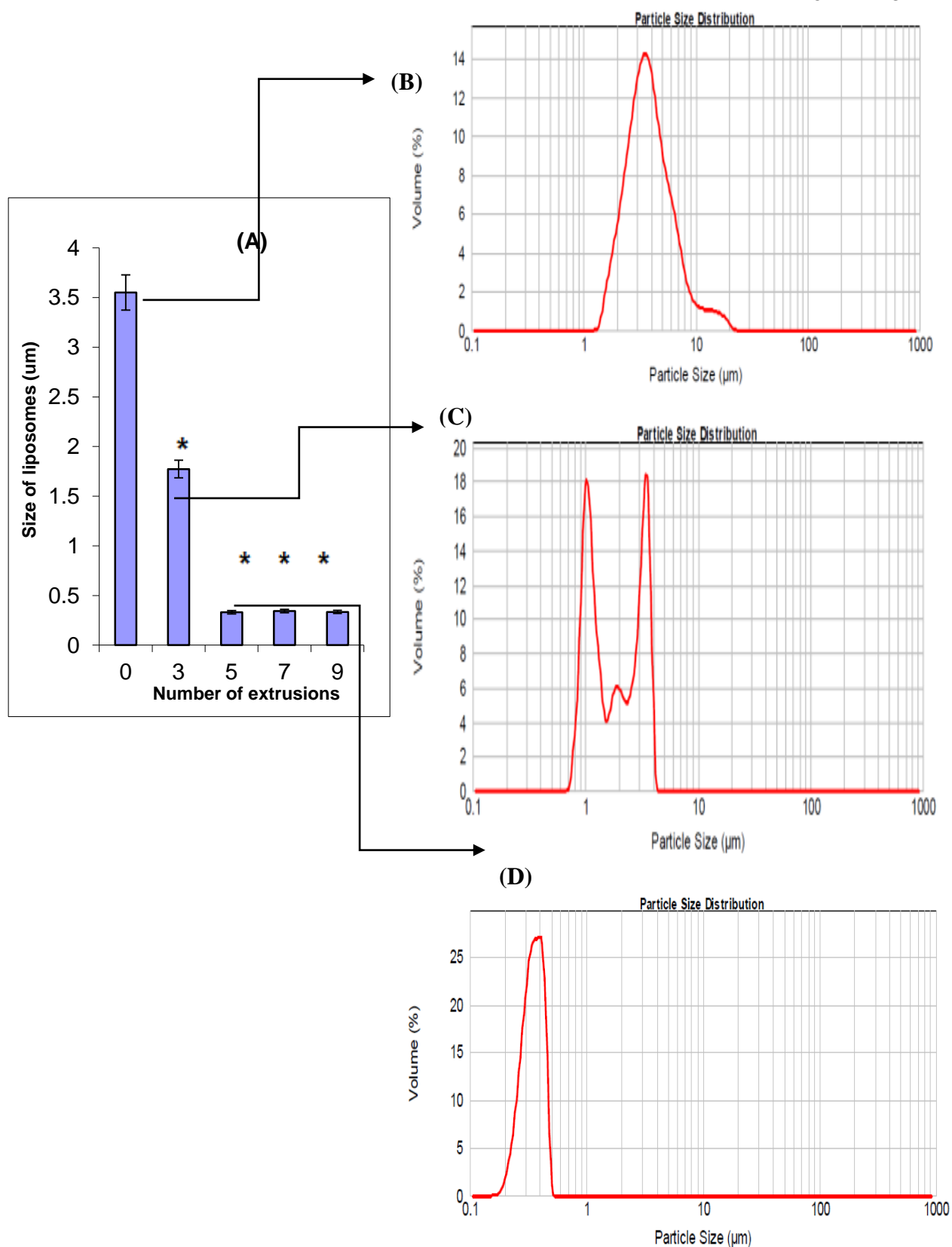


Figure 3.11: Relationship between number of extrusion cycles through the different membrane filters (5, 1, 0.8 and 0.4 µm pore size) on the (A) size of liposomes and (B,C,D) size distribution following 0, 3 and 5-7 extrusion cycles, respectively. (B-D) represents typical size distribution monographs generated by the Zetasizer Nanoseries analysis software. Data are mean ± SD, n=3; * $p < 0.05$ for 3,5,7,9 extrusions compared to 0 extrusions; $p > 0.05$ for 5,7,9 extrusions; B,C and D are typical of 3 different experiments.

The number of extrusion cycles through the different polycarbonate membrane filters with pore sizes (5, 1, 0.8 and 0.4 μm), and their effect on the size distribution of liposomes were also investigated (Figure 3.11).

As demonstrated in Figure 3.11, as the number of extrusion cycles increased from 1 to 5 cycles through each of the polycarbonate membrane filters, the measured size of liposomes decreased from $3.41 \pm 0.55 \mu\text{m}$ to $414.3 \pm 24.6 \text{ nm}$. However, further increases in the number of extrusion cycles (e.g. up to 9 cycles) resulted in no significant change in the size of liposomes ($p > 0.05$). Moreover, when the number of extrusion cycles increased from 1 to 7, the Pdi decreased from 0.970 ± 0.042 to 0.296 ± 0.026 . Also, further increase in the number of extrusion cycles (e.g. up to 9 cycles) resulted in no significant change in the Pdi of the liposomes ($p > 0.05$). In light of those findings, 7 extrusion cycles through each of the polycarbonate membrane filters were performed in this study.

3.3.5 Effect of extrusion on the properties of liposomes entrapping SS or OVA

The effect of extrusion on size, size distribution and drug entrapment was studied using liposomes manufactured via the ethanol-based proliposome method. The model drugs used in this study were OVA and SS (Table 3.6). The number of extrusions required when either OVA or SS were included in the liposomes was 7 extrusion cycles through the 5, 1, 0.8 and 0.4 μm membrane filters to generate 400 nm vesicles.

As shown in Table 3.6, no significant differences between SS and OVA ($p > 0.05$) were observed in terms of size and SPAN or Pdi of the generated liposomes. Overall, this indicates that the size of liposomes before or after extrusion is not dependent on the type of drug included, but is rather dependent on the manufacturing procedure, such as the number of extrusion cycles, as demonstrated earlier (Figure 3.11). In addition, Table 3.6 demonstrates that whilst extrusion had no effect on the zeta potential of SS and OVA liposomes, the zeta potential was markedly different between the SS and OVA liposomes, thus indicating that, contrary to the size and Pdi or SPAN, zeta potential is influenced by the type of drug included rather than manufacturing procedure.

Table 3.6: Size, SPAN and zeta potential of liposomes incorporating SS or OVA. Data are mean \pm SD, n=3; $P>0.05$ for size and SPAN; $*p<0.05$ for Zeta potential.

<i>Before extrusion</i>			
	Size (μm)	SPAN	Zeta potential (mV)
OVA liposomes	3.46 \pm 0.38	1.56 \pm 0.29	-6.37 \pm 0.47
SS liposomes	3.37 \pm 0.28	1.61 \pm 0.31	-4.44 \pm 0.45 *
<i>After extrusion</i>			
	Size (nm)	Pdi	Zeta potential (mV)
OVA liposomes	412.3 \pm 36.7	0.275 \pm 0.051	-6.82 \pm 0.61
SS liposomes	389.7 \pm 41.6	0.302 \pm 0.038	-4.16 \pm 0.52 *

The entrapment efficiency values were also investigated following extrusion of the OVA and SS liposomes (Figure 3.12). As shown in Figure 3.12, a significant reduction ($p<0.05$) in the entrapment efficiency values were apparent following extrusion of OVA and SS containing liposomes (i.e. 13.21 and 17.85%, respectively). These findings are in agreement with those of Szoka *et al.*, (1980) and Elhissi *et al.*, (2007), who reported that extrusion significantly reduces the entrapment of materials in liposomes. The decrease in entrapment efficiency is attributed to the reduction of the mean diameter of the liposomes, hence the internal space available for encapsulation of hydrophilic drugs is reduced (Schneider *et al.*, 1995; Winslow, 2006).

Figure 3.12 demonstrates that the entrapment efficiency of OVA in liposomes was significantly lower ($p<0.05$) than that of SS. This might be due to the molecular size of the entrapped materials; where unlike the small hydrophilic SS, OVA is a large protein of 45 kDa.

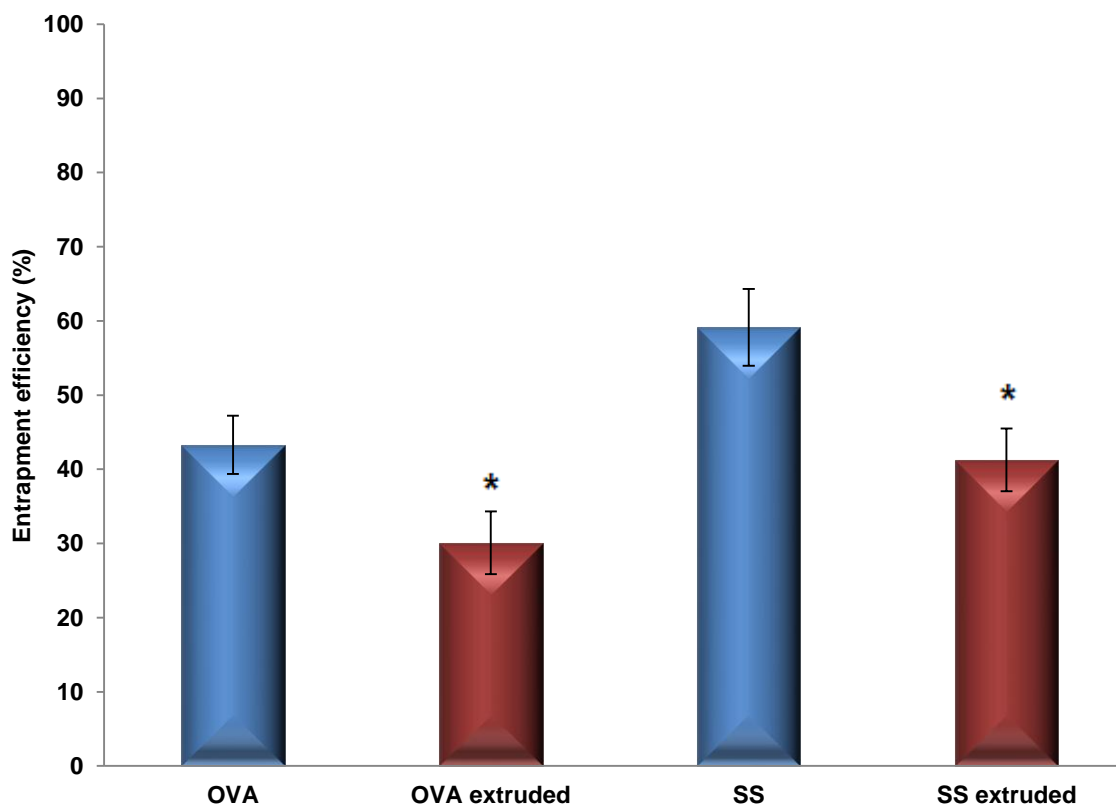


Figure 3.12: Entrapment efficiency of OVA and SS before and after extrusion of liposomes. Data are mean \pm SD, n=3; * $p < 0.05$ for OVA compared to OVA extruded and SS compared to SS extruded, respectively.

3.3.6 Inclusion of chitosan in liposome formulations

Chitosan was included in the liposome formulations in order to increase the mucoadhesive properties of the liposomes. Chitosan used in this study was a water soluble glutamate salt having a molecular weight of less than 200 kDa. The low molecular weight of chitosan may facilitate formation of uniform polymer–liposome complexes (Werle and Takeuchi, 2009), thus it can enhance the mucoadhesive properties of liposomes.

The concentrations of chitosan in the liposome formulations were 0.1, 0.2 or 0.3% w/v. The effect of chitosan concentration on the size, SPAN and zeta potential of liposomes was investigated and the entrapment efficiency of OVA in liposomes was studied. These chitosan concentrations have been previously used for liposome coating (Zaru *et al.*, 2009; Albasarah *et al.*, 2010; Zhuang *et al.*, 2010). Zaru *et al.*, (2009) demonstrated that 0.1% w/v chitosan resulted in

the highest coating efficiency to liposomes. On the other hand, Zhaung *et al.*, (2010) reported that 0.3% (w/v) was an optimal concentration for chitosan for the preparation of stable liposomes. Higher concentrations of chitosan have also been previously studied, however their use demonstrated low coating efficiencies (Galovic Rengel *et al.*, 2002; Zaru *et al.*, 2009).

Table 3.7 elucidates the effect of chitosan concentration on size and SPAN of liposomes. As demonstrated in Table 3.7, chitosan concentration had no effect ($p>0.05$) on the size or SPAN of liposomes. A similar finding on the effect of chitosan addition on the size of liposomes was previously reported by Werle *et al.*, (2009).

Table 3.7: Size and size distribution of freshly prepared liposomes prepared with a range of chitosan concentrations. Data are mean \pm SD, n=3; $p>0.05$ for size and SPAN measurements.

Chitosan concentration % (w/v)	Size (μm)	SPAN
0.0	3.46 \pm 0.38	1.56 \pm 0.29
0.1	3.28 \pm 0.29	1.64 \pm 0.41
0.2	3.19 \pm 0.36	1.58 \pm 0.28
0.3	3.22 \pm 0.43	1.71 \pm 0.36

The increase in zeta potential by addition of chitosan is attributed to the positive charge of the chitosan polymer (Davis, 1999b; Zaru *et al.*, 2009; Behera *et al.*, 2011). The increase in the zeta potential of liposomes possibly means that chitosan has adsorbed onto the surface of liposomes, which might be in the form of electrostatic interactions between the positively charged chitosan and the negatively charged surface of liposomes (Zaru *et al.*, 2009), or via hydrogen bonding between the polysaccharide molecules of the chitosan and the phospholipid head groups in the liposome bilayers (Perugini *et al.*, 2000).

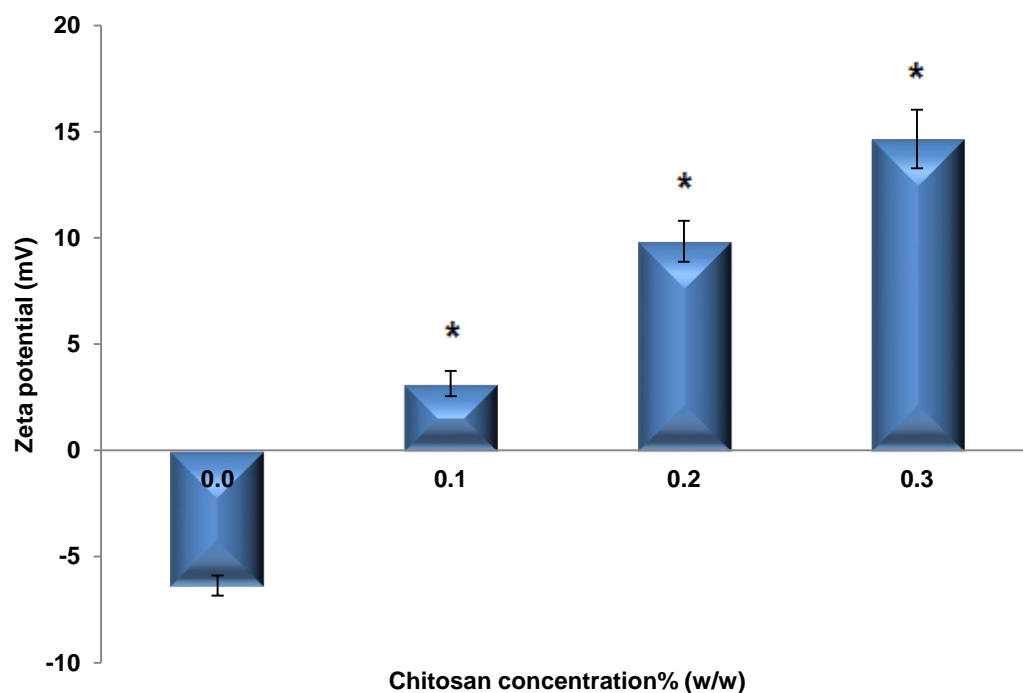


Figure 3.13: Zeta potential of liposomes upon inclusion of chitosan in a range of concentrations. Data are mean \pm SD, n=3; * $p < 0.05$ for 0.1, 0.2 and 0.3 % (w/w) chitosan compared to the absence of chitosan.

Many research findings have demonstrated that chitosan may increase the entrapment efficiency of drugs in liposomes (Phetdee *et al.*, 2008; Albasarah *et al.*, 2010). However, this was not in agreement with our findings using the proliposome technology to manufacture liposomes, since chitosan concentration was found not to affect ($p > 0.05$) the entrapment of OVA in liposomes in this study (Figure 3.14). The entrapment efficiency of OVA in liposomes was found to be $43.30 \pm 3.91\%$ before inclusion of chitosan, and 37.62 ± 3.58 , 40.15 ± 4.65 and $43.50 \pm 5.13\%$ after inclusion of 0.1, 0.2 and 0.3% (w/v) chitosan, respectively. The disagreement between these findings and the observations reported in the literature might be attributed to the use of different drugs or excipients within the liposomal formulations, or might be ascribed to the manufacturing procedure of liposomes using the proliposome technology.

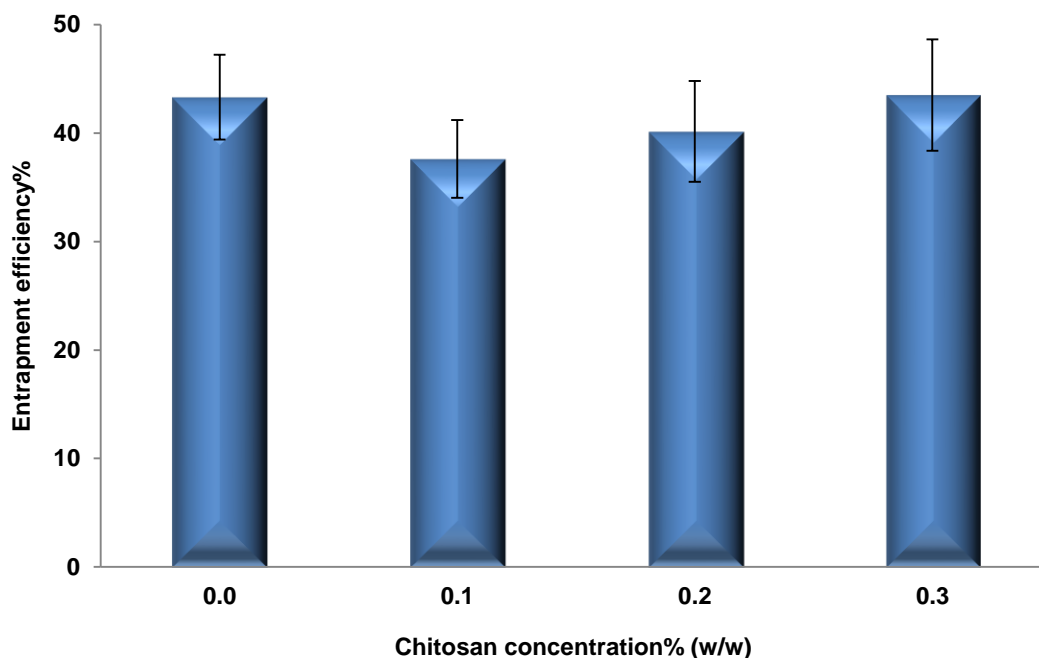


Figure 3.14: Effect of chitosan concentration on the entrapment efficiency of OVA in liposomes. Data are mean \pm SD, $n=3$; $p>0.05$ for all.

3.4 Conclusions

The results from this study give a rational basis for optimal parameters required for the preparation of liposomes via the ethanol-based proliposome method. Generated liposomes from the ethanol-based proliposome technology proved to be stable upon dilution and storage for duration of at least one week. Moreover, sample volume was found not to influence the characteristics of the generated liposomes, thus giving an indication of the potential scale-up of the proliposome technology, and warranting further studies using larger volumes of samples.

The validity of liposomes prepared via the modified ethanol-based proliposome method for the entrapment of different drug molecules such as SS and OVA was also demonstrated in this study. Moreover, the effect of cholesterol inclusion into the liposomal structure was evaluated, and in light of findings a ratio of (1:1) SPC to cholesterol was chosen as optimal for liposome preparation.

Size reduction of generated liposomes via the extrusion technique was also established to be the most suitable for the formulations studied, and 400 nm

vesicles entrapping SS and OVA were successfully prepared. The results from extrusion studies also demonstrated marked influences on the characteristics of generated liposomes, including a significant loss of the entrapped moieties following size reduction.

The incorporation of the mucoadhesive agent chitosan into the liposome formulation was established. Chitosan's incorporation was observed to significantly increase the positive charge of the liposomes, whilst having no marked influence on size of liposomes and entrapment efficiency values.

Overall, the validity of the modified ethanol-based proliposomes method for the generation of mucoadhesive 400 nm vesicles able to entrap different moieties (i.e. small hydrophilic drug SS and a 45 kDa protein OVA) was established. Also, optimal parameters for liposome preparation were elucidated.

CHAPTER 4

FORMULATION OF IgG LIPOSOMES USING THE ETHANOL-BASED PROLIPOSOMES METHOD

4.1 Introduction

Numerous therapeutic proteins and peptides have emerged in the market over the last century, and antibody pharmaceuticals in particular are gaining tremendous momentum. This increase in the popularity in antibodies is due to their specific action, ability to conjugate with other therapeutic entities, and the fact that technology advancement has made complete human antibodies available (Wang *et al.*, 2007).

The field of therapeutic antibodies is continuously expanding, and immunoglobulins (Ig) are used today for prophylaxis or the therapy of infectious diseases (Weltzin and Monath, 1999; Breedveld, 2000; Dellamary *et al.*, 2004; Maillet *et al.*, 2008b). Antibodies are often administered by parenteral routes, but recently non-invasive mucosal routes have been explored and showed promise of enhancing the therapeutic effects and reducing the side effects of antibodies (Garcia-Santana *et al.*, 2006). Despite the advantages antibodies possess, various hurdles are posed by their high molecular weight, including their limited ability to cross the cell membranes, short half-lives and instability (Pisal *et al.*, 2010).

Several strategies have been proposed to help circumvent the limitations and to improve the therapeutic effects of antibodies. Liposomal carriers in particular, due to being biocompatible, biodegradable, non-immunogenic and able to be conjugated with both hydrophobic and hydrophilic therapeutic agents, have attracted a lot of interest (Pisal *et al.*, 2010; Webster, 2010). Liposomes have been applied to a wide variety of proteins and have been investigated for the administration of IgG (Wong *et al.*, 1994; Dreffier *et al.*, 2003; Garcia-Santana *et al.*, 2006).

However, until the present, the proliposome technology to overcome the stability and scaling-up limitation of conventional liposomes has never been investigated for the administration of IgG.

The optimal parameters for formulating liposomes from ethanol-based proliposomes were established in Chapter 3, and the feasibility of entrapping a small hydrophilic drug SS, and the protein OVA was demonstrated. This chapter

evaluated the validity of liposomes generated via the ethanol-based proliposome method for the entrapment of immunoglobulin G (IgG), which is the main model protein in this thesis.

To assess the efficacy of the ethanol-based proliposomes method for the entrapment of IgG, liposomes entrapping IgG were also prepared via conventional thin film hydration method and particulate-based proliposome method, and the properties of the generated liposomes were compared. Moreover, the effect of the incorporation of the mucoadhesive polymers chitosan and alginate into liposome formulations was evaluated and the effect of size reduction of the mucoadhesive liposomes was investigated.

Liposomes prepared in this chapter were characterised in terms of particle size and size distribution, zeta potential and entrapment efficiency. The secondary structure and activity of IgG free in solution or incorporated into the liposomal formulation were determined in this study following size reduction and at different temperatures.

4.2 Methodology

4.2.1 Manufacture of IgG liposomes

Liposomes in this study were prepared using: thin film hydration method, particulate-based proliposome method and ethanol-based proliposomes method, as discussed earlier in Section 2.2.1. Different concentrations of IgG were incorporated into the liposomal structure (0.5, 1, 1.25, 2.5 or 5 mg/ml) and the concentration resulting in maximum entrapment was used throughout the study.

4.2.2 Characterisation of liposomes

IgG liposomes prepared in this study were characterised for (a) size distribution, (b) morphology, (c) zeta potential and (d) entrapment efficiency.

(a) Size distribution of liposomes

The size distribution of liposomes in this study was measured as previously discussed in Section 2.2.5 using the technologies of: (1) laser diffraction employing the Malvern Mastersizer 2000 instrument (Malvern Instruments Ltd, UK) or (2) dynamic light scattering (DLS) employing the Malvern Zetasizer Nanoseries (Malvern Instruments Ltd, UK). Laser diffraction was the technique employed for determining the size distribution of liposomes before size reduction, whilst DLS was the technique used for size reduced liposomes.

(b) Morphology of liposomes:

The morphology of the liposomes (before and after size reduction) was investigated using Cryo-TEM. Liposome samples were blotted on glow discharged carbon lacey carbon grid, plunged into nitrogen chilled liquid ethane and imaged on a JEOL 2010F TEM (200 kV FEG) with a 4K Gatan Ultrascan camera as described earlier in Section 2.2.6.

(c) Zeta potential:

The zeta potential of generated liposomes was analysed via the technology LDV using a Zetasizer Nanoseries (Malvern Instruments Ltd, UK), as elucidated in Section 2.2.7.

(d) Entrapment of IgG

The liposomal suspensions were centrifuged using a Beckman LM-80 ultracentrifuge device with a 70.1 Ti fixed angle rotor (Beckman Coulter Instruments) at a speed of 55,000 rpm (277,000 x g) for 45 minutes. The supernatant was then collected and analysed via HPLC to determine the entrapment efficiency of IgG according to the protocol previously discussed in Section 2.2.8 using an Agilent 1200 series HPLC system (Agilent Technologies, Palo Alto, CA) and an agilent SEC5 5 μ M- 300A column.

4.2.3 Formulation of mucoadhesive ethanol-based liposomes.

Different concentrations (0.1, 0.2 and 0.3% w/v) of the mucoadhesive agents protasan G213, an ultrapure chitosan glutamate salt, (Novamatrix, Belgium) and sodium alginate (Sigma Aldrich, UK) were dissolved in 4.5 ml HPLC water. The resultant solutions were then employed in the secondary hydration step of the ethanol-based liposomes to generate the mucoadhesive liposome dispersions.

4.2.4 Size reduction of ethanol-based liposomes

Generated liposome dispersions were reduced in size via ultrasonic vibrations using a probe sonicator (Vibra cell sonicator, Sonics and Materials Inc., Newtown, USA) according to the protocol previously discussed in Section 2.2.3. Probe sonication proceeded until desired size was achieved. The effect of sonication time on the size distribution and zeta potential of liposomes was determined using the Malvern Zetasizer Nanoseries (Malvern Instruments Ltd, UK) employing the techniques of DLS and LDV for the size distribution and zeta potential, respectively.

4.2.5 Secondary structure and activity of IgG

The secondary structure of IgG was investigated using CD. CD experiments were performed as previously described in Section 2.2.9, using a J-815 spectropolarimeter (Jasco, UK) coupled with a Peltier Jasco CFF-426S system for temperature control. Collated CD spectra of IgG both in solution or incorporated into liposomes were then estimated via the secondary structure algorithm CDSSTR using DICHROWEB (Greenfield, 2006).

To determine the immunogenic reactivity of IgG (activity), an easy titre IgG kit was used according to the protocol previously described in Section 2.2.10.

4.3 Results and discussion

4.3.1 Entrapment of IgG

As outlined earlier in Section 4.1, IgG was incorporated into liposomes using three different preparation methods: different concentrations of IgG were incorporated into the liposome formulations and the effect of IgG concentration on its entrapment efficiency in liposomes; and size, SPAN and zeta potential of generated liposomes was studied.

As shown in Figure 4.1, when the concentration of IgG increased from 0.5 mg/ml to 5 mg/ml in liposomes prepared by the thin film method, the entrapment efficiency markedly decreased ($p < 0.05$) from $17.13 \pm 2.97\%$ to $2.91 \pm 1.40\%$. The same trend of decrease in entrapment was also found for liposomes prepared by both proliposomal methods (particulate-based and ethanol-based). For the particulate-based proliposomes method, a decrease in the entrapment efficiency from $23.13 \pm 3.11\%$ to $7.1 \pm 1.65\%$ occurred upon increasing the IgG concentration from 0.5 to 5 mg/ml. Similarly, the entrapment efficiency of liposomes prepared by the ethanol-based proliposome method decreased from $29.90 \pm 2.47\%$ to $5.83 \pm 1.64\%$ as the concentration increased from 0.5 to 5 mg/ml.

These findings agreed with our previous finding for OVA (Section 3.3.3), where the entrapment efficiency decreased by increasing the concentration of the protein, and with the findings of Dreffier *et al.*, (2003), which demonstrated a higher encapsulation when 1 mg/ml IVIG was used in comparison to a 10 mg/ml. This trend might be attributed to the limited drug incorporation in liposomes, thus higher concentrations will not lead to enhanced drug encapsulation (Rogers *et al.*, 1990). In light of these findings, the 0.5 mg/ml of IgG was chosen to be the optimum concentration in the study, and the rest of the studies were performed using this concentration.

As displayed in Figure 4.1, amongst the three liposomal preparation methods, the ethanol-based proliposome method was found to entrap the highest amount of IgG (up to $29.90 \pm 2.47\%$) followed by the particulate-based method (up to $23.13 \pm 3.10\%$), while the thin film method was found to have the lowest entrapment efficiency for this protein (up to $17.13 \pm 2.97\%$). The low entrapment efficiency for hydrophilic drugs using the thin film method has been reported previously (Colletier *et al.*, 2002; Elhissi *et al.*, 2006a). Sharma and Sharma (1997) also reported the range of entrapment efficiency of hydrophilic drugs in thin film liposomes to be between 5 and 15%.

The superiority of the proliposome methods over many other methods of liposome preparation in terms of drug entrapment has also been previously demonstrated by Galovic Rengel *et al.*, (2002), who found that the entrapment of superoxide dismutase was 39-65% for liposomes generated by the ethanol-based proliposome method, 1-13% using the thin film method and 2-3% by using the dehydration rehydration method. Ishikawa *et al.*, (2004) demonstrated that the ethanol-based proliposome method offers superior encapsulation of BSA compared to the dehydration rehydration method, so that the entrapment was 41% and 15%, respectively, when liposomes were made from SPC.

Amongst the proliposome methods, the entrapment efficiency of hydrophilic drugs in ethanol-based proliposome method tends to be high. This might be attributed to the two-step hydration protocol, which optimizes encapsulation of the drug (Elhissi *et al.*, 2006a).

The entrapment efficiencies of IgG obtained in this study for the proliposome preparation method is similar to that obtained earlier by Garcia-Santana *et al.*, (2006), who found entrapment efficiency of IgG to be 30% in liposomes prepared by dehydration rehydration method. Furthermore, Shimizu *et al.*, (1993) also reported the entrapment efficiency for IgY, a chicken egg yolk immunoglobulin G, in rehydration dehydration liposomes to be 30% when incubated at 60 °C, agreeing with our findings using the ethanol-based proliposome method. Szoka and Papahadjopoulos (1978) also revealed similar entrapment efficiency for rabbit IgG in reverse phase evaporation technique liposomes (28-40%).

4.3.2 Size distribution of IgG liposomes

As described in Section 4.3.1, 0.5 mg/ml of IgG was chosen to be the optimum concentration in the study, and the rest of the studies were performed using this concentration. The effect of the liposome preparation method on the size, SPAN and zeta potential of the generated liposomes was also investigated (Figures 4.2-4.4).

As displayed in Figure 4.2, the size of liposomes generated from ethanol-based proliposomes was markedly smaller than the size of liposomes manufactured by thin film or particulate-based proliposome methods ($p < 0.05$), being $3.28 \pm 0.18 \mu\text{m}$, $6.49 \pm 0.21 \mu\text{m}$ and $5.64 \pm 0.26 \mu\text{m}$, respectively. The smaller size of liposomes generated from ethanol-based proliposomes could be attributed to the presence of fewer bilayers compared to vesicles formed by thin film or particulate-based proliposome methods (Elhissi *et al.*, 2006b).

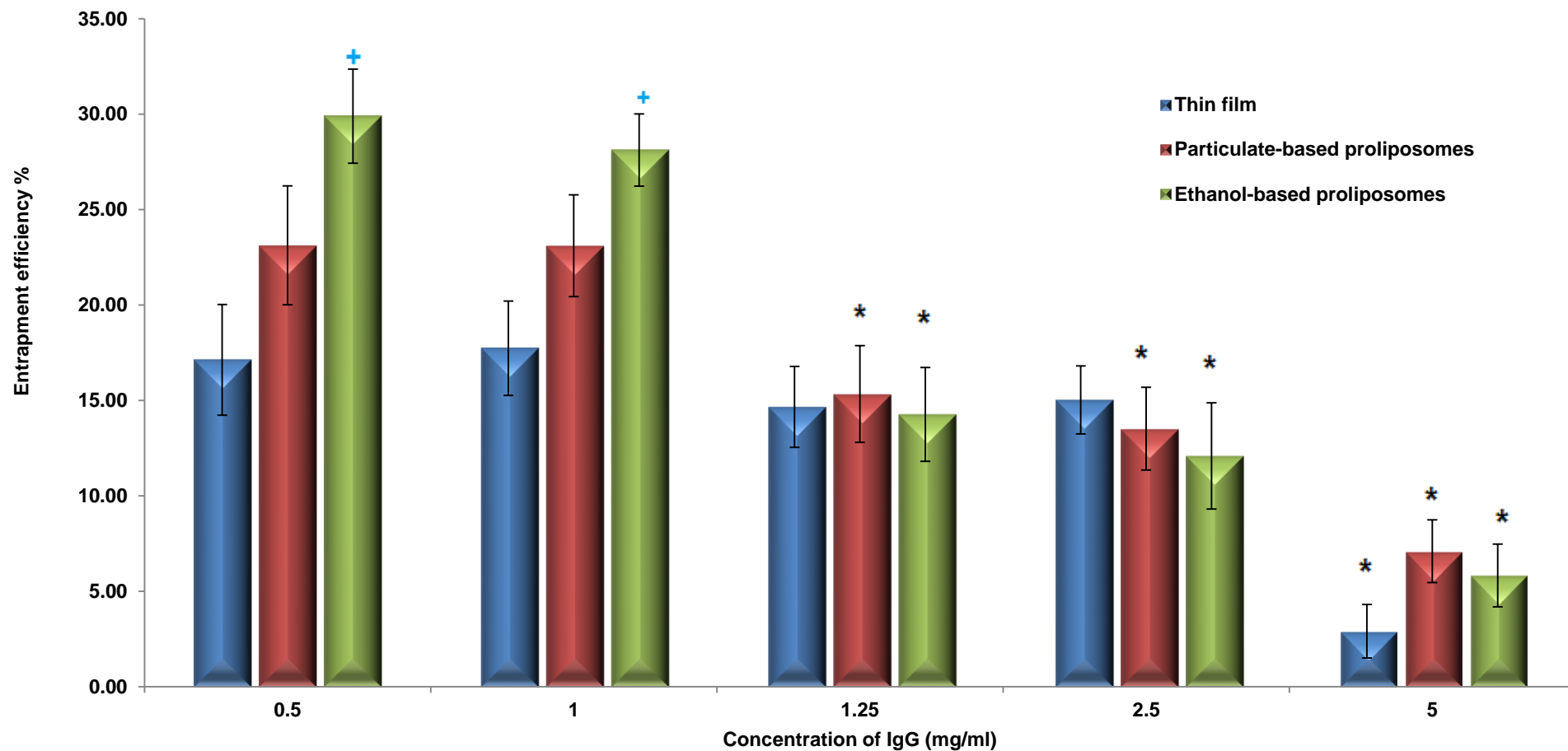


Figure 4.1: Entrapment efficiency of IgG used at various concentrations in liposomes manufactured using the thin film hydration or proliposome methods. Data are mean \pm SD, n=3; * $P < 0.05$ for 1.25, 2.5 and 5 mg/ml compared to lower concentrations; Also + $p < 0.05$ for Ethanol-based compared to Thin film and Particulate-based.

Also, liposomes generated from particulate-based proliposomes were smaller than those made using the thin film method, probably due to the presence of sucrose, which could affect the packing of the liposomes (Elhissi *et al.*, 2006b).

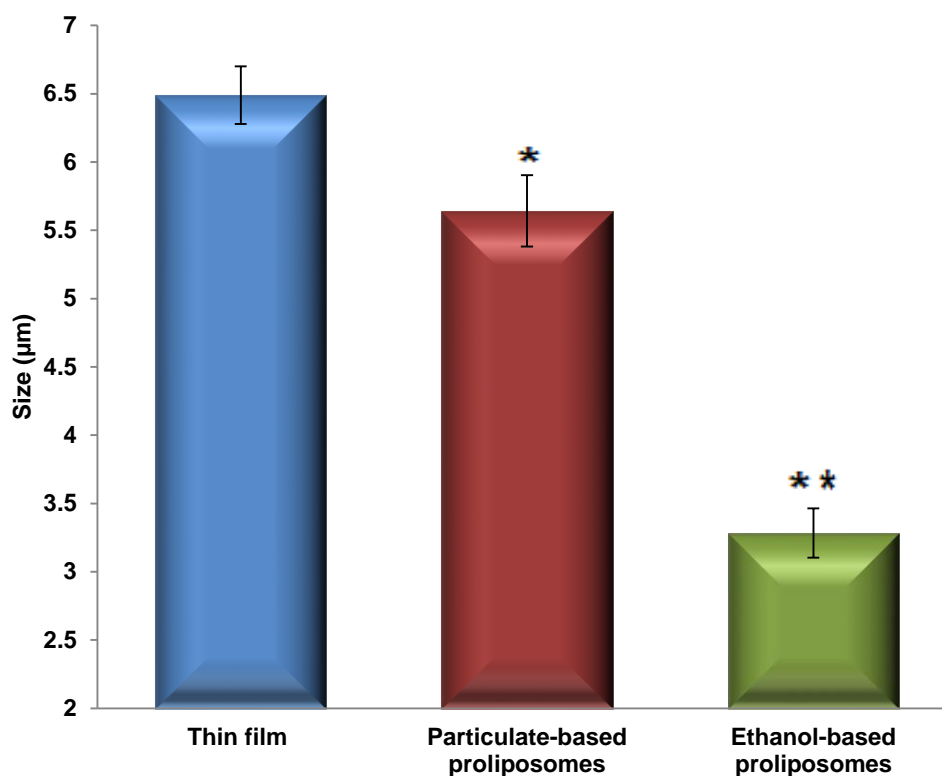


Figure 4.2: Size of liposomes prepared using ethanol-based proliposomes, particulate-based proliposomes or thin film hydration. Data are mean \pm SD, n=3; * $p < 0.05$ for Particulate-based compared to Thin film; ** $p < 0.001$ for Ethanol-based compared to Thin film.

The SPAN of liposomes (Figure 4.3) was found to be significantly different ($p > 0.05$) when employing the proliposome technologies (particulate-based and ethanol-based) and the thin film hydration technique, with lower SPAN values for the proliposome-generated vesicles, being 1.73 ± 0.12 and 1.80 ± 0.19 for liposomes generated from particulate-based proliposomes and liposomes generated from ethanol-based proliposomes, respectively. By contrast, the SPAN value for liposomes generated by the thin film method was 2.49 ± 0.24 .

High SPAN measurements indicate high size distribution, demonstrating that the proliposome methods are advantageous in this regard.

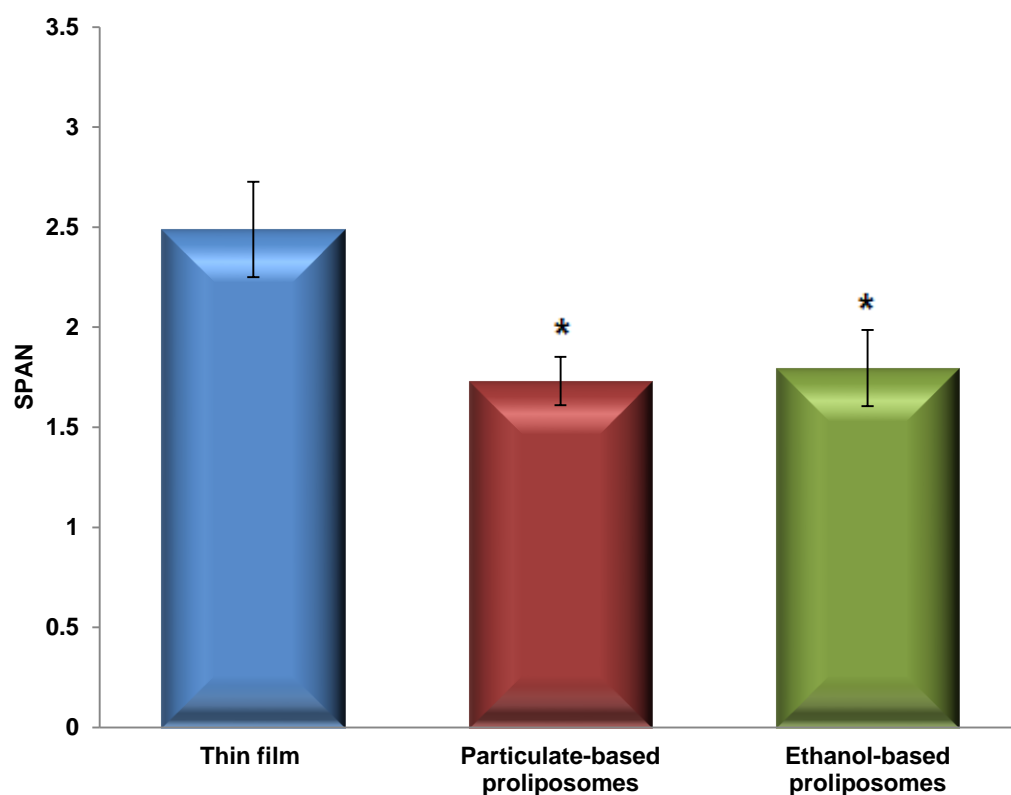


Figure 4.3: Size distribution of liposomes prepared using ethanol-based proliposomes, particulate-based proliposomes or thin film hydration. Data are mean \pm SD, $n=3$; * $p<0.05$ for Particulate-based and Ethanol-based proliposomes compared to Thin film

Additionally, the effect of the preparation method on the zeta potential of liposomes was investigated. Figure 4.4 demonstrates that there was no significant difference ($p>0.05$) in the zeta potential between the three methods. The slightly negative charge of the liposomes can be attributed to the lipid structure, whereby the hydroxyl groups could have oriented themselves on the outside of the bilayer. Also, the zeta potential was found to be markedly lower than drug-free liposomes prepared in Section 3.3.1 ($p<0.05$). This less negative zeta potential value could be due to the positive charge of IgG in the aqueous media, where it was found to be 1.89 ± 0.17 mV. This finding is in agreement with Dreffier *et al.*, (2003), who previously reported that the inclusion of IVIG in liposomal formulations reduces the zeta potential of the negatively charged vesicles. The outcomes from this study may also indicate that IgG might be

located at the liposome surfaces or partition between the liposome bilayers and the aqueous environment of the preparation. Further studies are required to confirm this finding.

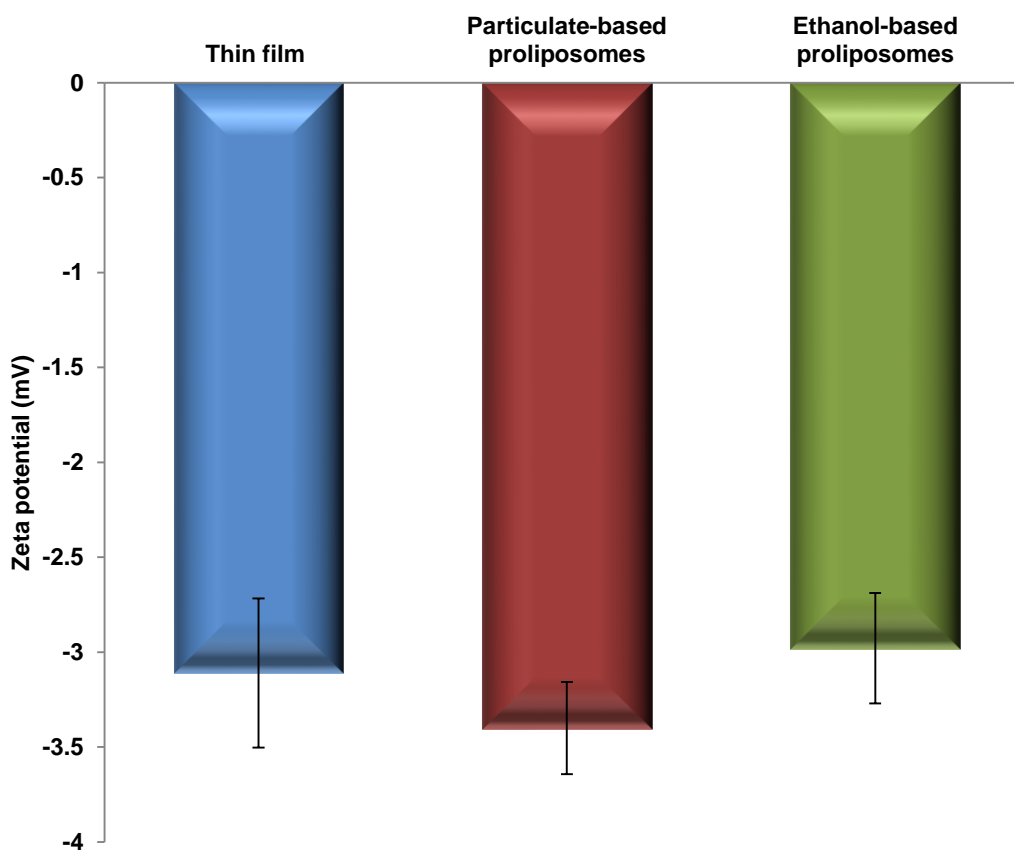


Figure 4.4: Zeta potential of liposomes prepared using ethanol-based proliposomes, particulate-based proliposomes or thin film hydration. Data are mean \pm SD, $n=3$; $p>0.05$ for all.

4.3.3 Addition of mucoadhesive agents to IgG liposomes generated from ethanol-based proliposomes

Using ethanol-based proliposomes, the effects of including either chitosan or alginate as mucoadhesive agents on the size, SPAN and zeta potential of IgG liposomes were studied. Moreover, the entrapment efficiency of IgG in the liposomes was investigated.

Chitosan is a well-known mucoadhesive agent which has been used in many studies to enhance the mucoadhesive properties of liposomes. Alginate is another well-known polysaccharide mucoadhesive which has been used to coat

liposomes in order to enhance their mucoadhesive properties (Wu *et al.*, 2003). Figure 4.5 illustrates the effect of incorporating different concentrations of mucoadhesive agents on the size of liposomes.

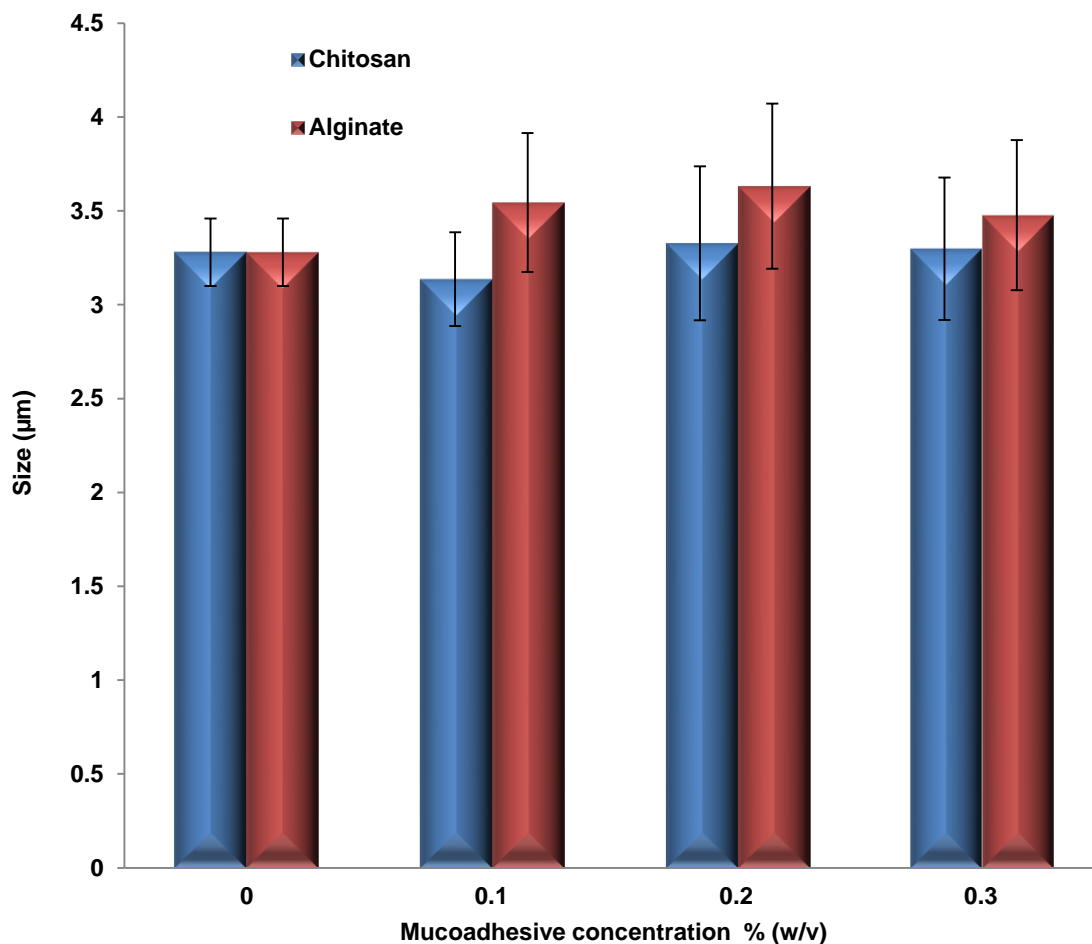


Figure 4.5: Effect of mucoadhesive agents' (chitosan and alginate) concentration on size of generated liposomes. Data are mean \pm SD, n=3; $p>0.05$ for all.

As displayed in Figure 4.5, Similar to the previous findings using OVA (Section 3.3.6), chitosan concentration had no effect ($p>0.05$) on the size of liposomes entrapping IgG. Also, alginate concentration was found not to affect the size of the generated liposomes ($p>0.05$), and no significant difference between the two mucoadhesive agents on the size of the liposomes was demonstrated ($p>0.05$). These findings indicate that the size of liposomes is not dependent on the type or concentration of the mucoadhesive polymer included, but rather on the manufacturing procedure of the liposomes. In addition, the SPAN values

(Figure 4.6) were found not to be markedly different between the two mucoadhesive agents and for the range of concentrations investigated ($p>0.05$). However, there is a trend of lower SPAN using the alginate polymer compared to the chitosan mucoadhesive agent.

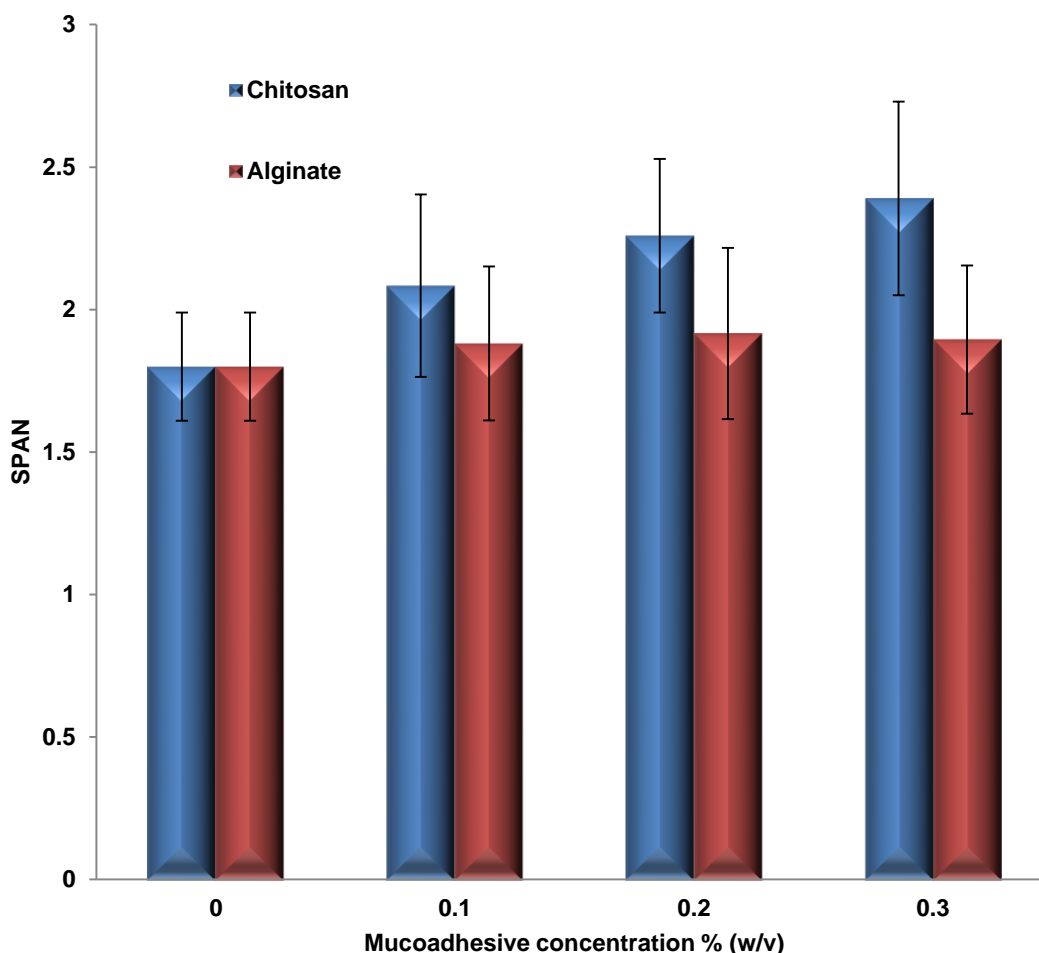


Figure 4.6: Effect of Mucoadhesive agents' (chitosan and alginate) concentration on SPAN of generated liposomes. Data are mean \pm SD, $n=3$; $p>0.05$ for all.

In contrast to the size and SPAN results, the zeta potential measurements (Figure 4.7) revealed a significant effect of the mucoadhesive concentration and type on the zeta potential of the IgG liposomes ($p<0.05$). Chitosan reversed the negative surface charge of liposomes to positive, whilst alginate intensified the negative charge of the vesicles, and the influence of both mucoadhesive polymers on the surface charge was dependent on polymer concentration. The

effect of both mucoadhesive polymers on the zeta potential of liposomes was statistically significant ($p < 0.05$).

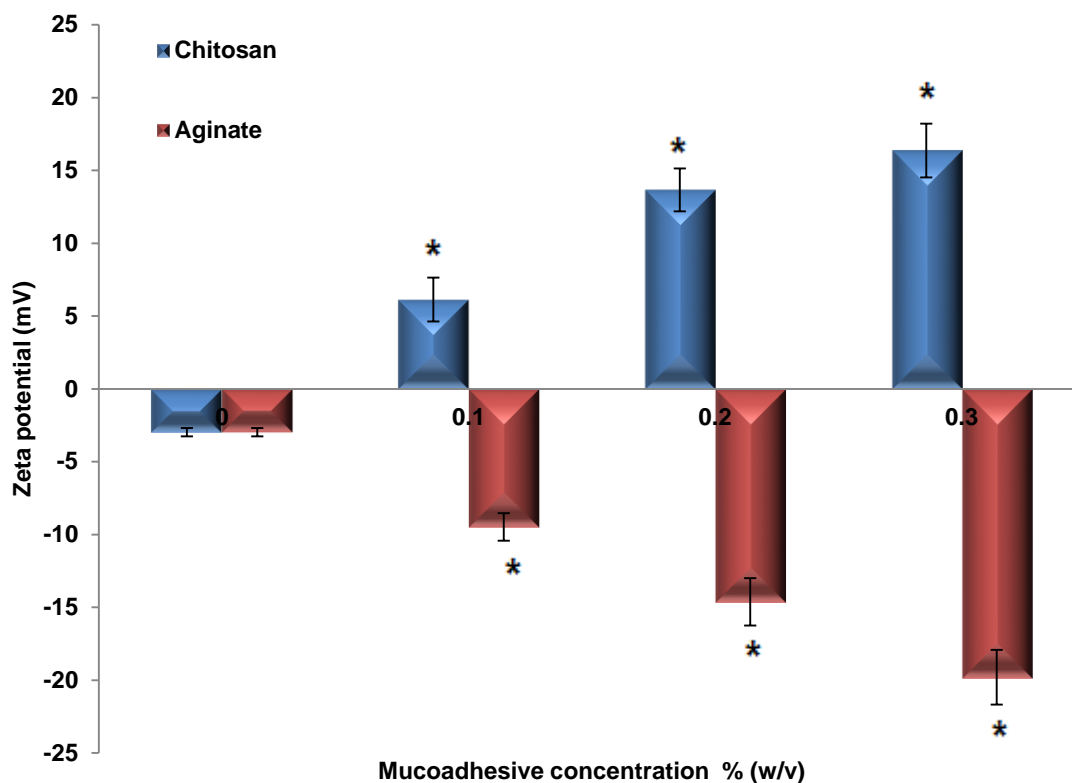


Figure 4.7: Effect of mucoadhesive agents' (chitosan and alginate) concentration on size of generated liposomes. Data are mean \pm SD, $n=3$; * $p < 0.05$ for either chitosan or alginate concentrations compared to their absence (i.e. 0% w/v).

The zeta potential of the vesicles was -2.98 ± 0.29 mV when no mucoadhesive was included. This slightly negative charge of the vesicles was reversed to positive 6.14 ± 1.51 mV upon inclusion of as low as 0.1% (w/v) chitosan, which was further increased by addition of higher chitosan concentrations to become 13.66 ± 1.47 mV and 16.37 ± 1.84 mV when chitosan concentrations were 0.2 and 0.3% (w/v), respectively (Figure 4.7). The positive zeta potential of liposomes that contain chitosan is attributed to the positive charge of the chitosan molecules, and may strongly indicate that chitosan has successfully coated the liposome surfaces. Also elucidated, in Figure 4.7, the zeta potential of liposomes after inclusion of alginate in 0.1, 0.2 and 0.3% (w/v) concentrations

were -9.48 ± 0.94 , -14.63 ± 1.63 and -19.80 ± 1.87 mV, respectively. These data can be attributed to the negative charge of the alginate (Chen *et al.*, 2009). This suggests that the alginate has coated the surfaces of liposomes.

In Section 3.3.6, the incorporation of chitosan in the concentrations of 0.1, 0.2 and 0.3% (w/v) in liposomal formulations did not significantly affect the entrapment efficiency of OVA ($p > 0.05$). However, unlike OVA, IgG was not entrapped at all in liposomes when chitosan was included even at very low concentrations (e.g. 0.1% w/w) (Figure 4.8). The failure of liposomes to entrap IgG when chitosan was included suggests that the mucoadhesive might have prevented the protein from associating with the liposome bilayers. The similar surface charge of the IgG protein and the chitosan mucoadhesive may have resulted in displacement of the protein by the chitosan and prevention of its association with the bilayers of the liposomes. Further studies to check the interaction of chitosan with IgG are required in the future in order to understand the reason for this phenomenon. An alternative to chitosan was then required to proceed with the study; hence the alginate mucoadhesive was employed.

It has been previously reported that inclusion of chitosan with liposomes containing the positively charged loperamide has markedly decreased the entrapment efficiency of the drug (Guo *et al.*, 2003). According to Guo *et al.*, (2003), the positive charge of chitosan had higher affinity with the phospholipid bilayers when compared to the drug, resulting in drug exclusion and marked decreases in its entrapment. The outcomes from this study strongly imply that IgG is likely to be adsorbed in the liposome surfaces or associate with the liposome bilayers rather than being encapsulated within the aqueous spaces of the vesicles.

Contrary to chitosan, the inclusion of alginate in the liposomal formulations led to a significant increase in the entrapment efficiency of IgG (Figure 4.8). The entrapment efficiency of IgG in liposomes without any alginate included in its formula was $29.90 \pm 2.47\%$. When alginate was included in a concentration of 0.1% (w/w) no significant change in the entrapment efficiency of IgG was observed ($p > 0.05$). However, when the concentration of alginate was increased to 0.2 or 0.3% (w/w), the entrapment of the protein significantly increased

($p < 0.05$) to be $43.71 \pm 2.54\%$ and $44.30 \pm 2.92\%$, respectively, with no significant differences between the two concentrations ($p > 0.05$). It is suggested that the negative charge of alginate has enhanced the positively charged protein to interact and associate with the bilayers, resulting in enhanced protein entrapment. In light of those findings, alginate was incorporated into the IgG liposomes at a concentration of 0.2% (w/w) throughout the study.

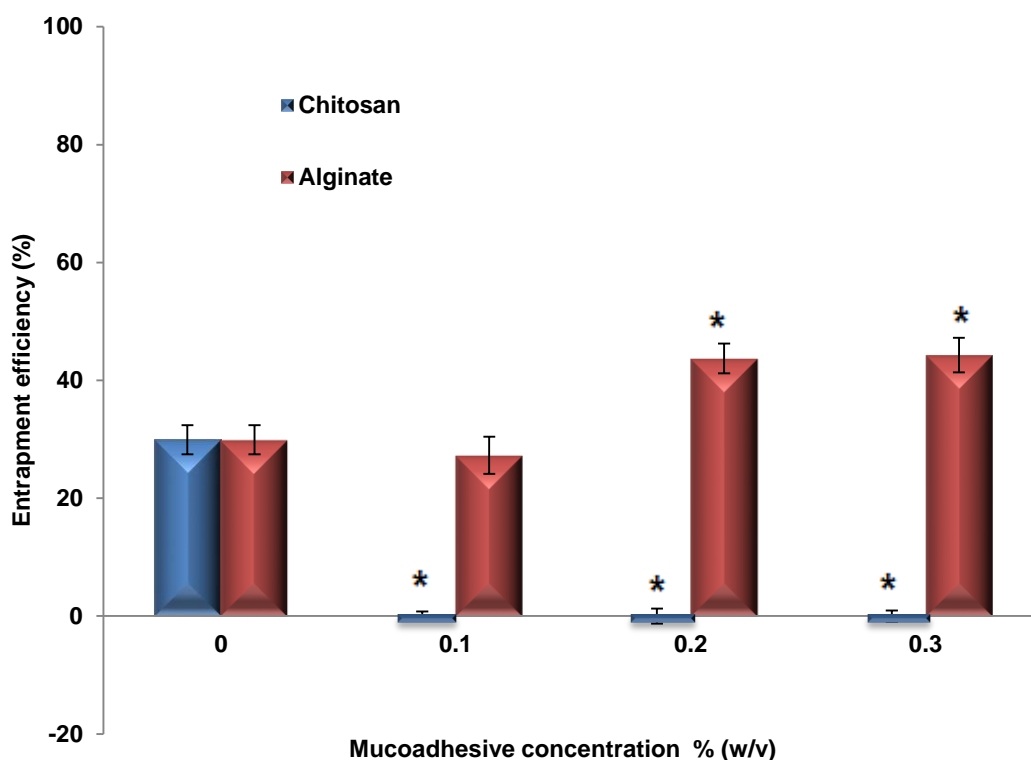


Figure 4.8: Mucoadhesive agents' (chitosan and alginate) concentration and its effect on entrapment efficiency of IgG in the generated liposomes. Data are mean \pm SD, $n=3$; * $p < 0.05$ for alginate or chitosan compared to their absence (i.e. 0% w/v)

4.3.4 Size reduction of IgG liposomes

The effect of size reduction of liposomes generated by the ethanol-based proliposome method incorporating IgG on size distribution, morphology, zeta potential and entrapment efficiency of the generated liposomes was investigated.

As discussed previously in Section 3.3.4, extrusion is an effective technique for size reduction of liposomes entrapping OVA. Nevertheless, this was not the case when IgG was chosen for encapsulation in liposomes, since a significant amount of IgG was trapped by the polycarbonate membrane filters upon extrusion, thus compromising the properties of the liposomes in terms of yield of the active ingredient (i.e. IgG). In order to avoid this problem, probe sonication was used to reduce the size of liposomes. Previously, it has been reported that IgG concentration decreased after filtration through a polycarbonate membrane filter from 10.5 g/L to 10 g/L thus, indicating that IgG adsorbs slightly to polycarbonate membrane filters (Walsh *et al.*, 1979). Yet, in this study, the adsorption was more pronounced, since extrusion was carried out through a series of different pore size polycarbonate membrane filters and for a set of seven extrusion cycles through each filter. In order to avoid this problem, probe sonication was used to reduce the size of liposomes.

By contrast, as observed with findings using OVA (Section 3.3.5), Walsh and Cole (Walsh and Coles, 1980) reported that albumin was not adsorbed by polycarbonate membrane filters, confirming the suitability of using extrusion as a method for the size reduction of OVA-based liposomes (Section 3.3.5).

Figure 4.9 demonstrates the effect of sonication time on the size and Pdi of the liposomes containing IgG and alginate. The size of liposomes significantly decreased from the original $3.63 \pm 0.44 \mu\text{m}$ to $946.9 \pm 46.3 \text{ nm}$ after only 1 minute of probe sonication. Further increase in sonication time to 2 minutes decreased the size of liposomes to 550.0 ± 34.1 , until liposomes reached a measured size of 388.1 ± 26.4 after a cumulative 4.5 minutes of probe sonication. In addition, there was no significant difference in the Pdi between liposomes sonicated for 1 or 3.5 minutes, and the Pdi approached its maximum value (i.e. just below 1). After 4 minutes of probe sonication a significant drop in Pdi to 0.613 ± 0.045 occurred, followed by a further marked drop in Pdi after a cumulative sonication duration of 4.5 minutes ($p < 0.05$), as the measured Pdi was 0.454 ± 0.039 .

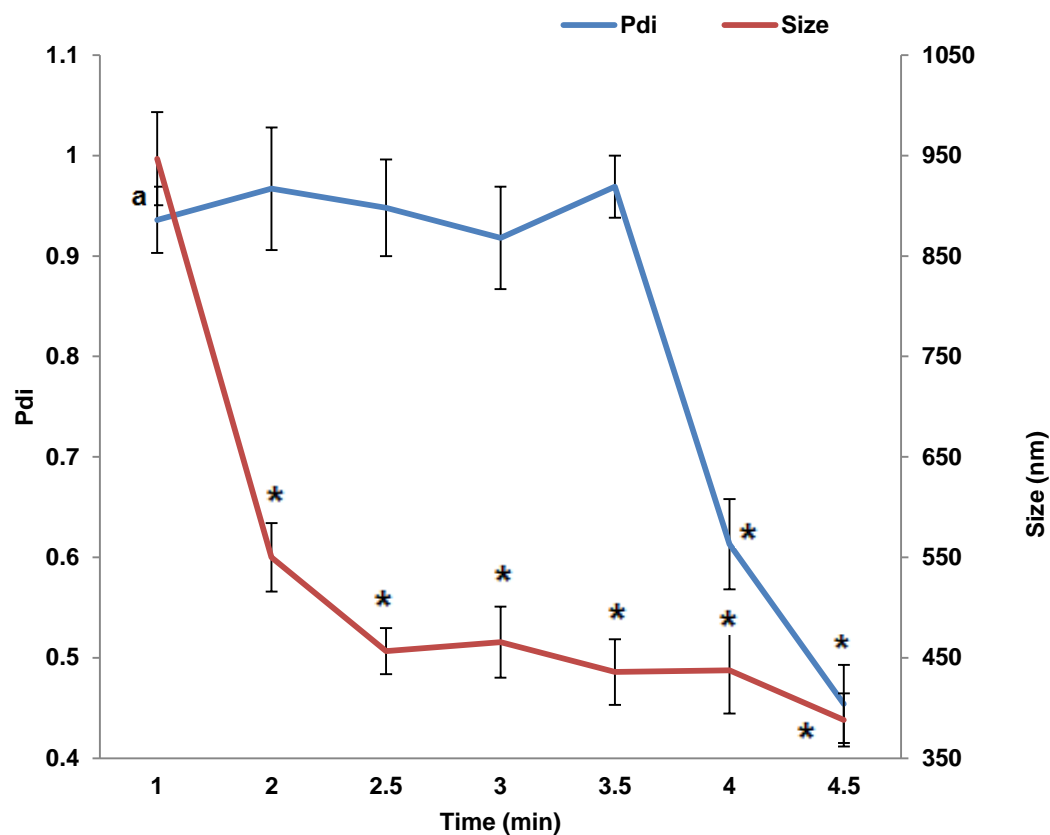


Figure 4.9: Probe sonication time and its effect on size and PDI of the generated liposomes. Data are mean \pm SD, $n=3$; * $p<0.05$ for size or PDI following the different sonication times compared to initial size and PDI (a).

Cryo-TEM studies performed demonstrated that, liposomes generated from the ethanol-based proliposome technology were predominantly MLVs (Figure 4.10a). Also displayed in (Figure 4.10b), sonication of the generated liposomes did not affect the multilamellar structure of liposomes.

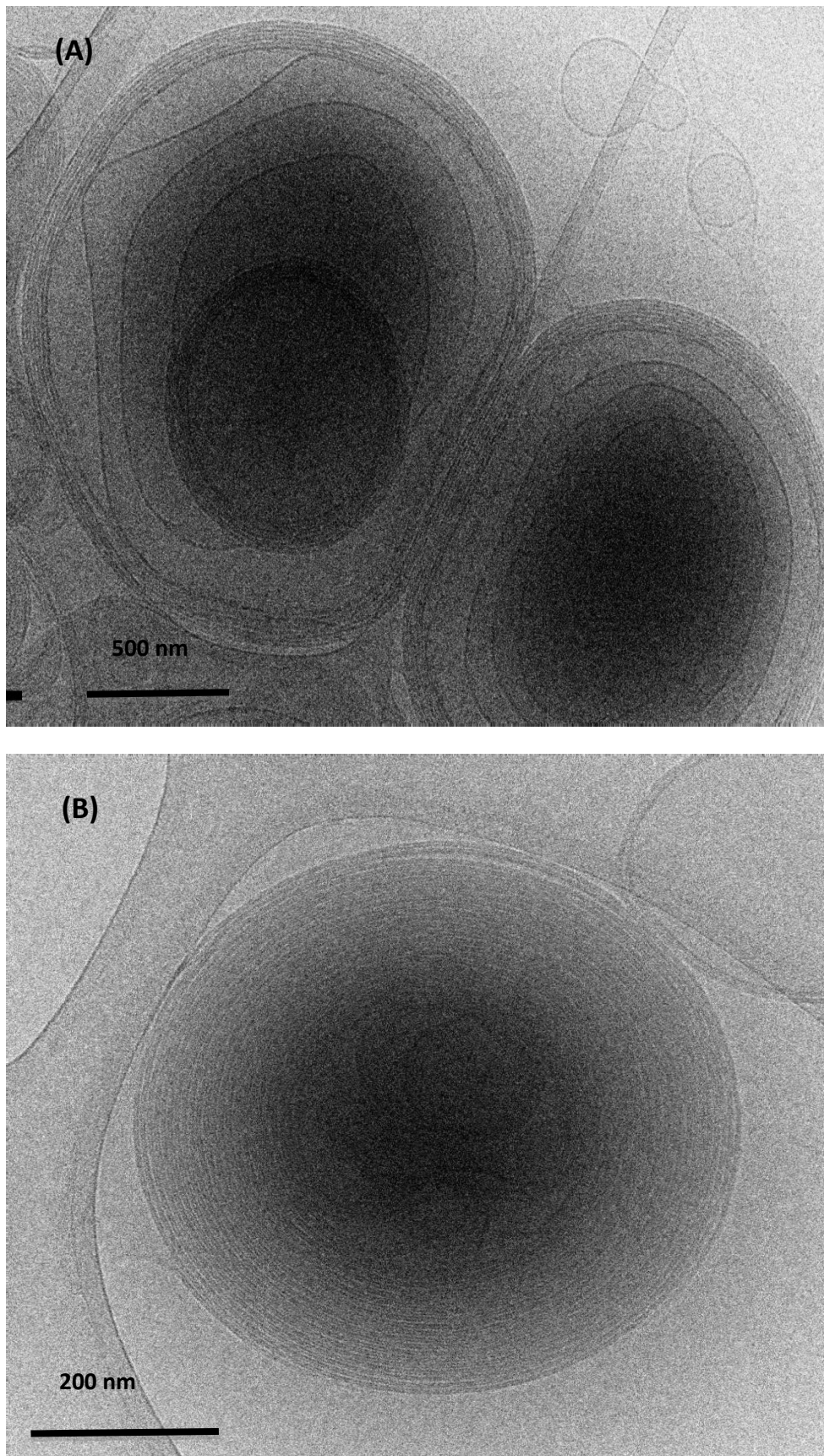


Figure 4.10: Cryo-TEM images of liposomal multilamellar structure (A) before and (B) after sonication. Typical of 4-6 different experiments.

The zeta potential was also measured and found not to change significantly after probe sonication ($p>0.05$) (Figure 4.11), where liposomes before probe sonication had a zeta potential value of -14.63 ± 1.63 mV and after 4.5 minutes of probe sonication had a value of -13.78 ± 2.13 mV. This finding was analogous to what was previously reported in (Section 3.3.5) for SS and OVA liposomes, where the main factor to affect the zeta potential was concluded to be the formulation composition.

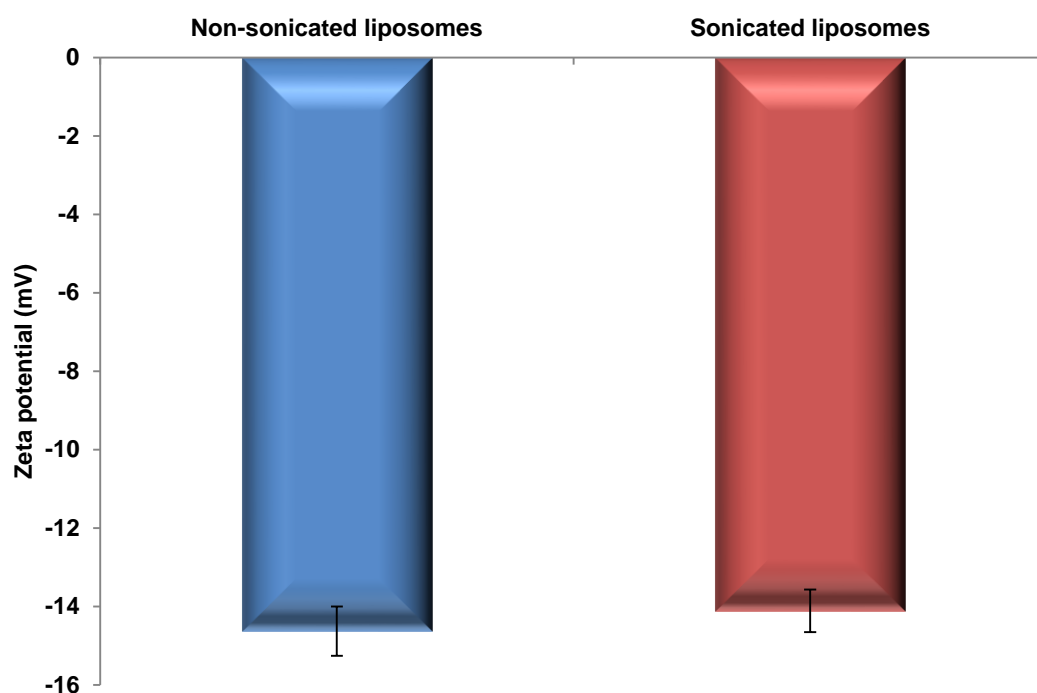


Figure 4.11: Effect of probe sonication on the zeta potential of liposomes. Data are mean \pm SD, n=3; $p>0.05$ for both formulations.

Contrary to the findings with OVA and SS based liposomes (Section 3.3.5), size reduction of IgG liposomes to 400 nm via probe sonication significantly increased ($p<0.05$) the entrapment efficiency of IgG in the liposomes from 43.71 ± 2.54 to $50.18\pm 2.87\%$ (Figure 4.12). This finding disagrees with previous findings reporting the decrease in the entrapment efficiency following size reduction (Szoka *et al.*, 1980; Elhissi *et al.*, 2007).

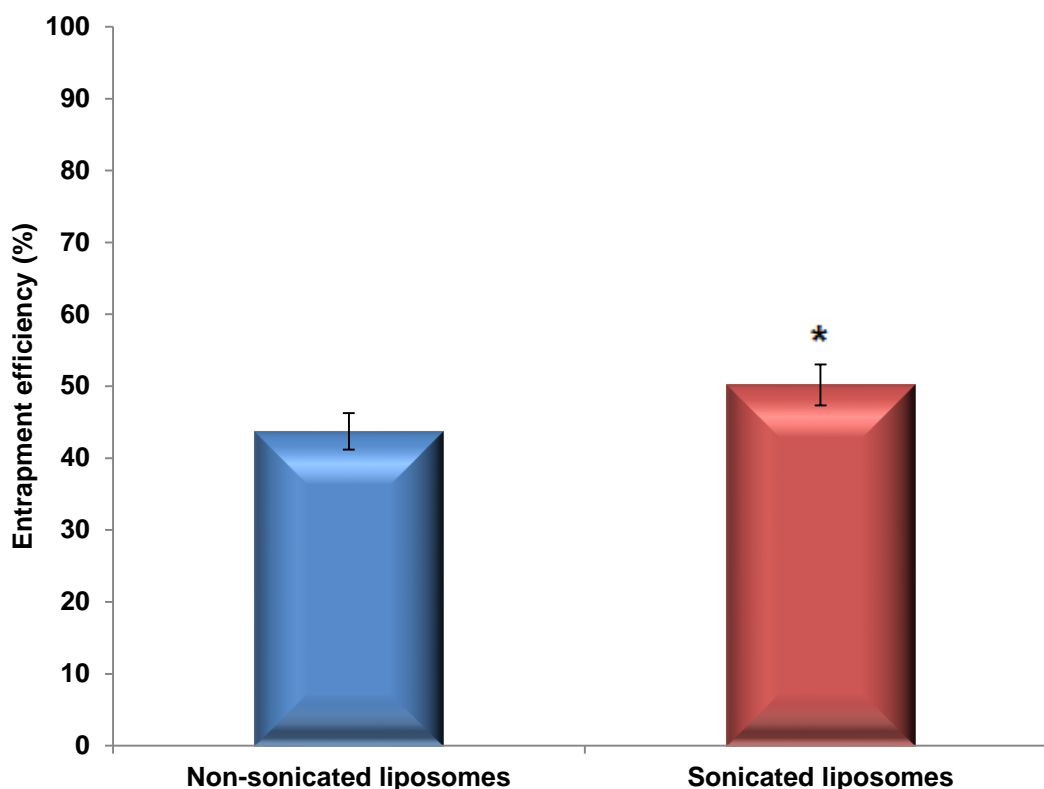


Figure 4.12: Effect of probe sonication on the entrapment efficiency of IgG in the generated liposomes. Data are mean \pm SD, n=3; * $p < 0.05$ for sonicated liposomes compared to non-sonicated liposomes.

A possible explanation for the results in this study could be the possible location or partitioning of the IgG on the outer surface of the liposomes. Therefore, an increase in the surface area of the bilayers after size reduction would be expected to increase the contact between the lipid bilayers and IgG, and hence enhance its entrapment. This justification may also explain the reduction in zeta potential demonstrated earlier for the IgG protein (Section 4.3.2) and their displacement when chitosan was included in the formulation (Section 4.3.3). Other studies reported similar findings, whereby size reduction led to an increase in entrapment efficiency (Dufour *et al.*, 1996; Phetdee *et al.*, 2008). Dufour *et al.*, (1996) previously reported an increase in the percentage of the enzyme immobilized on the surface of liposomes prepared by the ethanol-based proliposome method after sonication. They ascribed the enhanced entrapment to the higher surface area of the vesicles as a result of size reduction via sonication. Phetdee *et al.*, (2008) reported an increase in the

entrapment efficiency of tartaric acid from $51.1\pm 3.5\%$ to $68.3\pm 3.0\%$ after extrusion of liposomes.

4.3.5 Structural determination and activity of IgG.

As outlined in Section 4.2.5, CD was the method of choice in this study to determine the secondary structure of IgG. This was due to the fact that spectroscopic signals via CD are not affected by the presence of water, and CD can be used to determine the structure of IgG that is free in solution or incorporated into liposomes. Moreover, CD is suitable to study the IgG structure at different temperatures, thus enabling the detection of the structural changes induced by heat (Vermeer *et al.*, 1998). Figure 4.13 illustrates the α -Helix, Beta sheets, Beta turns and random coil (unordered) portions of the IgG in solution and bound to liposomes, as determined via CD.

As illustrated in Figure 4.13, the structure of IgG was significantly different ($p < 0.05$) for both the IgG in solution and IgG incorporated into liposomes. Whilst the α -Helix content was absent in the IgG solution, $47.7\pm 6.7\%$ appeared after its incorporation in the liposomal structure. Also, a significant reduction ($p < 0.05$) in the beta sheets content (i.e. from $52.0\pm 2.0\%$ to $25.7\pm 1.2\%$), beta turns content (from $19.5\pm 1.5\%$ to $6.3\pm 1.9\%$) and random coils content (from $28.5\pm 2.5\%$ to $20.7\pm 2.5\%$) was noticed when the IgG was incorporated into liposomes. The secondary structure of IgG in solution obtained from this study is consistent with literature reports, with the Beta sheet units being the predominant subunit and the presence of beta turns and random coils to a lesser extent (Amzel and Poljak, 1979; Vermeer *et al.*, 1998; Vermeer and Norde, 2000). On the other hand, the structure of the IgG incorporated into the liposomes closely resembles the previously reported CD structure of adsorbed IgG, with diminished beta sheets and beta turns content and the formation of the α -Helix subunits (Vermeer *et al.*, 1998). Sabin *et al.*, (2009) investigated the interaction of human IgG with dimyristoylphosphatidylcholine (DMPC) liposomes. Their results indicated that IgG was indeed adsorbed onto the

hydrophobic region of the liposomal membrane, thus explaining the change in the structure of IgG following its incorporation into liposomes.

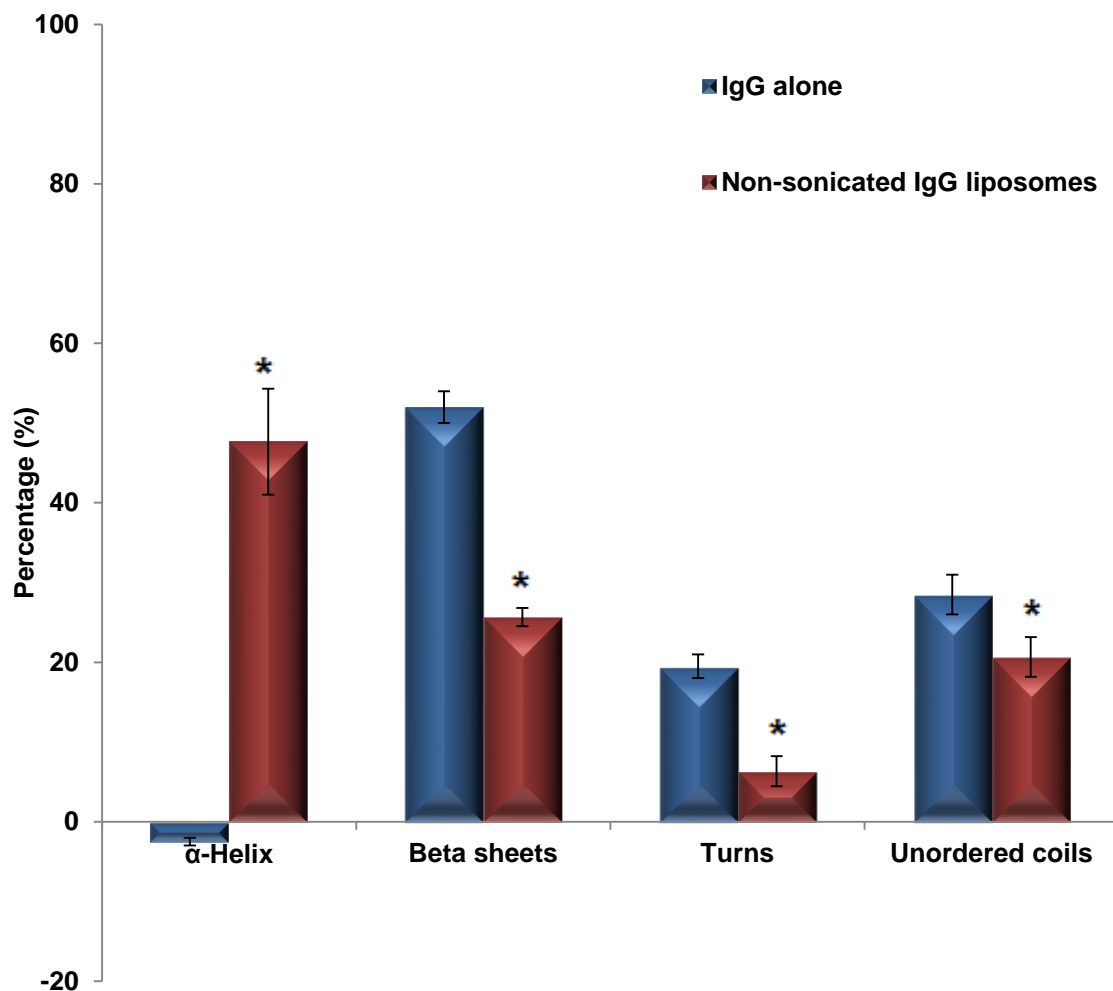


Figure 4.13: Secondary structure of IgG, both free in solution or incorporated into liposomes, as determined via CD. Data are mean \pm SD, n=3; * $p < 0.05$ for non-sonicated IgG liposomes compared to IgG alone.

In addition to determining the secondary structure of IgG, both free in solution and incorporated in liposomes, studies to determine the immunological activity of IgG were conducted (Figure 4.14). As demonstrated in Figure 4.14, IgG incorporated onto the liposomal membrane and IgG in solution were 100% active. The maintained activity of IgG following incorporation into liposome formulations can be attributed to the predicted end-on conformation of IgG onto

the liposome membrane, with the receptor binding portion (Fc) adsorbed onto the surface and the antigen binding sites facing the solution. Sabin *et al.*, (2009) concurred with this assumption, demonstrating that the Fc portion of the IgG is indeed the one inserted into the hydrophobic region of the liposomal bilayer, thus leaving the antigen binding region available on the outside of the liposomes. Moreover, Malmsten (1995) observed a similar end-on conformation of IgG on silica surfaces. This orientation of IgG can be attributed to the relatively lower structural stability of the Fc region in comparison to the Fab region, hence making it more ready to be adsorbed onto surfaces (Buijs *et al.*, 1996).

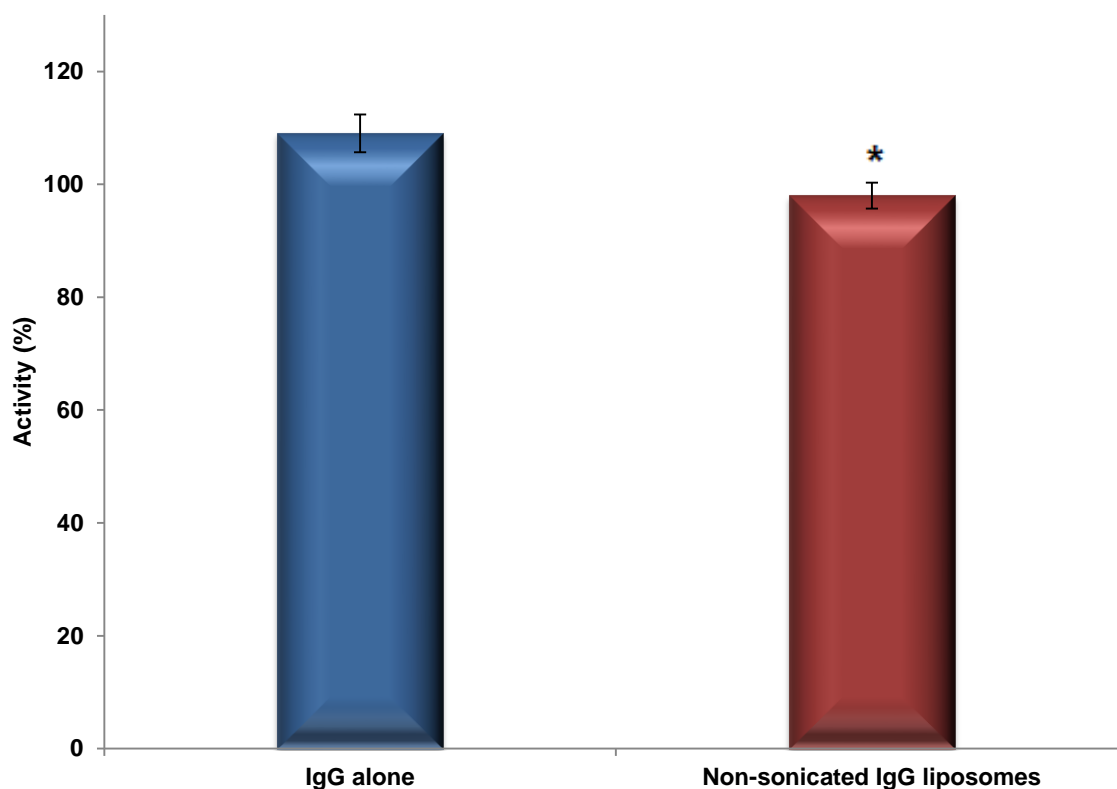


Figure 4.14: Activity of IgG free in solution or incorporated into liposomes, determined using the IgG easytitre kit. Data are mean \pm SD, n=3; * $p < 0.05$ for non-sonicated IgG liposomes compared to IgG alone.

4.3.6 Effect of temperature on the structure of IgG

The effect of temperature on the structure of IgG in solution or liposome formulation was assessed at temperatures between 20-80°C, as previously described in Section 4.2.5.

As demonstrated in Figure 4.15, the structure of IgG in solution was invariant up to a temperature of 60°C, with a CD that equals to zero mdeg at 206 nm and a minimum at 217 nm. However, at 70°C and 80°C, a significant ($p < 0.05$) reduction in the intensity at 217 was observed. This reduction in CD of the IgG at temperatures of 70 and 80°C indicates the loss of ordered structure of the protein (i.e. a decrease in the beta sheets' content and an increase in the unordered coils' contents), thus indicating possible denaturation of IgG. These results were analogous to the previous reports of Vermeer *et al.*, (1998) and Vermeer and Norde (2000), that temperatures above 65°C induce changes in the structure of IgG, with a notable decrease in the beta sheets and beta turns content and an increase in the random coils and alpha helix content.

Contrary to IgG in solution, IgG in the liposomal formulation was found to maintain its structure throughout the temperature range (Figure 4.16), thus indicating the preservation of the structure of IgG when incorporated into liposomes. Similar findings with adsorbed IgG were previously reported (Vermeer *et al.*, 1998).

4.3.7 Effect of size reduction on the structure and activity of IgG

As previously discussed in Section 4.3.4, probe sonication was the method of choice for size reduction of liposomes. Thus, the effect of probe sonication on the structure and activity of IgG in solution and liposomes was investigated (Figures 4.16 - 4.17).

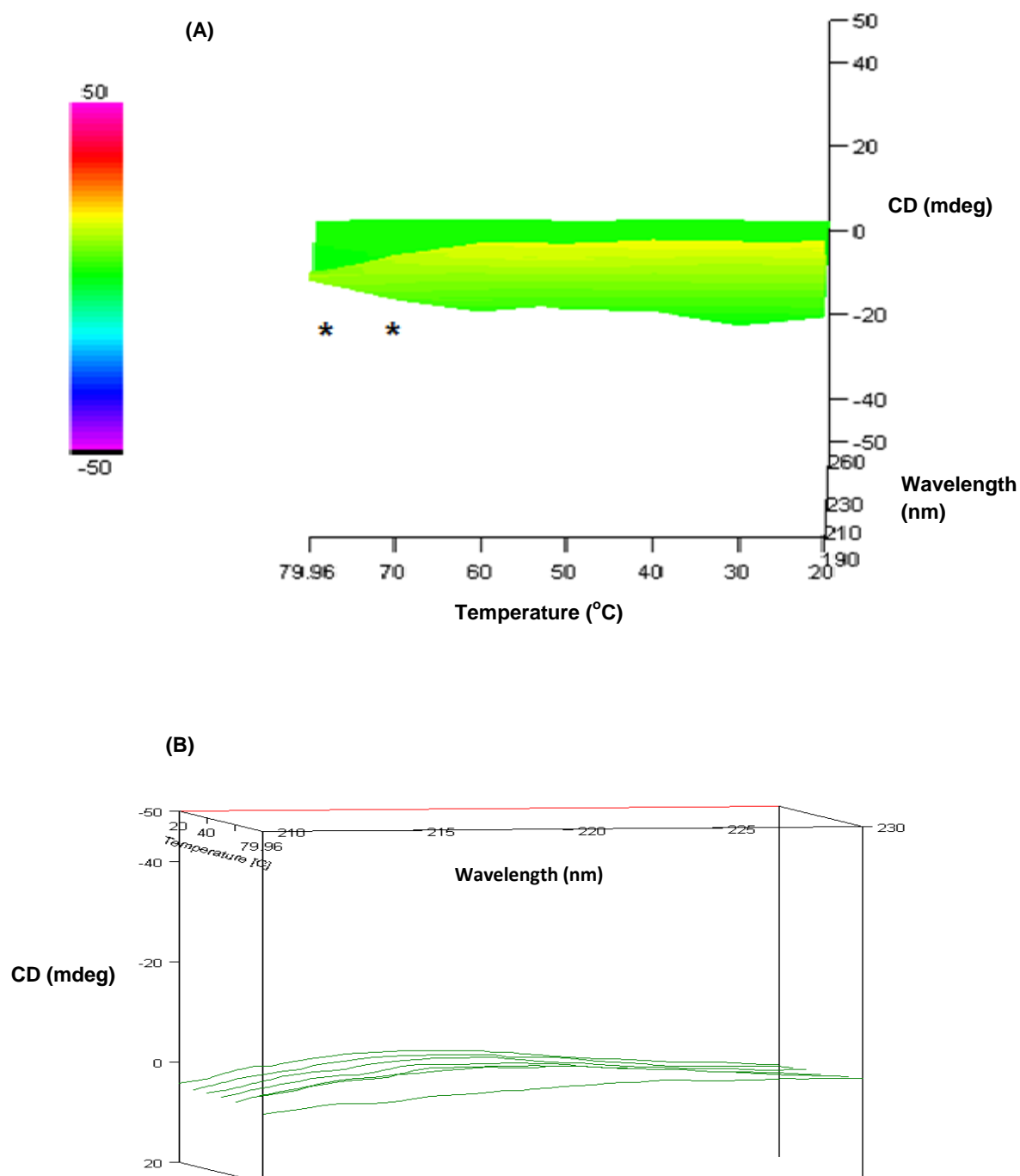


Figure 4.15: CD spectra of IgG in solution at temperatures between 20 °C and 70 °C. A 3D representation of (A) all the spectra combined and (B) the individual spectra at each temperature. Data are mean \pm SD, $n=3$; * $p<0.05$ for temperatures 70 °C and 80 °C compared to lower temperatures. A, B typical of 3 different experiments

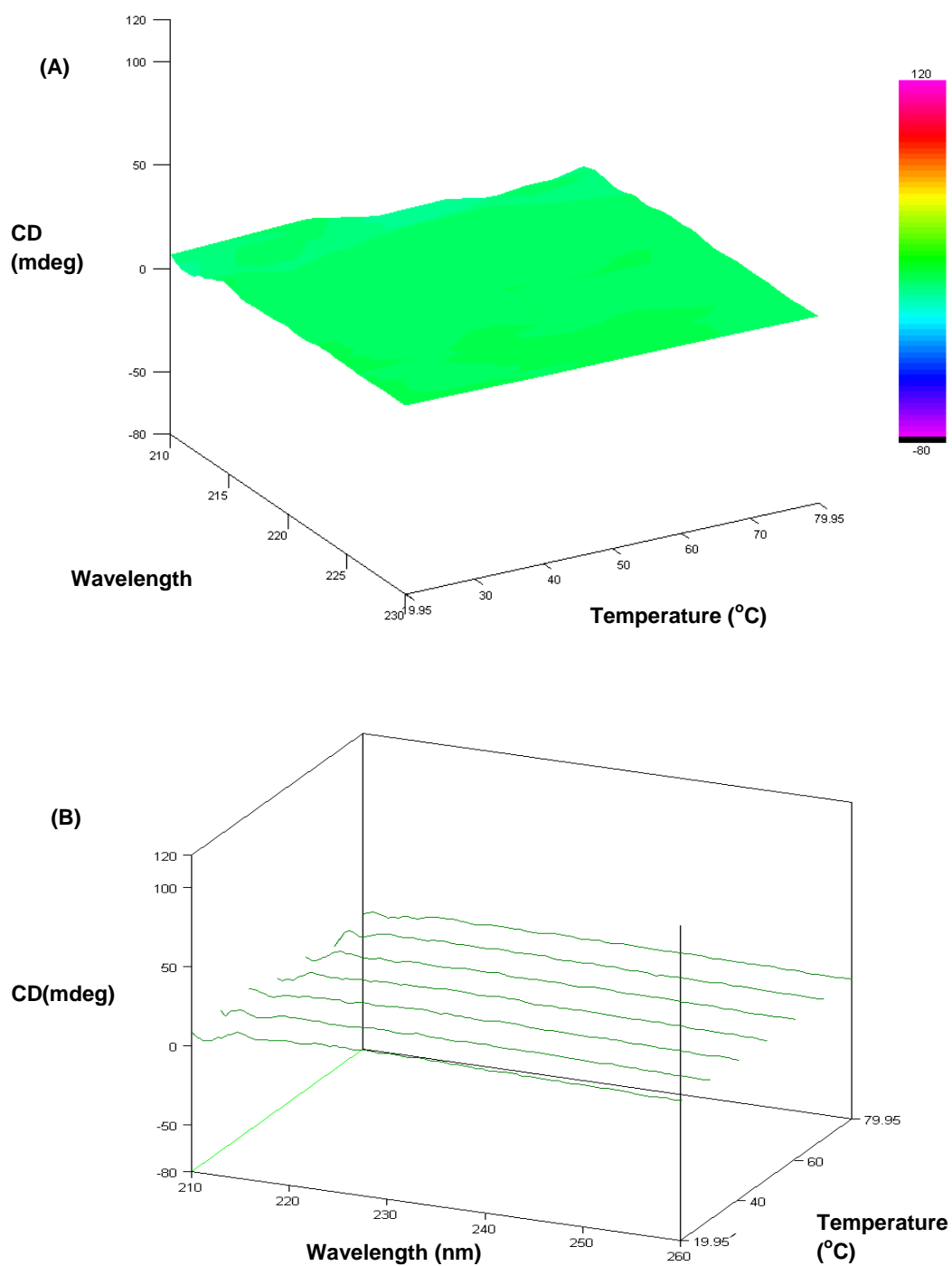


Figure 4.16: CD spectra of IgG incorporated in liposomes at temperatures between 20 °C and 70 °C. A 3D representation of (A) all the spectra combined and (B) the individual spectra at each temperature. Data are mean \pm SD, $n=3$; $p>0.05$ for all. A, B typical of 3 different experiments.

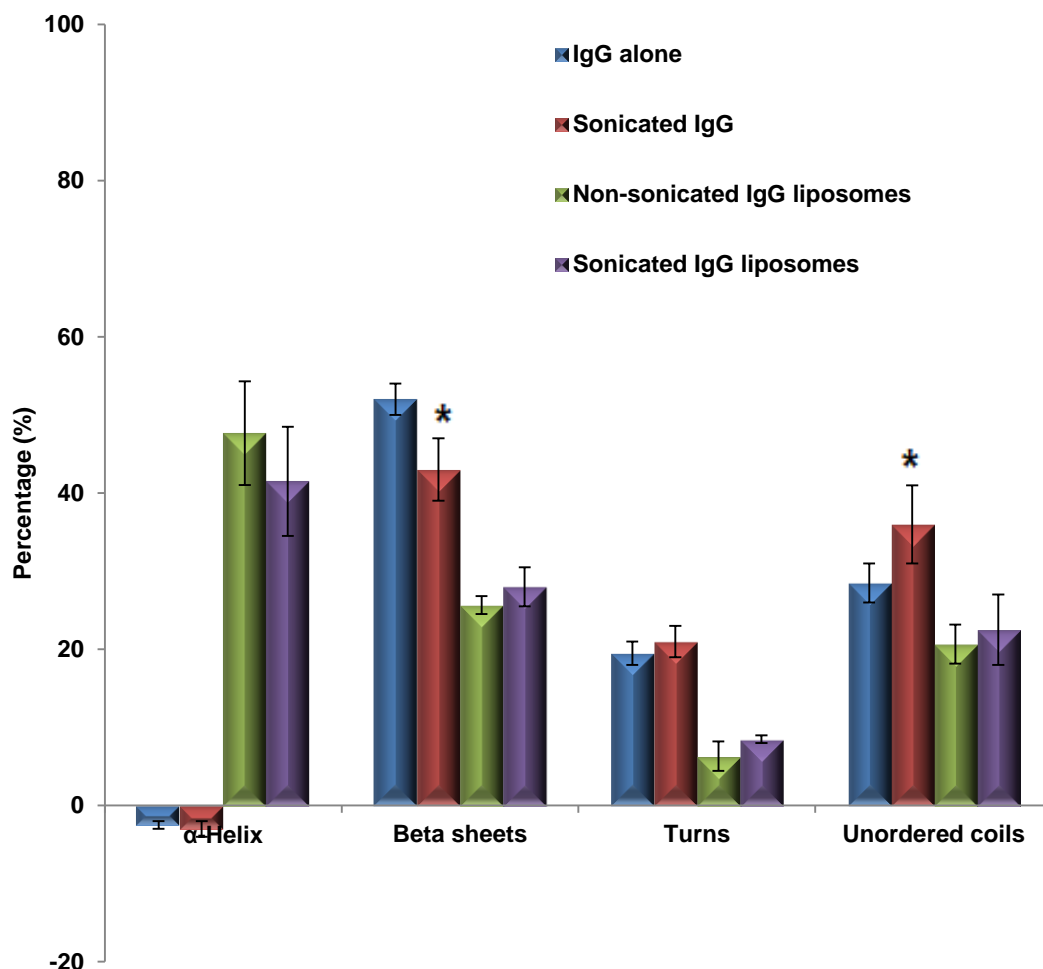


Figure 4.17: Secondary structure of IgG free and incorporated into liposomes before and after sonication. Data are mean \pm SD, $n=3$; * $p<0.05$ for IgG alone compared to sonicated IgG and Non-sonicated IgG liposomes compared to Sonicated IgG liposomes, respectively.

As shown in Figure 4.17, sonication of IgG solution caused no marked differences ($p>0.05$) in the α -Helix and beta turns content. The beta sheets content, on the other hand, was found to significantly decrease ($p<0.05$) (i.e. from 52.0 ± 2.0 to 43 ± 4.0 %) whilst the unordered random coils content was found to significantly increase ($p<0.05$) (i.e. from 28.5 ± 2.5 to 36 ± 5.0 %). Moreover, unlike the IgG in solution, no significant differences ($p>0.05$) in the secondary structure of the IgG bound to the liposomes were observed following

their size reduction.

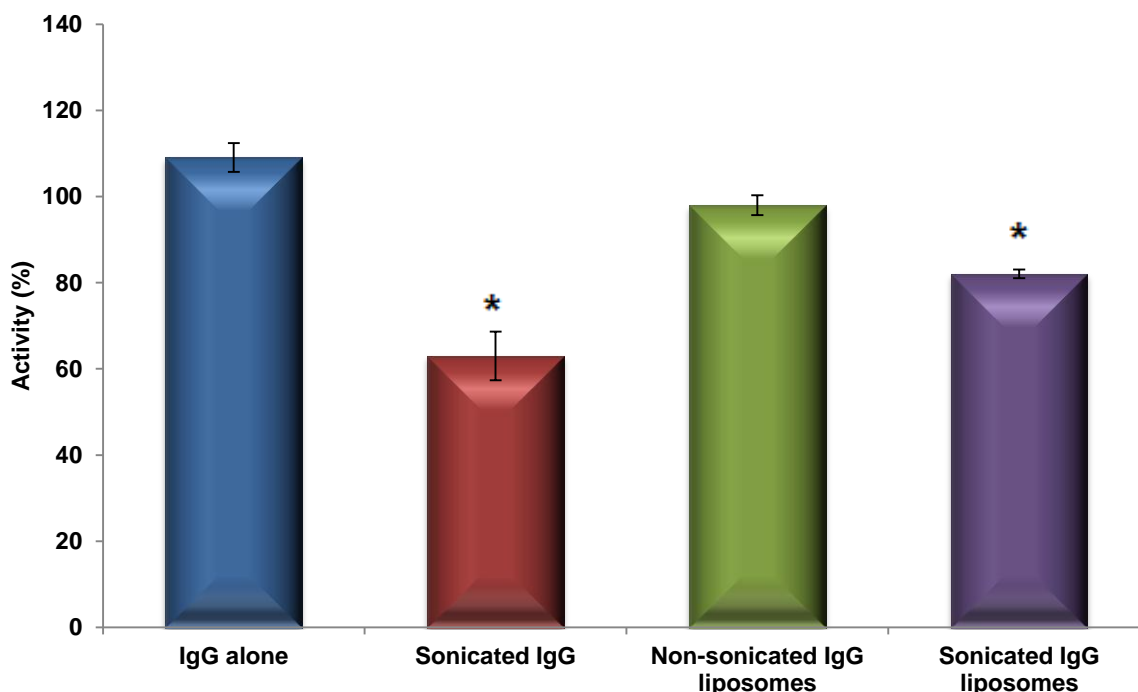


Figure 4.18: Activity of IgG free and incorporated into liposomes before and after sonication. Data are mean \pm SD, n=3; * $p<0.05$ for Sonicated IgG compared to IgG alone and Non-sonicated IgG liposomes compared to Sonicated IgG liposomes.

When the activity of IgG was investigated (Figure 4.18), both IgG in solution and IgG incorporated in liposomes demonstrated a significant loss ($p<0.05$) in activity following sonication by 46.09 and 15.95%, respectively. The loss of activity of IgG following sonication can be attributed to the shear stress and heat generation during sonication which may disrupt the activity of proteins (Morlock *et al.*, 1997; Zambaux *et al.*, 1999). This loss in activity of IgG upon sonication differs from the findings of Wang *et al.*, (2004), who reported that the integrity and immunoreactivity of IgG was not affected by sonication. This difference, however, may be attributed to the duration of sonication in their study, which was 30 seconds, compared to 4.5 minutes in our study.

Interestingly, despite the decrease in activity of both IgG in solution and in

liposome formulation, the decrease in activity for the IgG in solution was accompanied by a change in the secondary structure of the protein, whilst no correlation was observed for the IgG incorporated in liposomes. Moreover, the structural change of IgG in solution following sonication was typical of the previously reported structural change induced by heat (Section 4.3.6), with a distinguishable decrease in the beta sheets' content and an increase in the unordered content. These findings indicate that heat generation during sonication contributed to the loss of activity of IgG in solution. Furthermore, the previously reported structural stability to heat of liposome-IgG (Section 4.3.6) can therefore explain the higher maintained activity following sonication, since only shear force is expected to have caused this reduction in activity, whilst both heat and shear stress contribute to the reduction of the activity of the IgG in solution.

4.4 Conclusions

The results from this chapter confirmed the validity of liposomes prepared via the different methods for the entrapment of IgG, and demonstrated the superiority of liposomes prepared via the ethanol-based proliposome method for the entrapment of IgG over the other liposome preparation methods. Moreover, the findings in this chapter showed an inverse relationship between the IgG concentration incorporated into liposomes and the entrapment efficiency.

This study also established that mucoadhesive agents such as chitosan and alginate can be efficiently incorporated into the liposome structure. The nature of the incorporated mucoadhesive agent and its concentration were found to play an important role in determining the characteristics of the generated liposomes. For instance, whilst incorporation of chitosan in the liposomal structure led to total evacuation of IgG from the liposomes, the incorporation of alginate was found to enhance the entrapment efficiency of IgG.

Unlike findings in Chapter 3, the size reduction of liposomes entrapping IgG was demonstrated to lead to a marked increase in entrapment efficiency values

of IgG, indicating the possible allocation of the IgG on the liposomal surface. The performance of activity studies also confirmed these findings, since the activity of entrapped IgG was retained when incorporated into liposomes. This suggests that an end-on conformation of IgG on the liposomal surface occurred.

This study also demonstrates the utility of CD spectroscopy as a viable technique to study the conformation IgG both free in solution or incorporated into liposomes. CD results in this study demonstrated significant differences between the structures of IgG free in solution and incorporated in liposomes. CD results also suggested that the IgG is adsorbed onto liposomal surfaces, analogous to results previously reported for IgG adsorbed to hydrophobic surfaces (Vermeer *et al.*, 1998).

In addition to preserving the activity of incorporated IgG, liposomes prepared from ethanol-based proliposomes were found to enhance the stability of IgG to heat and shear stress, as demonstrated via CD and activity studies, respectively. This suggests the promise ethanol-based proliposome technology in the area of protein delivery.

Overall, novel mucoadhesive liposomal formulations generated from ethanol-based proliposomes entrapping IgG were prepared and characterised in this study. These formulations were found to have relatively high entrapment efficiency values of IgG, both in their submicron and micron range, and they will be used for the rest of this study.

CHAPTER 5

DELIVERY OF LIPOSOMES GENERATED FROM ETHANOL- BASED PROLIPOSOMES VIA MEDICAL NEBULISERS

5.1 Introduction

The investigation of non-invasive routes for the delivery of macromolecules has attracted tremendous biomedical and scientific interest in recent years. The pulmonary delivery of macromolecules as aerosols is one of the most interesting fields being studied (Edwards *et al.*, 1998).

Pulmonary delivery of molecules provides many advantages, such as improved bioavailability of drugs and enhanced patient compliance. Furthermore, the large surface area of the lung and its high vascularity permit rapid drug absorption into the systemic circulation (Farr *et al.*, 1987; Adjei and Gupta, 1994; Torchilin, 2006). Despite the many advantages offered by pulmonary delivery, the systemic bioavailability yield of inhaled macromolecules is low, mainly due to their low permeability and enzymatic degradation (Jorgensen and Nielson, 2010).

One proposed solution to overcome the limitations of pulmonary delivery is the encapsulation of macromolecules into liposomes, since liposomes can enhance the retention time of macromolecules in the pulmonary system and offer sustained release into the systemic circulation (Bi and Zhang, 2007). Furthermore, liposomes show high compatibility with pulmonary alveoli, since their phospholipids are natural components of the alveolar surfactants (Finley *et al.*, 1968).

Unfortunately, the number of clinically approved liposome formulations is limited because of the instability of liposome phospholipids in aqueous environment during storage. Various approaches have been employed to stabilize liposomes, such as the use of proliposomes, which are stable phospholipid formulations that generate liposomes upon addition of an aqueous phase (Payne *et al.*, 1986a; Payne *et al.*, 1986b; Perrett *et al.*, 1991).

A major challenge in aerosolizing liposome formulations is the liposome physical stability and the fragmentation of liposomes during nebulization (Taylor *et al.*, 1990a; Saari *et al.*, 1999; Elhissi *et al.*, 2006a). Various methods have been employed for improving the stability of liposomes during nebulization, including size reduction of liposomes prior to nebulization (Niven *et al.*, 1991; Finlay and Wong, 1998).

Different types of nebulisers have been studied for liposome delivery, including air-jet, ultrasonic and vibrating-mesh nebulisers. Various *in vitro* methods are well-established for studying the performance of medical nebulisers and examining the properties of their aerosolised droplets (O'Callaghan and Barry, 1997; Bisgaard *et al.*, 2001). Amongst the most important variables in defining the dose deposited are the aerosol particle size and respirable fraction, which is also known as the fine particle fraction (FPF) (Labiris and Dolovich, 2003).

Different technologies can be used to investigate the aerosol median size, namely time-of-flight (TOF), which gives indication on the MMAD (Vecellio *et al.*, 2001; Waldrep *et al.*, 2007) and laser diffraction, which measures the VMD of the aerosols (Clark, 1995).

This study investigated the feasibility of using different medical nebulisers for the delivery of liposomes generated from ethanol-based proliposomes entrapping IgG. The study further determined the effect of size reduction of liposomes (via sonication) on the performance of the nebulisers, characteristics of the generated aerosols and stability of the liposomes and their incorporated IgG.

The performance of the nebulisers for the delivery of a conventional IgG solution, probe-sonicated liposomes and non-sonicated liposomes was studied in terms of nebulization time, sputtering time, mass output and output rate. The generated aerosols on the other hand were assayed for particle size, size distribution, FPF and FPF output using the TOF and laser diffraction technologies. In addition, the physical stability of the liposomes was investigated by measuring the size and size distribution of the liposomes (non-sonicated and sonicated) prior to and after nebulization. Furthermore, the effect of size reduction of liposomes and nebulisation on the integrity of IgG (both free in solution and incorporated into the liposomal structure) was investigated in this study by means of assaying the secondary structure and activity of the protein.

5.2 Methodology

5.2.1 Preparation of IgG liposomes

Liposomes were manufactured as described in Section 2.2.1 by modifying the ethanol-based proliposome previously described by Perrett and co-workers (1991). They comprised 10 mg/ml lipid (2:1 SPC to cholesterol), 0.5 mg/ml IgG and 0.2% w/v mucoadhesive agent (sodium alginate) to make up a final volume of 5 ml using HPLC water. For the size reduction of liposomes, probe sonication for 4.5 minutes was employed to produce 400 nm vesicles, as previously described in Section 4.3.4. Furthermore, the IgG solution comprised of 0.5 mg/ml IgG in 5 ml HPLC water.

5.2.2 Determination of nebuliser performance

As outlined earlier in Section 2.2.11, three different nebulisers were employed in this study: An air-jet Pari Turbo Boy nebuliser (Pari GmbH, Germany), an Omron Micro Air NE-U22 vibrating-mesh nebuliser (Omron Healthcare, UK Ltd., UK) and a Polygreen ultrasonic nebuliser (Clement Clarke International, UK). Formulation (i.e. IgG solution or liposomes, non-sonicated or sonicated) (5 ml) was placed in the nebulisers, and as described in (Section 2.2.11) the time required for aerosol generation to become erratic “nebulisation time” and the duration of this erratic generation behaviour to cease “sputtering duration” were determined. Furthermore, studies to determine the aerosol mass output were performed, as previously elucidated in Section 2.2.11.

5.2.3 Determination of aerosol size distribution

Studies to determine the aerosol droplet size distribution (DSD) and the fine particle fraction (FPF) were conducted as described in Section 2.2.12, using both

the Malvern Spraytec laser diffraction instrument (Malvern Instruments Ltd, UK) and the Model 3321 Aerodynamic Particle Sizer[®] (APS) Spectrometer (TSI, UK). FPF output was determined in relation to mass and active protein output (see Section 2.2.12).

5.2.4 Characterisation of liposomes

Size and size distribution of liposomes before nebulization, in the nebulizer container and collected in the flask following nebulization (i.e. delivered liposomes) were determined as described previously using laser diffraction via the Mastersizer 2000 (Malvern Instruments Ltd, UK) or via dynamic light scattering (DLS) using the Malvern Zetasizer Nanoseries (Malvern Instruments Ltd, UK). The Mastersizer was employed for non-sonicated liposomes and the Zetasizer for probe-sonicated liposomes. Also, the morphology of the delivered liposomes (non-sonicated and sonicated) was investigated using cryo-TEM (see Section 2.2.6).

5.2.5 Determination of structure and activity of IgG

The secondary structure of IgG was determined as previously discussed in Section 2.2.9 via CD spectroscopy using a J-815 spectropolarimeter (Jasco, UK). CD spectra of IgG both in solution or incorporated into liposomes (non-sonicated and sonicated) were then estimated using DICHROWEB via the secondary structure algorithm CDSSTR (Greenfield, 2006). Moreover, the immunoreactivity of the protein was determined using an easy titre IgG kit according to the protocol previously described in Section 2.2.10.

5.3 Results and discussion

5.3.1 Determination of nebuliser performance

In this study the nebulisation time required for IgG solution, non-sonicated IgG liposomes and probe-sonicated IgG liposomes (400 nm) was investigated using three different nebulisers:

- 1- An air-jet Pari Turbo Boy nebuliser
- 2- A vibrating-mesh Omron MicroAir NE-U22 nebuliser
- 3- An ultrasonic Polygreen nebuliser

As previously outlined in Section 5.2.2, the time required for nebulisation to become erratic was investigated in this study and recorded as the “nebulisation time” (Figure 5.1). Also, the time required for the cessation of aerosol generation was determined and referred to as the “sputtering duration” (Figure 5.2).

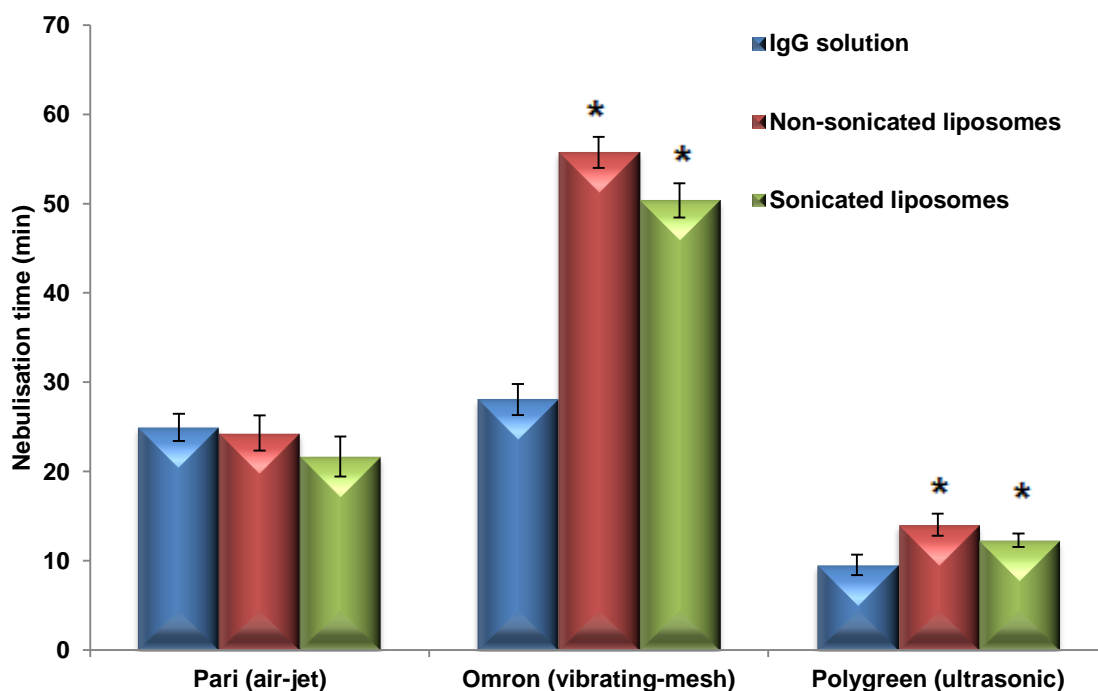


Figure 5.1: Nebulisation time of IgG solution and IgG liposomes before and after probe-sonication using Pari Turboboy (air-jet), Omron MicroAir (vibrating-mesh) and Polygreen (ultrasonic) nebulisers. Data are mean \pm SD, $n=3$; * $p < 0.05$ for Non-sonicated liposomes and Sonicated liposomes compared to IgG solution in the three nebulisers.

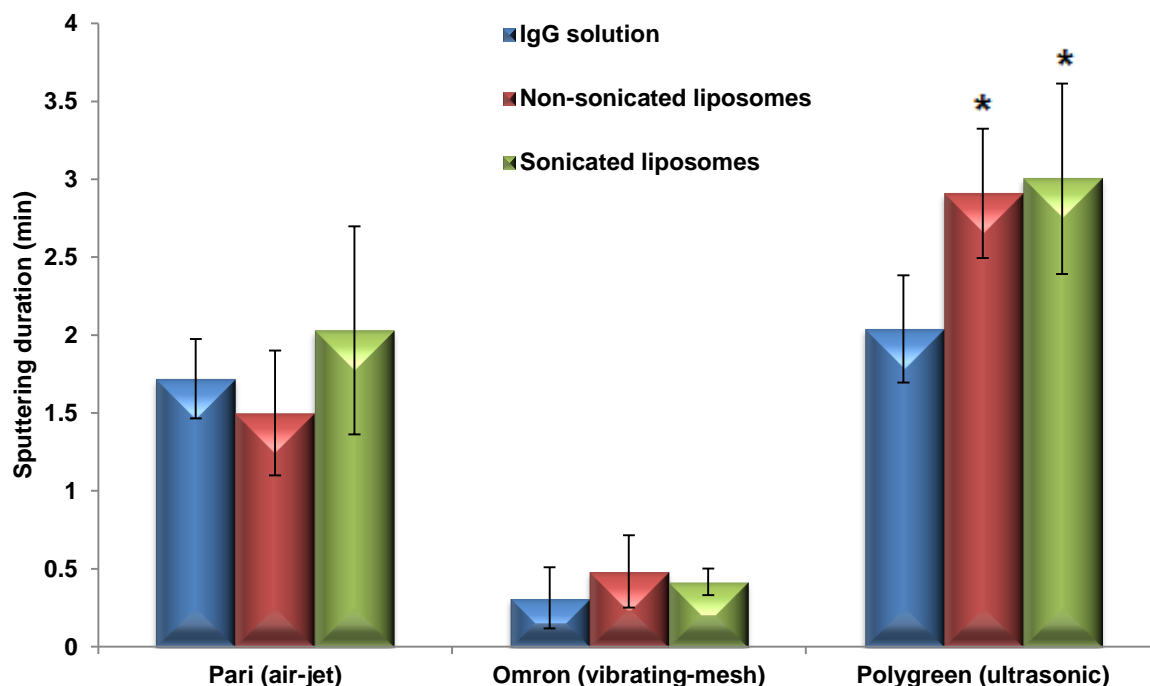


Figure 5.2: Sputtering duration of IgG solution and IgG liposomes before and after probe-sonication using Pari (air-jet), Omron (vibrating-mesh) and the Polygreen (ultrasonic) nebulisers. Data are mean \pm SD, n=3; * $p < 0.05$ for Non-sonicated liposomes and Sonicated liposomes compared to IgG solution in the three nebulisers.

As demonstrated in Figures 5.1-5.2, the time required for nebulisation of the different formulations using the Pari, Omron and Polygreen nebulisers differed significantly ($p < 0.05$), and where in the order of Omron > Pari > Polygreen. Also, unlike the Omron and the Polygreen nebulisers, the nebulisation time of the Pari device was similar for the different formulations ($p > 0.05$). Figure 5.1 also elucidates that when the Omron nebuliser was employed, the nebulisation time required for the IgG solution was 28.05 ± 1.74 minutes and that was prolonged to 50.36 ± 1.92 minutes and 55.74 ± 1.73 minutes for sonicated and non-sonicated liposomes, respectively. The prolonged time of nebulisation could be attributed to the increase of fluid viscosity when liposome formulations were used, whereby the viscosity of the liposomal suspension is expected to be higher than IgG solution due to the presence of a considerable amount of lipid (10 mg/ml) and alginate (2 mg/ml) in the liposome formulations. This effect of viscosity on the nebulisation time for the Omron can be attributed to the low energy of atomisation employed by the nebuliser (Ghazanfari *et al.*, 2007). Furthermore, due to the larger size of the

non-sonicated liposomes, the blockage of some of the mesh apertures is more likely to have occurred, resulting in prolonged nebulisation.

Also displayed in Figure 5.1, the Polygreen nebuliser was found to exhibit the shortest nebulisation time compared to the Pari and Omron nebulisers. This finding is analogous to earlier studies (Mercer, 1981; Sterk *et al.*, 1984; Mc Callion *et al.*, 1996b). Similar to the Omron nebuliser, nebulisation using the Polygreen device was significantly different ($p < 0.05$) amongst formulations, being 9.53 ± 1.14 , 12.28 ± 0.75 and 14.03 ± 1.25 minutes for the IgG solution, probe-sonicated IgG liposomes and non-sonicated IgG liposomes, respectively. The expected difference in physicochemical properties between formulations could be the reason for the difference in nebulisation time.

As discussed in Section 1.2.4.3, droplet formation in ultrasonic nebulisers results from the disintegration of capillary waves. Those capillary waves have an amplitude directly proportional to the liquid viscosity and hence suppression of the atomisation process is expected when the fluid viscosity is high (Boguslaskii and Eknadiosyants, 1969).

Unlike the Omron and ultrasonic nebulisers, nebulisation using the Pari (Figure 5.1) was independent of formulation, since no significant differences ($p > 0.05$) were found in the nebulisation time between formulations. This finding did not agree with previous reports, which demonstrated a prolongation of the time required for nebulisation in air-jet nebulisers when high viscosity solutions were used (McCallion *et al.*, 1995). The disagreement with the findings of McCallion *et al.*, (1995) might be attributed to the effectiveness of the Pari Turbo Boy compressor employed in our study and its suitability for the delivery of formulations with higher viscosity, or because of the possible lowering of surface tension when using liposomes (Elhissi *et al.*, 2011b).

Similar to nebulisation results, marked differences were found to exist in the sputtering duration for the different nebulisers ($p < 0.05$), being in the order: Polygreen > Pari > Omron (Figure 5.2). Moreover, contrary to the Omron and Pari nebulisers, the formulation type affected the sputtering duration for the Polygreen device ($p < 0.05$). Whilst sputtering duration was 2.04 ± 0.34 minutes for the IgG solution, it was markedly prolonged to 2.91 ± 0.42 and 3.00 ± 0.61 minutes for the

non-sonicated and sonicated liposomes, respectively. These results therefore indicate that the viscosity parameter is mostly influential on ultrasonic nebulisers, which came in agreement with the findings of Steckel and Eskandar (2003).

Despite the fact that nebulisation was carried out to dryness, nebulisation does not usually result in complete atomization of the preparations, hence, the mass output does not reach 100%, and some of the fluid remains as a dead residual volume within the nebuliser (Clay *et al.*, 1983). In this study, the effect of nebuliser type and formulation on the mass output was also investigated (Figure 5.3).

Figure 5.3 demonstrated that mass output was significantly different between the different nebulisers ($p < 0.05$). Despite the long nebulisation time required by the Omron nebuliser, its mass output was very high, having an average value of 96.4%. This high mass output of the Omron nebuliser has been demonstrated previously (Elhissi and Taylor, 2005; Elhissi *et al.*, 2006a). Furthermore, Vecellio *et al.*, (2006) and Dolovich and Dhand, (2011) reported that vibrating-mesh nebulisers have lower residual volumes than air-jet and ultrasonic nebulisers.

The ultrasonic nebuliser by contrast generated the lowest mass output (approximately 65%). Furthermore, the mass output of the Pari nebuliser was found to lie in between the Polygreen and Omron outputs, and had an average value of 85.3%.

Also elucidated in Figure 5.3, the nature of formulation did not significantly influence the mass output for the different nebulisers ($p > 0.05$). Therefore, despite the effect formulations had on the nebulisation time of Omron and Polygreen nebulisers, the mass output was not compromised. The Results from this study thus indicate that the design and method of action of the nebuliser rather than the nature of the formulation is the main determinant of the mass output.

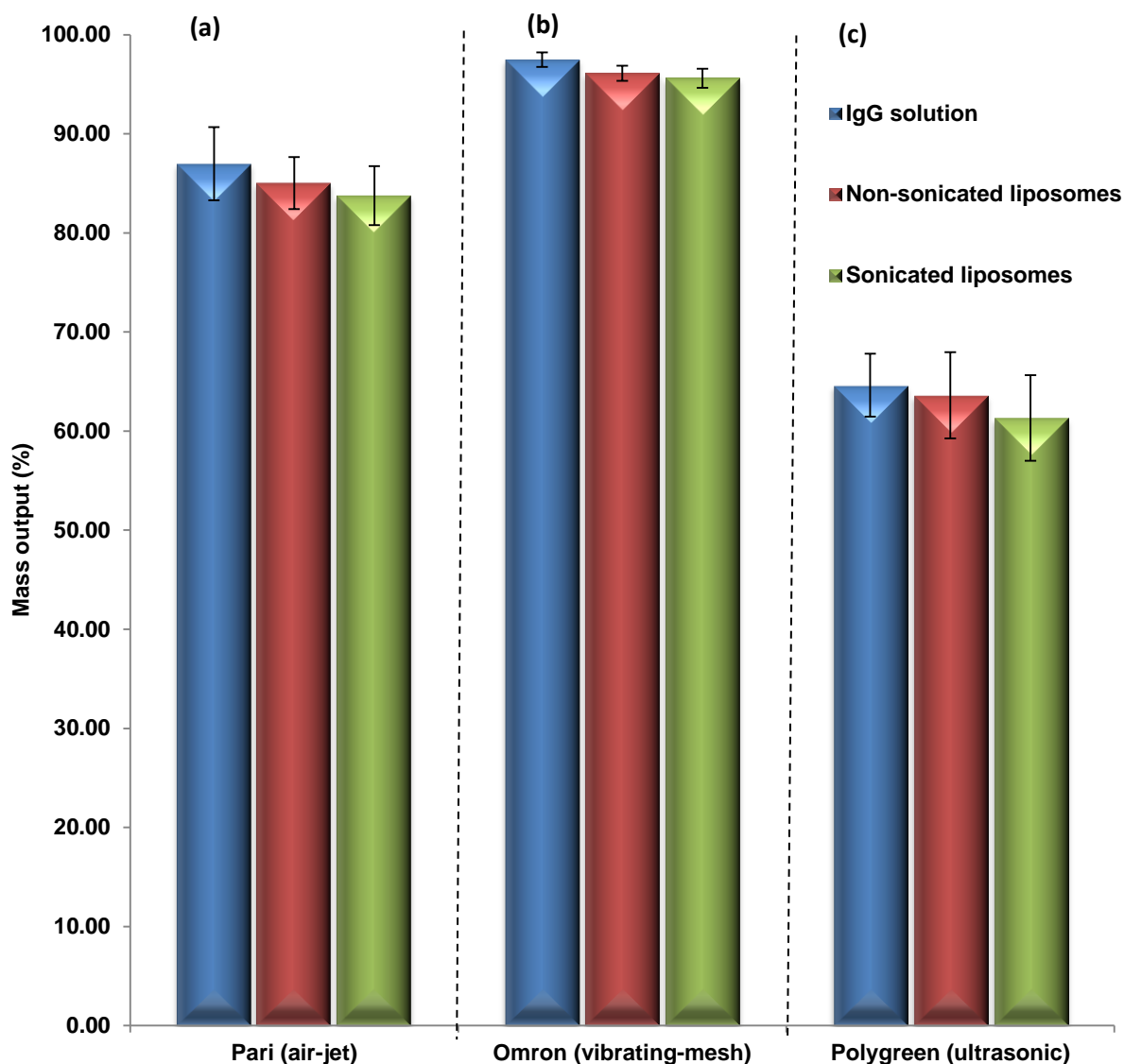


Figure 5.3: Mass output for IgG solution and IgG liposomes before and after probe-sonication using; (a) Pari (air-jet), (b) Omron (vibrating-mesh) and (c) the Polygreen (ultrasonic) nebulisers. Data are mean \pm SD, $n=3$; $p>0.05$ for the three different formulations in all three nebulisers.

In addition to nebulisation time, sputtering duration and mass output, the output rates using the different nebulisers were determined in this study for the three different formulations (Figure 5.4). As displayed in Figure 5.4, the three nebulisers differed significantly ($p<0.05$) in their output rate. The output rate values were in the order of: Polygreen > Pari > Omron. Also, contrary to the Omron and Polygreen, the output rate of the Pari nebuliser was independent on formulation ($p>0.05$).

The output rate of the protein solution using the Omron nebuliser was 173.84 ± 1.32 mg/min as demonstrated in Figure 5.4. This, however, was found to significantly decrease ($p < 0.05$) to 86.69 ± 0.68 mg/min and 95.35 ± 0.96 for the non-sonicated and sonicated liposomes, respectively. The slower rate of nebulisation of liposomes using the Omron might be attributed to the expected higher viscosity of the liposome formulations. Also, possible blockage of some of the meshes by large liposome is thought to have occurred following nebulisation. This can also explain the slowest output rates demonstrated for non-sonicated liposomes.

The Polygreen nebuliser on the other hand exhibited the highest output rate values amongst the devices investigated (Figure 5.4). Also, for the Polygreen nebuliser, the output rate of the IgG solution was significantly higher ($p < 0.05$) than the two liposome preparations which demonstrated similar output rates ($p > 0.05$). This therefore indicates that, like in the Omron nebuliser, the size of the liposomes in the Polygreen nebuliser affects the nebulisers performance.

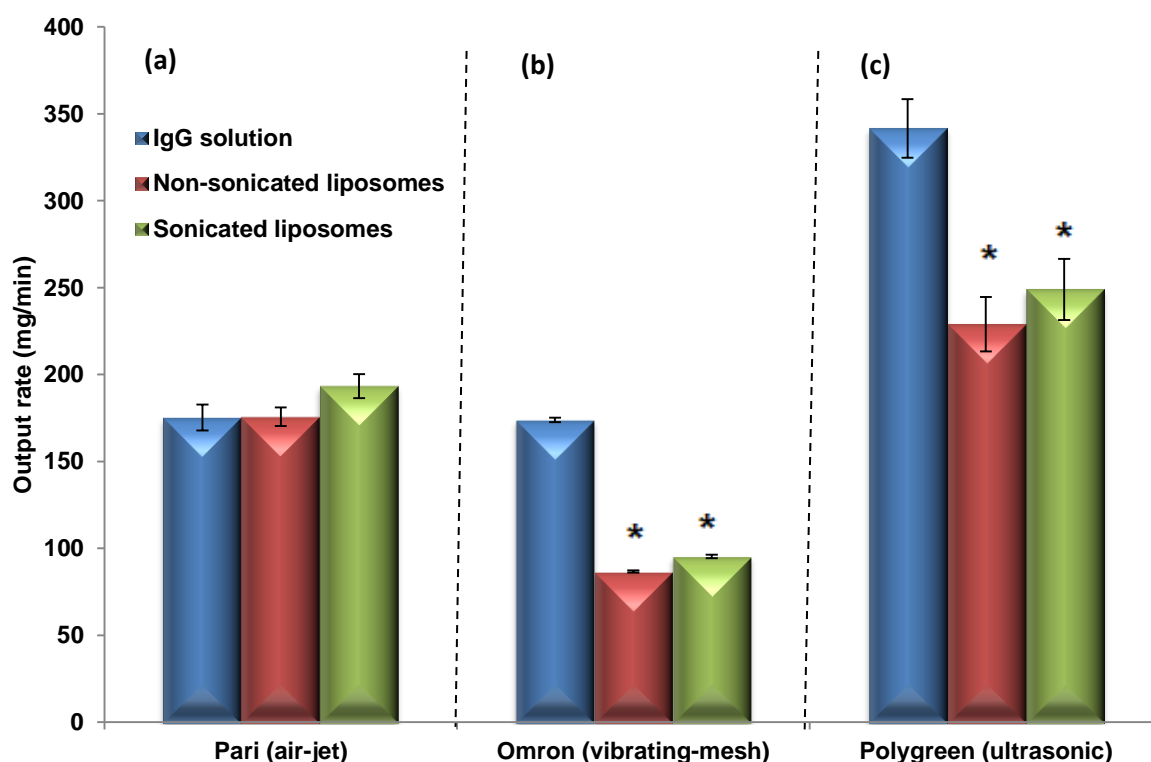


Figure 5.4: Output rate of IgG solution and IgG liposomes before or after sonication using; (a) Pari (air-jet), (b) Omron (vibrating-mesh) and (c) Polygreen (ultrasonic) nebulisers. Data are mean \pm SD, $n=3$; * $p < 0.05$ for IgG solution compared to Non-sonicated liposomes and Sonicated liposomes in the three nebulisers.

5.3.2 Aerosol droplet size and Respirable output

In the present study, the effect of using the different nebulisers on the DSD of the generated aerosols from three different formulations, an IgG solution and IgG liposomes (non-sonicated and sonicated) was examined. Two different methods for the measurement of the droplet sizes were employed:

- 1- Laser diffraction using the Spraytec instrument
- 2- TOF using the APS instrument

Figures 5.5-5.6 illustrate the size of droplets generated for the three formulations using the three nebulisers as measured via the APS and Spraytec.

As shown in Figures 5.5, the size of the generated droplets was calculated differently by the two instruments ($p < 0.05$). The size of the droplets were smaller using the APS for all nebulisers and formulations ($p < 0.05$) (Figure 5.5). The instruments employed utilise different principles in calculating particle size, justifying the difference in the measured size of particles.

These differences in the readings between the APS and Spraytec can be attributed to the distinct differences between the technologies employed for aerosol droplet size analysis in both instruments. Particle-counting methods such as that using TOF in a course of a single analysis consider only a few thousands particles. By contrast, millions of particles are considered in laser diffraction measurements, hence leading to considerable differences in the interpreted size distribution between the two size analysis mechanisms (Kippax, 2005). Moreover, TOF technology accelerates particles in an air stream before size measurement, resulting in possible solvent evaporation from the droplets and subsequent small size measurements. Additionally, the high shear caused by this mechanism might distort the droplets, making them appear to be smaller in aerodynamic size (Mitchell and Nagel, 2004; Kippax, 2005).

The SPAN values were found to be considerably lower ($p < 0.05$) when using laser diffraction despite the larger size of the droplets (Figure 5.6). The high SPAN values recorded by the APS might be attributed to the high shear force applied and subsequent distortion of the droplet dimensions, thus giving higher polydispersity measurements.

In spite of the differences between the two technologies employed, the nebulisers exhibited the same trend in the droplet size and SPAN measurements (Figures 5.5-5.6), with the Omron generating significantly larger droplet size ($p < 0.05$) than the Pari (air-jet) and the Polygreen (ultrasonic) nebulisers. The air-jet and ultrasonic nebulisers employed in this study have exhibited no significant differences ($p > 0.05$) in terms of droplet sizes, regardless of formulation and size analysis technology. In addition, regardless of the aerosol size analysis mechanism, no marked differences ($p > 0.05$) in the SPAN were observed between the three nebulisers.

The large droplet size generated by the mesh nebuliser compared to ultrasonic and air-jet nebulisers has been previously reported (Elhissi, 2005). The large droplet size generated by the Omron mesh nebuliser can be attributed to the limited input of shearing energy when compared to the air-jet or the ultrasonic nebulisers.

The similarity in droplet size for aerosols generated by the air-jet and ultrasonic devices in this study differs from the previous findings of previous researchers (Mc Callion *et al.*, 1996a; Elhissi *et al.*, 2011b), who reported that the size of droplets generated by the ultrasonic nebulisers were larger than those generated by jet nebulisers. This could be due to the use of different models of ultrasonic and air-jet devices in this study.

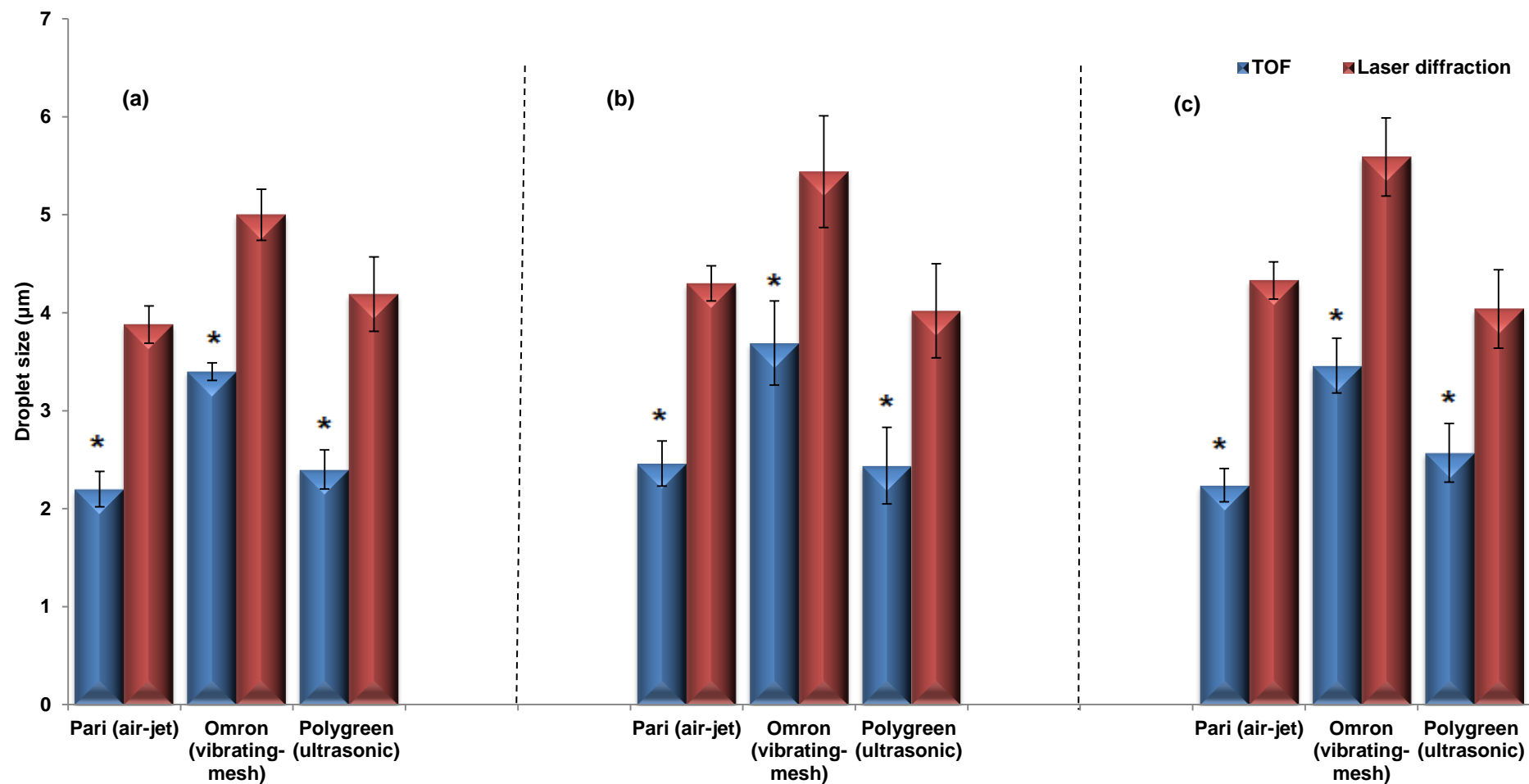


Figure 5.5: Droplet size measured using the TOF and laser diffraction Spraytec for (a) IgG solution, (b) non-sonicated liposomes and (c) sonicated liposomes. Data are mean \pm SD, n=3; * $p < 0.05$ for TOF compared to laser diffraction; $p > 0.05$ for the different formulations in all three nebulisers.

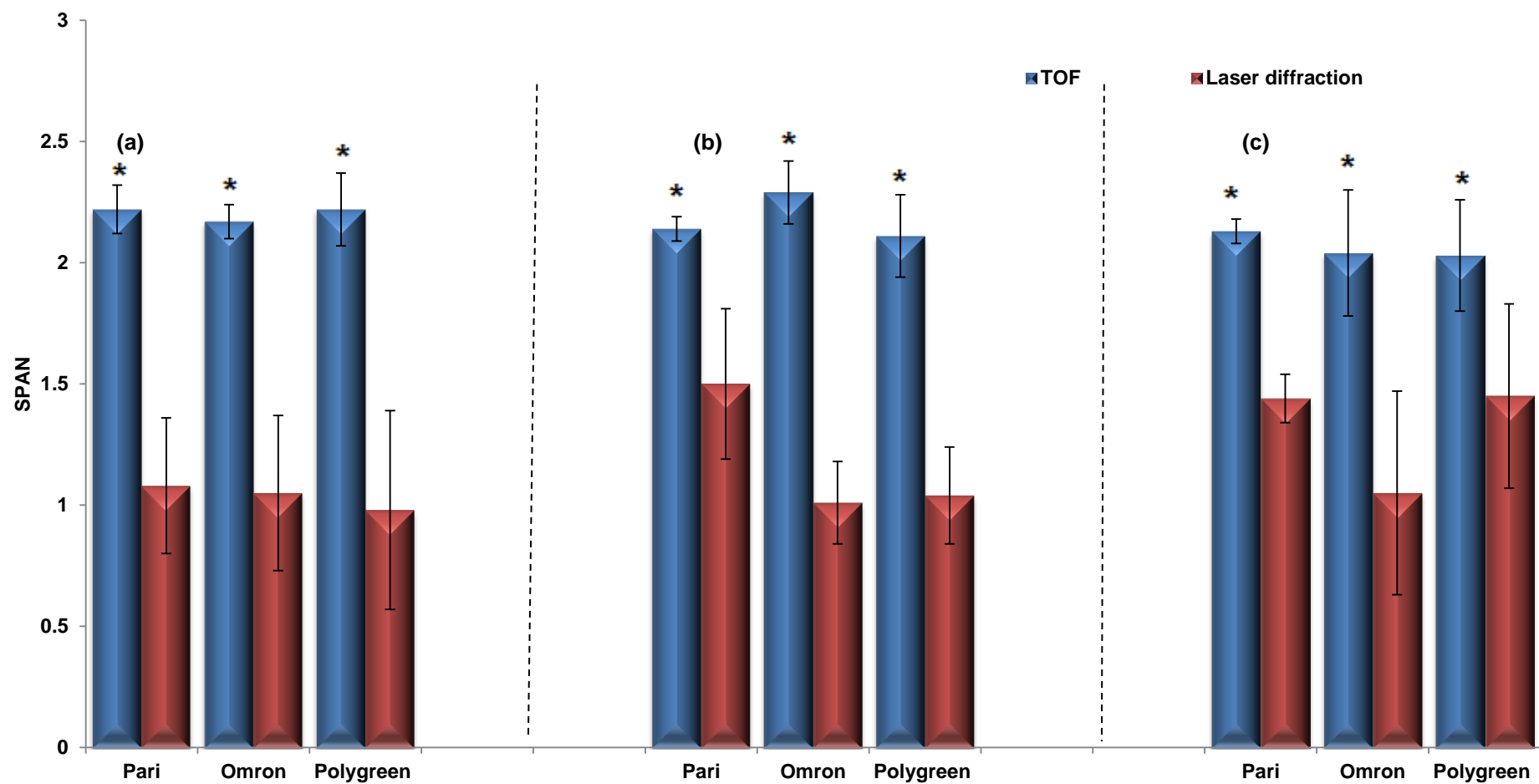


Figure 5.6: SPAN of the droplets measured using the TOF and laser diffraction technology for (a) IgG solution, (b) non-sonicated liposomes and (c) sonicated liposomes. Data are mean \pm SD, $n=3$; * $p < 0.05$ for TOF compared to laser diffraction; $p > 0.05$ for the different formulations in all three nebulisers.

Atomization theory suggests that as the viscosity increases the mean diameter of nebulised droplets may increase (Elhissi *et al.*, 2011a). However, this was not the case in this study, since no significant differences ($p>0.05$) in the droplet sizes or SPAN values were demonstrated for the different formulations. This finding can be due to the relatively small differences in the viscosities of the different formulations investigated in this study.

In addition to the mean droplet size, the FPF of the three formulations in the different nebulisers was determined via laser diffraction and TOF size analysis technologies (Figure 5.7). Aerosol particle size is an important factor affecting lung deposition. For particles to deposit in the bronchioles and alveolar region, they should have a particle size smaller than approximately 5 μm , and these particles will be described as “respirable” or as FPF (O’Callaghan and Barry, 1997).

As displayed in Figure 5.7, the FPF percentage was significantly higher ($p<0.05$) when analysed by the APS than the Spraytec for all the different nebulisers and formulations. These higher FPF values in the TOF measurements can be attributed to the smaller droplet size measured by that technology.

Furthermore, no significant differences ($p>0.05$) were found between the FPF of the Pari air-jet nebuliser and the Polygreen ultrasonic nebuliser. The Omron nebuliser on the other hand exhibited a significantly lower FPF ($p<0.05$) than the other nebulisers. This again can be attributed to the larger droplet median size values generated by the Omron mesh nebuliser. Also, due to the similar aerosol droplet sizes generated from the different formulations in the nebulisers, no differences in the FPF were observed ($p>0.05$).

The FPF output relative to the total mass output was also determined in this study for the three different formulations in the different nebulisers. FPF output was calculated using the two size analysis mechanisms (Figure 5.8).

Figure 5.8 also demonstrated that the FPF output results for the three nebulisers were significantly higher ($p<0.05$) when measured using the APS. This can be ascribed to the larger proportion of FPF measured using the TOF technology. Also, the three nebulisers differed significantly ($p<0.05$) in their FPF output when measured using the APS and the FPF output was in the range of Pari > Omron >

Polygreen. On the other hand, when the FPF output was determined using the Spraytec instrument, droplets generated by the Pari nebuliser exhibited a higher ($p < 0.05$) FPF output than both the Omron and Polygreen. There were no significant differences between the ultrasonic and the Omron nebulisers using laser diffraction ($p > 0.05$). This indicates that the interpretation of differences in size of nebulised droplets can be dependent on the size measurement mechanism.

Additionally, Figure 5.8 demonstrated that there were no significant differences ($p > 0.05$) in the FPF output between the different formulations in all nebulisers using TOF or laser diffraction size analysis technologies. The results determined were inherently dependent on the total output data (outlined previously in Section 5.3.1) and the FPF results presented previously in this section.

5.3.3 Influence of nebulisation on the size distribution and morphology of liposomes

The effect of nebulisation on the size and SPAN or Pdi of liposomes was also investigated in the study. IgG liposomes and probe-sonicated IgG liposomes were nebulised using:

- 1- Pari Turbo Boy (air-jet)
- 2- Omron MicroAir NE-U22 (vibrating-mesh)
- 3- Polygreen (ultrasonic)

The size and SPAN or Pdi were determined before nebulisation. Size distribution analysis was also conducted after the completion of nebulisation for both delivered liposomes, and those remained within the nebuliser's residual volume (Tables 5.1-5.2). In addition to size distribution analysis of liposomes before and after nebulisation, morphology studies were conducted to study the influence of nebulisation on the morphology of liposomes (non-sonicated and sonicated) (Figures 5.9-5.10).

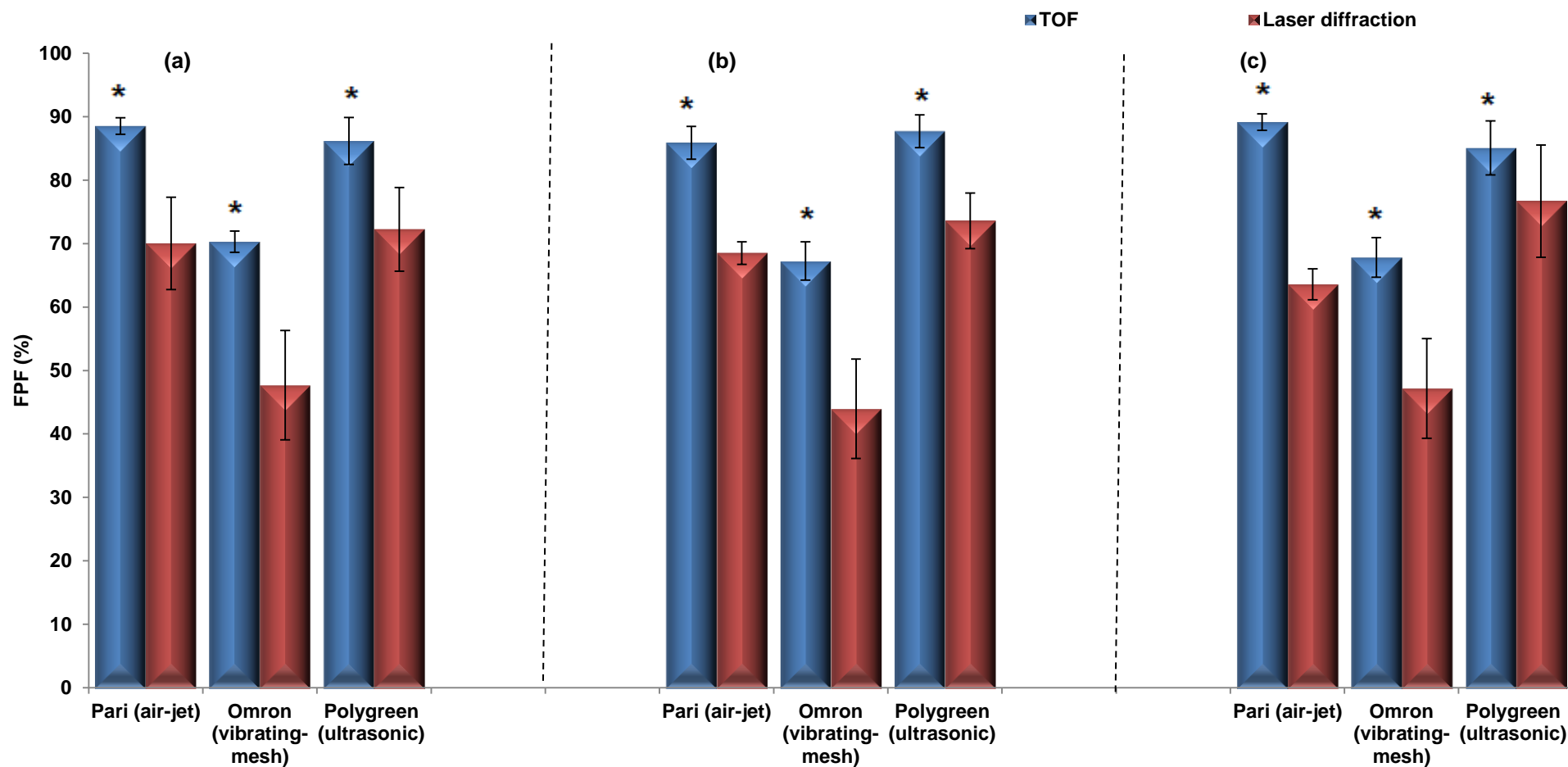


Figure 5.7: FPF from the different nebulisers using the TOF and laser diffraction technology for (a) IgG solution, (b) non-sonicated liposomes and (c) sonicated liposomes. Data are mean \pm SD, $n=3$; * $p < 0.05$ for TOF compared to laser diffraction; $p > 0.05$ for the different formulations in all three nebulisers.

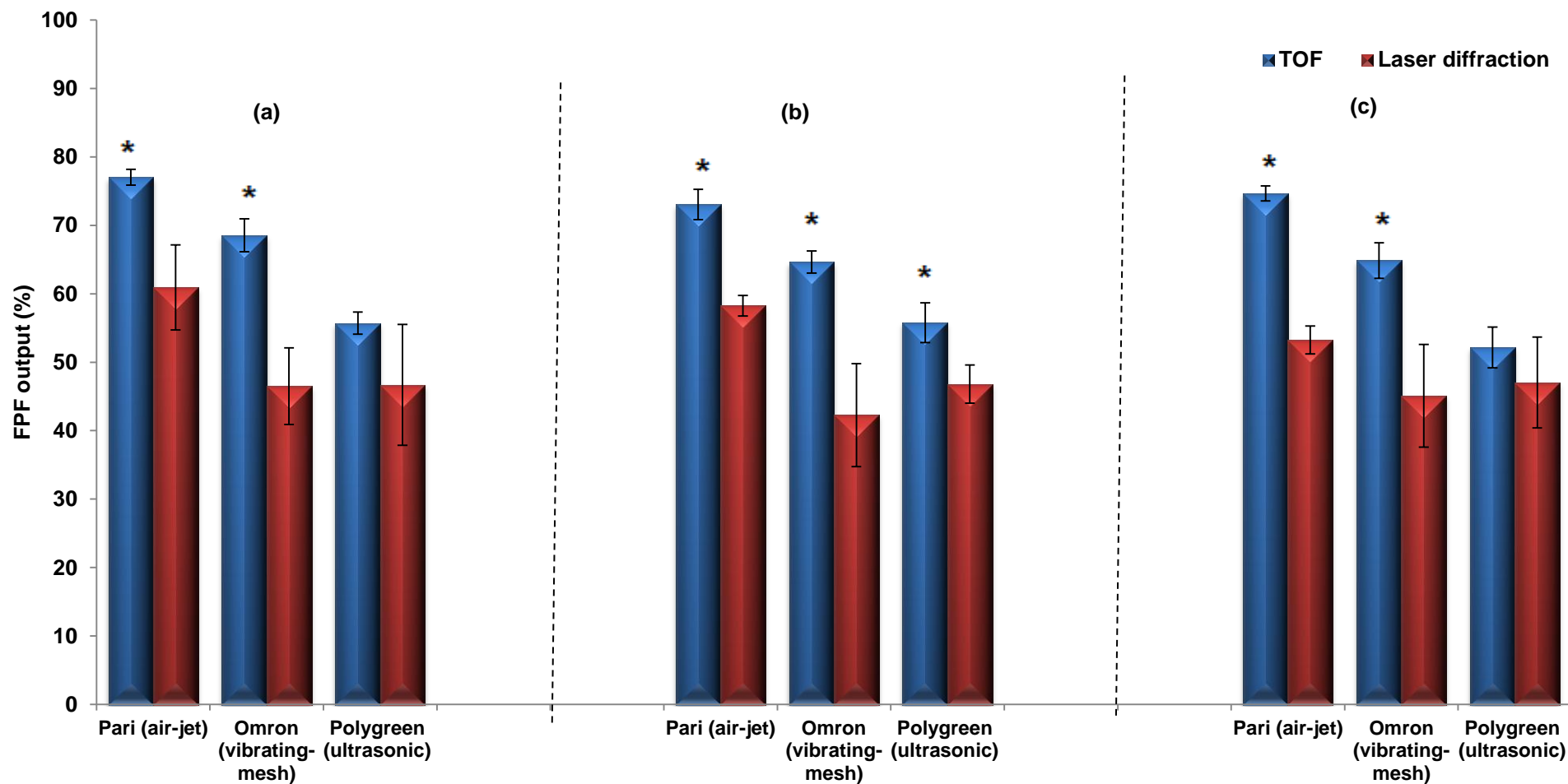


Figure 5.8: FPF output from the different nebulisers using the TOF and laser diffraction technology for (a) IgG solution, (b) non-sonicated liposomes and (c) sonicated liposomes. Data are mean \pm SD, $n=3$; * $p < 0.05$ for TOF compared to laser diffraction; $p > 0.05$ for the different formulations in all three nebulisers.

As shown in Table 5.1 non-sonicated liposomes significantly decreased in size after nebulisation via the Omron nebuliser ($p < 0.05$). However, there was no significant decrease in the size of probe-sonicated liposomes after nebulisation ($p > 0.05$) (Table 5.2). Moreover, the SPAN and Pdi of the non-sonicated and probe-sonicated liposomes, respectively did not markedly change ($p > 0.05$) following nebulisation through Omron.

The decrease in size of the non-sonicated liposomes after nebulisation via the Omron nebuliser might be attributed to the extrusion effect of liposomes through the perforated plate of the nebuliser that consists of around 6000 tapered apertures (3 μm in diameter) (Dhand, 2002; Dhand, 2003). However as the size of the liposomes was reduced to 400 nm, the vesicles were found to be more stable to nebulisation through Omron thus giving indication on the possible use of size reduction as a method to stabilise liposomes to nebulisation.

Furthermore, whilst liposomes remaining in the Omron's reservoir had the same size as the original non-sonicated liposomes before nebulisation, the SPAN of the liposomes remaining in the nebuliser's reservoir was found to significantly increase ($p < 0.05$) from 1.68 ± 0.27 to 2.31 ± 0.33 , indicating the possible failure of large liposomes or liposomal aggregates to pass through the mesh pores. On the other hand, no significant differences in the size or size distribution of the probe-sonicated liposomes remaining in the nebuliser compared to the probe-sonicated liposomes before nebulisation were observed ($p > 0.05$).

Nebulisation of non-sonicated liposomes via the air-jet nebuliser led to a significant decrease ($p < 0.05$) in their size (i.e. from 3.36 ± 0.28 to 2.10 ± 0.25 μm). Moreover, unlike nebulisation of probe-sonicated liposomes via Omron, probe-sonicated liposomes were found to significantly decrease ($p < 0.05$) in size following nebulisation via the air-jet nebuliser, where a decrease in size from 403.2 ± 54.9 to 277.0 ± 18.3 nm was observed. Furthermore, the size distribution of the non-sonicated and probe-sonicated liposomes remained similar, as no effect of processing within the nebuliser was observed ($p > 0.05$).

Table 5.1: Size and size distribution of non-sonicated liposomes before nebulisation, after nebulisation and what is remaining in the nebuliser reservoir. Measurements were carried out using laser diffraction or dynamic light scattering (DLS). Data are mean \pm SD, n=3; $p>0.05$ for size and SPAN measurements before nebulisation; $^x p<0.05$ for size and SPAN measurements for before nebulisation compared to delivered liposomes and residual content; $^+ p<0.05$ for size and SPAN of delivered liposomes and residual content for Polygreen compared to Pari and Omron; $^+ p<0.05$ for size of delivered liposomes and residual content between Pari and Omron.

<i>Non-sonicated liposomes</i>			
<u>Size (μm)</u>			
	Before nebulisation	Delivered liposomes	Residual content
Pari (air-jet)	3.36 \pm 0.28	2.10 \pm 0.25 ^x	2.56 \pm 0.36 ^x
Omron (vibrating-mesh)	3.36 \pm 0.28	2.71 \pm 0.21 ^{+ x}	3.43 \pm 0.42 ^{+ x}
Polygreen (ultrasonic)	3.36 \pm 0.28	1149.3 \pm 51.7 nm (DLS) ^{* x}	1464.0 \pm 45.3 nm (DLS) ^{* x}
<u>SPAN or Pdi</u>			
	Before nebulisation	Delivered liposomes	Residual content
Pari (air-jet)	1.68 \pm 0.27	1.78 \pm 0.31	2.78 \pm 0.21 ^x
Omron (vibrating-mesh)	1.68 \pm 0.27	1.44 \pm 0.23	2.31 \pm 0.33 ^x
Polygreen (ultrasonic)	1.68 \pm 0.27	0.441 \pm 0.202 (Pdi) [*]	0.887 \pm 0.110 (Pdi) [*]

Table 5.2: Size and size distribution of sonicated liposomes before nebulisation, after nebulisation and what is remaining in the nebuliser reservoir. Measurements were carried out using dynamic light scattering (DLS). Data are mean \pm SD, n=3; $p>0.05$ for size and SPAN measurements before nebulisation; $^x p<0.05$ for size and SPAN measurements for before nebulisation compared to delivered liposomes and residual content; $^* P<0.05$ for size and SPAN of delivered liposomes and residual content for Polygreen compared to Pari and Omron; $^+ p<0.05$ for size of delivered liposomes and residual content between Pari and Omron.

<i>Sonicated liposomes</i>			
<u>Size (nm)</u>			
	Before nebulisation	Delivered liposomes	Residual content
Pari (air-jet)	403.2 \pm 54.9	277.0 \pm 18.3 ⁺ x	330.8 \pm 09.4 x
Omron (vibrating-mesh)	403.2 \pm 54.9	361.2 \pm 20.2	343.5 \pm 29.6
Polygreen (ultrasonic)	403.2 \pm 54.9	207.0 \pm 48.0 x *	223.6 \pm 31.9 x *
<u>Pdi</u>			
	Before nebulisation	Delivered liposomes	Residual content
Pari (air-jet)	0.753 \pm 0.247	0.600 \pm 0.152	0.974 \pm 0.026
Omron (vibrating-mesh)	0.753 \pm 0.247	0.709 \pm 0.230	0.853 \pm 0.147
Polygreen (ultrasonic)	0.753 \pm 0.247	0.442 \pm 0.025 x *	0.558 \pm 0.248 x

The reason for the size reduction of both non-sonicated liposomes and probe-sonicated vesicles following air-jet nebulisation can be attributed to vesicle fragmentation when they are drawn through the inlet of the nebuliser and mixed with the high speed jet. Moreover, the impact of the aerosolised droplets onto the baffles might have decreased the size of the liposomes (Taylor *et al.*, 1990b). Saari *et al.*, (1999) have reported a marked reduction in liposome size following air-jet nebulisation for both beclomethasone dipropionate DLPC and DPPC liposomes, from 3.49 to 0.83 μm and from 5.07 to 0.91 μm , respectively. Liposomes remaining in the Pari's reservoir were also found to markedly decrease in size ($p < 0.05$) when compared to vesicles before nebulisation. Moreover, the SPAN of the non-sonicated liposomes remaining in the reservoir of the nebuliser was significantly higher ($p < 0.05$) than the SPAN of the liposomes before nebulisation, where an increase in the SPAN from 1.68 ± 0.27 to 2.78 ± 0.21 was observed. This might be attributed to the possible increase in the concentration of the liposomes inside the nebuliser due to evaporation of the solvent during aerosolisation, thus leading to accumulation of liposomes in the reservoir and possibly formation of liposome aggregates.

As outlined in Tables 5.1-5.2, both the non-sonicated liposomes and probe-sonicated liposomes significantly decreased in size ($p < 0.05$) following nebulisation via the Polygreen nebuliser. Leung *et al.*, (1996) reported that nebulisation of egg PC liposomes using a Medix ultrasonic nebuliser lead to the decrease in vesicle size from $5.71 \pm 0.02 \mu\text{m}$ to $0.97 \pm 0.05 \mu\text{m}$. During ultrasonic nebulisation aerosol droplets are generated via cavitation bubbles and/or capillary waves. Any of these mechanisms involved in droplet formation combined with the presence of baffles and constant recycling of the fluid is expected to disrupt the liposomal structures (Leung *et al.*, 1996).

Additionally, unlike the Omron and Pari, size and size distribution of the non-sonicated liposomes were analysed using DLS via the Zetasizer, rather than laser diffraction, following nebulisation by the Polygreen device. The reason for that was the very low obscuration value of the liposomes under laser diffraction, which was not sufficient to measure the size via the laser diffraction Mastersizer instrument. In general, ultrasonic nebulisers are unsuitable for the delivery of

liposomes (Leung *et al.*, 1996; Bridges and Taylor, 1998; Elhissi and Taylor, 2005), indicating that the new design ultrasonic devices are consistent with old ultrasonic devices in that regard.

Also shown in Tables 5.1-5.2, non-sonicated liposomes and probe-sonicated liposomes remaining in the ultrasonic reservoir significantly decreased ($p < 0.05$) in size following nebulisation via the Polygreen nebuliser. The Pdi of the liposomes remaining in the nebuliser was also higher ($p < 0.05$) than the delivered liposomes, where an increase from 0.441 ± 0.202 to 0.887 ± 0.110 was observed. This increase in Pdi can be attributed to accumulation and subsequent aggregation in the reservoir during atomisation. It has been previously reported that like air-jet nebulisers an increase in the concentration of the drug solution occurs after ultrasonic nebulisation (O'Callaghan and Barry, 1997).

Furthermore, studies using cryo-TEM demonstrated that nebulisation via the three different nebulisers did not affect the morphology of liposomes (both non-sonicated and sonicated), and the multilamellar structure of the liposomes was still maintained (Figures 5.9-5.10).

5.3.4 Structure and activity of IgG following nebulisation

In this section the secondary structure and activity of IgG in solution or liposome formulations (non-sonicated and sonicated) were investigated after nebulization by the three different nebulizers: the air-jet nebulizer Pari Turboboy, the vibrating-mesh nebulizer Omron MicroAir and the ultrasonic nebulizer Polygreen.

Figures 5.11-5.13 illustrate the effect of nebulization on the secondary structure and activity of IgG in solution and IgG in liposome preparations (non-sonicated and sonicated).

As demonstrated in Figure 5.11, there were no significant differences in the structure of IgG, both in solution or bound to liposomes, before and after nebulisation, and regardless of nebuliser type ($p > 0.05$). On the other hand,

when the activity of IgG was investigated, both IgG in solution and in liposomes demonstrated a significant reduction ($p < 0.05$) in their activity following nebulisation (Figures 5.12-5.13). Amongst the nebulisers studied, the Omron least reduced the activity of IgG, by 18.69 ± 1.24 , 15.90 ± 2.74 and 16.61 ± 2.42 % for the solution, non-sonicated liposomes and sonicated liposomes, respectively. On the other hand, nebulisation via the Polygreen nebuliser was found to lead to the highest loss in protein activity. The magnitude of activity loss was by 88.81 ± 1.20 , 88.99 ± 0.95 and 50.39 ± 2.20 % for the solution, non-sonicated liposomes and sonicated vesicles, respectively. Furthermore, nebulisation through the Pari was found to lie in between the Omron nebuliser and the Polygreen ultrasonic devices, with 61.16 ± 4.92 , 73.58 ± 1.95 and 48.85 ± 0.94 % losses in activity for the solution, non-sonicated liposomes and sonicated liposomes, respectively.

The loss of activity using the different nebulisers can be attributed to the shear stress and aggregation of the protein molecules during nebulisation. Maillet *et al.*, (2008a) investigated the amount of IgG aggregates following nebulisation using Aeronex Pro vibrating-mesh nebuliser, PARI LC+ air-jet nebuliser and SYST_AM LS290 ultrasonic nebuliser. The results from their study indicated that aggregation was minimal following the use of the vibrating-mesh nebuliser and the highest following ultrasonic nebulisation. These results have been attributed to the prolonged continuous shearing within the air-jet and ultrasonic devices. By contrast, the mesh nebulisers may offer lower shear forces and shearing seems to occur only during extrusion through the mesh pores. Various studies have demonstrated a higher efficiency of vibrating-mesh nebulisers over other types of nebulisers for the delivery of liposomes incorporating hydrophilic drugs (Elhissi *et al.*, 2006a; 2007; Kleemann *et al.*, 2007).

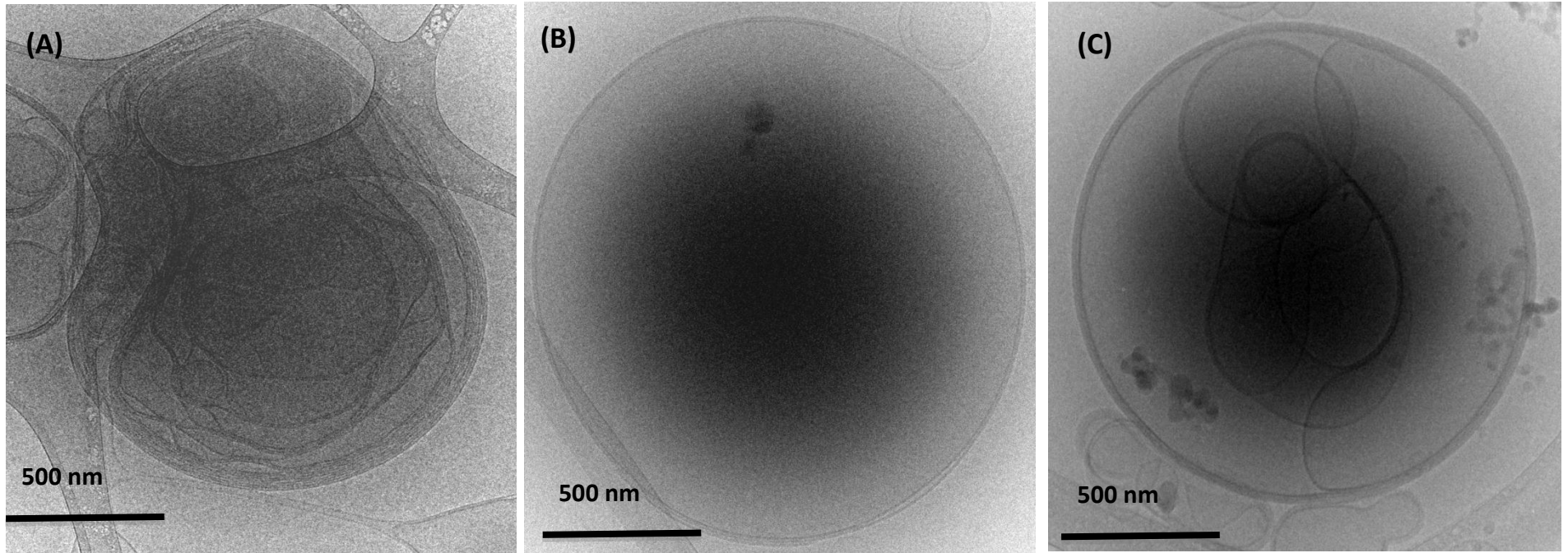


Figure 5.9: Cryo-TEM images of liposomes (non-sonicated) following nebulisation via (a) Pari air-jet nebuliser, (b) Omron vibrating-mesh nebuliser and (c) Polygreen ultrasonic nebuliser. Typical of 4-6 different experiments.

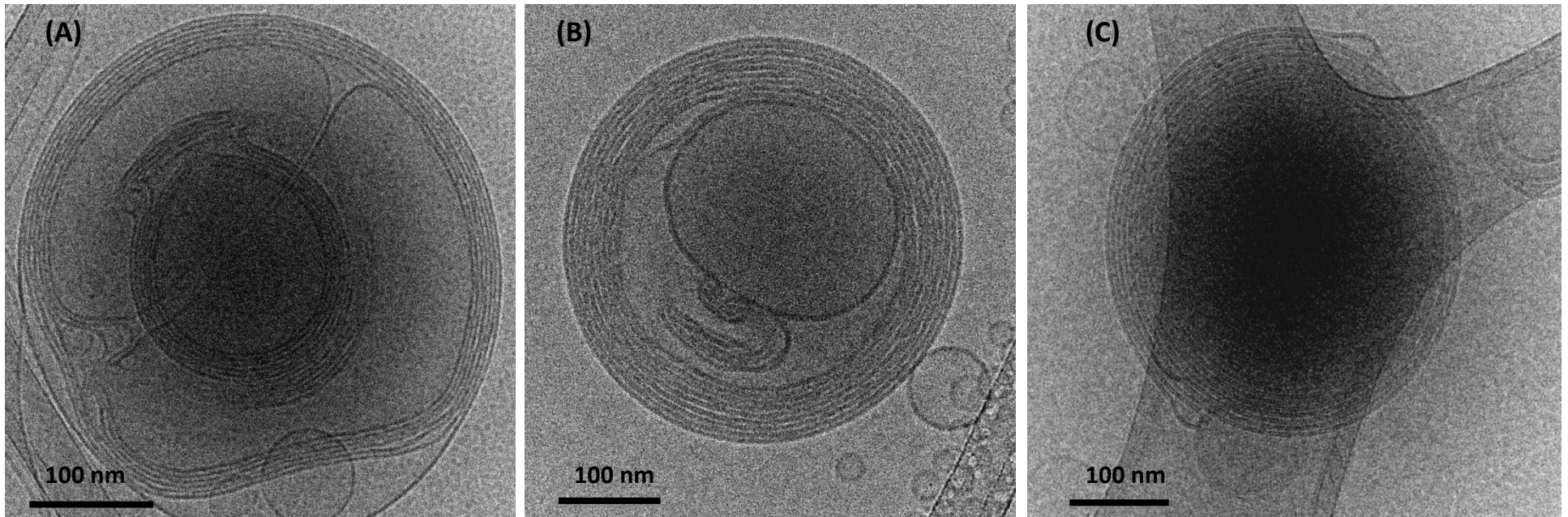


Figure 5.10: Cryo-TEM images of liposomes (sonicated) following nebulisation via (a) Pari air-jet nebuliser, (b) Omron vibrating-mesh nebuliser and (c) Polygreen ultrasonic nebuliser. Typical of 4-6 different experiments.

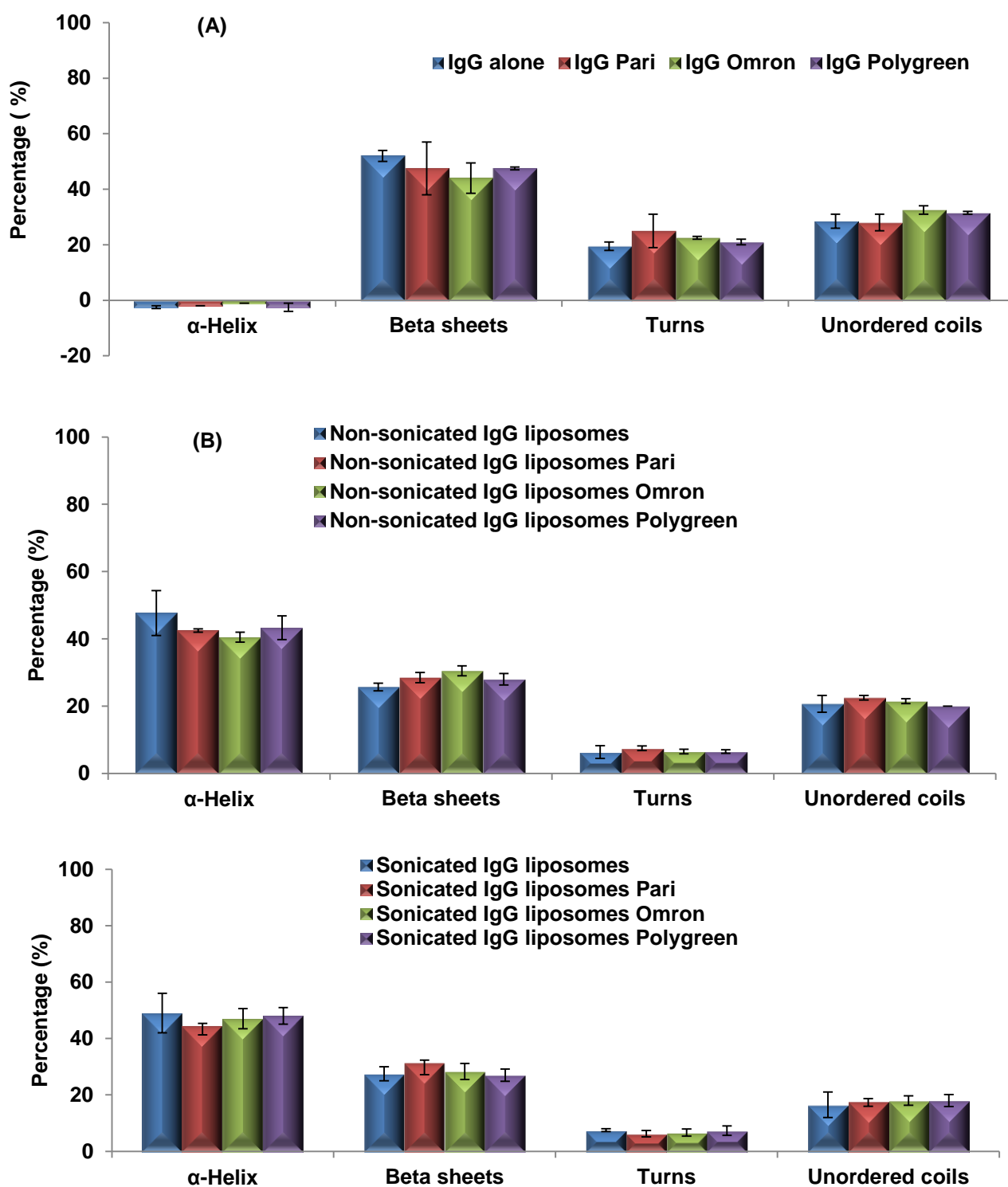


Figure 5.11: Nebulisation of (A) IgG and IgG bound to liposomes ((B) non-sonicated and (C) sonicated), via Pari, Omron and Polygreen nebulisers, and its effect on the secondary structure of IgG. Data are mean \pm SD, $n=3$; $p > 0.05$ for all formulations in the different nebulisers.

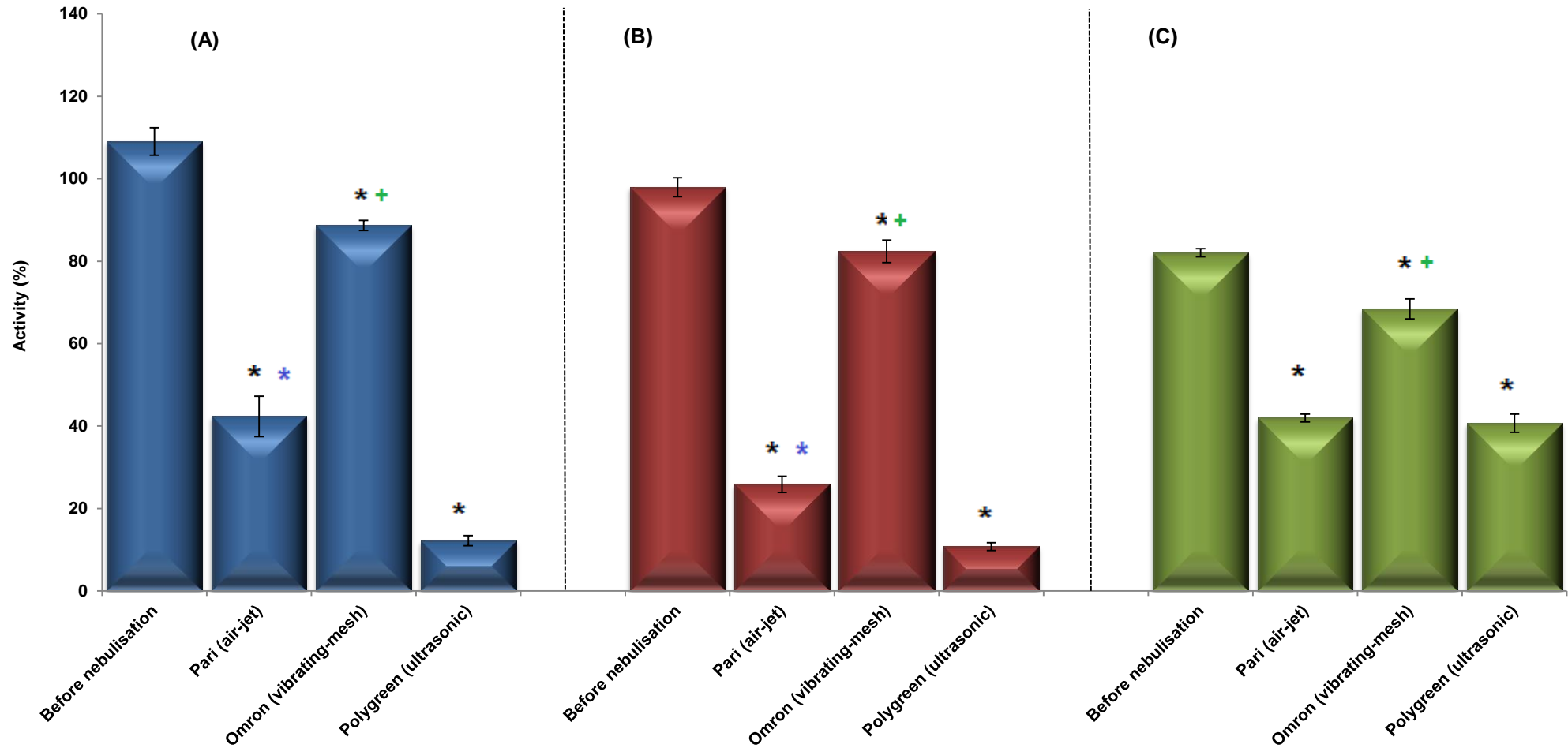


Figure 5.12: Nebulisation of IgG bound to liposomes ((A) non-sonicated and (B) sonicated) and (C) IgG solution, via Pari, Omron and Polygreen nebulisers, and its effect on the activity of IgG. Data are mean \pm SD, n=3; * $p < 0.05$ for Pari, Omron and Polygreen compared to before nebulisation; + $p < 0.05$ for Omron compared to Pari and Polygreen; * $p < 0.05$ for Pari compared to Polygreen.

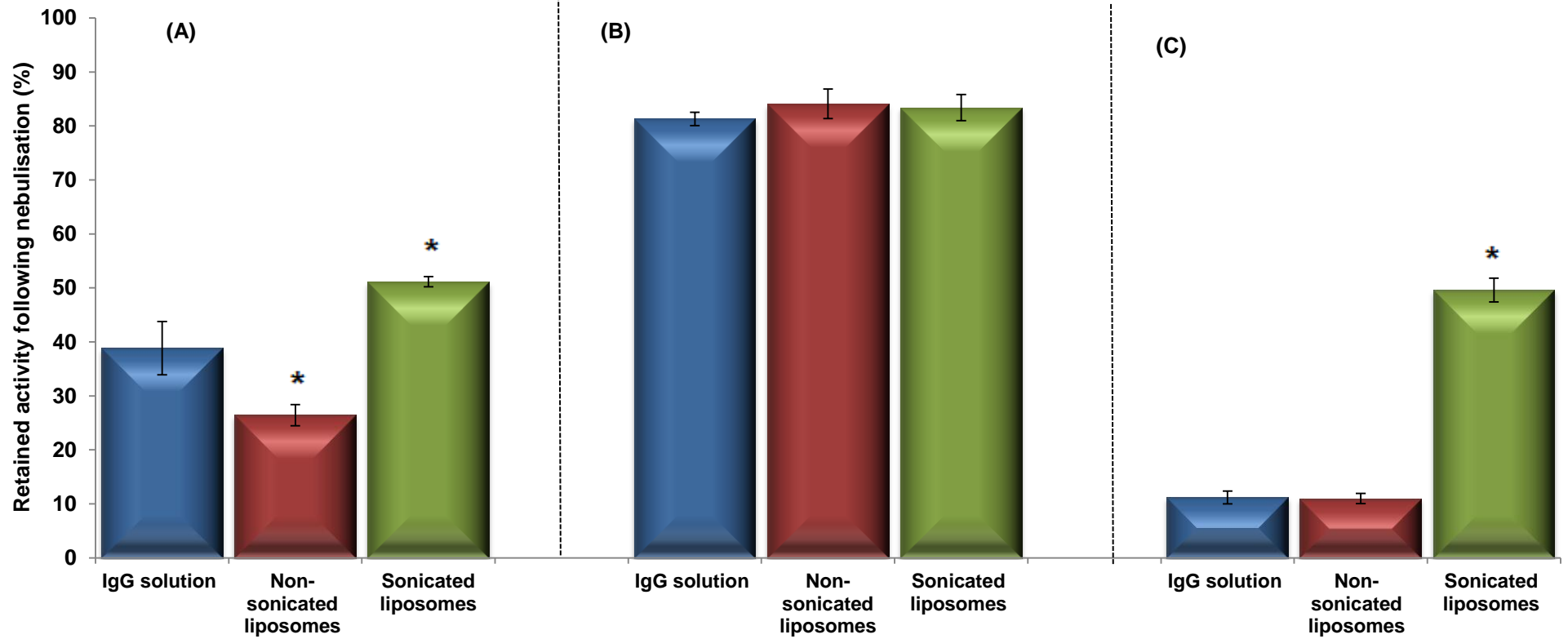


Figure 5.13: Nebulisation of IgG and IgG bound to liposomes (non-sonicated and sonicated), via (A) Pari, (B) Omron and (C) Polygreen nebulisers, and its effect on the activity of IgG relative to before nebulisation. Data are mean \pm SD, $n=3$; * $p<0.05$ for non-sonicated liposomes or sonicated liposomes compared to IgG solution.

Furthermore, the loss of activity following nebulisation was found to directly correlate with the results in Section 5.3.3, which demonstrate the effect of nebulisation on liposomes' structure. It is noteworthy that the nebuliser with the least disruptive effect on liposomal structure (i.e. the Omron) demonstrated the least reduction in activity, whilst the nebuliser with the highest disruptive effect on liposomes (i.e. the Polygreen) demonstrated the highest reduction in activity.

Also, as demonstrated in Figure 5.13, sonication of liposomes was found to markedly enhance the retained activity of IgG following nebulisation, especially for the Pari and Polygreen nebulisers ($p < 0.05$). This enhanced retained activity can be attributed to the previously mentioned enhancement effect of size reduction on the stability of liposomes (Section 5.3.3).

As shown in Section 5.3.2, the FPF output percentage relative to the total mass output was determined using TOF and laser diffraction. In this section the FPF output percentage relative to the active IgG delivered was investigated (Figure 5.14).

As demonstrated in Figure 5.14, the FPF output percentage relative to the active IgG delivered was significantly lower ($p < 0.05$) than the previously reported FPF output percentage results relative to the mass output (Section 5.3.2). Moreover, the FPF output using TOF technology was significantly higher than laser diffraction technology due to the smaller droplet sizes measured using the TOF as discussed earlier (see Section 5.3.2).

Also illustrated in Figure 5.14, both FPF output results using TOF and laser diffraction followed the same trend for the different formulations using the different nebulisers, and the order in FPF output was as follows: Omron > Pari > Polygreen. The results from this study further confirmed previous reports (O'Callaghan *et al.*, 1989; O'Callaghan and Barry, 1997), highlighting the importance of calculating the FPF output percentage relative to the active output, rather than the mass output, which has been used in some previous studies (Kradjan and Lakshminarayan, 1985; Douglas *et al.*, 1986; McCallion *et al.*, 1996b).

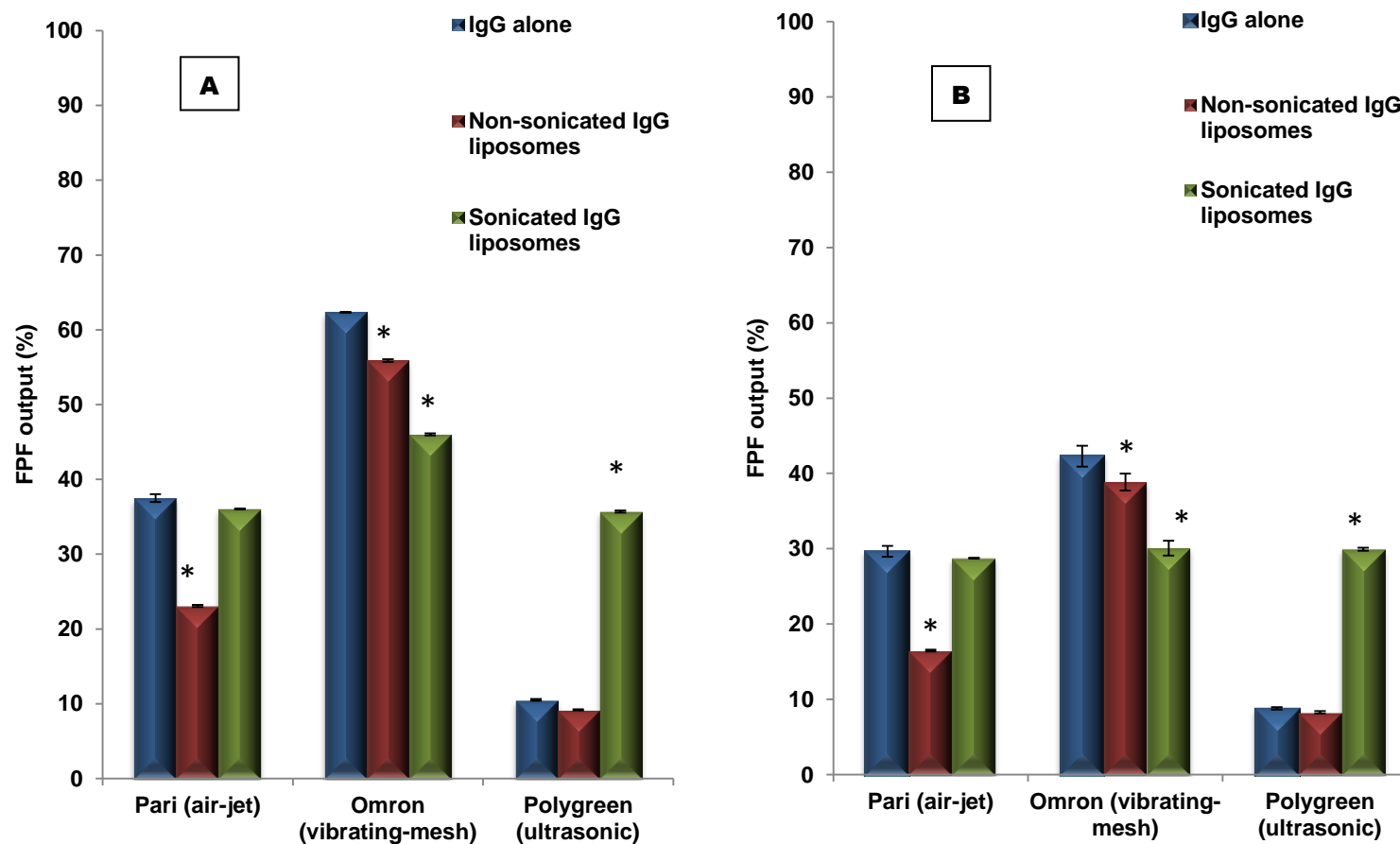


Figure 5.14: FPF output% relative to the active IgG delivered, using the (A) TOF and (B) laser diffraction technologies for the, IgG solution, non-sonicated liposomes and sonicated liposomes. Data are mean \pm SD, n=3; * $p < 0.05$ for non-sonicated IgG liposomes or sonicated IgG liposomes compared to IgG solution.

5.4 Conclusions

The results from this study have demonstrated that the three different nebulisers varied in their performance. Moreover, marked differences existed in the nebulisation time, sputtering duration, output rate and mass output values between the different nebulisers. In addition to the nebuliser type, the formulation itself was found to affect the performance of the nebulisers.

Furthermore, the validity of delivering multilamellar liposomes prepared from proliposomes via medical nebulisers has been established, although fragmentation of liposomes was demonstrated following the use of nebulisers. Also, size reduction of liposomes was proven viable as a technique to improve the stability of liposomes to nebulization.

Although the stability of IgG was found to be significantly ($p < 0.05$) reduced following nebulisation, its incorporation into the liposomal structure was found to enhance its retained activity, especially when incorporated into sonicated liposomes.

Additionally, the results from this study have further demonstrated that amongst the different studied nebulisers, the vibrating-mesh nebuliser (Omron) exhibited the longest nebulisation time. However, it was the least disruptive to liposomal structure and retained the highest activity of IgG when it was used, hence it proves to be the most suitable for the nebulisation of liposomes, especially when proteins are incorporated in their structure.

CHAPTER 6

DELIVERY OF LIPOSOMES VIA NASAL SPRAYS

6.1 Introduction

The nasal cavity has been used as a route of drug administration since ancient times, and there has been heightened interest in the exploitation of the nose for systemic drug administration in recent years. The high permeability of the nasal surfaces is implicit in this approach, along with its non-invasive nature and avoidance of gastrointestinal and hepatic metabolism (Banga and Chien, 1988; Song *et al.*, 2004; Pires *et al.*, 2009).

Despite its advantages, the nasal mucosa represents an obstacle for the uptake of large molecules, particularly peptides and proteins (Illum, 2006; Pires *et al.*, 2009). Nevertheless, these drawbacks can be overcome by using drug carrier systems such as liposomes (Türker *et al.*, 2004). Liposomes have been demonstrated to have good bioadhesive characteristics, especially when a mucoadhesive agent is incorporated into liposome formulation (Jain *et al.*, 2007). Furthermore, liposomes demonstrated the ability to slow the rate of drug clearance from the nose as well as protect the drug from enzymatic degradation in nasal secretions (Kato *et al.*, 1993; Law *et al.*, 2001).

In addition to the nature of formulation, factors like site of deposition and rate of clearance of the drug from the nasal cavity affect the absorbance of the drug, and therefore its therapeutic effect (Hardy *et al.*, 1985; Harris *et al.*, 1988).

Various dosage forms have been utilized to deliver medications to the nasal cavity, but liquid preparations are the most widely used. Liquid formulations for intranasal delivery can be administered by means of sprays, drops, propellant driven metered dose inhalers, squeeze bottles or compressed air nebulisers (Kublik and Vidgren, 1998). Due to their convenience, dose consistency and the ability to administer both solutions and suspensions, sprays have become the preferred devices for delivery of nasal formulations. Most of the preparations in the market nowadays are delivered by metered-dose pump sprays and a variety of metered volumes, pumps and nozzle types are commercially available (Foo *et al.*, 2007; Kushwaha *et al.*, 2011).

Spray devices and drug formulations affect the characteristics of the spray plume, including its unique geometric and droplet properties. Characteristics of the

resulting spray plume are believed to have a profound influence on the resulting nasal deposition patterns (Foo, 2007; Foo *et al.*, 2007). These spray characteristics generated by the device are dependent not only on the spray nozzle design, but also on the properties of the formulation (Dayal *et al.*, 2004; Guo and Doub, 2006). Adequate choice of the nasal device along with designing a suitable formulation is therefore necessary in optimizing the nasal delivery.

In the USA, the Food and Drug Administration (FDA) CDER has established a set of industry guidelines and regulations to market nasal products (CDER, 2002; 2003). The FDA recommends that several *in vitro* tests should be used to assess nasal delivery. These include parameters which allow the quantity and reproducibility of drug to be investigated, and tests to examine the droplet size distribution and spray geometry (i.e. the characteristics of the expanding spray plume) (Newman *et al.*, 2004).

While significant efforts have been made to study the influence of spray characteristics on nasal deposition, little research has focused on the interactions between nasal delivery device and formulation and the effect of that on drug deposition in the nasal cavity. Furthermore, literature lacks information elucidating the effect of nasal devices on liposomes and liposome-entrapped materials (Foo, 2007).

This study investigated the effects of formulation, whether IgG solution or IgG liposomes (non-sonicated or sonicated) on dose accuracy and characteristics of the resulting spray plume. This study was conducted using a mucosal atomisation device (MAD) which was then compared with two different nasal pump sprays. The effect of device on the dose accuracy and spray cloud characteristics was determined for the different formulations.

Moreover, the effect of the different nasal devices on the physical integrity of liposomes (non-sonicated and sonicated) was examined. Parallel to this, the effect of nasal device on the structure and activity of IgG, alone or incorporated into liposomes, was determined.

6.2 Methodology

6.2.1 Preparation of IgG liposomes

Liposomes were manufactured as discussed earlier in Section 2.2.1 by adapting the ethanol-based proliposome method described by Perrett and co-workers (1991). Liposomes comprised 10 mg/ml lipid (2:1 SPC to cholesterol), 0.5 mg/ml IgG and 0.2% w/v mucoadhesive agent (sodium alginate) to make up a final volume of 5 ml using HPLC water. For size reduction of liposomes, probe sonication for 4.5 minutes was employed to produce 400 nm vesicles, as previously described in Section 4.3.4. Furthermore, IgG solution comprising 0.5 mg/ml IgG in 5 ml HPLC water was prepared for comparison with the liposome formulation.

6.2.2 Determination of the shot weight and dose accuracy of nasal devices

The shot weight and dose accuracy of the different nasal devices were determined according to the FDA guidelines (CDER, 2002; 2003). Three nasal devices were employed in this study: a MAD (Wolfe Tory Medical Inc., Salt Lake City, UT) and two nasal pump sprays (Model VP3/93, Valois) from a Beconase[®] aq. nasal spray, and (Model VP7/100, Valois) from a Nasacort[®] aq. nasal spray, referred to as “nasal spray A” and “nasal spray B”, respectively. The number of actuations required to prime the nasal devices, number of full actuations and number of actuations in the tail-off phase were determined in this study as discussed in Section 2.2.13. Studies to determine the shot weight and actuation duration were also conducted, as described in Section 2.2.13.

6.2.3 Determination of nasal spray characteristics

As outlined in Section 6.1, the characteristics of the spray cloud generated from the nasal devices can be assessed by a variety of means, including DSD, spray pattern and plume geometry.

The fluid (5 ml) was placed in the nasal devices and (as described in Section 2.2.13), the size and SPAN of the generated droplets were analysed using the Malvern Spraytec laser diffraction instrument (Malvern Instruments Ltd, UK). The spray pattern and plume geometry were performed according to the FDA guidelines (CDER, 2002; 2003). The impaction technique was employed to determine the spray pattern of the nasal devices whilst high-speed photography was used to determine the plume geometry of the nasal devices (see Section 2.2.14).

6.2.4 Characterisation of liposomes following spraying

Determination of the size and size distribution of liposomes were performed as previously described in Section 2.2.5. Measurement of the size of non-sonicated liposomes before and after spraying was conducted via laser diffraction using the Malvern Mastersizer 2000, whilst DLS using the Malvern Zetasizer Nanoseries was employed to determine the size and size distribution of the probe sonicated liposomes.

6.2.5 Determination of structure and activity of IgG

The secondary structure of IgG was determined as described in Section 2.2.9 using CD. CD experiments were performed using a J-815 spectropolarimeter (Jasco, UK). Collated CD spectra of IgG both in solution or incorporated into liposomes were then estimated via the secondary structure algorithm CDSSTR using DICHROWEB (Greenfield, 2006). Moreover, an easy titre IgG kit was used to measure the immunoreactivity of the protein according to the protocol previously described in Section 2.2.10.

6.3 Results and discussion:

6.3.1 Priming and tail off characteristics

As mentioned earlier in Section 6.1, it is important for data on nasal sprays to include pump priming parameters (Gibson, 2001). Figure 6.1 illustrates the effect

of formulation on the number of actuations required to prime the nasal devices, the number of full actuations achieved via the nasal devices and number of actuations required in the tail-off phase.

As shown in Figure 6.1, no priming was required for the MAD device and no tail-off behaviour was noticed. This is due to the design of the MAD, since it is simply a manually operated syringe connected to a mucosal atomization device. Therefore, the user manually controls the dose through the MAD. This also explains the high accuracy in the number of full actuations generated, which is reflected in the small standard deviations. Furthermore, due to the manual operation of the device, no significant changes ($p>0.05$) were observed between the different formulations and the number of actuations depended solely on the user.

Contrary to the MAD, both nasal pump sprays A and B required priming, and exhibited tail-off behaviour as the formulations ran out. Both nasal sprays required 2-5 actuations to prime the devices with no significant differences found between the two devices for the three different formulations ($p>0.05$). The numbers of priming actuations conformed with the manufacturers' directions.

The number of full actuations on the other hand differed significantly between the two nasal pumps ($p<0.05$). Whilst nasal spray A delivered 44 ± 3 , 40 ± 4 and 41 ± 4 full actuations for the IgG solution, non-sonicated liposomes and sonicated liposomes, respectively, nasal spray B delivered 31 ± 4 , 26 ± 3 and 27 ± 4 full actuations for the IgG solution, non-sonicated liposomes and sonicated liposomes, respectively. The difference between the nasal pump sprays can be attributed to the designs of the nasal sprays, specifically the volume of the metering chamber (Marx and Birkhoff, 2011). Studies conducted to measure the shot weight also confirmed the same conclusion (Figure 6.2), whereby the lower numbers of actuations exhibited by nasal spray A were associated with a larger shot weight, and the larger numbers of actuations exhibited by nasal spray B were associated with a smaller shot weight. Moreover, as demonstrated in Figure 6.1 and Figure 6.2, no significant differences were found between the different formulations in both nasal pump sprays ($p>0.05$). The numbers of actuations in the tail-off phase were also found to be similar between the nasal pump sprays ($p>0.05$).

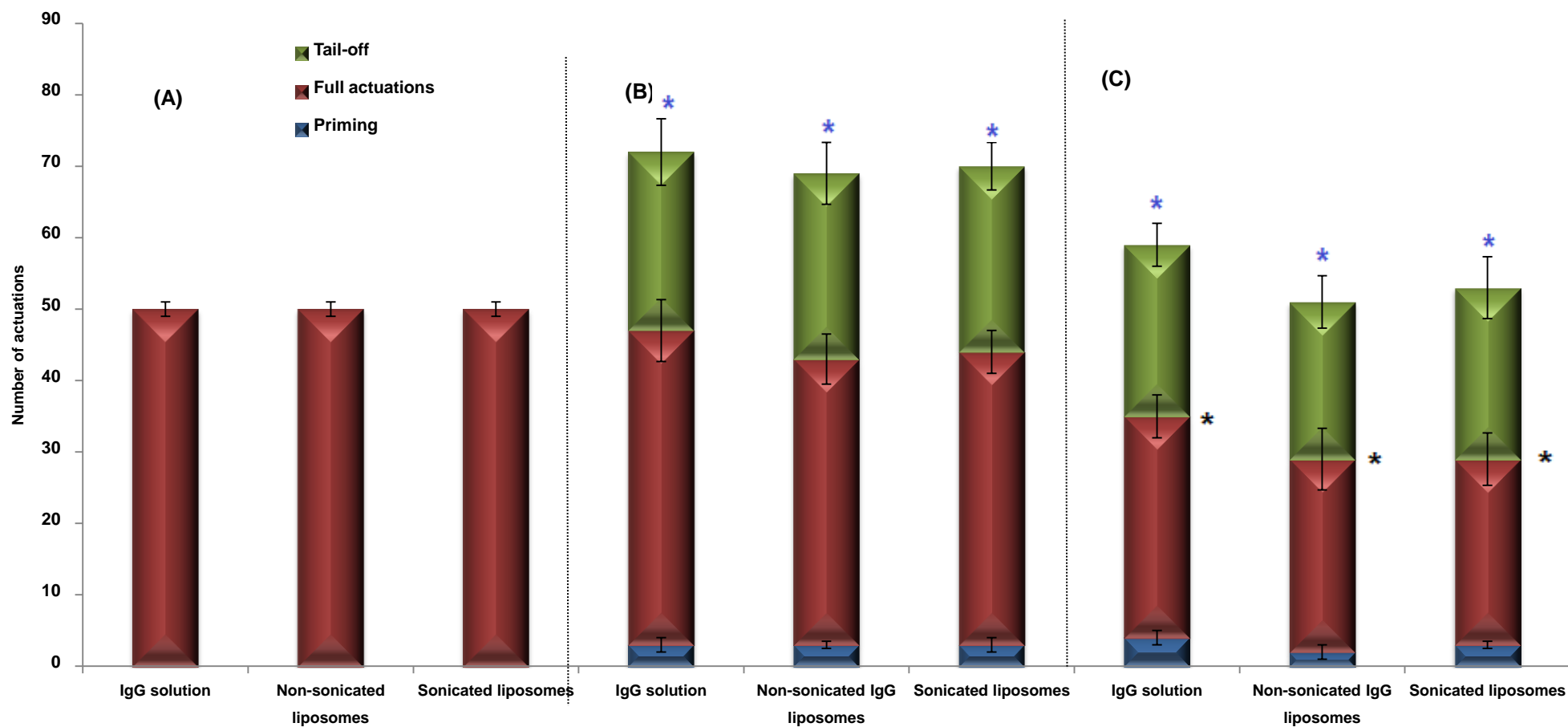


Figure 6.1: Number of actuations required priming the nasal devices, number of full actuations generated and number of actuations in the tail-off phase for the different formulations in nasal devices: (A) MAD (B) nasal spray A (C) nasal spray B. Data are mean \pm SD, $n=3$; $p>0.05$ for the number of actuations in the priming and tail-off phase for nasal sprays A and B; $p>0.05$ for number of actuations in the MAD; * $p<0.05$ for number of full actuations between Nasal spray A and B; * $p<0.05$ in the total number of actuations for Nasal sprays A and B compared to the MAD.

Results from this study indicate that the number of actuations and shot weight are primarily affected by the design of device rather than the nature of formulation. These findings came in agreement with Harris *et al.*, (1988), who observed no differences in the dose accuracy between different formulations containing 0, 0.25 or 0.5 % methylcellulose.

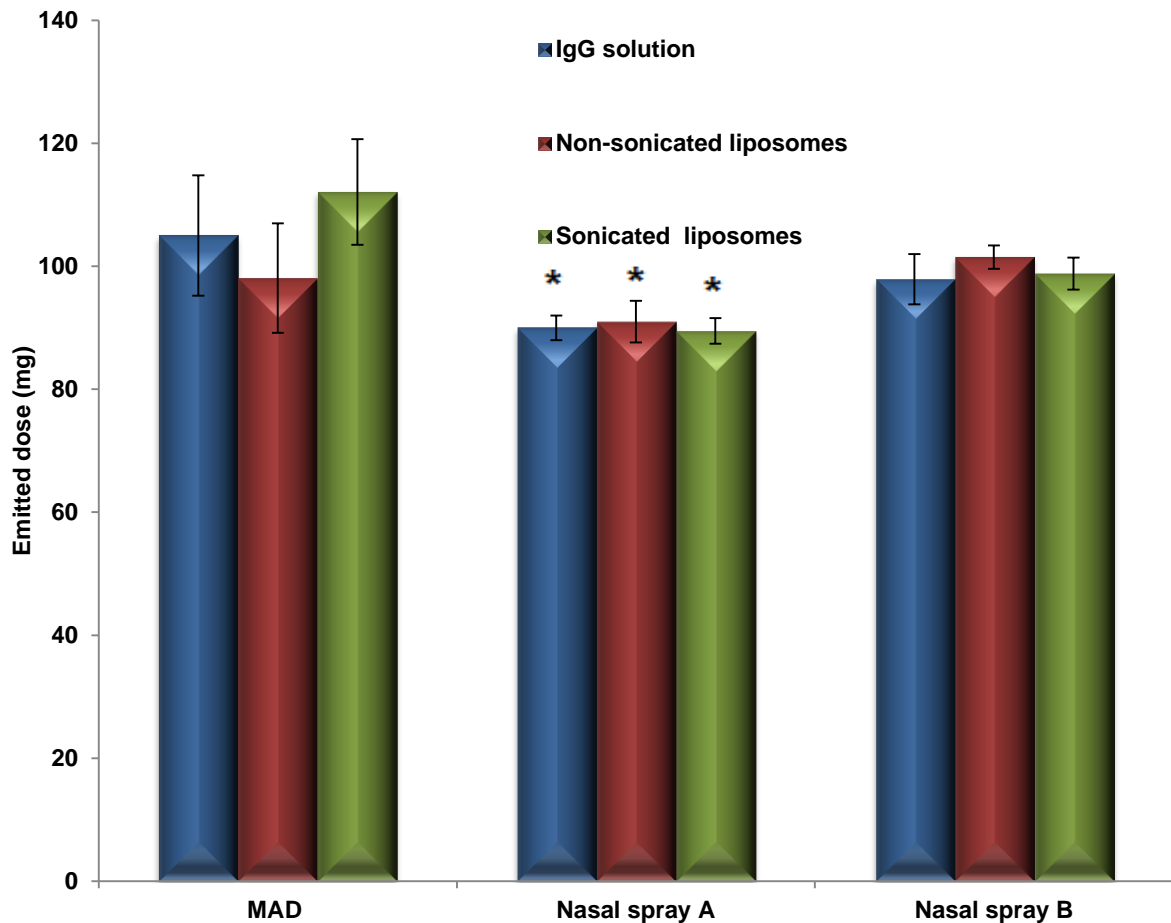


Figure 6.2: The emitted dose from the nasal devices for the different formulations. Data are mean \pm SD, n=3; * $p < 0.05$ for nasal spray A compared to nasal spray B and the MAD.

In addition to the dose accuracy reflected by the number of full actuations and the shot weight, the total time required per actuation was investigated (Figure 6.3).

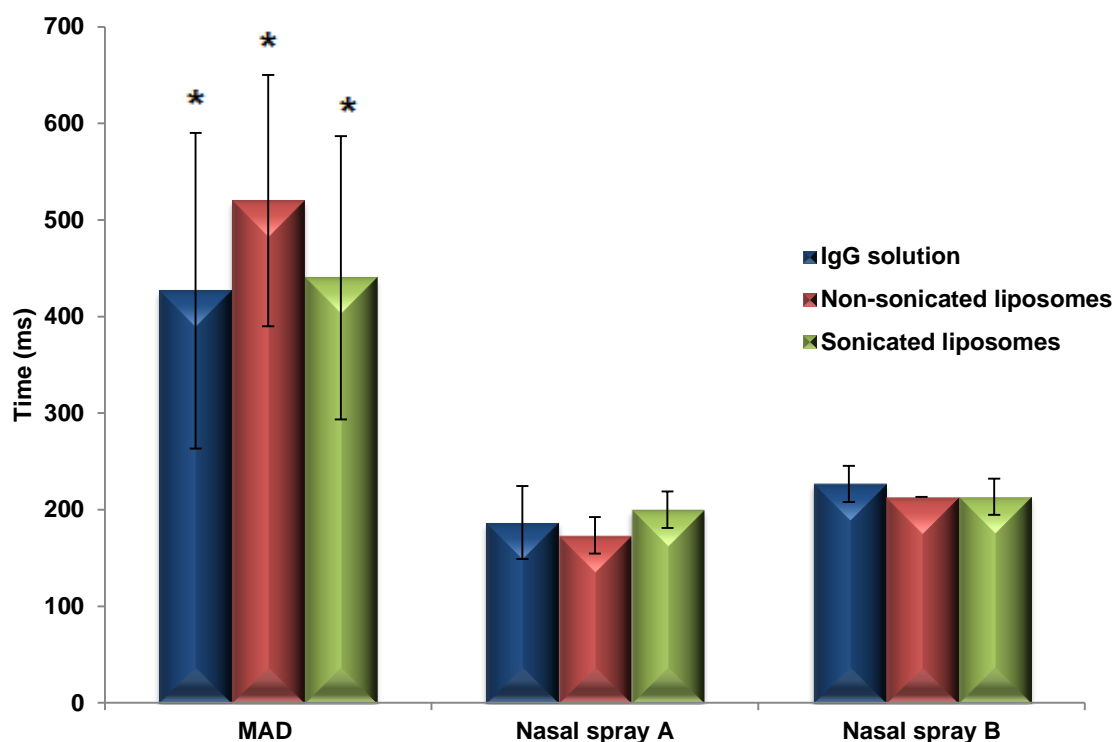


Figure 6.3: The time required per actuation for the different formulations through the nasal devices. Data are mean \pm SD, $n=3$; * $p<0.05$ for MAD compared to nasal sprays A and B; $p>0.05$ between nasal sprays A and B.

As demonstrated in Figure 6.3, the total time per actuation was found not to significantly differ between nasal sprays A and B ($p>0.05$). Conversely, the time required per actuation in the MAD device was found to be considerably longer than both nasal sprays A and B. The time per actuation through the MAD was found to be 426.67 ± 163.33 , 520 ± 130 and 440 ± 146.66 ms for IgG solution non-sonicated liposomes and sonicated liposomes, respectively. On the other hand, the time required per actuation was found to be 186.67 ± 37.7 , 173.33 ± 18.85 and 200 ± 18.85 ms for IgG solution, non-sonicated liposomes and sonicated liposomes, respectively upon using nasal spray A; and 226.67 ± 18.85 , 213.33 and 213.33 ± 18.85 ms upon using nasal spray B.

In addition, no marked differences were observed in the time required per actuation amongst the different formulations in all three nasal devices ($p>0.05$). These differences between the different devices are ascribed to their designs, and like the actuation results previously discussed in Section 6.3.1, the nature of the formulation was found to have no effect on the time per actuation ($p>0.05$).

As described in Section 2.2.14, each actuation through the nasal device is comprised of three phases: formation phase, evolution phase and dissipation phase. Examples of images of the different phases are illustrated in Figures 6.4-6.6 for the three nasal devices.

As observed from the Images 5.6-5.8, the duration of the formation, evolution and dissipation phase through the nasal pump sprays were the same (i.e. 80 ms each phase). The MAD on the other hand was characterised by a long formation and dissipation phases (i.e. 160 ms each) and shorter evolution phase (i.e. 120 ms). The absence of a pump system in MAD in comparison to the nasal pump sprays can thus explain this different behaviour between the devices.

6.3.2 Droplet size distribution (DSD)

The DSD and fraction of droplets below 10 μm are amongst the critical parameters defining the performance and efficiency of nasal devices (Dayal *et al.*, 2004). Moreover, those parameters can be possible predictors of the ability of droplets to target the lung (Kippax *et al.*, 2011) or the nasal cavity (Kippax and Fracassi, 2003). In this section the effects of formulation on the DSD and the fraction of droplets below 10 μm using the three nasal devices were evaluated (Table 6.1).

As demonstrated in Table 6.1, the trend in droplet size for both nasal sprays A and B was the same: non-sonicated liposomes > sonicated liposomes > IgG solution, with significant differences between the IgG solution and non-sonicated liposomes for both nasal sprays ($p < 0.05$). This trend in DSD can be attributed to the expected increase in viscosity of liposomes (non-sonicated and sonicated) in comparison to the IgG solution, where incorporation of lipid and alginate is expected to increase the viscosity of the formulations.

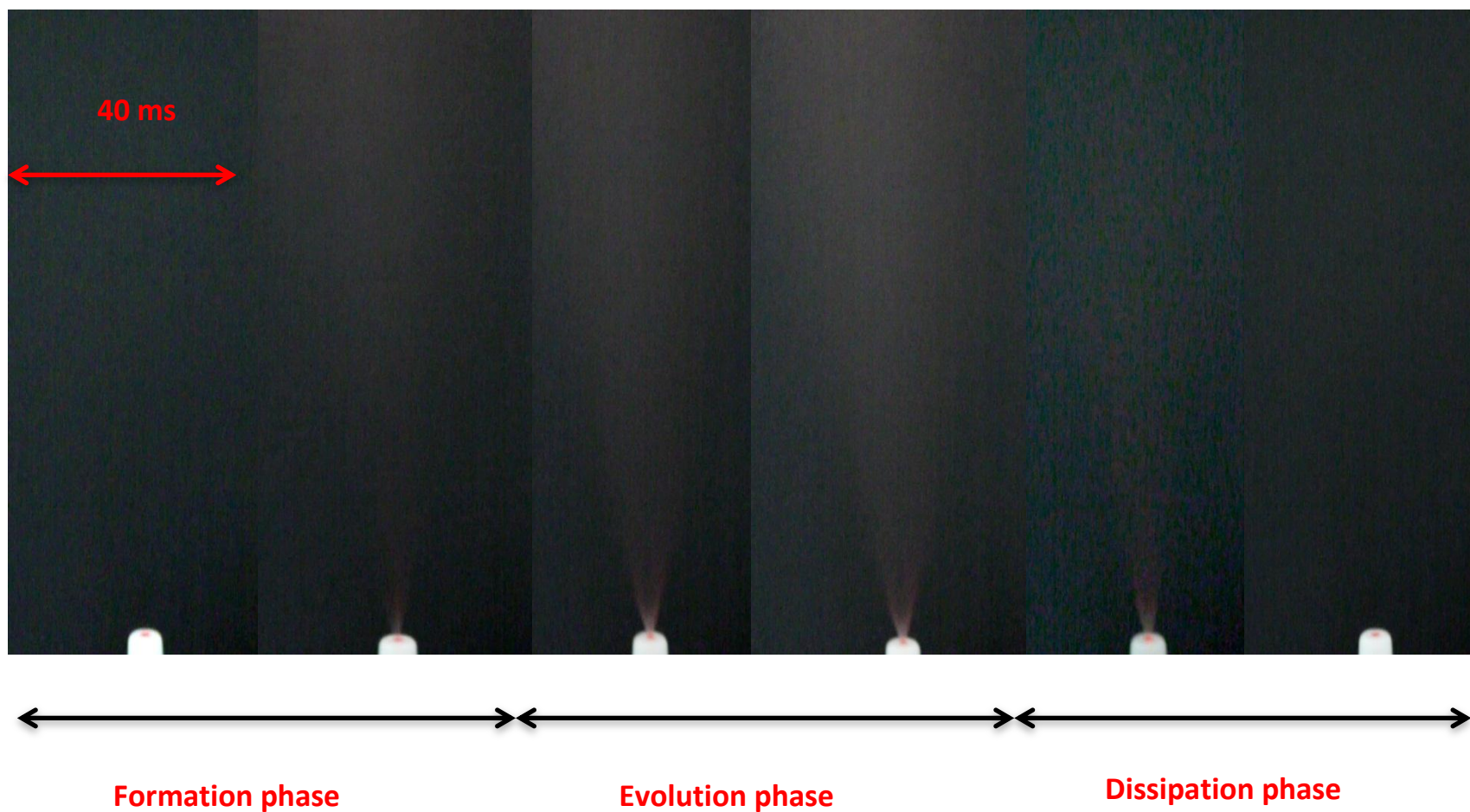


Figure 6.4: Time course frames (40 ms) of an evolving plume from nasal spray A showing the different phases of cloud spray development. Typical of 4-6 different experiments.

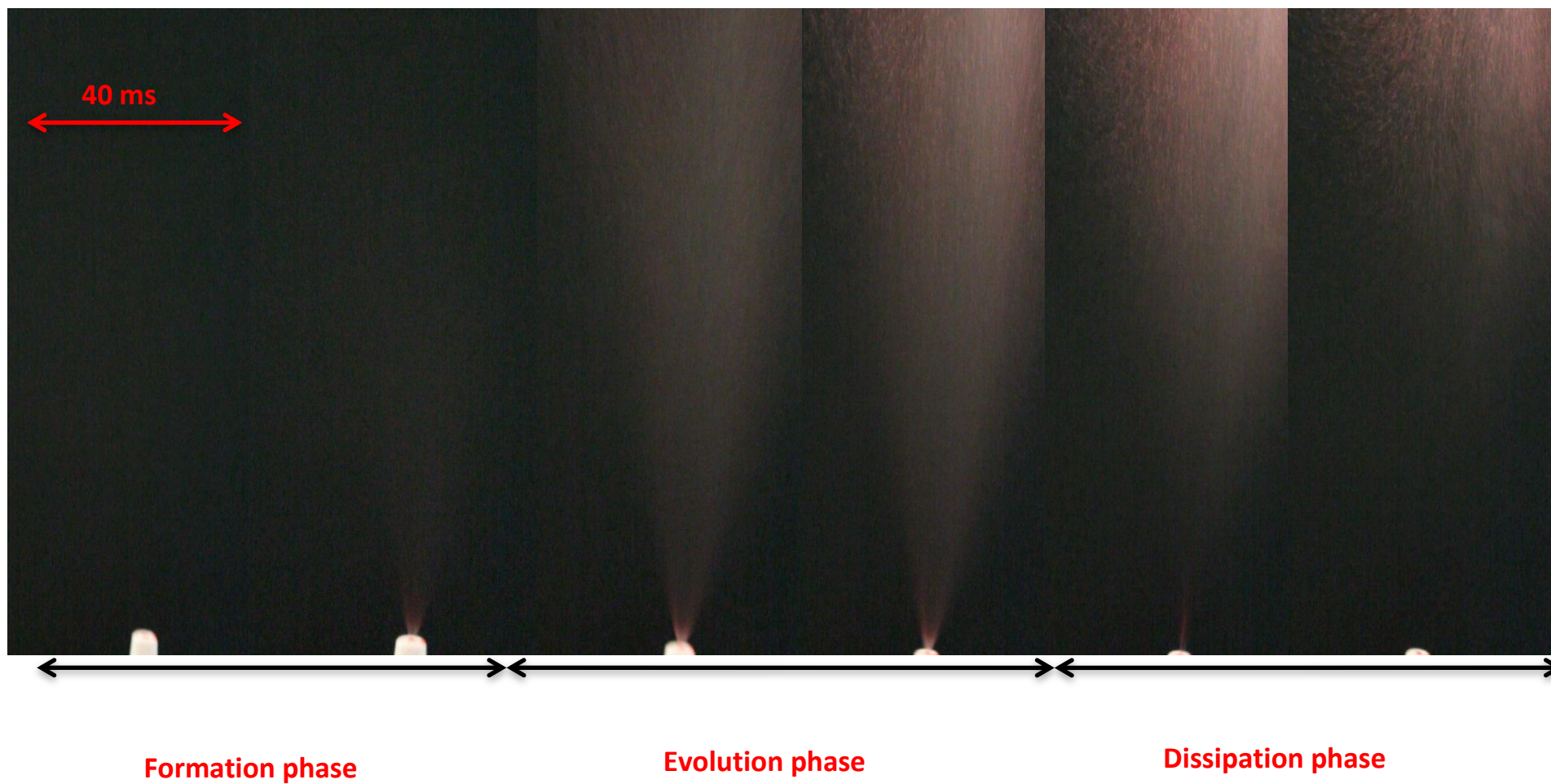


Figure 6.5: Time course frames (40 ms) of an evolving plume from nasal spray B showing the different phases of cloud spray development. Typical of 4-6 different experiments.

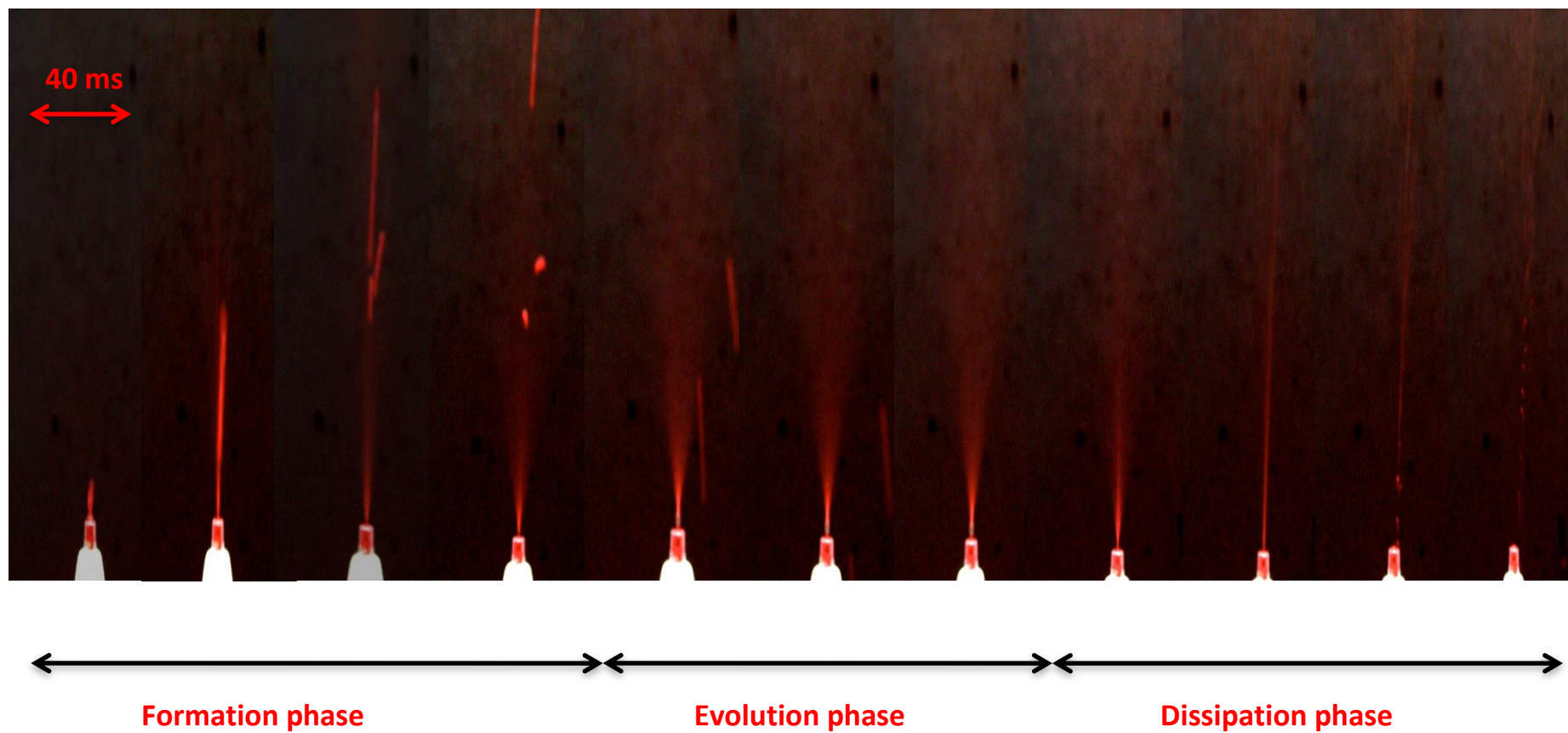


Figure 6.6: Time course frames (40 ms) of an evolving plume from the MAD showing the different phases of cloud spray development. Typical of 4-6 different experiments.

Kippax *et al.*, (2010) evaluated the effect of increasing the viscosity of aqueous solution on the DSD of nasal sprays using different concentrations (0%-1.5%) of polyvinylpyrrolidone (PVP). They reported an increase in the droplet size with increasing solution viscosity, which is in agreement with our findings in this study. These results were also supported by Harris *et al.*, (1988), who reported an increase in the DSD of nasal sprays from 51 to 200 μm as the concentration of methylcellulose increased from 0 to 0.5 %. Moreover, Foo (2007) compared the DSD produced by 37% sucrose solution (viscosity = 4.24 cP) and water (viscosity = 0.94 cP) using different nasal devices. The results from that study also demonstrated a significantly higher DSD for the 37% sucrose solution in comparison to water.

It was also demonstrated in Table 6.1 that droplets generated by the nasal spray B were larger than those of nasal spray A. This can be attributed to differences in the designs of the devices specifically the dimensions of the orifice in the nasal sprays. This increase in droplet particle size is expected to increase the deposition in the anterior region of the nasal cavity (Cheng *et al.*, 2001).

Contrary to both nasal spray A and nasal spray B, the droplet size generated by the MAD was found not to be affected by the nature of formulation ($p > 0.05$). This can be attributed to the high standard deviations of the droplet size readings when the MAD device was employed, and the possible differences in the velocity or stroke strength exerted on the MAD. Guo and Doub (2006) evaluated the effect of actuating parameters such as stroke velocity, acceleration and stroke length using an electronic automatic actuator on the characteristics of nasal sprays. The results from their study indicated a significant effect of the stroke velocity on the droplet size of particles, whereby an increase in velocity from 20 mm/s to 60 mm/s resulted in a decrease in the mean droplet size of sprays from 45 μm to 30 μm , respectively.

Table 6.1: The droplet size, SPAN and particle fraction < 10 μm for the different formulations using different nasal devices. Data are mean \pm SD, n=3; $p>0.05$ for the SPAN and Droplet<10 μm (%) for all formulations; * $p<0.05$ for the droplet size of sonicated liposomes and non-sonicated liposomes compared to the IgG solution for nasal sprays A and B.

<u>Droplet size (μm)</u>			
	IgG solution	Sonicated liposomes	Non-sonicated liposomes
Nasal spray A	54.87 \pm 3.51	59.74 \pm 1.68 *	68.43 \pm 3.01 *
Nasal spray B	59.42 \pm 3.41	64.10 \pm 5.11 *	76.83 \pm 4.52 *
MAD	68.99 \pm 8.88	65.11 \pm 20.24	72.75 \pm 20.02
<u>SPAN</u>			
	IgG solution	Sonicated liposomes	Non-sonicated liposomes
Nasal spray A	3.41 \pm 1.01	4.21 \pm 0.67	3.33 \pm 0.31
Nasal spray B	4.76 \pm 0.31	3.31 \pm 1.63	3.01 \pm 0.71
MAD	6.30 \pm 1.51	4.26 \pm 1.54	3.34 \pm 2.08
<u>Droplets <10 μm (%)</u>			
	IgG solution	Sonicated liposomes	Non-sonicated liposomes
Nasal spray A	3.93 \pm 1.47	6.26 \pm 1.29	6.71 \pm 1.38
Nasal spray B	4.19 \pm 1.44	3.35 \pm 2.47	6.87 \pm 2.05
MAD	5.04 \pm 2.11	4.33 \pm 1.43	8.31 \pm 6.52

Unlike the droplet size, the SPAN and fraction of droplets below 10 μm were not affected by the nature of the formulation ($p>0.05$). Moreover, no significant differences were also observed in the SPAN and the fraction of droplets below 10 μm between the different nasal devices.

According to findings of Harris *et al.*, (1988), optimum mean droplet size diameter for nasal delivery lies within the range of 59 to 80 μm . Hence, indicating that droplets generated via the different nasal devices and formulations in our study are considered to be optimal for nasal delivery.

6.3.3 Spray pattern and plume geometry

In addition to the DSD, shot weight and actuating properties of nasal devices, the spray pattern and plume geometry of the generated cloud from the different nasal devices are important factors that can be used to evaluate the performance of the nasal devices (Harrison, 2000). Furthermore, the spray pattern and plume geometry can be used to predict the possible deposition site within the nasal cavity (Newman *et al.*, 2004; Foo, 2007)

In this section studies were conducted in order to investigate the effect of formulation and nasal device on the spray pattern and plume geometry of the generated cloud (Table 6.2). Figures 6.7-6.9 also show example images of the plumes and spray patterns of the different formulations sprayed using the different nasal devices.

As demonstrated in Table 6.2 and Figures 6.7-6.9, significant differences ($p<0.05$) in plume geometry measurements existed between the devices. First, with regard to the plume angle, it was in the order of: nasal spray B > nasal spray A > MAD for all the formulations. Secondly, the plume width at 3 cm was found to be dependent on the plume angle, and thus was found to be significantly higher for nasal spray B, followed by nasal spray A and the least plume width was demonstrated by the MAD device. Finally, contrary to the plume width, the total plume height was found to decrease as the plume angle increased, and thus was highest for the MAD device and the lowest plume height was exhibited by nasal spray B. These

differences in plume angles between the different devices are expected to have implications on the site of deposition within the nasal cavity, as it has been previously demonstrated that deposition in the anterior region of the nasal cavity increases with increasing the plume angle, whilst deposition in the turbinate region increases with decreasing the plume angle (Cheng *et al.*, 2001; Foo *et al.*, 2007). Thus, it is suggested that the anterior deposition will be highest when the nasal spray B is employed, whilst turbinate deposition might be highest when the MAD device is used.

Furthermore, as displayed in Table 6.2 and Figures 6.7-6.9, the spray pattern was differed considerably when using different devices. Whilst nasal pumps A and B were found to exhibit more oval and larger spray patterns, the MAD exhibited significantly smaller and irregularly shaped spray patterns. The average ovality ratio were 1.07 and 1.11 for the nasal spray pumps A and B, respectively and 1.73 for the MAD device.

In a study conducted by Makidon *et al.*, (2010), the characteristics of sprays generated from both a single dose Becton, Dickinson and Company (BD) accuspray nasal device and a Pfeiffer nasal pump nasal spray were compared. Results from their study demonstrated a significant difference ($p < 0.05$) in ovality ratio between the devices, being respectively 3.6 ± 1.9 and 1.2 ± 0.1 for the single dose nasal device and the nasal pump device. This may indicate that a more oval spray pattern is exhibited when employing nasal pump sprays. These results came in high agreement with the results from the present study.

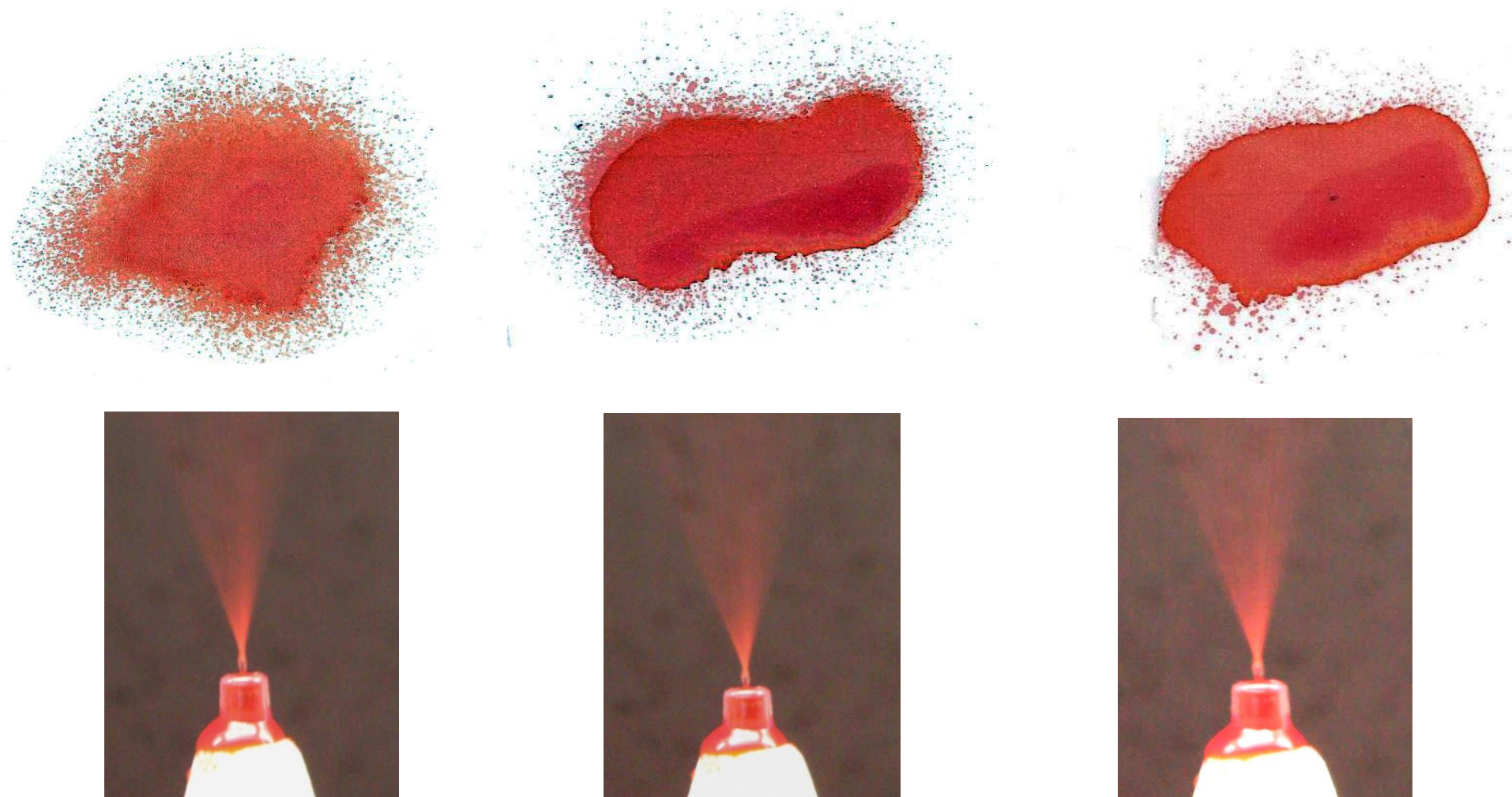


Figure 6.7: Images of the plumes and the spray patterns using the MAD for (A) the IgG solution (B) non-sonicated IgG liposomes and (C) sonicated IgG liposomes. Typical of 4-6 different experiments.

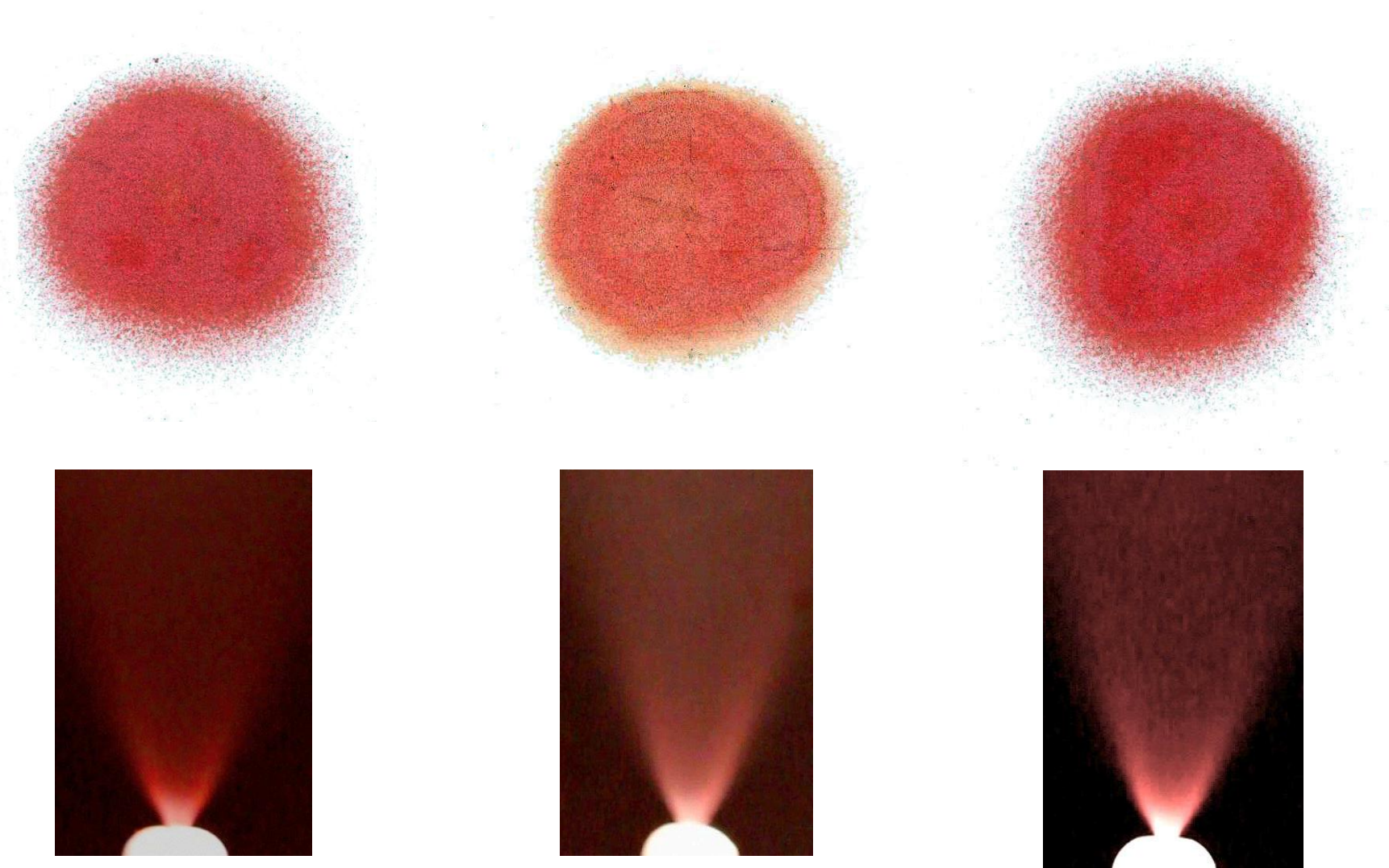


Figure 6.8: Images of the plumes and the spray patterns using nasal spray A for (A) the IgG solution (B) non-sonicated IgG liposomes and (C) sonicated IgG liposomes. Typical of 4-6 different experiments.

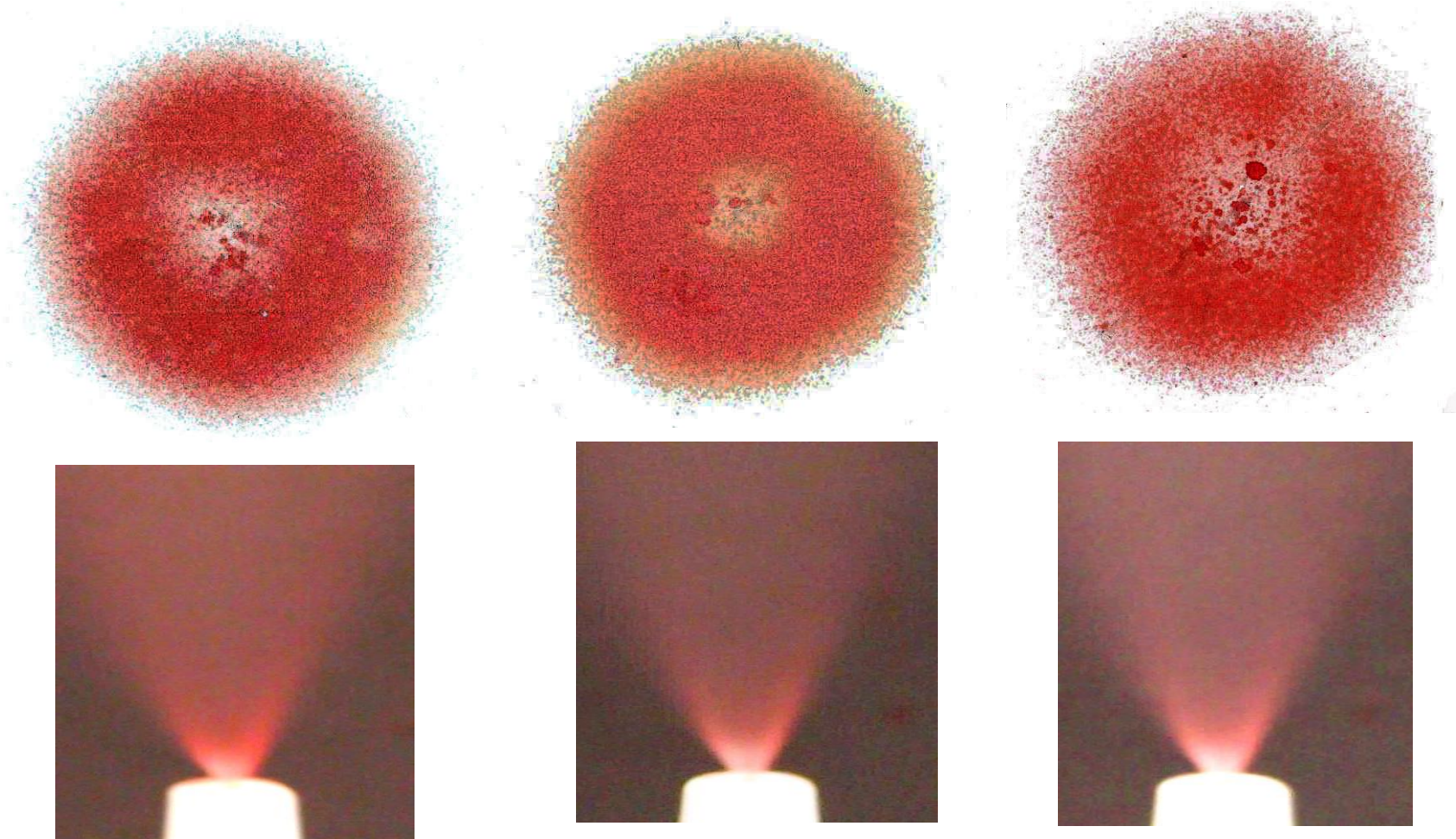


Figure 6.9: Images of the plumes and the spray patterns using nasal spray B for (A) the IgG solution (B) non-sonicated IgG liposomes and (C) sonicated IgG liposomes. Typical of 4-6 different experiments.

Table 6.2: The (A) plume geometry and (B) spray pattern of the generated spray cloud. Data are mean \pm SD, n=3; $p>0.05$ among all the plume geometry parameters for the different formulations; $p<0.05$ for the cone angle and width at 3 cm parameters among the different devices; * $p<0.05$ for the total plume height of the MAD device compared to nasal sprays A and B; $p>0.05$ in spray pattern parameters for all formulations; * $p<0.05$ in the different spray pattern parameters for nasal sprays A and B compared to the MAD; * $p<0.05$ in the D_{\min} and D_{\max} data for nasal spray A compared to nasal spray B and the MAD.

(A) Plume geometry

	<i>IgG solution</i>			<i>Sonicated liposomes</i>			<i>Non-sonicated liposomes</i>		
	Cone angle	Width at 3 cm	Total plume height (cm)	Cone angle	Width at 3 cm	Total plume height (cm)	Cone angle	Width at 3 (cm)	Total plume height (cm)
MAD	34.00 \pm 0.82	1.97 \pm 0.05	58.20 \pm 6.09*	35.00 \pm 0.94	2.03 \pm 0.09	62.73 \pm 5.26*	33.33 \pm 1.25	1.90 \pm 0.08	60.97 \pm 4.60*
Nasal spray A	44.33 \pm 1.25	2.56 \pm 0.09	48.97 \pm 3.21	43.00 \pm 0.82	2.47 \pm 0.12	47.03 \pm 3.95	42.66 \pm 0.47	2.50 \pm 0.08	50.17 \pm 2.76
Nasal spray B	49.66 \pm 1.25	3.07 \pm 0.05	44.60 \pm 4.25	48.33 \pm 0.94	3.00 \pm 0.08	45.57 \pm 3.27	48.66 \pm 0.47	2.80 \pm 0.16	44.43 \pm 3.62

(B) Spray pattern

	<i>IgG solution</i>			<i>Sonicated liposomes</i>			<i>Non-sonicated liposomes</i>		
	D_{\min} (cm)	D_{\max} (cm)	Ovality	D_{\min} (cm)	D_{\max} (cm)	Ovality	D_{\min} (cm)	D_{\max} (cm)	Ovality
MAD	3.00 \pm 0.29	4.27 \pm 0.42	1.42 \pm 0.20	2.20 \pm 0.29	4.43 \pm 0.34	2.01 \pm 0.31	2.33 \pm 0.21	4.13 \pm 0.29	1.77 \pm 0.20
Nasal spray A	4.33 \pm 0.12*	4.77 \pm 0.12	1.10 \pm 0.04*	4.47 \pm 0.12*	4.97 \pm 0.12	1.11 \pm 0.04*	4.43 \pm 0.12*	5.00 \pm 0.22*	1.13 \pm 0.06*
Nasal spray B	5.73 \pm 0.17**	6.20 \pm 0.8**	1.08 \pm 0.15*	5.63 \pm 0.21**	5.93 \pm 0.26**	1.05 \pm 0.06*	5.43 \pm 0.17**	5.93 \pm 0.21**	1.09 \pm 0.05*

In addition, as demonstrated in Figures 6.7-6.9, the nature of the spray pattern was different in nasal spray B compared to nasal spray A and the MAD, where unlike the latter devices, the spray pattern was found to be hollow in nasal spray B in comparison to full spray patterns generated by nasal spray A and the MAD. In a study conducted by Inthavong *et al.*, (2011), the effect of the hollow cone and full cone spray patterns generated from an internal atomiser on the deposition inside the nasal cavity was evaluated. The results from their study indicated that hollow cone spray patterns deposited more in the middle regions of the nasal cavity when compared to the full cone spray pattern.

As demonstrated in Table 6.2 and Figures 6.7-6.9, for each device, formulation had no significant effects on the spray pattern and plume angle ($p>0.05$). These findings disagree with previous studies that reported a dependence of the spray pattern and plume geometry on the nature of formulation, mainly its viscosity (Dayal *et al.*, 2004; Foo, 2007). This disagreement might be attributed to the small difference in viscosity between our formulations in comparison to those used by previous studies.

6.3.4 Liposomes before and after spraying

Despite the fast-growing research on the applicability of liposomes in nasal delivery, as yet there have been no published studies demonstrating the effect of the nasal devices themselves on the size and size distribution of liposomes.

To ascertain the effect of dispensing the IgG liposomes (non-sonicated and sonicated) using nasal devices, the physical integrity of liposomes, by means of measuring their size, size distribution and morphology following spraying was examined (Figures 6.10-6.12).

As illustrated in Figure 6.10, spraying using the different nasal had no marked effect ($p>0.05$) on the size of non-sonicated or sonicated liposomes. The Pdi of the sonicated liposomes and SPAN non-sonicated liposomes were also not affected by spraying ($p>0.05$). Additionally, cryo-TEM studies conducted revealed that delivery of liposomes (non-sonicated and sonicated) via the different nasal devices

did not affect its morphology, since the multilamellar structure of the liposomes was maintained following spraying (Figures 6.11-6.12).

These results demonstrate the great promise that nasal sprays could offer in the field of liposome delivery to the respiratory tract, where unlike nebulisers which lead to significant fragmentation of liposomes, as demonstrated in chapter 4, nasal sprays demonstrated an ability of preserving the physical integrity of liposomes. However, this advantage of using nasal sprays over nebulisers is true only if deposition in the nose using nasal sprays can replace the need for targeting the deep lung via using nebulisers.

6.3.5 Effect of spraying on the structure and activity of IgG

In this Section the structure and activity of IgG in solution and in liposome formulations (non-sonicated or sonicated) have been analysed before and after spraying using the MAD device, and nasal pump sprays A and B (Figure 6.13).

As demonstrated in Figures 6.13-6.15, spraying using the three different nasal devices was found not to significantly affect the structure of IgG ($p>0.05$), both in solution and in liposome formulations (non-sonicated or sonicated). Moreover, contrary to using nebulisers, the use of nasal sprays has been found not to affect the activity of IgG in solution or in liposomes ($p>0.05$) (Figures 6.14-6.15) and the activity of IgG was about 100% for all formulations sprayed by the different devices.

It was demonstrated earlier in Section 5.3.3 that fragmentation of liposomes incorporating IgG can lead to a reduction in the activity of IgG. The preservation of the activity of IgG in this study further confirms that theory, since liposomes were previously demonstrated to be unaffected by spraying (Section 6.3.4).

This is the first study conducted to test the effect of nasal devices (for liquid formulations) on the integrity of liposomes or IgG. The positive outcomes from the study demonstrated by the preserved integrity of the liposomes and IgG following spraying, elucidates the great potential that nasal sprays can possess.

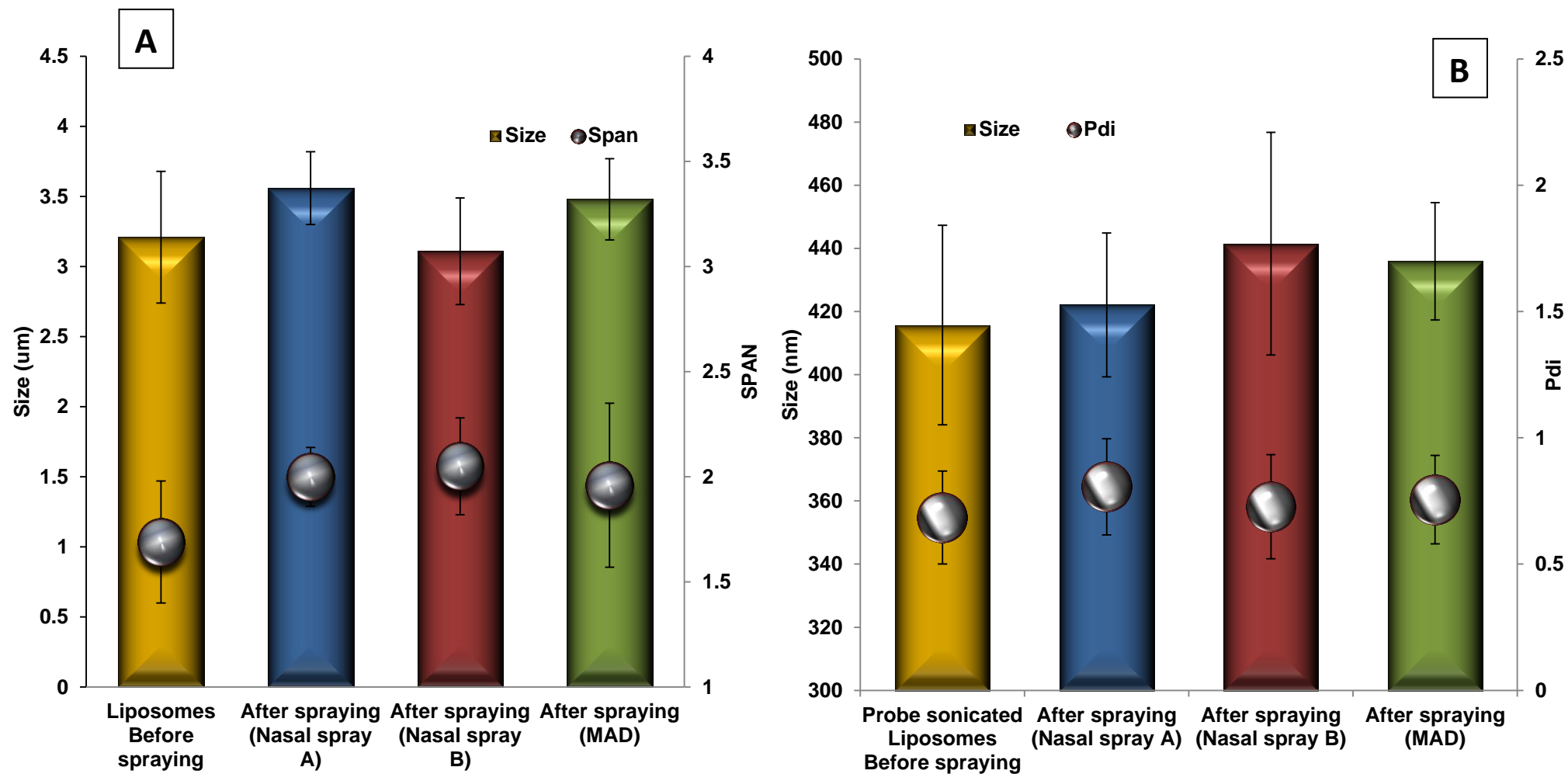


Figure 6.10: Size and size distribution of (A) non-sonicated liposomes and (B) sonicated vesicles using different nasal devices. Data are mean \pm SD, $n=3$; $p>0.05$ for all size and SPAN data.

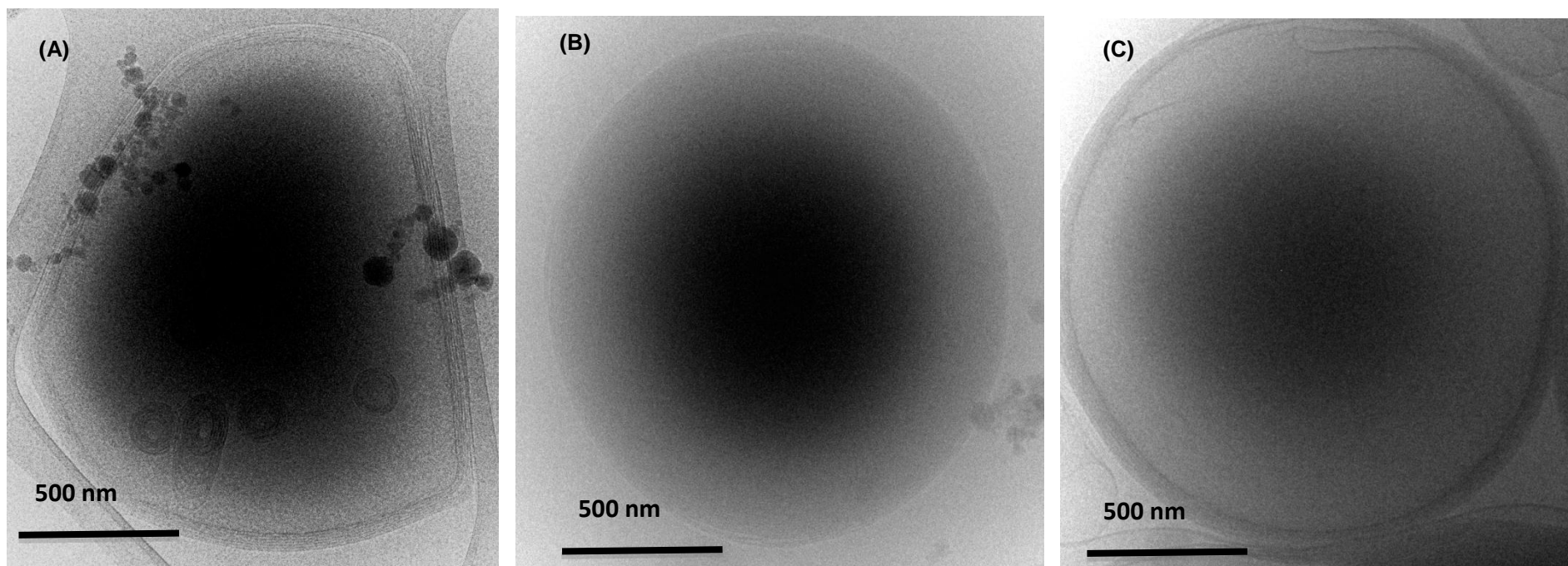


Figure 6.11: Cryo-TEM images of multilamellar liposomes (non-sonicated) following spraying via the (A) MAD, (B) nasal spray A and (C) nasal spray B. Typical of 4-6 different experiments.

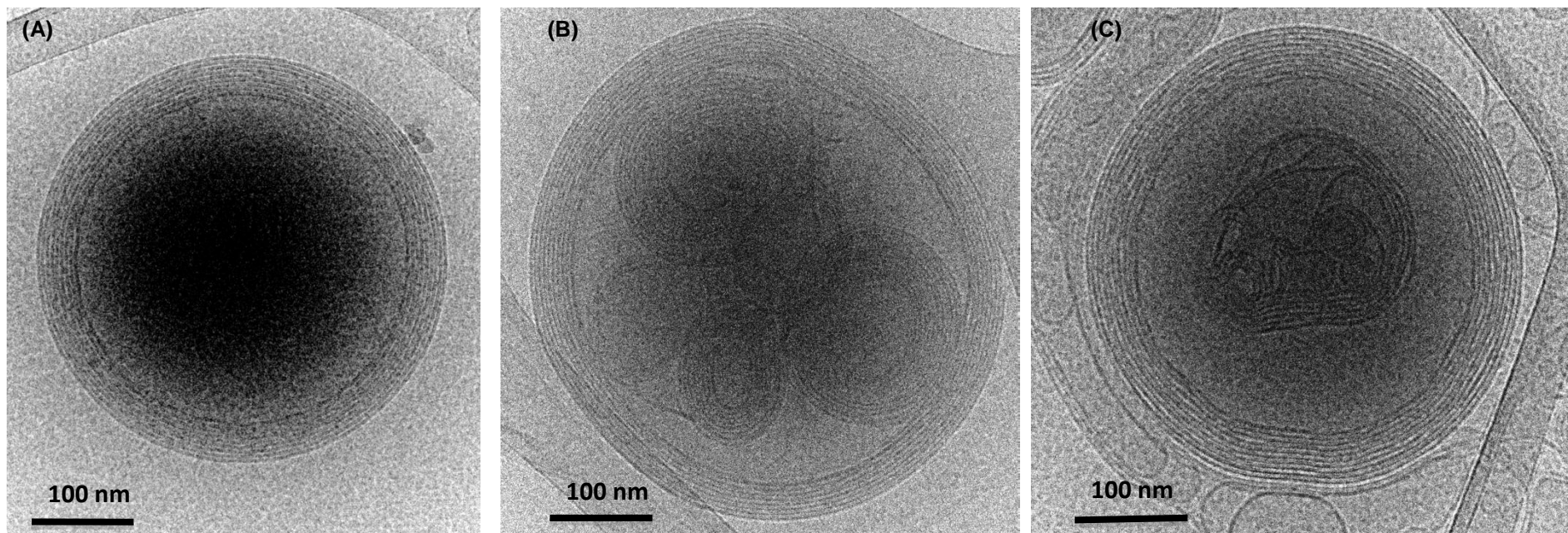


Figure 6.12: Cryo-TEM images of multilamellar liposomes (sonicated) following spraying via the (a) MAD, (b) nasal spray A and (c) nasal spray B. Typical of 4-6 different experiments.

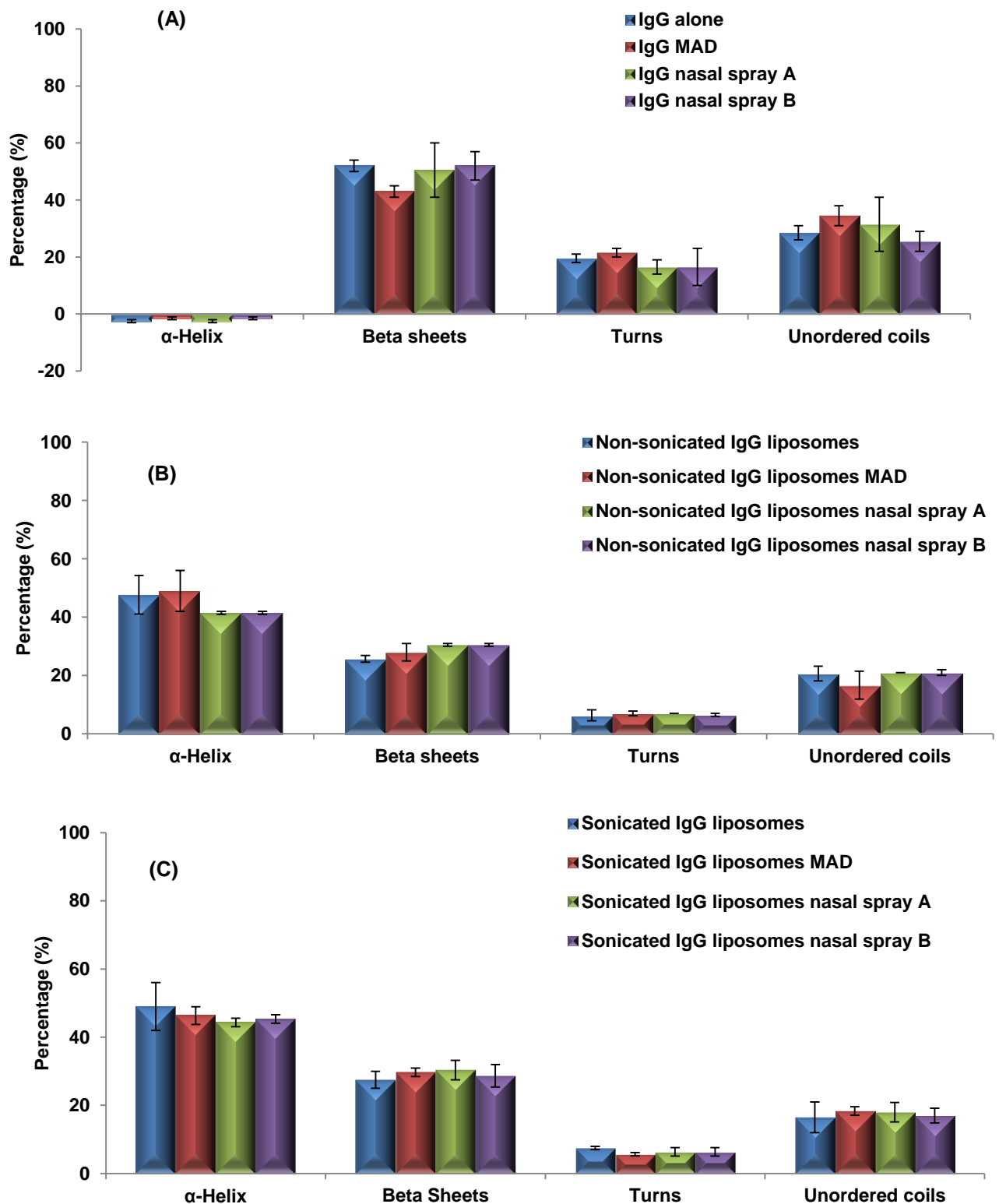


Figure 6.13: Spraying of (A) IgG and IgG bound to liposomes ((B) non-sonicated and (C) sonicated), using a MAD and two nasal pump sprays A and B, and its effect on the secondary structure of IgG. Data are mean \pm SD, $n=3$; $p>0.05$ among the different formulations in the three nasal devices.

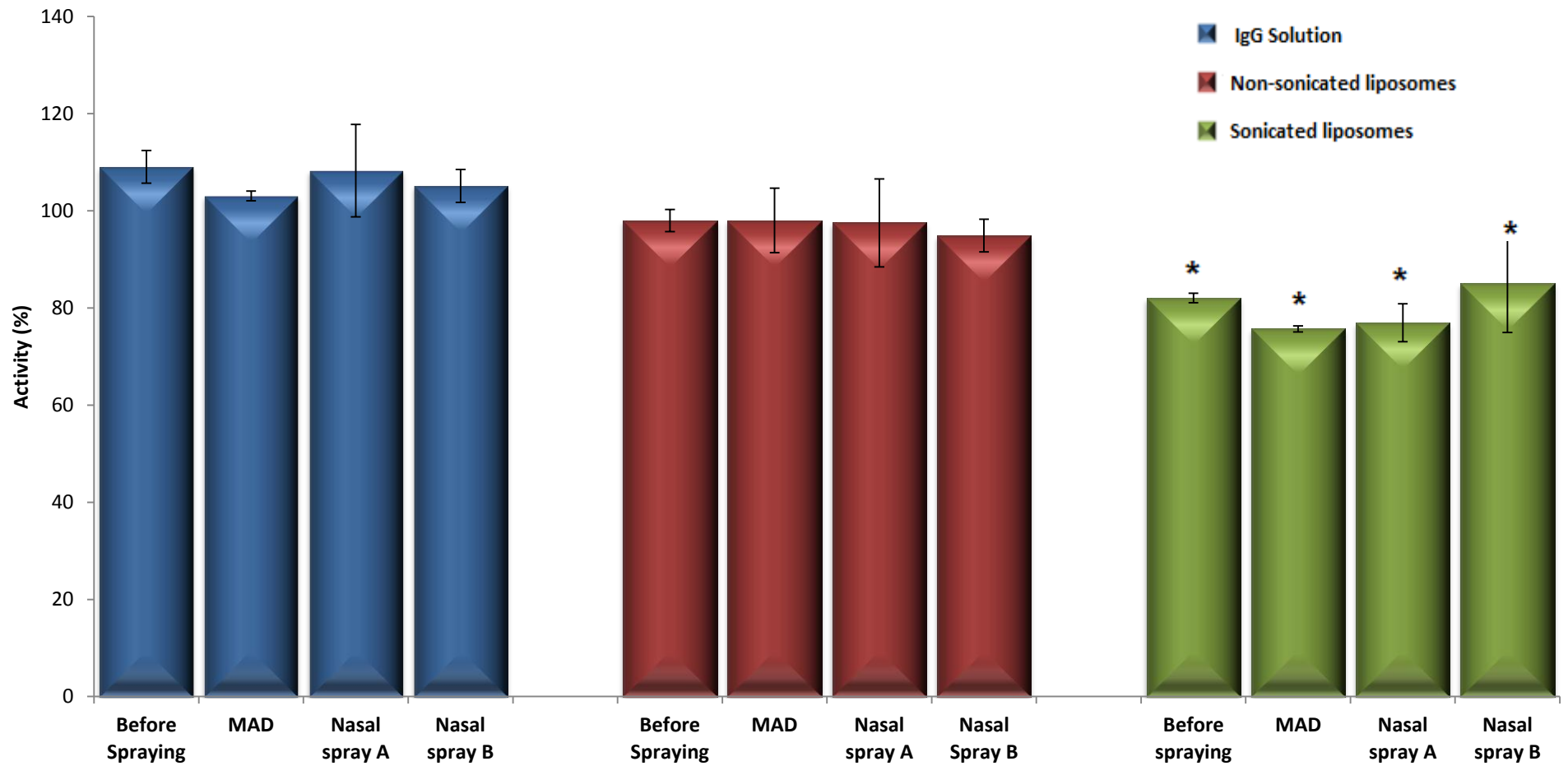


Figure 6.14: Spraying of IgG and IgG bound to liposomes (non-sonicated or sonicated), using a MAD and two nasal pump sprays A and B, and its effect on the activity of IgG. Data are mean \pm SD, $n=3$; * $p < 0.05$ for sonicated liposomes compared to non-sonicated liposomes and the IgG solution.

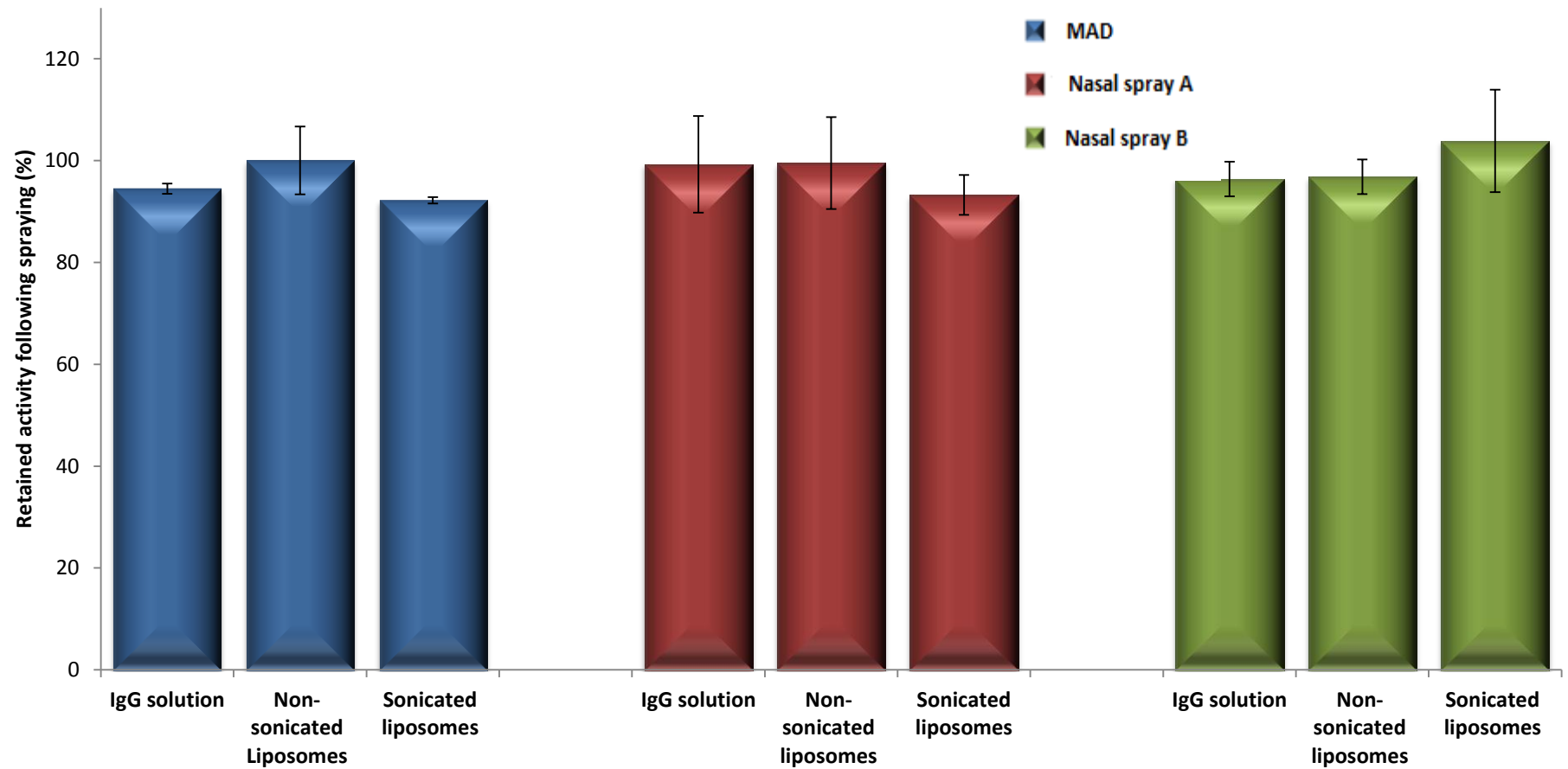


Figure 6.15: Spraying of IgG and IgG bound to liposomes (non-sonicated and sonicated), using a MAD and two nasal pump sprays A and B, and its effect on the activity of IgG relative to before nebulisation. Data are mean \pm SD, $n=3$; $p>0.05$ among the different formulations in all three nasal devices.

6.4 Conclusions

The results obtained from this study provide a rational basis for device and liposomal formulation selection of nasal spray delivery systems. In fact, this is the first study that examines the effect of incorporating liposomal formulations in nasal devices and examining the effect liposomal formulations on the spray characteristics of various devices. Based on DSD, plume geometry and spray pattern results, nasal pump sprays were demonstrated to be superior to the MAD in delivering spray plumes with uniform DSD, wider plume angles and more uniform spray patterns. All of these are postulated to achieve better deposition in the nasal cavity, and are expected to deposit more in the anterior non-ciliated region of the nose, thus leading to a slower clearance from the nose, hence promising an enhanced therapeutic effect.

The results from this study were also the first to elucidate that all nasal devices examined managed to preserve both the physical integrity of liposomes (non-sonicated and sonicated) and their incorporated IgG moiety. Considering those results, the potential benefits both intranasal administration and proliposome technology offer great promise for using liposomal formulation incorporating proteins in intranasal delivery.

CHAPTER 7

GENERAL CONCLUSIONS AND FUTURE WORK

The potential of drug delivery via the respiratory tract as an alternative to non-invasive systemic delivery of therapeutic agents has been attracting a lot of attention. Nowadays, both pulmonary delivery and nasal delivery are amongst the top four routes in the drug delivery market. The potential growth of those sectors is also extensive owing to the promise they demonstrate in the delivery of macromolecules such as peptides and proteins. Despite the advantages of delivery via the respiratory tract, the duration of activity following administration is short when the drug is formulated as a solution. Also, the activity of some proteins and peptides might be compromised following deposition in the respiratory system. Consequently, controlled drug delivery systems have been investigated as alternatives to conventional drug solutions. Amongst the controlled-release systems, liposomes are considered very promising owing to their biocompatibility and biodegradability. Liposomes are postulated to overcome the limitations of respiratory tract delivery by offering sustained release and enhancing the local retention time of drugs (Gregoriadis, 1993). In addition, liposomes are nontoxic, since they contain lipids similar to those found in the pulmonary walls (Finley *et al.*, 1968). Unfortunately, liposomes are unstable in aqueous dispersions. Also, conventional methods of liposome manufacture, such as the thin film hydration method, are difficult to scale-up and they often demonstrate low entrapment efficiency of hydrophilic materials (New, 1990b).

In this and other studies various methods have been employed to manufacture stable phospholipid systems that would generate liposomes prior to administration; one of these systems is proliposomes (Payne *et al.*, 1986a; Payne *et al.*, 1986b; Perrett *et al.*, 1991). Proliposomes are stable phospholipid formulations which readily generate liposomes upon the addition of an aqueous phase, thereby overcoming the drawbacks of liposomes made by the thin-film method (Elhissi *et al.*, 2007). To further enhance the stability of liposomes during nebulisation, the incorporation of cholesterol into the liposomal formulation (Leung *et al.*, 1996) and size reduction of liposomes have been suggested. Furthermore, to prolong the residence time of liposome formulations in the respiratory tract, the incorporation of mucoadhesive agents has proven to be viable.

General Conclusions

This study was specifically designed to fabricate novel mucoadhesive liposomes in the submicron range via the ethanol-based capable of entrapping IgG and to investigate the effects of various medical nebulisers and nasal spray devices on the integrity of formulated IgG liposomes.

Studies in this project gave a rational basis for optimal parameters required in manufacturing liposomes via the ethanol-based proliposome method. Resultant liposomes were easy to prepare and stable upon storage, and they demonstrated a potential for large-scale manufacturing. Also, the generated liposomes proved to be capable of entrapping considerable proportions of various materials, including: the small hydrophilic drug SS (EE up to 59%); the 43 kDa model protein antigen OVA (EE up to 43%); and the 150 kDa immunoglobulin IgG (EE up to 50%).

The present results also show that IgG liposomes were also prepared via the conventional thin film hydration method and the particulate-based proliposome method. The latter methods of liposomes manufacture proved valid for the entrapment of IgG. However, liposomes generated from ethanol-based proliposomes were found to be superior to the other manufacturing techniques, since they had higher EE values of IgG.

Studies to incorporate mucoadhesive agents into liposome formulations were attempted in order to prolong the retention of the liposomes in the respiratory tract. The results from those studies demonstrated that mucoadhesive agents such as chitosan or alginate can be efficiently incorporated into liposomes. The nature and concentration of those agents, however, markedly influenced the properties of the liposomes. For instance, whilst the incorporation of alginates led to enhanced IgG entrapment, the incorporation of chitosan caused the entrapment of IgG in liposomes to be negligible so that the EE was almost 0%.

Moreover, studies were conducted to reduce the size of liposomes to the submicron range in an attempt to enhance liposome stability. The results from those studies proved that various size reduction techniques were successful; however, depending on the nature of the entrapped material, a suitable size

reduction technique should be chosen. For instance, whilst extrusion proved valid for liposomes entrapping OVA and SS, it could not be used for liposomes entrapping IgG, since IgG adsorption on filters may occur. However, probe sonication proved valid as a size reduction technique of IgG liposomes.

Overall, novel mucoadhesive liposomes in the submicron size range entrapping considerable amounts of IgG were developed. These liposomes were prepared via the ethanol-based proliposome technology; therefore they can overcome the stability and scaling-up limitations of liposomes.

Following the manufacture of IgG liposome formulations (non-sonicated or sonicated), the potential of delivery of the formulations via medical nebulisers and nasal sprays of various operating principles was studied, and the performance of devices and properties of generated aerosol clouds were investigated using different formulations.

The Results from those studies showed a marked influence of formulation on the performance of medical nebulisers and the characteristics of clouds generated from nasal sprays. For instance, the use of IgG liposomes compared to IgG solution was found to prolong nebulisation time of the vibrating-mesh and ultrasonic nebulisers, whilst having no marked effects on the characteristics of the generated aerosol from the different nebulisers (i.e. aerosol DSD and FPF). On the other hand, formulations did not affect the performance of nasal devices. Nevertheless, generated cloud was strongly influenced by formulation type. For example, IgG liposomes increased the size of droplets generated by both nasal spray pump sprays.

The effect of device on liposomes' physical stability and IgG integrity was also investigated. The results demonstrated that the use of medical nebulisers caused liposome fragmentation, without affecting the multilamellar morphology of the liposomes. Also, with the use of medical nebulisers, a marked loss in the activity of IgG was demonstrated. However, the secondary structure of IgG was maintained. Furthermore, marked differences existed amongst the nebulisers themselves, and the vibrating-mesh nebuliser was found to have the least effect on fragmentation of liposomes and reducing activity of IgG.

Overall, the retained activity of IgG was demonstrated to be higher following their incorporation into liposomes, especially sonicated liposomes, suggesting that liposomes have protected IgG during nebulisation.

Contrary to medical nebulisers, nasal sprays did not affect the physical stability or morphology of liposomes, or the integrity of IgG. Hence the use of nasal sprays for liposome delivery proved to have a great potential.

In conclusion, the results from this study have clearly demonstrated that the proliposome technology can be successfully employed to incorporate IgG. The findings further demonstrated the feasibility of using proliposomes in respiratory tract delivery, particularly using nasal devices.

The Scope For Future Studies

Findings in this study present an important rationale for the commencement of experiments, and future work in this area could involve improving liposome stability to nebulisation, possibly by optimising liposome formulation or nebuliser design (for instance, collaboration with the manufacturers of nebulisers to reduce the shear stress that nebulisers generate on liposomes). This can perhaps be achieved by reducing the frequency of vibrations. Also, alternatively other devices such as soft mist inhalers may be investigated.

Furthermore, using the ethanol-based proliposome technology, the study of the thermal behaviour of IgG-liposomes with and without the mucoadhesive agents, chitosan and alginate, may comprise a part of future investigations.

The promise drawn by nasal sprays in preserving the physical stability of liposomes as well as the activity of IgG warrants further investigations. For instance, different designs of nasal spray pumps and devices, including the novel nasal spray pump EquadelTM (Valois Inc., France) could be investigated.

Further characterisation results may also be carried out using laser-based spray pattern and plume geometry measurement instrumentation. Also, the use of

impactors and nasal cast models are important in order to support the present findings regarding aerosol and spray characterisation.

Finally, this project could be extended to involve more *in vitro* studies using cell cultures and *in vivo* studies using animals. A correlation between the *in vivo* and *in vitro* will be established in order to enhance the reliability of the *in vitro* studies.

CHAPTER 8

REFERENCES

- Abdelrahim MEA (2009) Relative bioavailability of terbutaline to the lung following inhalation using different methods, in *Institute of Pharmaceutical Innovation, School of Pharmacy*, University of Bradford, Bradford, pp:38-50.
- Adjei A and Gupta P (1994) Pulmonary delivery of therapeutic peptides and proteins. *Journal of Controlled Release* **29**:361-373.
- Ahn B-N, Kim S-K and Shim C-K (1995a) Preparation and evaluation of proliposomes containing propranolol hydrochloride. *Journal of Microencapsulation* **12**:363-375.
- Ahn B-N, Kim S-K and Shim C-K (1995b) Proliposomes as an intranasal dosage form for the sustained delivery of propranolol. *Journal of Controlled Release* **34**:203-210.
- Albasarah YY, Somavarapu S, Stapleton P and Taylor KM (2010) Chitosan-coated antifungal formulations for nebulisation. *Journal of Pharmacy and Pharmacology* **62**:821-828.
- Allen TM (1998) Liposomal drug formulations. Rationale for development and what we can expect for the future. *Drugs* **56**:747-756.
- Allen TM and Chonn A (1987) Large unilamellar liposomes with low uptake into the reticuloendothelial system. *FEBS Letters* **223**:42-46.
- Allen TM and Everest JM (1983) Effect of liposome size and drug release properties on pharmacokinetics of encapsulated drug in rats. *Journal of Pharmacology and Experimental Therapeutics* **226**:539-544.
- Alpar HO, Bowen JC and Brown MRW (1992) Effectiveness of liposomes as adjuvants of orally and nasally administered tetanus toxoid. *International Journal of Pharmaceutics* **88**:335-344.
- Alsarra IA, Hamed AY and Alanazi FK (2008) Acyclovir liposomes for intranasal systemic delivery: Development and pharmacokinetics evaluation. *Drug Delivery* **15**:313-321.
- Alves GP and Santana MHA (2004) Phospholipid dry powders produced by spray drying processing: structural, thermodynamic and physical properties. *Powder Technology* **145**:139-148.
- Amzel LM and Poljak RJ (1979) Three-dimensional structure of immunoglobulins. *Annual Review of Biochemistry* **48**:961-997.
- Anabousi S, Kleemann E, Bakowsky U, Kissel T, Schmehl T, Gessler T, Seeger W, Lehr CM and Ehrhardt C (2006) Effect of PEGylation on the stability of liposomes during nebulisation and in lung surfactant. *Journal Of Nanoscience And Nanotechnology* **6**:3010-3016.
- Anderson PJ (2005) History of aerosol therapy: liquid nebulization to MDIs to DPIs. *Respiratory Care* **50**:1139-1150.
- Arora P, Sharma S and Garg S (2002) Permeability issues in nasal drug delivery. *Drug Discovery Today* **7**:967-975.
- Arumugam K, Subramanian GS, Mallayasamy SR, Averineni RK, Reddy MS and Udupa N (2008) A study of rivastigmine liposomes for delivery into the brain through intranasal route. *Acta Pharmaceutica* **58**:287-297.

- Aulton ME (2007) *Pharmaceutics: The Design and manufacture of medicines*. Churchill Livingstone, Edinburgh, UK, pp:540-563.
- Aurora J (2002) Development of Nasal Delivery Systems: A Review. *Drug Development and Delivery* **2**:70-73.
- Banga AK and Chien YW (1988) Systemic delivery of therapeutic peptides and proteins. *International Journal of Pharmaceutics* **48**:15-50.
- Bangham AD, Standish MM and Watkins JC (1965) Diffusion of univalent ions across the lamellae of swollen phospholipids. *Journal of Molecular Biology* **13**:227-238.
- Barreras F, Amaveda H and Lozano A (2002) Transient high-frequency ultrasonic water atomization. *Experiments in Fluids* **33**:405-413.
- Basu SC and Basu M (2002) *Liposome Methods and Protocols*, Humana Press, Totowa, New Jersey, pp:1-17.
- Behera T, Swain P and Sahoo SK (2011) Antigen in chitosan coated liposomes enhances immune responses through parenteral immunization. *International Immunopharmacology* **11**:907-914.
- Betageri GV (1993) Liposomal encapsulation and stability of dideoxyinosine triphosphate. *Drug Development and Industrial Pharmacy* **19**:531-539.
- Betageri GV and Yatvin MB (2002) Proliposomes for oral drug administration. *Cellular & Molecular Biology Letters* **7**:278.
- Bi R and Zhang N (2007) Liposomes as a Carrier for Pulmonary Delivery of Peptides and Proteins. *Journal of Biomedical Nanotechnology* **3**:332-341.
- Bisgaard H, O'Callaghan C and Smaldone GC (2001) *Drug Delivery to the Lung*, Taylor & Francis, New York, pp:1-21.
- Boguslaskii Y and Eknadiosyants O (1969) Physical mechanism of the acoustic atomization of a liquid. *Soviet Physics - Acoustics* **15**:14-21.
- Born J, Lange T, Kern W, McGregor GP, Bickel U and Fehm HL (2002) Sniffing neuropeptides: a transnasal approach to the human brain. *Nature Neuroscience* **5**:514-516.
- Brayden DJ (2003) Controlled release technologies for drug delivery. *Drug Discovery Today* **8**:976-978.
- Breedveld FC (2000) Therapeutic monoclonal antibodies. *The Lancet* **355**:735-740.
- Brgles M, Jurasin D, Sikiric MD, Frkanec R and Tomasic J (2008) Entrapment of ovalbumin into liposomes--factors affecting entrapment efficiency, liposome size, and zeta potential. *Journal of Liposome Research* **18**:235-248.
- Bridges PA and Taylor KM (2000) An investigation of some of the factors influencing the jet nebulisation of liposomes. *International Journal of Pharmaceutics* **204**:69-79.
- Bridges PA and Taylor KMG (1998) Nebulisers for the generation of liposomal aerosols. *International Journal of Pharmaceutics* **173**:117-125.

- Bridges PA and Taylor KMG (2001) The effects of freeze-drying on the stability of liposomes to jet nebulization. *Journal of Pharmacy and Pharmacology* **53**:393-398.
- Buijs J, Norde W and Lichtenbelt JWT (1996) Changes in the Secondary Structure of Adsorbed IgG and F(ab')₂ Studied by FTIR Spectroscopy. *Langmuir* **12**:1605-1613.
- CDER (2002) Guidance for Industry: Nasal Spray and Inhalation Solution, Suspension, and Spray Drug Products. Chemistry, Manufacturing, and Controls Documentation., in *US Department of Health and Human Services, Food and Drug Administration*, pp:1-43.
- CDER (2003) Guidance for Industry: Bio-availability and Bioequivalence Studies for Nasal Aerosols and Nasal Sprays for Local Action., in *US Department of Health and Human Services, Food and Drug Administration*, pp:1-25.
- Chasin L (2010) Introduction to molecular and cellular biology (Lecture 3), University of columbia, pp:1-10.
- Chen A, Haddad D and Wang R (2009) Analysis of Chitosan-Alginate Bone Scaffolds. *Rutgers University, New Jersey Governor's School of Engineering & Technology*, pp:1-8.
- Cheng YS, Holmes TD, Gao J, Guilmette RA, Li S, Surakitbanharn Y and Rowlings C (2001) Characterization of nasal spray pumps and deposition pattern in a replica of the human nasal airway. *Journal of aerosol medicine : The Official Journal of The International Society for Aerosols In Medicine* **14**:267-280.
- Chien YW, Su KSE and Chang SF (1989) *Nasal Systemic Drug Delivery*, M. Dekker, New York, pp:1-9.
- Chougule M, Padhi B and Misra A (2008) Development of spray dried liposomal dry powder inhaler of dapsone. *AAPS PharmSciTech* **9**:47-53.
- Chougule MB, Padhi BK, Jinturkar KA and Misra A (2007) Development of dry powder inhalers. *Recent Patents on Drug Delivery & Formulation* **1**:11-21.
- Chrystyn H (2007) The Diskus™: a review of its position among dry powder inhaler devices. *International Journal of Clinical Practice* **61**:1022-1036.
- Clark AR (1995) The use of laser diffraction for the evaluation of the aerosol clouds generated by medical nebulizers. *International Journal of Pharmaceutics* **115**:69-78.
- Clay MM, Pavia D, Newman SP, Lennard-Jones T and Clarke SW (1983) Assessment of jet nebulisers for lung aerosol therapy. *The Lancet* **2**:592-594.
- Cockcroft DW, Hurst TS and Gore BP (1989) Importance of evaporative water losses during standardized nebulized inhalation provocation tests. *Chest* **96**:505-508.
- Colletier JP, Chaize B, Winterhalter M and Fournier D (2002) Protein encapsulation in liposomes: efficiency depends on interactions between protein and phospholipid bilayer. *BMC Biotechnology* **2**:1-8.
- Conley J, Yang H, Wilson T, Blasetti K, Di Ninno V, Schnell G and Wong JP (1997) Aerosol delivery of liposome-encapsulated ciprofloxacin: aerosol characterization and efficacy against *Francisella tularensis* infection in mice. *Antimicrobial Agents and Chemotherapy* **41**:1288-1292.

- Costantino HR, Illum L, Brandt G, Johnson PH and Quay SC (2007) Intranasal delivery: Physicochemical and therapeutic aspects. *International Journal of Pharmaceutics* **337**:1-24.
- Crommelin DJA and Sindelar RD (1997) *Pharmaceutical Biotechnology: An Introduction for Pharmacists and Pharmaceutical Scientists*, Harwood Academic Publishers, pp:25-33.
- Crompton GK (2004) How to achieve good compliance with inhaled asthma therapy. *Respiratory Medicine* **98**:S35-S40.
- Daley-Yates PT and Baker RC (2001) Systemic bioavailability of fluticasone propionate administered as nasal drops and aqueous nasal spray formulations. *British Journal of Clinical Pharmacology* **51**:103-105.
- Davis S (1999a) Delivery of peptide and non-peptide drugs through the respiratory tract. *Pharmaceutical Science and Technology Today* **2**:450-456.
- Davis SS (1999b) Delivery of peptide and non-peptide drugs through the respiratory tract. *Pharmaceutical Science & Technology Today* **2**:450-456.
- Dayal P, Shaik MS and Singh M (2004) Evaluation of different parameters that affect droplet-size distribution from nasal sprays using the Malvern Spraytec. *Journal of Pharmaceutical Sciences* **93**:1725-1742.
- Dellamary L, Smith DJ, Bloom A, Bot S, Guo GR, Deshmuk H, Costello M and Bot A (2004) Rational design of solid aerosols for immunoglobulin delivery by modulation of aerodynamic and release characteristics. *Journal of Controlled Release* **95**:489-500.
- Dennis JH, Stenton SC, Beach JR, Avery AJ, Walters EH and Hendrick DJ (1990) Jet and ultrasonic nebuliser output: use of a new method for direct measurement of aerosol output. *Thorax* **45**:728-732.
- Desai TR, Hancock RE and Finlay WH (2002) A facile method of delivery of liposomes by nebulization. *Journal of Controlled Release* **84**:69-78.
- Devillier P, Grassin-Delyle S, Naline E, Buenestado A, Blouquit-Laye S and Advenier C (2010) Intranasal delivery of systemic drugs: a new route for opioid drugs. *Therapie* **65**:475-481.
- Dhand R (2002) Nebulizers that use a vibrating mesh or plate with multiple apertures to generate aerosol. *Respiratory Care* **47**:1406-1416.
- Dhand R (2003) New nebuliser technology – aerosol generation by using a vibrating mesh or plate with multiple apertures, Business briefing: Long-term healthcare strategies, pp:1-4.
- Ding W-X, Qi X-R, Fu Q and Piao H-S (2007) Pharmacokinetics and pharmacodynamics of sterylglucoside-modified liposomes for levonorgestrel delivery via nasal route. *Drug Delivery* **14**:101-104.
- Dini L, Di Giulio A, Pavan A, Ravagnan G and Mossa G (1991) Size and stability of dipalmitoylphosphatidylcholine/cholesterol unilamellar vesicles are affected by interaction with proteins. *Biochimica et Biophysica Acta* **1062**:108-112.

- Dolovich MB and Dhand R (2011) Aerosol drug delivery: developments in device design and clinical use. *The Lancet* **377**:1032-1045.
- Dondeti P, Zia H and Needham TE (1996) Bioadhesive and formulation parameters affecting nasal absorption. *International Journal of Pharmaceutics* **127**:115-133.
- Douglas J, Leslie M, Crompton G and Grant I (1986) A comparative study of two doses of salbutamol nebulized at 4 and 8 litres per minute in patients with chronic asthma. *British Journal of Diseases of the Chest* **80**:55-58.
- Dreffier C, Ramise F and Dubernet C (2003) Pulmonary administration of IgG loaded liposomes for passive immunoprophylaxy. *International Journal of Pharmaceutics* **254**:43-47.
- Du Plessis J, Ramachandran C, Weiner N and Müller DG (1996) The influence of lipid composition and lamellarity of liposomes on the physical stability of liposomes upon storage. *International Journal of Pharmaceutics* **127**:273-278.
- Dufour P, Vuilleumard JC, Laloy E and Simard RE (1996) Characterization of enzyme immobilization in liposomes prepared from proliposomes. *Journal of Microencapsulation* **13**:185-194.
- Düzgüneş N (2005) *Liposomes*, In Methods in Enzymology, Volume 391, Part E, Düzgüneş N, Elsevier Academic Press, pp:71-97.
- Edwards DA, Ben-Jebria A and Langer R (1998) Recent advances in pulmonary drug delivery using large, porous inhaled particles. *Journal of Applied Physiology* **85**:379-385.
- Edwards KA and Baeumner AJ (2006) Analysis of liposomes. *Talanta* **68**:1432-1441.
- Elhissi A, Gill H, Ahmed W and Taylor K (2011a) Vibrating-mesh nebulization of liposomes generated using an ethanol-based proliposome technology. *Journal of Liposome Research* **21**:173-180.
- Elhissi A, Taylor K and Ahmed W (2011b) *Nanocarrier Systems for Drug Delivery for the Treatment of Asthma: Liposomes as Model Carrier Systems*, LAP Lambert Academic Publishing, Berlin, pp:60-97.
- Elhissi AM, Faizi M, Naji WF, Gill HS and Taylor KM (2007) Physical stability and aerosol properties of liposomes delivered using an air-jet nebulizer and a novel micropump device with large mesh apertures. *International Journal of Pharmaceutics* **334**:62-70.
- Elhissi AM, Karnam KK, Danesh-Azari MR, Gill HS and Taylor KM (2006a) Formulations generated from ethanol-based proliposomes for delivery via medical nebulizers. *The Journal of Pharmacy and Pharmacology* **58**:887-894.
- Elhissi AM, O'Neill MA, Roberts SA and Taylor KM (2006b) A calorimetric study of dimyristoylphosphatidylcholine phase transitions and steroid-liposome interactions for liposomes prepared by thin film and proliposome methods. *International Journal of Pharmaceutics* **320**:124-130.
- Elhissi AMA (2005) Proliposome formulations for delivery via medical nebulisers, in *School of Pharmacy p 267*, University of London, London, pp:30-69.

- Elhissi AMA and Taylor KMG (2005) Delivery of liposomes generated from proliposomes using air-jet, ultrasonic, and vibrating-mesh nebulisers. *Journal of Drug Delivery Science and Technology* **15**:261-265.
- Fangmark I and Carpin JC (1996) Protein nebulization. *Journal of Aerosol Science* **27**, Supplement 1:S231-S232.
- Fangmark I and Carpin JC (1998) Stability of urease during aerosolization: The effect of operating conditions. *Journal of Aerosol Science* **29**:279-288.
- Farina DJ (2010) Regulatory aspects of nasal and pulmonary spray drug products (chapter 10) in *Handbook of Non-Invasive Drug Delivery Systems* (Vitthal SK ed) William Andrew Publishing, Boston, pp:247-290.
- Farr SJ, Kellaway IW and Carman-Meakin B (1987) Assessing the potential of aerosol-generated liposomes from pressurised pack formulations. *Journal of Controlled Release* **5**:119-127.
- Fasman GD (1996) *Circular Dichroism and the Conformational Analysis of Biomolecules*, Plenum Press, New York, pp:25-69.
- Felnerova D, Viret J-Fo, Glvock R and Moser C (2004) Liposomes and virosomes as delivery systems for antigens, nucleic acids and drugs. *Current Opinion in Biotechnology* **15**:518-529.
- Ferron GA, Kerrebijn KF and Weber J (1976) Properties of aerosols produced with three nebulizers. *The American Review Respiratory Disease* **114**:899-908.
- Finlay WH and Wong JP (1998) Regional lung deposition of nebulized liposome-encapsulated ciprofloxacin. *International Journal of Pharmaceutics* **167**:121-127.
- Finley TN, Pratt SA, Ladman AJ, Brewer L and McKay MB (1968) Morphological and lipid analysis of the alveolar lining material in dog lung. *Journal of Lipid Research* **9**:357-365.
- Flament MP, Leterme P and Gayot A (1999) Influence of the technological parameters of ultrasonic nebulisation on the nebulisation quality of α 1 protease inhibitor (α 1PI). *International Journal of Pharmaceutics* **189**:197-204.
- Foo MY (2007) Deposition pattern of nasal sprays in the human nasal airway interactions among formulation, device, anatomy and administration techniques, PhD dissertation, University of Iowa, Ann Arbor, MI, pp:48-72.
- Foo MY, Cheng Y-S, Su W-C and Donovan MD (2007) The influence of spray properties on intranasal deposition. *Journal of Aerosol Medicine-Deposition Clearance and Effects in The Lung* **20**:495-508.
- Galovic Rengel R, Barisic K, Pavelic Z, Zanic Grubisic T, Cepelak I and Filipovic-Grcic J (2002) High efficiency entrapment of superoxide dismutase into mucoadhesive chitosan-coated liposomes. *European Journal Of Pharmaceutical Sciences* **15**:441-448.
- Garcia-Santana MA, Duconge J, Sarmiento ME, Lanio-Ruiz ME, Becquer MA, Izquierdo L and Acosta-Dominguez A (2006) Biodistribution of liposome-entrapped human gamma-globulin. *Biopharmaceutics and Drug Disposition* **27**:275-283.

- Gardner DE, Crapo JD and McClellan RO (1993) *Toxicology of the Lung*, Raven Press, New York, pp:83-107.
- Ghazanfari T, Elhissi AM, Ding Z and Taylor KM (2007) The influence of fluid physicochemical properties on vibrating-mesh nebulization. *International Journal of Pharmaceutics* **339**:103-111.
- Ghosh TK and Jasti BR (2005) *Theory and Practice of Contemporary Pharmaceutics*, CRC Press, New York, pp:479-525.
- Gibson M (2001) *Pharmaceutical Preformulation and Formulation: A Practical Guide from Candidate Drug Selection to Commercial Dosage Form*, Taylor & Francis, pp:342-374.
- Gilbert BÄ, Knight C, Alvarez FÄ, Waldrep JÄ, Rodarte JÄ, Knight V and Eschenbacher WÄ (1997) Tolerance of Volunteers to Cyclosporine A-dilauroylphosphatidylcholine Liposome Aerosol. *American Journal of Respiratory and Critical Care Medicine* **156**:1789-1793.
- Gomez-Hens A and Fernandez-Romero J (2006) Analytical methods for the control of liposomal delivery systems. *TrAC Trends in Analytical Chemistry* **25**:167-178.
- Graf P, HallÉN H and Juto JE (1995) Benzalkonium chloride in a decongestant nasal spray aggravates rhinitis medicamentosa in healthy volunteers. *Clinical & Experimental Allergy* **25**:395-400.
- Greenfield NJ (2006) Using circular dichroism spectra to estimate protein secondary structure. *Nature Protocols* **1**:2876-2890.
- Gregoriadis G (1988) *Liposomes as drug carriers: recent trends and progress*, John and Sons, UK, pp:3-19.
- Gregoriadis G (1993) *Liposome technology: Liposome preparation and related techniques*, volume 1, Informa Health Care, pp:67-82.
- Guo C and Doub WH (2006) The influence of actuation parameters on *in vitro* testing of nasal spray products. *Journal Of Pharmaceutical Sciences* **95**:2029-2040.
- Guo J, Ping Q, Jiang G, Huang L and Tong Y (2003) Chitosan-coated liposomes: characterization and interaction with leuprolide. *International Journal of Pharmaceutics* **260**:167-173.
- Gupta V, Barupal AK and Ramteke S (2008) Formulation development and *in vitro* characterization of proliposomes for topical Delivery of aceclofenac. *Indian Journal of Pharmaceutical Sciences* **70**:768-775.
- Hardy JG, Lee SW and Wilson CG (1985) Intranasal drug delivery by spray and drops. *Journal of Pharmacy and Pharmacology* **37**:294-297.
- Harris AS, Nilsson IM, G.-Wagner Z and Alkner U (1986) Intranasal administration of peptides: Nasal deposition, biological response, and absorption of desmopressin. *Journal of Pharmaceutical Sciences* **75**:1085-1088.
- Harris AS, Svensson E, Wagner ZG, Lethagen S and Nilsson IM (1988) Effect of viscosity on particle size, deposition, and clearance of nasal delivery systems containing desmopressin. *Journal of Pharmaceutical Sciences* **77**:405-408.

- Harrison LI (2000) Commentary on the FDA draft guidance for bioequivalence studies for nasal aerosols and nasal sprays for local action: an industry view. *Journal of Clinical Pharmacology* **40**:701-707.
- Hernandez-Caselles T, Villalain J and Gomez-Fernandez JC (1990) Stability of liposomes on long term storage. *The Journal Of Pharmacy And Pharmacology* **42**:397-400.
- Hernández VA and Scholz F (2008) The Electrochemistry of Liposomes. *Israel Journal of Chemistry* **48**:169-184.
- Hess D, MacIbtyre N, Mishoe S, Galvin W and Adams A (2012) *Respiratory Care: Principles and practice*, Jones & Bartlett Publishers, pp:304-336.
- Hess DR (2000) Nebulizers: principles and performance. *Respiratory Care* **45**:609-622.
- Heyder J (1982) Particle transport onto human airway surfaces. *European Journal of Respiratory Diseases Supplement* **119**:29-50.
- Heyder J, Armbruster L, Gebhart J, Grein E and Stahlhofen W (1975) Total deposition of aerosol particles in the human respiratory tract for nose and mouth breathing. *Journal of Aerosol Science* **6**:311-328.
- Heyder J, Gebhart J, Rudolf G, Schiller CF and Stahlhofen W (1986) Deposition of particles in the human respiratory tract in the size range 0.005-155 μm . *Journal of Aerosol Science* **17**:811-825.
- Huang W-H, Yang Z-J, Wu H, Wong Y-F, Zhao Z-Z and Liu L (2010) Development of liposomal salbutamol sulfate dry powder inhaler formulation. *Biological And Pharmaceutical Bulletin* **33**:512-517.
- Huang YY and Wang CH (2006) Pulmonary delivery of insulin by liposomal carriers. *Journal of Controlled Release* **113**:9-14.
- Hussain AA (1998) Intranasal drug delivery. *Advanced Drug Delivery Reviews* **29**:39-49.
- Hwang B-Y, Jung B-H, Chung S-J, Lee M-H and Chang-Koo S (1997) *In vitro* skin permeation of nicotine from proliposomes. *Journal of Controlled Release* **49**:177-184.
- Illum L (2003) Nasal drug delivery--possibilities, problems and solutions. *Journal of Controlled Release* **87**:187-198.
- Illum L (2006) Nasal clearance in health and disease. *Journal of Aerosol Medicine-Deposition Clearance and Effects In The Lung* **19**:92-99.
- Inthavong K, Ge Q, Se CMK, Yang W and Tu JY (2011) Simulation of sprayed particle deposition in a human nasal cavity including a nasal spray device. *Journal of Aerosol Science* **42**:100-113.
- Ip AY, Arakawa T, Silvers H, Ransone CM and Niven RW (1995) Stability of recombinant consensus interferon to air-jet and ultrasonic nebulization. *Journal of Pharmaceutical Sciences* **84**:1210-1214.
- Ishikawa H, Shimoda Y and Matsumoto K (2004) Preparation of liposomal microcapsules by proliposome method with soybean lecithin. *Journal of the Faculty of Agriculture Kyushu University* **49**:119-127.

- Jain AK, Chalasani KB, Khar RK, Ahmed FJ and Diwan PV (2007) Muco-adhesive multivesicular liposomes as an effective carrier for transmucosal insulin delivery. *Journal of Drug Targeting* **15**:417-427.
- Jesorka A and Orwar O (2008) Liposomes: technologies and analytical applications. *Annual Review of Analytical Chemistry* **1**:801-832.
- Jindal SK, SK Jindal MD and Shankar P (2011) *Textbook of Pulmonary and Critical Care Medicine*, Jaypee Brothers, Medical Publishers, pp:9-18.
- Joki S, Saano V, Nuutinen J, Virta P, Karttunen P, Silvasti M and Toskala E (1996) Effects of some preservative agents on rat and guinea pig tracheal and human nasal ciliary beat frequency. *American Journal of Rhinology* **10**:181-186.
- Jorgensen L and Nielson HM (2010) *Delivery Technologies for Biopharmaceuticals: Peptides, Proteins, Nucleic Acids and Vaccines*, John Wiley & Sons, pp:227-241.
- Joshi MR and Misra A (2001) Liposomal budesonide for dry powder inhaler: preparation and stabilization. *AAPS Pharmaceutical Science and Technology* **2**:44-53.
- Jung BH, Chung BC, Chung S-J, Lee M-H and Shim C-K (2000) Prolonged delivery of nicotine in rats via nasal administration of proliposomes. *Journal of Controlled Release* **66**:73-79.
- Kaiser HB, Findlay SR, Georgitis JW, Grossman J, Ratner PH, Tinkelman DG, Roszko P, Zegarelli E and Wood CC (1995) Long-term treatment of perennial allergic rhinitis with ipratropium bromide nasal spray 0.06%. *Journal of Allergy and Clinical Immunology* **95**:1128-1132.
- Kanaoka E, Nagata S and Hirano K (1999) Stabilization of aerosolized IFN- γ by liposomes. *International Journal of Pharmaceutics* **188**:165-172.
- Karn PR, Vanic Z, Pepic I and Skalko-Basnet N (2011) Mucoadhesive liposomal delivery systems: the choice of coating material. *Drug Development And Industrial Pharmacy* **37**:482-488.
- Katare OP, Vyas SP and Dixit VK (1990) Effervescent granule based proliposomes of ibuprofen. *Journal of Microencapsulation* **7**:455-462.
- Katare OP, Vyas SP and Dixit VK (1995) Enhanced *in vivo* performance of liposomal indomethacin derived from effervescent granule based proliposomes. *Journal of Microencapsulation* **12**:487-493.
- Kato Y, Hosokawa T, Hayakawa E and Ito K (1993) Influence of liposomes on tryptic digestion of insulin *Biological & Pharmaceutical Bulletin* **16**:740-744.
- Kellaway IW and Farr SJ (1990) Liposomes as drug delivery systems to the lung. *Advanced Drug Delivery Reviews* **5**:149-161.
- Kelly SM, Jess TJ and Price NC (2005) How to study proteins by circular dichroism. *Biochimica et Biophysica Acta (BBA) - Proteins & Amp; Proteomics* **1751**:119-139.
- Khanna C, Anderson PM, Hasz DE, Katsanis E, Neville M and Klausner JS (1997) Interleukin-2 liposome inhalation therapy is safe and effective for dogs with spontaneous pulmonary metastases. *Cancer* **79**:1409-1421.

- Khatri L, Taylor KM, Craig DQ and Palin K (2001) An assessment of jet and ultrasonic nebulisers for the delivery of lactate dehydrogenase solutions. *International Journal of Pharmaceutics* **227**:121-131.
- Khatri L, Taylor KMG, Craig DQM and Palin K (2004) The stability of liposome entrapped lactate dehydrogenase to nebulisation. *Journal of Pharmacy and Pharmacology* **56**:S41-S41.
- Kippax P (2005) Appraisal of the laser diffraction particle-sizing technique. *Pharmaceutical Technology*, pp:88-96.
- Kippax P and Fracassi J (2003) Particle size characterisation in nasal sprays and aerosols, Lab Plus International, pp:1-2.
- Kippax P, Huck D, Levoguer C, Virden A and Suman J (2011) Characterizing A Nasal Spray Formulation From Droplet To API Particle Size. *Pharmaceutical Technology Europe* **23**:1-6.
- Kippax P, Suman J, Virden A and Williams G (2010) Effects of viscosity, pump mechanism and nozzle geometry on nasal spray droplet size. *ILASS – Europe 2010*, pp:1-6.
- Kirby C and Gregoriadis G (1999) Liposomes, in *Encyclopedia of Controlled Drug Delivery* (Mathiowitz E ed) John Wiley & Sons, New York, pp:461–492.
- Kleemann E, Schmehl T, Gessler T, Bakowsky U, Kissel T and Seeger W (2007) Iloprost-containing liposomes for aerosol application in pulmonary arterial hypertension: formulation aspects and stability. *Pharmaceutical Research* **24**:277-287.
- Kleinstreuer C, Zhang Z and Donohue JF (2008) Targeted drug-aerosol delivery in the human respiratory system. *Annual Review of Biomedical Engineering*, pp:195-220.
- Koch M (2003) The growing market for nasal drug delivery. *Pharmatech*, pp:1-3.
- Korsholm KS, Agger EM, Foged C, Christensen D, Dietrich J, Andersen CS, Geisler C and Andersen P (2007) The adjuvant mechanism of cationic dimethyldioctadecylammonium liposomes. *Immunology* **121**:216-226.
- Kradjan WA and Lakshminarayan S (1985) Efficiency of air compressor-driven nebulizers. *Chest* **87**:512-516.
- Kublik H and Vidgren MT (1998) Nasal delivery systems and their effect on deposition and absorption. *Advanced Drug Delivery Reviews* **29**:157-177.
- Kushwaha SKS, Keshari RK and Rai AK (2011) Advances in nasal trans-mucosal drug delivery. *Journal of Applied Pharmaceutical Science* **1**:21-28.
- Labiris NR and Dolovich MB (2003) Pulmonary drug delivery. Part I: physiological factors affecting therapeutic effectiveness of aerosolized medications. *British Journal of Clinical Pharmacology* **56**:588-599.
- Lapinski MM, Castro-Forero A, Greiner AJ, Ofoli RY and Blanchard GJ (2007) Comparison of liposomes formed by sonication and extrusion: rotational and translational diffusion of an embedded chromophore. *Langmuir* **23**:11677-11683.
- Lasic DD, Joannic R, Keller BC, Frederik PM and Auvray L (2001) Spontaneous vesiculation. *Advances in Colloid and Interface Science* **89-90**:337-349.

- Law M (2000) Plant sterol and stanol margarines and health. *British Medical Journal* **320**:861-864.
- Law SL, Huang KJ, Chou VHY and Cherng JY (2001) Enhancement of nasal absorption of calcitonin loaded in liposomes. *Journal of Liposome Research* **11**:165-174.
- Lee HJ, Ahn B-N, Paik WH, Shim C-K and Lee MG (1996) Inverse targeting of reticuloendothelial system-rich organs after intravenous administration of adriamycin-loaded neutral proliposomes containing poloxamer 407 to rats. *International Journal of Pharmaceutics* **131**:91-96.
- Lee MK, Choi L, Kim MH and Kim CK (1999) Pharmacokinetics and organ distribution of cyclosporin A incorporated in liposomes and mixed micelles. *International Journal of Pharmaceutics* **191**:87-93.
- Leung KKM, Bridges PA and Taylor KMG (1996) The stability of liposomes to ultrasonic nebulisation. *International Journal of Pharmaceutics* **145**:95-102.
- Litzinger DC, Buiting AM, van Rooijen N and Huang L (1994) Effect of liposome size on the circulation time and intraorgan distribution of amphipathic poly(ethylene glycol)-containing liposomes. *Biochimica et Biophysica Acta* **1190**:99-107.
- Loffert DT, Ikle D and Nelson HS (1994) A comparison of commercial jet nebulizers. *Chest* **106**:1788-1792.
- Maggi L, Bruni R and Conte U (1999) Influence of the moisture on the performance of a new dry powder inhaler. *International Journal of Pharmaceutics* **177**:83-91.
- Maherani B, Arab-tehrany E, Kheiriloom A, Reshetov V, Stebe MJ and Linder M (2012) Optimization and characterization of liposome formulation by mixture design. *The Analyst* **137**:773-786.
- Maillet A, Congy-Jolivet N, Le Guellec S, Vecellio L, Hamard S, Courty Y, Courtois A, Gauthier F, Diot P, Thibault G, Lemarie E and Heuze-Vourc'h N (2008a) Aerodynamical, immunological and pharmacological properties of the anticancer antibody cetuximab following nebulization. *Pharmaceutical Research*, **25**:1318-1326.
- Maillet A, Congy-Jolivet N, Le Guellec S, Vecellio L, Hamard S, Courty Y, Courtois A, Gauthier F, Diot P, Thibault G, Lemarie E and Heuze-Vourc'h N (2008b) Aerodynamical, immunological and pharmacological properties of the anticancer antibody cetuximab following nebulization. *Pharmaceutical Research* **25**:1318-1326.
- Makidon PE, Nigavekar SS, Bielinska AU, Mank N, Shetty AM, Suman J, Knowlton J, Myc A, Rook T and Baker JR, Jr. (2010) Characterization of stability and nasal delivery systems for immunization with nanoemulsion-based vaccines. *Journal Of Aerosol Medicine And Pulmonary Drug Delivery* **23**:77-89.
- Malmsten M (1995) Ellipsometry studies of the effects of surface hydrophobicity on protein adsorption. *Colloids and Surfaces B: Biointerfaces* **3**:297-308.
- Malvern-Instruments (2004) Zetasizer Nano Series User Manual, www.malvern.com. {accessed on 14/06/2012}.

- Malvern-Instruments (2011) Laser diffraction particle sizing, www.malvern.com. {accessed on 14/06/2012}.
- Marjan JMJ and Allen TM (1996) Long circulating liposomes: past, present and future. *Biotechnology Advances* **14**:151-175.
- Martin SR and Schilstra MJ (2008) Circular Dichroism and Its Application to the Study of Biomolecules, in *Methods in Cell Biology* (Dr. John JC and Dr. H. William Detrich, III eds), Academic Press, pp:263-293.
- Marx D and Birkhoff M (2011) Multi-Dose Container for Nasal and Ophthalmic Drugs: A Preservative Free Future?, In *Drug Development - A Case Study Based Insight Into Modern Strategies* (Rundfeldt C ed), Intech, pp:509-523.
- Mc Callion ONM, Taylor KMG, Thomas M and Taylor AJ (1996a) The influence of surface tension on aerosols produced by medical nebulisers. *International Journal of Pharmaceutics* **129**:123-136.
- Mc Callion ONM, Taylor KMG, Thomas M and Taylor AJ (1996b) Nebulisation of monodisperse latex sphere suspensions in air jet and ultrasonic nebulisers. *International Journal of Pharmaceutics* **133**:203-214.
- McCallion ONM, Taylor KMG, Bridges PA, Thomas M and Taylor AJ (1996a) Jet nebulisers for pulmonary drug delivery. *International Journal of Pharmaceutics* **130**:1-11.
- McCallion ONM, Taylor KMG, Thomas M and Taylor AJ (1995) Nebulization of Fluids of Different Physicochemical Properties with Air-Jet and Ultrasonic Nebulizers. *Pharmaceutical Research* **12**:1682-1688.
- McCallion ONM, Taylor KMG, Thomas M and Taylor AJ (1996b) Nebulisation of monodisperse latex sphere suspensions in air jet and ultrasonic nebulisers. *International Journal of Pharmaceutics* **133**:203-214.
- McCullough KC and Summerfield A (2009) Targeting the porcine immune system--particulate vaccines in the 21st century. *Developmental and Comparative Immunology* **33**:394-409.
- McMartin C, Hutchinson LEF, Hyde R and Peters GE (1987) Analysis of structural requirements for the absorption of drugs and macromolecules from the nasal cavity. *Journal of Pharmaceutical Sciences* **76**:535-540.
- Mercer TT (1981) Production of therapeutic aerosols; principles and techniques. *Chest* **80**:813-818.
- Mercer TT, Goddard RF and Flores RL (1968) Output characteristics of three ultrasonic nebulizers. *Annals of Allergy, Asthma & Immunology* **26**:18-27.
- Mestecky, J., Moldoveanu, z., Michalek, M. S, Morrow, D. C, Compans, W. R, Schafer, P. D, Russell and W. M (1997) Current options for vaccine delivery systems by mucosal routes. *Journal of Controlled Release* **48**:243-257.
- Misra A, Ganesh S, Shahiwala A and Shah SP (2003) Drug delivery to the central nervous system: a review. *Journal of Pharmacy and Pharmaceutical Sciences* **6**:252-273.

- Mistry A, Stolnik S and Illum L (2009) Nanoparticles for direct nose-to-brain delivery of drugs. *International Journal of Pharmaceutics* **379**:146-157.
- Mitchell J, Nagel M, Wiersema K and Doyle C (2003) Aerodynamic particle size analysis of aerosols from pressurized metered-dose inhalers: Comparison of andersen 8-stage cascade impactor, next generation pharmaceutical impactor, and model 3321 aerodynamic particle sizer aerosol spectrometer. *AAPS, Pharmaceutical Science and Technology* **4**:425-433.
- Mitchell JP and Nagel MW (2004) Particle size analysis of aerosols from medicinal inhalers *KONA* **22**:32-64.
- Molina MJ and Rowland FS (1974) Stratospheric sink for chlorofluoromethanes: chlorine atom-catalysed destruction of ozone. *Nature* **249**:810-812.
- Morimoto K, Yamaguchi H, Iwakura Y, Miyazaki M, Nakatani E, Iwamoto T, Ohashi Y and Nakai Y (1991) Effects of proteolytic enzyme inhibitors on the nasal absorption of vasopressin and an analogue. *Pharmaceutical Research* **8**:1175-1179.
- Morlock M, Koll H, Winter G and Kissel T (1997) Microencapsulation of rh-erythropoietin, using biodegradable poly(d,l-lactide-co-glycolide): protein stability and the effects of stabilizing excipients. *European Journal of Pharmaceutics and Biopharmaceutics* **43**:29-36.
- Mozafari MR (2005) Liposomes: an overview of manufacturing techniques. *Cellular & Molecular Biology Letters* **10**:711-719.
- Muers MF (1997) Overview of nebuliser treatment. *Thorax* **52 Supplement 2**:S25-30.
- Muramatsu K, Maitani Y, Takayama K and Nagai T (1999) The relationship between the rigidity of the liposomal membrane and the absorption of insulin after nasal administration of liposomes modified with an enhancer containing insulin in rabbits. *Drug Development and Industrial Pharmacy* **25**:1099-1105.
- Mygind N and Dahl R (1998) Anatomy, physiology and function of the nasal cavities in health and disease. *Advanced Drug Delivery Reviews* **29**:3-12.
- Nastruzzi C (2005) *Lipospheres In Drug Targets And Delivery: Approaches, Methods, And Applications*, CRC Press, pp:91-103.
- Nerbrink O, Dahlback M and Hansson HC (1994) Why do medical nebulizers differ in their output and particle size characteristics? *Journal of aerosol medicine : the official journal of the International Society for Aerosols in Medicine* **7**:259-276.
- New RRC (1990) *Liposomes: a practical approach*, IRL Press at Oxford University Press, Oxford, pp:1-27.
- Newman S and Gee-Turner A (2005) The Omron MicroAir vibrating mesh technology nebuliser, a 21st century approach to inhalation therapy. *Journal of Applied Therapeutic Research* **5**:29-33.
- Newman SP (2005) Principles of metered-dose inhaler design. *Respiratory Care* **50**:1177-1190.
- Newman SP, Pitcairn GR and Dalby RN (2004) Drug delivery to the nasal cavity: *In vitro* and *in vivo* assessment. *Critical Reviews in Therapeutic Drug Carrier Systems* **21**:21-66.

- Ning MY, Guo YZ, Pan HZ, Yu HM and Gu ZW (2005) Preparation and evaluation of proliposomes containing clotrimazole. *Chemical & Pharmaceutical Bulletin (Tokyo)* **53**:620-624.
- Ninomiya A, Ogasawara K, Kajino K, Takada A and Kida H (2002) Intranasal administration of a synthetic peptide vaccine encapsulated in liposome together with an anti-CD40 antibody induces protective immunity against influenza A virus in mice. *Vaccine* **20**:3123-3129.
- Niven RW and Brain JD (1994) Some functional aspects of air-jet nebulizers. *International Journal of Pharmaceutics* **104**:73-85.
- Niven RW, Carvajal TM and Schreier H (1992) Nebulization of Liposomes. III. The Effects of Operating Conditions and Local Environment. *Pharmaceutical Research* **9**:515-520.
- Niven RW, Ip AY, Mittelman S, Prestrelski SJ and Arakawa T (1995) Some factors associated with the ultrasonic nebulization of proteins. *Pharmaceutical Research* **12**:53-59.
- Niven RW, Ip AY, Mittelman SD, Farrar C, Arakawa T and Prestrelski SJ (1994) Protein nebulization: I. Stability of lactate dehydrogenase and recombinant granulocyte-colony stimulating factor to air-jet nebulization. *International Journal of Pharmaceutics* **109**:17-26.
- Niven RW, Prestrelski SJ, Treuheit MJ, Ip AY and Arakawa T (1996) Protein nebulization II. Stabilization of G-CSF to air-jet nebulization and the role of protectants. *International Journal of Pharmaceutics* **127**:191-201.
- Niven RW and Schreier H (1990) Nebulization of Liposomes. I. Effects of Lipid Composition. *Pharmaceutical Research* **7**:1127-1133.
- Niven RW, Speer M and Schreier H (1991) Nebulization of Liposomes. II. The Effects of Size and Modeling of Solute Release Profiles. *Pharmaceutical Research* **8**:217-221.
- Noakes T (2002) Medical aerosol propellants. *Journal of Fluorine Chemistry* **118**:35-45.
- Norris A and Rowe-Jones J (2006) Infections and foreign bodies in the ear, nose and throat. *Surgery (Oxford)* **24**:299-303.
- O'Callaghan C and Barry PW (1997) The science of nebulised drug delivery. *Thorax* **52 Supplement 2**:S31-44.
- O'Callaghan C, Clarke AR and Milner AD (1989) Inaccurate calculation of drug output from nebulisers. *European Journal of Pediatrics* **148**:473-474.
- Oguchi K, Ikegami M, Jacobs H and Jobe A (1985) Clearance of large amounts of natural surfactants and liposomes of dipalmitoylphosphatidylcholine from the lungs of rabbits. *Experimental Lung Research* **9**:221-235.
- Park JM, Ahn BN, Yoon EJ, Lee MG, Shim CK and Kim CK (1994) The pharmacokinetics of methotrexate after intravenous administration of methotrexate-loaded proliposomes to rats. *Biopharmaceutics & Drug Disposition* **15**:391-407.
- Payne NI, Browning I and Hynes CA (1986a) Characterization of proliposomes. *Journal of Pharmaceutical Sciences* **75**:330-333.

- Payne NI, Timmins P, Ambrose CV, Ward MD and Ridgway F (1986b) Proliposomes: a novel solution to an old problem. *Journal of Pharmaceutical Sciences* **75**:325-329.
- Perrett S, Golding M and Williams WP (1991) A simple method for the preparation of liposomes for pharmaceutical applications: characterization of the liposomes. *Journal of Pharmacy and Pharmacology* **43**:154-161.
- Perugini P, Genta I, Pavanetto F, Conti B, Scalia S and Baruffini A (2000) Study on glycolic acid delivery by liposomes and microspheres. *International Journal of Pharmaceutics* **196**:51-61.
- Phalen RF and Phalen RN (2011) *Introduction to Air Pollution Science: A Public Health Perspective*, Jones & Bartlett Learning, Burlington, MA, pp: 43-60.
- Phetdee M, Polnok A and Viyoch J (2008) Development of chitosan-coated liposomes for sustained delivery of tamarind fruit pulp's extract to the skin. *International Journal of Cosmetic Science* **30**:285-295.
- Pierce scientific (2010) IgG easy-titre kit manual, pp:1-5.
- Pierce scientific (2011) BCA protein assay kit, pp:1-7.
- Pires A, Fortuna A, Alves G and Falcao A (2009) Intranasal drug delivery: how, why and what for? *Journal of Pharmacy and Pharmaceutical Sciences* **12**:288-311.
- Pisal DS, Kosloski MP and Balu-Iyer SV (2010) Delivery of therapeutic proteins. *Journal of Pharmaceutical Sciences* **99**:2557-2575.
- Presti FT, Pace RJ and Chan SI (1982) Cholesterol-phospholipid interaction in membranes. 2. Stoichiometry and molecular packing of cholesterol-rich domains. *Biochemistry* **21**:3831-3835.
- Pritchard J (2005) The future of metered-dose inhalers. *Pharmaceutical Technology Europe* **17**:27-28.
- Quraishi MS, Jones NS and Mason JDT (1997) The nasal delivery of drugs. *Clinical Otolaryngology & Allied Sciences* **22**:289-301.
- Rathbone MJ, Hadgraft J and Roberts MS (2003) *Modified-Release Drug Delivery Technology*, Marcel Dekker, pp:857-863.
- Rau JL, Ari A and Restrepo RD (2004) Performance comparison of nebulizer designs: constant-output, breath-enhanced, and dosimetric. *Respiratory Care* **49**:174-179.
- Reusch W (1999) Virtual Text of Organic Chemistry. www2.chemistry.msu.edu/faculty/reusch/VirtTxtJml/intro1.htm {accessed on 15/08/2012}.
- Riaz M (1995) Review article : stability and uses of liposomes. *Pakistan Journal of Pharmaceutical Sciences* **8**:69-79.
- Rogers JA, Betageri GV and Choi YW (1990) Solubilization of Liposomes by Weak Electrolyte Drugs. I. Propranolol. *Pharmaceutical Research* **7**:957-961.

- Rojanarat W, Changsan N, Tawithong E, Pinsuwan S, Chan H-K and Srichana T (2011) Isoniazid proliposome powders for inhalation—preparation, characterization and cell culture studies. *International Journal of Molecular Sciences* **12**:4414-4434.
- Rongen HAH, Bult A and van Bennekom WP (1997) Liposomes and immunoassays. *Journal of Immunological Methods* **204**:105-133.
- Rosada RS, de la Torre LG, Frantz FG, Trombone APF, Zarate-Blades CR, Fonseca DM, Souza PRM, Brandao IT, Masson AP, Soares EG, Ramos SG, Faccioli LH, Silva CL, Santana MHA and Coelho-Castelo AAM (2008) Protection against tuberculosis by a single intranasal administration of DNA-hsp65 vaccine complexed with cationic liposomes. *BMC Immunology* **9**:1-13.
- Rozgony NR, Fang C, Kuczmarski MF and Bob H (2010) Vitamin B(12) deficiency is linked with long-term use of proton pump inhibitors in institutionalized older adults: could a cyanocobalamin nasal spray be beneficial? *Journal of Nutrition for the Elderly* **29**:87-99.
- Rubin BK (2010) Air and soul: the science and application of aerosol therapy. *Respiratory Care* **55**:911-921.
- Rubin BK and Durotoye L (2004) How do patients determine that their metered-dose inhaler is empty? *Chest* **126**:1134-1137.
- Saari M, Vidgren MT, Koskinen MO, Turjanmaa ViMH and Nieminen MM (1999) Pulmonary distribution and clearance of two beclomethasone liposome formulations in healthy volunteers. *International Journal of Pharmaceutics* **181**:1-9.
- Sabin J, Prieto G, Messina PV, Ruso JM, Hidalgo-Alvarez R and Sarmiento F (2005) On the effect of Ca²⁺ and La³⁺ on the colloidal stability of liposomes. *Langmuir* **21**:10968-10975.
- Sabin J, Prieto G, Ruso J, Hidalgo-Álvarez R and Sarmiento F (2006) Size and stability of liposomes: A possible role of hydration and osmotic forces. *The European Physical Journal E: Soft Matter and Biological Physics* **20**:401-408.
- Sabin J, Prieto G, Ruso JM, Messina PV, Salgado FJ, Nogueira M, Costas M and Sarmiento F (2009) Interactions between DMPC liposomes and the serum blood proteins HSA and IgG. *The Journal of Physical Chemistry B* **113**:1655-1661.
- Salib RJ and Howarth PH (2003) Safety and tolerability profiles of intranasal antihistamines and intranasal corticosteroids in the treatment of allergic rhinitis. *Drug Safety* **26**:863-893.
- Saunders KB (1965) Misuse of inhaled bronchodilator agents. *British Medical Journal* **1**:1037-1038.
- Schata M, Jorde W and Richarz-Barthauer U (1991) Levocabastine nasal spray better than sodium cromoglycate and placebo in the topical treatment of seasonal allergic rhinitis. *Journal of Allergy and Clinical Immunology* **87**:873-878.
- Schneider T, Sachse A, Röβling G and Brandl M (1995) Generation of contrast-carrying liposomes of defined size with a new continuous high pressure extrusion method. *International Journal of Pharmaceutics* **117**:1-12.
- Schreier H, Gonzalez-Rothi RJ and Stecenko AA (1993) Pulmonary delivery of liposomes. *Journal of Controlled Release* **24**:209-223.

- Schreier H, McNicol KJ, Ausborn M, Soucy DM, Derendorf H, Stecenko AA and Gonzalez-Rothi RJ (1992) Pulmonary delivery of amikacin liposomes and acute liposome toxicity in the sheep. *International Journal of Pharmaceutics* **87**:183-193.
- Schultz RK (1995) Drug delivery characteristics of metered-dose inhalers. *Journal of Allergy and Clinical Immunology* **96**:284-287.
- Segata, S, Tezak and D (2006) Spontaneous formation of vesicles. *Advances in Colloid and Interface Science* **121**:51-75.
- Shah NM, Parikh J, Namdeo A, Subramanian N and Bhowmick S (2006) Preparation, characterization and *in vivo* studies of proliposomes containing Cyclosporine A. *Journal of Nanoscience and Nanotechnology* **6**:2967-2973.
- Shahiwala A and Misra A (2006) Preliminary investigation of the nasal delivery of liposomal leuprorelin acetate for contraception in rats. *Journal of Pharmacy and Pharmacology* **58**:19-26.
- Sharma A and Sharma US (1997) Liposomes in drug delivery: Progress and limitations. *International Journal of Pharmaceutics* **154**:123-140.
- Shim C and Williams MH (1980) The adequacy of inhalation of aerosol from canister nebulizers. *American Journal of Medicine* **69**:891-894.
- Shimizu M, Miwa Y, Hashimoto K and Goto A (1993) Encapsulation of chicken egg yolk immunoglobulin G (IgY) by liposomes. *Bioscience, Biotechnology, and Biochemistry* **57**:1445-1449.
- Smith PK, Krohn RI, Hermanson GT, Mallia AK, Gartner FH, Provenzano MD, Fujimoto EK, Goeke NM, Olson BJ and Klenk DC (1985) Measurement of protein using bicinchoninic acid. *Analytical Biochemistry* **150**:76-85.
- Smola M, Vandamme T and Sokolowski A (2008) Nanocarriers as pulmonary drug delivery systems to treat and to diagnose respiratory and non respiratory diseases. *International Journal Of Nanomedicine* **3**:1-19.
- Smyth HDC, Smyth HH and Hickey AJ eds (2011) *Controlled Pulmonary Drug Delivery*, Springer, New York, pp:51-75.
- Soane RJ, Frier M, Perkins AC, Jones NS, Davis SS and Illum L (1999) Evaluation of the clearance characteristics of bioadhesive systems in humans. *International Journal of Pharmaceutics* **178**:55-65.
- Song KH, Chung SJ and Shim CK (2002) Preparation and evaluation of proliposomes containing salmon calcitonin. *Journal of Controlled Release*, **84**:27-37.
- Song Y, Wang Y, Thakur R, Meidan VM and Michniak B (2004) Mucosal drug delivery: membranes, methodologies, and applications. *Critical Reviews in Therapeutic Drug Carrier Systems* **21**:195-256.
- Stanaland BE (2004) Once-daily budesonide aqueous nasal spray for allergic rhinitis: a review. *Clinical Therapeutics* **26**:473-492.

- Steckel H and Eskandar F (2003) Factors affecting aerosol performance during nebulization with jet and ultrasonic nebulizers. *European journal of pharmaceutical sciences : official journal of the European Federation for Pharmaceutical Sciences* **19**:443-455.
- Sterk PJ, Plomp A, van de Vate JF and Quanjer PH (1984) Physical properties of aerosols produced by several jet- and ultrasonic nebulizers. *Bulletin European Pathophysiology of Respiration* **20**:65-72.
- Stewart JC (1980) Colorimetric determination of phospholipids with ammonium ferrothiocyanate. *Analytical Biochemistry* **104**:10-14.
- Storm G and Crommelin DJA (1998) Liposomes: quo vadis? *Pharmaceutical Science & Technology Today* **1**:19-31.
- Szoka F, Jr. and Papahadjopoulos D (1978) Procedure for preparation of liposomes with large internal aqueous space and high capture by reverse-phase evaporation. *Proceedings of the National Academy of Sciences of the United States of America* **75**:4194-4198.
- Szoka F, Olson F, Heath T, Vail W, Mayhew E and Papahadjopoulos D (1980) Preparation of unilamellar liposomes of intermediate size (0.1-0.2 μmol) by a combination of reverse phase evaporation and extrusion through polycarbonate membranes. *Biochim Biophys Acta* **601**:559-571.
- Tafaghodi M, Jaafari M-R and Sajadi Tabassi SA (2006) Nasal immunization studies using liposomes loaded with tetanus toxoid and CpG-ODN. *European Journal Of Pharmaceutics And Biopharmaceutics* **64**:138-145.
- Taylor KMG and Hoare C (1993) Ultrasonic nebulisation of pentamidine isethionate. *International Journal of Pharmaceutics* **98**:45-49.
- Taylor KMG and McCallion ONM (1997) Ultrasonic nebulisers for pulmonary drug delivery. *International Journal of Pharmaceutics* **153**:93-104.
- Taylor KMG and McCallion ONM (2002) Ultrasonic nebulizers, in *Encyclopedia of Pharmaceutical Technology* (Swarbrick J and Boylan JC eds) Marcel Dekker, New York, pp:2840-2847.
- Taylor KMG, Taylor G, Kellaway IW and Stevens J (1990a) The stability of liposomes to nebulisation. *International Journal of Pharmaceutics* **58**:57-61.
- Ten RM, Anderson PM, Zein NN, Temesgen Z, Clawson ML and Weiss W (2002) Interleukin-2 liposomes for primary immune deficiency using the aerosol route. *International Immunopharmacology* **2**:333-344.
- Thomas DA, Myers MA, Wichert B, Schreier H and Gonzalez-Rothi RJ (1991) Acute effects of liposome aerosol inhalation on pulmonary function in healthy human volunteers. *Chest* **99**:1268-1270.
- Torchilin VP (2006) *Nanoparticulates As Drug Carriers*, Imperial College Press, London, pp:367-386.
- Torchilin VP and Weissig V (2003) *Liposomes: A Practical Approach*, Oxford University Press, pp:31-72.

- Tortorella D, Ulbrandt ND and London E (1993) Simple centrifugation method for efficient pelleting of both small and large unilamellar vesicles that allows convenient measurement of protein binding. *Biochemistry* **32**:9181-9188.
- Turanek J, Zaluska D and Neca J (1997) Linkup of a fast protein liquid chromatography system with a stirred thermostated cell for sterile preparation of liposomes by the proliposome-liposome method: application to encapsulation of antibiotics, synthetic peptide immunomodulators, and a photosensitizer. *Analytical Biochemistry* **249**:131-139.
- Türker S, Onur E and Ózer Y (2004) Nasal route and drug delivery systems. *Pharmacy World & Science* **26**:137-142.
- Ugwoke MI, Agu RU, Verbeke N and Kinget R (2005) Nasal mucoadhesive drug delivery: Background, applications, trends and future perspectives. *Advanced Drug Delivery Reviews* **57**:1640-1665.
- Uhumwangho MU and Okor RS (2005) Current trends in the production and biomedical applications of liposomes: a review. *Journal of Medicine and Biomedical Research* **4**:9-21.
- Vecellio L (2006) The mesh nebuliser: a recent technical innovation for aerosol delivery. *Breathe* **2**:253-260.
- Vecellio L, Grimbert D, Becquemin MH, Boissinot E, Le Pape A, Lemarie E and Diot P (2001) Validation of laser diffraction method as a substitute for cascade impaction in the European Project for a Nebulizer Standard. *Journal of Aerosol Medicine : The Official Journal of The International Society For Aerosols In Medicine* **14**:107-114.
- Vemuri S and Rhodes CT (1995) Preparation and characterization of liposomes as therapeutic delivery systems: a review. *Pharmaceutica Acta Helveticae* **70**:95-111.
- Vermeer AW, Bremer MG and Norde W (1998) Structural changes of IgG induced by heat treatment and by adsorption onto a hydrophobic Teflon surface studied by circular dichroism spectroscopy. *Biochimica et Biophysica Acta* **1425**:1-12.
- Vermeer AW and Norde W (2000) The thermal stability of immunoglobulin: unfolding and aggregation of a multi-domain protein. *Biophysical Journal* **78**:394-404.
- Vyas SP, Goswami SK and Singh R (1995) Liposomes based nasal delivery system of nifedipine: development and characterization. *International Journal of Pharmaceutics* **118**:23-30.
- Vyas SP and Sakthivel T (1994) Pressurized Pack-Based Liposomes for Pulmonary Targeting of Isoprenaline, Development and Characterization. *Journal of Microencapsulation* **11**:373-380.
- Waldrep JC, Berlinski A and Dhand R (2007) Comparative analysis of methods to measure aerosols generated by a vibrating mesh nebulizer. *Journal of Aerosol Medicine : the official journal of the International Society for Aerosols in Medicine* **20**:310-319.

- Waldrep JC, Keyhani K, Black M and Knight V (1994) Operating characteristics of 18 different continuous-flow jet nebulizers with beclomethasone dipropionate liposome aerosol. *Chest* **105**:106-110.
- Waldrep JC, Knight CM, Black MB, Gilbert BE, Knight V, Eschenbacher W and Scherer PW (1997) Pulmonary delivery of beclomethasone liposome aerosol in volunteers. *Chest* **111**:316-323.
- Wallace DV, Dykewicz MS, Bernstein DI, Blessing-Moore J, Cox L, Khan DA, Lang DM, Nicklas RA, Oppenheimer J, Portnoy JM, Randolph CC, Schuller D, Spector SL and Tilles SA (2008) The diagnosis and management of rhinitis: an updated practice parameter. *Journal of Allergy and Clinical Immunology* **122**:S1-S84.
- Walsh RL and Coles ME (1980) Binding of ige and other proteins to microfilters. *Clinical Chemistry* **26**:496-498.
- Walsh RL, Coles ME and Geary TD (1979) Evaluation of 2 commercially available laser nephelometers and their recommended methods for measurement of serum immunoglobulin-g. *Clinical Chemistry* **25**:151-156.
- Wang CH and Huang YY (2003) Encapsulating protein into preformed liposomes by ethanol-destabilized method. *Artificial Cells, Blood Substitutes, and Immobilization Biotechnology* **31**:303-312.
- Wang J, Chua KM and Wang C-H (2004) Stabilization and encapsulation of human immunoglobulin G into biodegradable microspheres. *Journal of Colloid And Interface Science* **271**: 92-101.
- Wang W, Singh S, Zeng DL, King K and Nema S (2007) Antibody structure, instability, and formulation. *Journal Of Pharmaceutical Sciences* **96**:1-26.
- Washington N, Washington C and Wilson CG (2001) *Physiological Pharmaceutics: Barriers to Drug Absorption*, Taylor & Francis, London, pp:199-210.
- Webster TJ (2010) *Nanotechnology Enabled In Situ Sensors for Monitoring Health*, Springer, pp:9-14.
- Weissig V (2010) *Liposomes: Methods and Protocols, Volume 1: Pharmaceutical Nanocarriers*, Humana Press, pp:1-27.
- Weltzin R and Monath TP (1999) Intranasal antibody prophylaxis for protection against viral disease. *Clinical Microbiology Reviews* **12**:383-393.
- Wen MM (2011) Olfactory targeting through intranasal delivery of biopharmaceutical drugs to the brain: current development. *Discovery Medicine* **11**:497-503.
- Werle M and Takeuchi H (2009) Chitosan-aprotinin coated liposomes for oral peptide delivery: Development, characterisation and *in vivo* evaluation. *International Journal of Pharmaceutics* **370**:26-32.
- Whitmore L and Wallace BA (2008) Protein secondary structure analyses from circular dichroism spectroscopy: Methods and reference databases. *Biopolymers* **89**: 392-400.
- Winslow RM (2006) *Blood Substitutes*, Elsevier Academic Press, San Diego, California, pp:499-514.

- Wong JP, Stadnyk LL and Saravolac EG (1994) Enhanced protection against respiratory influenza A infection in mice by liposome-encapsulated antibody. *Immunology* **81**:280-284.
- Woolfrey SG, Taylor G, Kellaway IW and Smith A (1988) Pulmonary absorption of liposome-encapsulated 6-carboxyfluorescein. *Journal of Controlled Release* **5**:203-210.
- Wu ZH, Ping QN, Lai JM and Wei Y (2003) Hypoglycemic effect of polysaccharide-coated insulin liposomes after oral administration in mice. *Acta Pharmaceutica Sinica* **38**:138-142.
- Yan-yu X, Yun-mei S, Zhi-peng C and Qi-neng P (2006) Preparation of silymarin proliposome: A new way to increase oral bioavailability of silymarin in beagle dogs. *International Journal of Pharmaceutics* **319**:162-168.
- Zambaux MF, Bonneaux F, Gref R, Dellacherie E and Vigneron C (1999) Preparation and characterization of protein C-loaded PLA nanoparticles. *Journal of Controlled Release* **60**:179-188.
- Zaru M, Manca M-L, Fadda AM and Antimisiaris SG (2009) Chitosan-coated liposomes for delivery to lungs by nebulisation. *Colloids and Surfaces B: Biointerfaces* **71**:88-95.
- Zhan H (1999) A method for quick measurement of protein binding to unilamellar vesicles. *Journal of Biochemical and Biophysical Methods* **41**:13-19.
- Zhang J, Guan P, Wang T, Chang D, Jiang T and Wang S (2009) Freeze-dried liposomes as potential carriers for ocular administration of cytochrome c against selenite cataract formation. *The Journal Of Pharmacy and Pharmacology* **61**:1171-1178.
- Zhuang J, Ping Q, Song Y, Qi J and Cui Z (2010) Effects of chitosan coating on physical properties and pharmacokinetic behavior of mitoxantrone liposomes. *International Journal of Nanomedicine* **5**:407-416.
- Zou Y, Ling Y-H, Reddy S, Priebe W and Perez-Soler R (1995) Effect of vesicle size and lipid composition on the *in vivo* tumor selectivity and toxicity of the non-cross-resistant anthracycline annamycin incorporated in liposomes. *International Journal of Cancer* **61**:666-671.